

2019-03-27

Development of Amino Acid-based Solid Sorbents for Post-Combustion CO₂ Capture

Uehara, Yusuke

Uehara, Y. (2019). Development of amino acid-based solid sorbents for post-combustion CO₂ capture (Doctoral thesis, University of Calgary, Calgary, Canada). Retrieved from <https://prism.ucalgary.ca>.
<http://hdl.handle.net/1880/110112>

Downloaded from PRISM Repository, University of Calgary

UNIVERSITY OF CALGARY

Development of Amino Acid-based Solid Sorbents for Post-Combustion CO₂ Capture

by

Yusuke Uehara

A THESIS

SUBMITTED TO THE FACULTY OF GRADUATE STUDIES

IN PARTIAL FULFILMENT OF THE REQUIREMENTS FOR THE

DEGREE OF DOCTOR OF PHILOSOPHY

GRADUATE PROGRAM IN CHEMICAL AND PETROLEUM ENGINEERING

CALGARY, ALBERTA

March, 2019

© Yusuke Uehara 2019

Abstract

Carbon dioxide (CO₂) has been recognized as a major greenhouse gas causing global warming. Post-combustion CO₂ capture is a crucial technology to directly capture CO₂ in flue gases emitted from industries like coal- and gas-fired power plants. The principal goal of this thesis project is developing novel and efficient amino acid (AA)-based solid sorbents for post-combustion CO₂ capture. Amino acid anion-functionalized ionic liquids (AAILs) have been synthesized and mainly employed as promising AA-based materials for CO₂ capture study, due to their good reactivity with CO₂.

Three major research topics have been arranged, associated with the primary goal; namely 1) fundamental comparative CO₂ capture study, 2) comprehensive CO₂ capture study of supported AAIL sorbents and 3) development of promising supports for AAILs. In the first topic, supported AAIL sorbents exhibited higher CO₂ adsorption capacities than the corresponding supported AA sorbents with the same AA content, whereas pure AAs themselves hardly adsorbed CO₂. In the second topic, the effect of cation and anion in AAILs on CO₂ adsorption-desorption of the supported AAIL sorbents were investigated thoroughly. As a result, it was found that cations with larger molecular size can lead to higher reaction stoichiometry of the supported AAILs with CO₂. Regarding AA anions, AAs having linear side chains with only primary amino groups gave rise to higher capacities than ones having complicated side chains with secondary and tertiary amino groups, regardless of the number of amino groups in the side chains. The effect of water vapor on the adsorption-desorption was evaluated as well. In the presence of water vapor, the supported AAIL sorbents slightly reduced their CO₂ uptakes, since the water content hindered the reaction of AAILs with CO₂. In the third topic, some strategies to develop more efficient mesoporous silica supports that can improve the CO₂ capture performances of the supported AAIL sorbents

have been explored through investigations on the effects of textural properties and remaining surfactants of supports on the CO₂ capture. As a result, it has been found that pore-expansion of or leaving the surfactant in a support are effective ways to enhance the capacities.

Among the supported AAIL sorbents studied so far, 60 wt% 1-ethyl-3-methylimidazolium lysine ([EMIM][Lys])-loaded PE-SBA-15 and SBA-15-SA sorbents exhibited the highest CO₂ adsorption capacities of 1.5 mmol/g-sorbent at 30 °C under a dry gas inlet (15% CO₂). It is expected that the capacities can be still elevated to an optimum capacity range of 2–4 mmol/g-sorbent by any modifications of AAILs and/or supports. Some recommendations to improve the CO₂ capture performances are described at the end of this thesis.

Acknowledgments

I would like to express the deepest appreciation to my supervisor, Dr. Nader Mahinpey, for providing me with the opportunity to carry out my PhD thesis research in the Energy and Environment Research Group (EERG) under his supervision. His generous advices and supports have always been a great help in continuing and then completing my doctoral program as well as thesis project there.

I would also like to offer special thanks to my supervisory committee members, examination committee members and examiners, Dr. Hector De la Hoz Siegler, Dr. Sathish Ponnurangam, Dr. Edward Ted P.L. Roberts, Dr. George Kisa Hayashi Shimizu and Dr. Amr Henni (the external examiner from University of Regina) for taking their time and providing valuable comments on my thesis.

I have had a lot of supports and encouragements from the EERG members throughout my PhD program as well. In particular, Dr. Abhimanyu Jayakumar has greatly helped me with acquiring the experimental and quantification procedures of TGA-MS analysis system. Dr. Davood Karami has also given me beneficial comments and assists when conducting experiments and writing paper in case of needs.

In addition, I am very grateful to the Natural Sciences and Engineering Research Council (NSERC) of Canada for funding my work, through its Industrial Research Chairs (IRC) program.

Dedication

This thesis is dedicated to my beloved family for their everlasting love and spiritual support to me at any time.

Table of contents

Abstract	ii
Acknowledgments.....	iv
Dedication	v
List of Tables	xii
List of Figures	xiv
List of Schemes.....	xxi
List of Symbols, Abbreviations and Nomenclature	xxii
 CHAPTER 1: INTRODUCTION	 1
1.1 Overview	1
1.2 Literature review	8
1.2.1 Reaction scheme of AAs with CO ₂	9
1.2.2 Amine-loaded solid sorbents and support materials	11
1.2.3 Effect of water vapor on CO ₂ adsorption–desorption	14
1.2.4 Amino acid anion-functionalized ionic liquids	16
1.3 Objectives and structure of the thesis.....	18
1.4 Outcomes of the thesis	21
1.5 References	22
 CHAPTER 2: FUNDAMENTAL CO ₂ CAPTURE STUDY USING PURE SOLID AMINO ACIDS AND SUPPORTED AMINO ACIDS	 30
2.1 Introduction	30
2.2 Experimental section	31

2.2.1. Materials.....	31
2.2.2. Immobilization of AAs into PMMA support	31
2.2.3. CO ₂ capture experiment under dry or humidified gas flow	32
2.3 Results and discussion.....	34
2.3.1 CO ₂ adsorption performances of pure solid AAs	34
2.3.2 CO ₂ adsorption performances of supported AA sorbents	36
2.4 Conclusions	38
2.5 References	39
CHAPTER 3: EFFECT OF WATER VAPOR ON CO ₂ SORPTION–DESORPTION	
BEHAVIORS OF SUPPORTED AMINO ACID IONIC LIQUID SORBENTS ON POROUS	
MICROSPHERES	41
3.1 Presentation of the article.....	41
3.2 Abstract	42
3.3 Introduction	43
3.4 Experimental section.....	46
3.4.1 Materials.....	46
3.4.2 Synthesis of [EMIM][AA]	46
3.4.3 Preparation of supported [EMIM][AA] or AA on PMMA	47
3.4.4 Characterization	48
3.4.5 CO ₂ capture experiment	48
3.4.6 Quantification of CO ₂ and H ₂ O adsorbed in humidified CO ₂ flow condition	49
3.4.7 Temperature-programmed desorption (TPD).....	49
3.5 Results and discussion.....	50

3.5.1 Characterization	50
3.5.2 Comparison of CO ₂ capture performance of [EMIM][AA]- and AA-PMMA under dry CO ₂ flow	51
3.5.3 Effect of water vapor in inlet gases on CO ₂ sorption of [EMIM][AA]- and AA-PMMA	56
3.5.4 Effect of water vapor in flow gases on CO ₂ desorption behavior	61
3.5.5 Cyclic CO ₂ sorption-desorption in both dry and humidified CO ₂ conditions.....	63
3.6 Conclusions	65
3.7 Supporting Information	66
3.7.1 Characterization	66
3.7.2 Error analysis	68
3.7.3 Tabular data of CO ₂ capture capacities	70
3.8 References	71
CHAPTER 4: ROLES OF CATION AND ANION OF AMINO ACID ANION– FUNCTIONALIZED IONIC LIQUIDS IMMOBILIZED INTO A POROUS SUPPORT FOR CO ₂ CAPTURE	76
4.1 Presentation of the article	76
4.2 Abstract	78
4.3 Introduction	79
4.4 Experimental section	81
4.4.1 Synthesis of [EMIM][AA] and [P ₄₄₄₄][AA].....	83
4.4.2 Immobilization of AAIL into PMMA microspheres	83
4.4.3 Characterization	84

4.4.4	CO ₂ sorption test under dry or humidified gas flow	84
4.4.5	Temperature programmed desorption (TPD)	85
4.5	Results and discussion.....	86
4.5.1	Effect of cation of AAIL on CO ₂ adsorption performance under dry CO ₂ inlet	87
4.5.2	Effect of anion of AAIL on CO ₂ adsorption performance under dry CO ₂ inlet.....	91
4.5.3	Kinetic analysis of CO ₂ adsorption in dry CO ₂ flow	92
4.5.4	Comparison of CO ₂ and H ₂ O adsorption behaviors under humidified CO ₂ inlet.....	98
4.5.5	TPD behaviors of CO ₂ adsorbed in dry and humidified gas flow	104
4.6	Conclusions	106
4.7	Supporting Information	108
4.8	References	119
CHAPTER 5: CO ₂ ADSORPTION USING AMINO ACID IONIC LIQUID–IMPREGNATED		
MESOPOROUS SILICA SORBENTS WITH DIFFERENT TEXTURAL PROPERTIES.....		123
5.1	Presentation of the article.....	123
5.2	Abstract	125
5.3	Introduction	126
5.4	Experimental	128
5.4.1	Synthesis of AAIL.....	128
5.4.2	Synthesis of mesoporous silica supports.....	128
5.4.3	Immobilization of AAIL into supports.....	130
5.4.4	Characterization	131
5.4.5	CO ₂ adsorption experiments	131
5.5	Results and discussion.....	132

5.5.1 Characterization of pure and [EMIM][Lys]-impregnated mesoporous silicas	132
5.5.2 CO ₂ adsorption performances of the [EMIM][Lys]-impregnated sorbents with 50 wt% loading	140
5.5.3 Effect of pore expansion of support on the CO ₂ adsorption performance	145
5.6 Conclusions	153
5.7 References	154
CHAPTER 6: AMINO ACID IONIC LIQUID–MODIFIED MESOPOROUS SILICA	
SORBENTS WITH REMAINING SURFACTANT FOR CO ₂ CAPTURE.....	161
6.1 Presentation of the article	161
6.2 Abstract	163
6.3 Introduction	164
6.4 Experimental section	166
6.4.1 Synthesis of materials	166
6.4.4.1 [EMIM][Lys]	166
6.4.4.2 Mesoporous silica supports.....	166
6.4.4.3 [EMIM][Lys]-loaded mesoporous silica sorbents	168
6.4.4.4 Characterization	168
6.4.4.5 CO ₂ adsorption test	169
6.5 Results and discussion.....	170
6.5.1 Characterization	171
6.5.5.1 TGA behavior	171
6.5.5.2 Pore property.....	172
6.5.2 CO ₂ capture performance	176

6.5.2.1 As-prepared mesoporous silicas	176
6.5.2.2 [EMIM][Lys]-loaded mesoporous silica sorbents with remaining surfactant	177
6.5.2.3 Cyclic CO ₂ capture performances of [EMIM][Lys]-loaded mesoporous silica sorbents	181
6.5.2.4 Effect of addition of surfactant	184
6.5.2.5 Effect of pore-expansion.....	186
6.6 Conclusions	188
6.7 References	189
CHAPTER 7: CONCLUSIONS AND RECOMMENDATIONS FOR FUTURE STUDY	194
7.1 Relation between chapters.....	194
7.2 Summaries.....	196
7.2.1 Fundamental comparative CO ₂ capture study.....	196
7.2.2 Comprehensive CO ₂ capture study of supported AAILs	198
7.2.3 Development of promising supports for AAILs	199
7.2.4 Overall conclusions	201
7.3 Recommendations for future study	202
7.3.1 CO ₂ adsorption capacity.....	203
7.3.2 CO ₂ /N ratio	204
7.3.3 Stability in cyclic CO ₂ adsorption–desorption.....	205
7.3.4 Tolerance to impurities.....	205
7.4 References	206
APPENDIX: COPYRIGHT PERMISSIONS.....	208

List of Tables

Table 1.1. 20 types of α -AAs, their 3 letter codes and R functional groups.	7
Table 1.2. Classification of α -AAs.....	8
Table 2.1. Structures and side chains of Lys, Arg and Gly.....	30
Table 3.1. Molecular structures of AAs.....	47
Table 3.2. CO ₂ sorption capacities of [EMIM][AA]-PMMA and AA-PMMA sorbents under dry CO ₂ inlet condition (2.3% CO ₂ and balance N ₂) along with corresponding literature values.	53
Table 3.3. Comparison of CO ₂ sorption capacities of [EMIM][AA]-PMMA and AA-PMMA sorbents under dry CO ₂ (2.3% CO ₂ and balance N ₂) and humidified CO ₂ (2.3% CO ₂ , 2.1% H ₂ O and balance N ₂) conditions.	57
Table S3.1. Surface areas and pore volumes of PMMA, [EMIM][Lys]-PMMA with 10 wt% and 50 wt% loadings, and Lys-PMMA with 5 wt% and 20 wt% loadings.	66
Table S3.2. CO ₂ capture capacities for three CO ₂ sorption runs of Lys-PMMA sorbent with the loading of 20 wt%, the averages and standard deviations (S.D.) in dry and humidified gas inlet conditions, respectively.	68
Table S3.3. CO ₂ capture capacities of 1-ethyl-3-methylimidazolium amino acid ([EMIM][AA])-PMMA sorbents with various loadings under dry CO ₂ inlet (2.3% CO ₂ and balance N ₂) and TGA temperature of 30 °C.	70
Table S3.4. CO ₂ capture capacities of amino acid (AA)-PMMA sorbents with various loadings under dry CO ₂ inlet (2.3% CO ₂ and balance N ₂) and TGA temperature of 30 °C.	71
Table 4.1. Molecular structures of AA anions.	82
Table 4.2. Molecular structures of EMIM and P ₄₄₄₄ cations.	82

Table 4.3. CO ₂ capture capacities of [EMIM][AA]-PMMA (50 wt%) and [P ₄₄₄₄][AA]-PMMA (50 wt%) in dry CO ₂ flow condition (2.3% CO ₂ and balance N ₂) at 30 °C.	89
Table 4.4. CO ₂ capture capacities and k_s values of [EMIM][Lys]-PMMA (50 wt%) and pure PMMA obtained at different CO ₂ inlet concentrations and 30 °C using Thermax 500 or Perkin-Elmer STA 6000 TGA.	96
Table S4.1. Surface areas and pore volumes of PMMA, [EMIM][Lys]-PMMA, [P ₄₄₄₄][Lys]-PMMA and [P ₄₄₄₄][Gly]-PMMA with various loadings.	108
Table 5.1. Textural properties of as-prepared mesoporous silica and PMMA supports.....	133
Table 5.2. Textural properties of [EMIM][Lys]-loaded mesoporous silica and PMMA sorbents with different loadings.	134
Table 6.1. Description of the mesoporous silica supports used in this work.	170
Table 6.2. Textural properties of as-prepared mesoporous silica supports.	173
Table 6.3. Textural properties of [EMIM][Lys]-loaded mesoporous silica sorbents with different [EMIM][Lys] loadings.....	175

List of Figures

Figure 1.1. The schematic diagrams of (a) pre-combustion, (b) post-combustion and (c) oxy-combustion CO ₂ capture.	2
Figure 1.2. Simplified diagram of aqueous amine scrubbing unit.	4
Figure 1.3. General structure of α -AAs (neutral form).	7
Figure 2.1. The schematic of TGA-MS analysis system.	32
Figure 2.2. CO ₂ desorption–adsorption experimental program over one cycle.	33
Figure 2.3. TGA weight change of pure Gly in humidified gas flow during 5 cyclic run (adsorption condition of 2.3% CO ₂ , 2.1% H ₂ O and balance N ₂ flow and 30 °C).	34
Figure 2.4. TGA weight change of pure Arg in humidified gas flow during 5 cyclic run (adsorption condition of 2.3% CO ₂ , 2.1% H ₂ O and balance N ₂ flow and 30 °C).	35
Figure 2.5. TGA weight change of pure Lys in humidified gas flow during 5 cyclic run (adsorption condition of 2.3% CO ₂ , 2.1% H ₂ O and balance N ₂ flow and 30 °C).	35
Figure 2.6. Dynamic CO ₂ adsorption performances of 20 wt% AA-loaded PMMA sorbents at 30 °C under 2.3 % CO ₂ and balance N ₂ flow.	37
Figure 2.7. Plot of AA loadings vs. CO ₂ adsorption capacity of AA-PMMA sorbents with different loadings at 30 °C under 2.3 % CO ₂ and balance N ₂ flow.	37
Figure 3.1. CO ₂ adsorption behaviors of [EMIM][AA]-PMMA and AA-PMMA sorbents under dry CO ₂ flow (2.3% CO ₂ and balance N ₂) with time.	51
Figure 3.2. Relationship between AA content in the supported sorbent and CO ₂ capture capacity obtained under the dry CO ₂ flow (2.3% CO ₂ and balance N ₂).	54
Figure 3.3. Amounts of CO ₂ and H ₂ O uptakes of (a) [EMIM][AA]-PMMA (50 wt%) and (b) AA-PMMA (20 wt%) sorbents during the adsorption step in dry and humidified CO ₂	

conditions.	58
Figure 3.4. Comparison of CO ₂ adsorption behaviors of (a) [EMIM][Gly]-PMMA (50 wt%) and (b) Arg-PMMA (20 wt%) with time under dry and humidified CO ₂ inlet gas conditions.	59
Figure 3.5. CO ₂ desorption behaviors of (a) [EMIM][Gly]-PMMA (50 wt%) and (b) Arg-PMMA (20 wt%) with change in TGA reactor temperature under dry and humidified CO ₂ inlet gas conditions.	62
Figure 3.6. Changes in CO ₂ capture capacities of [EMIM][AA]-PMMA (50 wt%) run under the dry CO ₂ (2.3% CO ₂ and balance N ₂) and humidified CO ₂ (2.3% CO ₂ , 2.1% H ₂ O and balance N ₂) flow with the number of cycles.	64
Figure S3.1. TGA curves of PMMA, [EMIM][Lys]-PMMA with 10 wt% and 50 wt% loadings, and as-prepared [EMIM][Lys] (N ₂ atmosphere, heating rate of 10 °C /min).	67
Figure S3.2. TGA curves of PMMA, Lys-PMMA with 5 wt% and 20 wt% loadings, and pure Lys (N ₂ atmosphere, heating rate of 10 °C /min).	67
Figure S3.3. Three repetitive CO ₂ sorption run behaviors of Lys-PMMA sorbent with the loading of 20 wt% in (a) dry and (b) humidified gas CO ₂ conditions.	69
Figure 4.1. Change in CO ₂ uptake of [EMIM][AA]-PMMA and [P ₄₄₄₄][AA]-PMMA sorbents with the loadings of 50 wt% under dry CO ₂ inlet condition (2.3% CO ₂ and balance N ₂) with time at 30 °C (AA: Gly, Lys or His).	87
Figure 4.2. Relationship between AAIL loadings and CO ₂ capture capacities of [EMIM][AA]- or [P ₄₄₄₄][AA]-PMMA sorbent under dry CO ₂ flow condition (2.3% CO ₂ and balance N ₂) at 30 °C (AA: Gly, Lys or His).	88
Figure 4.3. Relationship between AAIL loadings and CO ₂ capture capacities of [EMIM][AA]-PMMA sorbents under dry CO ₂ flow condition (2.3% CO ₂ and balance N ₂) at	

30 °C (AA: Gly, Lys, His, Ala, BALA or Arg).....	91
Figure 4.4. Plot of (a) k_s and (b) k_D of AAIL-PMMA sorbent under dry CO ₂ flow condition (2.3% CO ₂ and balance N ₂) at 30 °C vs AAIL loading in the sorbent.	94
Figure 4.5. Arrhenius plots of k_s for [EMIM][Lys]-PMMA and [P ₄₄₄₄][Lys]-PMMA (50 wt%) adsorption data obtained at different adsorption temperatures and 15% of CO ₂ concentration.	97
Figure 4.6. Amounts of CO ₂ and H ₂ O uptakes of (a) [EMIM][AA]-PMMA (50 wt%), and (b) [P ₄₄₄₄][AA]-PMMA (50 wt%) sorbents in dry (2.3% CO ₂ and balance N ₂) and humidified gas (2.3% CO ₂ , 2.1% H ₂ O and balance N ₂) inlets at 30 °C (AA: Gly, Lys or His).....	99
Figure 4.7. Amounts of CO ₂ and H ₂ O uptakes of Lys-PMMA (20 wt%) sorbent in the dry and humidified gas inlets at 30 °C.	100
Figure 4.8. CO ₂ sorption behaviors of (a) [EMIM][Lys]-PMMA (50 wt%), (b) [P ₄₄₄₄][Lys]-PMMA (50 wt%) and (c) Lys-PMMA (20 wt%) sorbents with time under dry (2.3% CO ₂ and balance N ₂) and humidified gas (2.3% CO ₂ , 2.1% H ₂ O and balance N ₂) inlets at 30 °C.	101
Figure 4.9. CO ₂ and H ₂ O sorption behaviors of (a) [EMIM][Lys]-PMMA (50 wt%) and (b) [P ₄₄₄₄][Lys]-PMMA (50 wt%) sorbents with time under humidified gas flow (2.3% CO ₂ , 2.1% H ₂ O and balance N ₂) at 30 °C.	103
Figure 4.10. TPD behaviors of CO ₂ adsorbed in dry and humidified gas flow conditions for (a) [EMIM][Lys]-PMMA (50 wt%), (b) [P ₄₄₄₄][Lys]-PMMA (50 wt%) and (c) Lys-PMMA (20 wt%) sorbents with TGA temperature.....	105
Figure S4.1. TGA curves of PMMA, [EMIM][Lys]-PMMA and [P ₄₄₄₄][Lys]-PMMA with 10 and 50 wt% loadings, and as-prepared [EMIM][Lys] and [P ₄₄₄₄][Lys] under N ₂ atmosphere at a heating rate of 10 °C /min.....	109

Figure S4.2. Fitted curves for CO ₂ sorption experimental data of [EMIM][Gly]-PMMA sorbents with different loadings.	110
Figure S4.3. Fitted curves for CO ₂ sorption experimental data of [EMIM][Lys]-PMMA sorbents with different loadings.	111
Figure S4.4. Fitted curves for CO ₂ sorption experimental data of [EMIM][His]-PMMA sorbents with different loadings.	112
Figure S4.5. Fitted curves for CO ₂ sorption experimental data of [EMIM][Ala]-PMMA sorbents with different loadings.	113
Figure S4.6. Fitted curves for CO ₂ sorption experimental data of [EMIM][BALA]-PMMA sorbents with different loadings.	114
Figure S4.7. Fitted curves for CO ₂ sorption experimental data of [EMIM][Arg]-PMMA sorbents with different loadings.	115
Figure S4.8. Fitted curves for CO ₂ sorption experimental data of [P ₄₄₄₄][Gly]-PMMA sorbents with different loadings.	116
Figure S4.9. Fitted curves for CO ₂ sorption experimental data of [P ₄₄₄₄][Lys]-PMMA sorbents with different loadings.	117
Figure S4.10. Fitted curves for CO ₂ sorption experimental data of [P ₄₄₄₄][His]-PMMA sorbents with different loadings.	118
Figure 5.1. N ₂ adsorption–desorption isotherms of as-prepared and [EMIM][Lys]-impregnated (a) SBA-15, (b) MCM-41 and (c) KIT-6S.	135
Figure 5.2. N ₂ adsorption–desorption isotherms of as-prepared and [EMIM][Lys]-impregnated PMMA.	136
Figure 5.3. BJH pore size distributions of as-prepared and [EMIM][Lys]-impregnated (a)	

SBA-15, (b) MCM-41 and (c) KIT-6S.....	137
Figure 5.4. BJH pore size distributions of as-prepared and [EMIM][Lys]-impregnated (50 wt%) PMMA.....	138
Figure 5.5. (a) TGA curves and (b) DTGA curves of pure [EMIM][Lys], pure supports (SBA-15, KIT-6S and PMMA) and [EMIM][Lys]-impregnated SBA-15 sorbents with various loadings under N ₂ atmosphere at a heating rate of 10 °C/min.	139
Figure 5.6. CO ₂ adsorption performances of (a) [EMIM][Lys]-loaded sorbents with 50 wt% loading and (b) as-prepared SBA-15 and KIT-6S supports with time at 30 °C.	141
Figure 5.7. Plot of D_p of as-prepared supports with CO ₂ capture capacities of [EMIM][Lys]-impregnated (50 wt%) sorbents at 30 °C.....	143
Figure 5.8. Plot of V_p of as-prepared supports with CO ₂ capture capacities of [EMIM][Lys]-impregnated (50 wt%) sorbents at 30 °C.....	143
Figure 5.9. Plot of S_{BET} of as-prepared supports with CO ₂ capture capacities of [EMIM][Lys]-impregnated (50 wt%) sorbents at 30 °C.....	144
Figure 5.10. BJH pore size distributions of as-prepared and [EMIM][Lys]-impregnated (50 wt%) PE-SBA-15.	146
Figure 5.11. CO ₂ adsorption performances of [EMIM][Lys]-impregnated (50 wt%) PE-SBA-15, SBA-15 and PMMA sorbents with time at 30 °C in the units of mol/mol-AAIL.	146
Figure 5.12. Relationship between D_p of pure supports and CO ₂ capture capacities of [EMIM][Lys]-impregnated (50 wt%) sorbents in the units of mol/mol-AAIL.....	147
Figure 5.13. Plot of [EMIM][Lys] loadings with CO ₂ capture capacities of [EMIM][Lys]-impregnated PE-SBA-15, SBA-15 and PMMA sorbents in the units of (a) mmol/g-sorb and	

(b) mol/mol-AAIL.....	150
Figure 5.14. Appearances of [EMIM][Lys]-impregnated (a) SBA-15 and (b) PMMA sorbents with various loadings.	151
Figure 5.15. Changes in CO ₂ adsorption capacities of [EMIM][Lys]-impregnated (50 wt%) PE-SBA-15, SBA-15 and PMMA sorbents with the number of CO ₂ adsorption–desorption cycles.....	153
Figure 6.1. TGA profiles of as-prepared [EMIM][Lys] and mesoporous silica supports under N ₂ atmosphere at a heating rate of 10 °C/min.	172
Figure 6.2. BJH pore size distributions of as-prepared (a) MCM-41, (b) SBA-15 and (c) PE-SBA-15.....	174
Figure 6.3. Dynamic CO ₂ adsorption performances of as-prepared (a) MCM-41 and (b) SBA-15 with and without the remaining surfactant under 15% CO ₂ (balance N ₂) flow and 30 °C.....	176
Figure 6.4. Dynamic CO ₂ adsorption performances of 50 wt% [EMIM][Lys]-loaded (a) MCM-41 and (b) SBA-15 sorbents with and without the remaining surfactant under 15% CO ₂ (balance N ₂) flow and 30 °C.....	178
Figure 6.5. Plot of [EMIM][Lys] loading vs. CO ₂ adsorption capacity of [EMIM][Lys]-loaded MCM-41 and SBA-15 sorbents with and without the remaining surfactant under 15% CO ₂ (balance N ₂) flow and 30 °C in units of (a) mmol/g-sorbent and (b) mol/mol-AAIL.....	180
Figure 6.6. Cyclic CO ₂ capture performances of 50wt% [EMIM][Lys]-loaded SBA-15 and SBA-15-SA sorbents under the adsorption condition of 15% CO ₂ (balance N ₂) flow and 30 °C, and desorption condition of 100% N ₂ flow and 100 °C.	181
Figure 6.7. Cyclic CO ₂ capture performance of 50wt% [EMIM][Lys]-loaded SBA-15-SA	

sorbent under different desorption temperature of 80, 100 or 120 °C in 100% N ₂ flow; the adsorption condition is 15% CO ₂ (balance N ₂) flow and 30 °C.....	182
Figure 6.8. CO ₂ adsorption capacities of 50 wt% [EMIM][Lys]-loaded MCM-41 (or MCM-41-SA) sorbents with and without an added CTAB under 15% CO ₂ (balance N ₂) flow and 30 °C.....	185
Figure 6.9. Plot of [EMIM][Lys] loading vs. CO ₂ adsorption capacity of [EMIM][Lys]-loaded SBA-15 and PE-SBA-15 sorbents with and without the remaining surfactant under 15% CO ₂ (balance N ₂) flow and 30 °C in units of (a) mmol/g-sorbent and (b) mol/mol-AAIL.....	187
Figure 7.1. Relation between Chapters.	194
Figure 7.2. Molecular structures of PEI (left) and TEPA (right).....	204

List of Schemes

Scheme 1.1. Proposed reaction mechanism of supported amines with CO ₂ in (A) the absence and (B) presence of water vapor.....	15
Scheme 1.2. Preparation process of AAILs with [EMIM] ⁺ by a neutralization method.....	17
Scheme 3.1. Preparation process of AAILs with [EMIM] ⁺ by neutralization method.	45
Scheme 5.1. Assumed reaction scheme of [EMIM][AAs] with CO ₂	148

List of Symbols, Abbreviations and Nomenclature

Symbols

A_1, A_2	double exponential model parameters, mmol g^{-1}
A_D	relative contribution of diffusion barrier for overall adsorption process
A_S	relative contribution of surface barrier for overall adsorption process
C_{CO_2}	volumetric concentration of CO_2 in flow gas
C_e	molar CO_2 uptake per gram of sorbent after reaching adsorption equilibrium, mmol g^{-1}
C_t	molar CO_2 uptake per gram of sorbent at time t , mmol g^{-1}
D_P	BJH adsorption average pore diameter
Δt	time step for TGA or MS readings (= 6s)
k_D	diffusion rate constant, min^{-1}
k_S	surface rate constant, min^{-1}
M_e	experimental mass gain of sorbent after reaching CO_2 adsorption equilibrium, g
M_t	experimental mass gain of sorbent at time t , g
S_{BET}	BET surface area
T	temperature
V_P	BJH adsorption cumulative pore volume
W_{sorbent}	sample weight of sorbent

Abbreviations

AA	amino acid
AAIL	amino acid ionic liquid or amino acid anion-functionalized ionic liquid
AAS	amino acid salt
Ala	L-alanine
Arg	L-arginine
BALA	β -alanine
BET	the Brunauer-Emmet-Teller analysis or method
BJH	the Barrett-Joyes-Halenda analysis or method
CCS	CO ₂ capture and storage
CTAB	cetyltrimethylammonium bromide
DEA	diethanolamine
DTGA	differential thermogravimetric analysis
Gly	glycine
His	L-histidine
IEA	International Energy Agency
IGCC	integrated gasification combined cycle
IL	ionic liquid
IPCC	the International Panel on Climate Change
Lys	L-lysine
MDEA	N-methyldiethanolamine
MEA	monoethanolamine

MOF	metal-organic framework
M.W.	molecular weight
PEI	polyethyleneimine
PE-MCM-41	pore expanded MCM-41
PE-SBA-15	pore expanded SBA-15
PMMA	polymethylmethacrylate
sorb	sorbent
TEOS	tetraethyl orthosilicate
TEPA	tetraethylenepentamine
TGA	thermogravimetric analysis or analyzer
TSIL	task-specific ionic liquid

Nomenclature

AMP	2-amino-2-methyl-1-propanol
BMIM	1-butyl-3-methylimidazolium
CO ₂	carbon dioxide
EMIM	1-ethyl-3-methylimidazolium
MCM-41-SA	MCM-41 not calcined
N ₁₁₁₁	tetramethylammonium
N ₂₂₂₂	tetraethylammonium
N ₆₆₆₁₄	triethyl(tetradecyl)ammonium
P123	triblock copolymer EO20-PO70-EO20
P ₄₄₄₄	tetrabutylphosphonium

P ₆₆₆₁₄	trihexyl(tetradecyl)phosphonium
PE-SBA-15-SA	PE-SBA-15 not calcined
TMB	1,3,5-trimethylbenzene

Chapter 1: Introduction

1.1 Overview

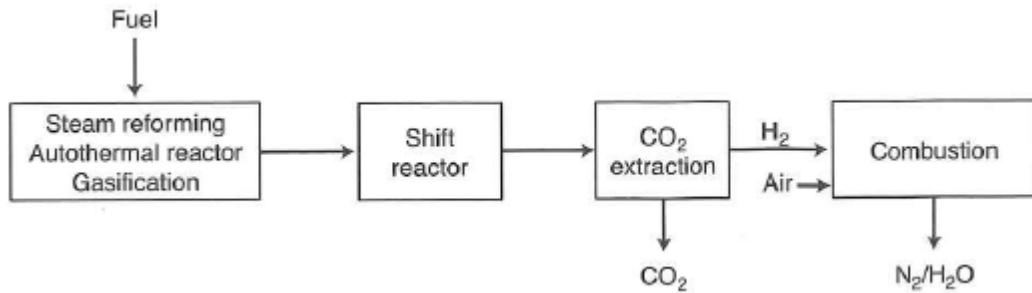
Moderating carbon dioxide (CO₂) emission from human activities has been a considerable concern in recent years as it is generally recognized that CO₂ is one of greenhouse gases affecting global warming. The International Panel on Climate Change (IPCC) has indeed stated in its fifth assessment report that human activities are a main cause of the global warming monitored from the middle of twentieth century [1]. Approximately 30% of anthropogenic sources of the CO₂ emission are originated from combustion of fossil fuels such as coal and oil for power generation [2]. In spite of the environmentally negative impact, it is expected that fossil fuels will exist as the major energy resource from now on [3]. Nevertheless, Copenhagen Accord requests that the global temperature rise be controlled to 2 °C by 2100 [4]. International Energy Agency (IEA) also has pointed out that CO₂ capture and storage (CCS) is required and the contribution should be 19% in 2050 in order to achieve the goal of the ± 2 °C temperature control. It is therefore crucial to develop efficient CCS technologies from large point sources like coal-fired power plants.

There are three approaches to CO₂ capture from large point sources: pre-combustion capture, post-combustion capture and oxy-combustion capture [5,6]. The descriptions of each technology are as follows [6]:

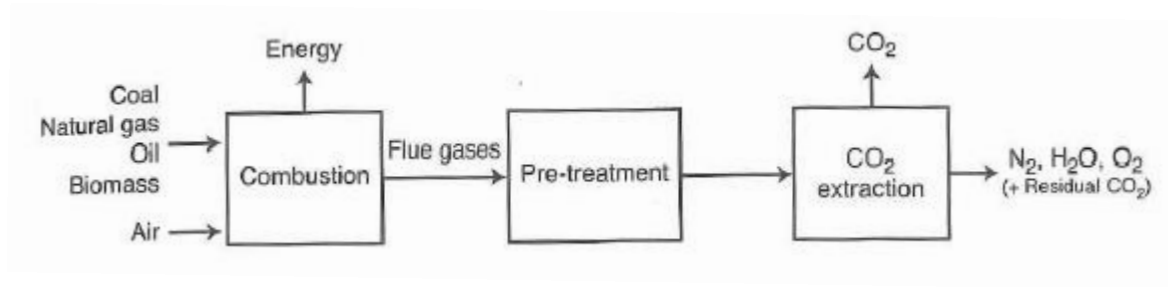
- Pre-combustion CO₂ capture process consists of converting the initial fuel into a mixture of hydrogen (H₂) and carbon dioxide (CO₂), followed by burning the hydrogen in a suitable thermal installation after extracting the CO₂;
- Post-combustion CO₂ capture is a technology for capturing CO₂ directly in flue gases

emitted from combustion or industrial installation like blast furnace;

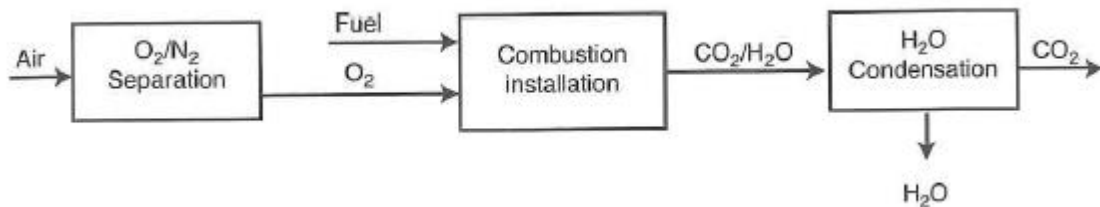
- Oxy-combustion CO₂ capture process consists of conducting combustion either in oxygen or using a metal oxide. As a result, the flue gases generated contain mainly CO₂ and water with virtually no nitrogen.



(a) Pre-combustion CO₂ capture



(b) Post-combustion CO₂ capture



(c) Oxy-combustion CO₂ capture

Figure 1.1. The schematic diagrams of (a) pre-combustion, (b) post-combustion and (c) oxy-combustion CO₂ capture [6].

The schematic diagrams of pre-combustion, post-combustion and oxy-combustion CO₂ capture processes are also described in Figure 1.1(a), (b) and (c), respectively [6]. Pre-combustion CO₂ capture can be applied to integrated gasification combined cycle or IGCC plants, whereas post-combustion and oxy-combustion CO₂ capture can be utilized to conventional coal- or gas-fired power plants [7]. Post-combustion CO₂ capture technology has a big advantage that it can be easily retrofitted on existing installations [6], making it considerably competitive in cost compared with the other two technologies [5]. In contrast, the main disadvantage of post-combustion CO₂ capture is that, since it involves a flue gas in air, which has a low CO₂ concentration (i.e. generally below 15%), the gas volume to be processed to capture only CO₂ becomes correspondingly very high, causing proportionally large equipment [5,6].

Aqueous amine scrubbing is a conventional technology for post-combustion CO₂ capture, which is widely used with an operating experience of over 80 years since the technology was developed in 1930 for the first time [8]. Figure 1.2 presents a simplified diagram of aqueous amine scrubbing unit [6]. The amine solvent captures CO₂ in the absorber (absorption column). After the (CO₂-rich) amine solvent is sent to the regenerator (stripping column), the bottom of the regenerator is heated to break the chemical bond of the amines with CO₂ so that the CO₂ is released from the solvent. Then, the regenerated (CO₂-lean) solvent is returned to the absorber. Various aqueous amine solutions including monoethanolamine (MEA), diethanolamine (DEA), *N*-methyldiethanolamine (MDEA) and 2-amino-2-methyl-1-propanol (AMP) have been extensively practiced for the chemical absorption of CO₂ from gas streams in natural gas, refinery off-gases and syngas processing for many years [7]. The aqueous amine scrubbing is expected to be the dominant technology for CO₂ capture until 2030 [8]. However, this

technology suffers from some disadvantages such as equipment corrosion, thermal and chemical degradation of the solvents, requirement of large absorber volume and high regeneration energy consumption due to the presence of huge amounts of water [4,7]. Therefore, it is desirable to develop new sorbents to overcome those drawbacks.

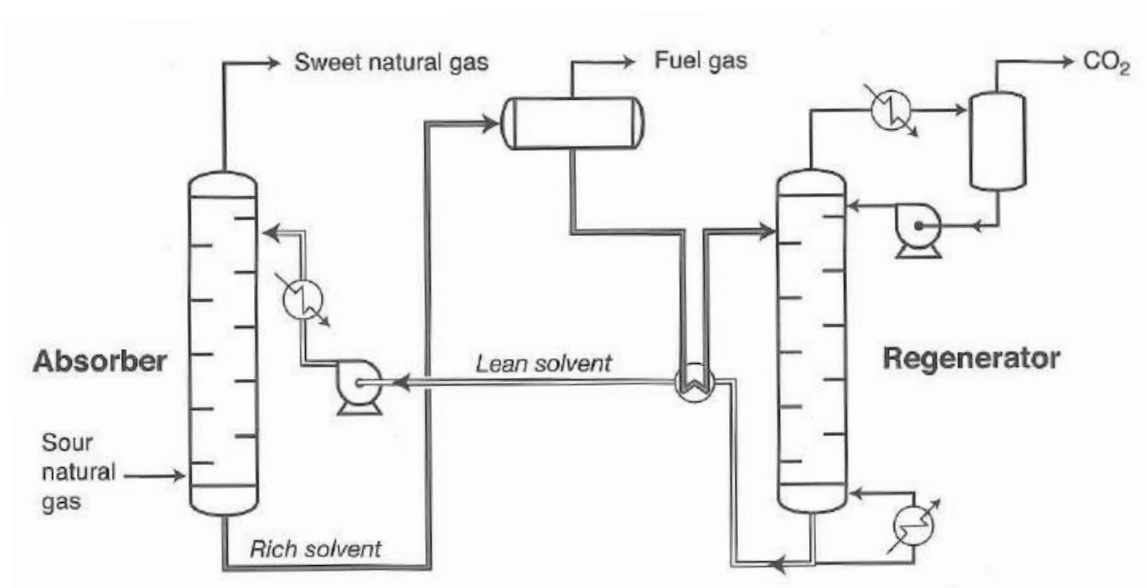


Figure 1.2. Simplified diagram of aqueous amine scrubbing unit [6].

Solid sorbents are expected as alternatives to conventional aqueous amines because solid sorbents can reduce a regeneration energy requirement due to the absence of water [7], which can also lead to reduction in the equipment installation area. Solid sorbents are categorized as physical adsorbents and chemical adsorbents. Physical adsorbents include activated carbon, zeolite, mesoporous silica and metal-organic framework (MOF), while chemical adsorbents include alkali metal carbonate and supported amine-based sorbents. Physical adsorbents typically suffer from low selectivity and high sensitivities to moisture, temperature and pressure. In contrast, chemical sorbents do not have such disadvantages, but these types of sorbents have to

overcome high heat of reaction and chemical stability [7]. Low selectivity and high sensitivity to moisture cause considerable complications in removing only CO₂ from flue gases, since flue gases generally contain some fraction of water vapor. Therefore, chemical adsorbents are considered more promising for post-combustion CO₂ capture than physical adsorbents. It is desirable that CO₂ adsorbents satisfy the following criteria [3,7]:

- CO₂ adsorption capacity: the equilibrium CO₂ adsorption capacity is one of the most important factors in considering the investment cost of the capture system, as it demands the amount of adsorbent needed. It is suggested that an optimum CO₂ adsorption capacity should be 2–4 mmol/g-sorbent, according to a report by Ho et al [9];
- CO₂ selectivity: the selectivity of adsorbents towards CO₂ directly affects the purity of CO₂ captured, which in turn plays an important role in the economics of CO₂ adsorption and sequestration processes. As flue gases contain some fraction of water vapor, adsorbents should exhibit high CO₂ capacity in the presence of the water vapor;
- Adsorption-desorption kinetics: adsorption-desorption kinetics for CO₂ controls the cycle time in a fluid-bed adsorption operation. Fast adsorption-desorption kinetics are crucial under the operating conditions;
- Stability during cyclic adsorption–desorption: the lifetime of adsorbents for cyclic adsorption-desorption is an important factor as it has a direct impact on the economics in a commercial scale operation;
- Tolerance to impurities in flue gas: flue gases contain impurities like SO₂ as well as water vapor. Solid CO₂ sorbents should be resistant to contaminants in a flue gas. Also, removal of impurities such as SO_x and NO_x will be required as CO₂ adsorbents generally have high affinities to those impurities;

- Sorbent cost: This is also one of the important factors to be considered in developing a promising solid sorbent.

Amino acids (AAs) are attractive materials as candidates of chemical adsorbents for CO₂ removal, as AAs have amino groups (–NH₂) in their structures like amines, which can react with CO₂ [10–12]. In addition, other benefits of AAs are that they have little impact on environment, high biodegradability and low volatility [13–15]. However, investigations on CO₂ capture using AA-based solid sorbents have been considerably less than amine-based solid sorbents. My PhD thesis project focuses on developing novel AA based solid sorbents for post-combustion CO₂ capture. AAs are organic compounds consisting of amine group (–NH₂), carboxyl group (–COOH) and a side chain (R group) specific to each AA as described in Figure 1.3. AAs are classified as α –, β –, γ – and δ –AAs, according to which carbon atom the amino group is attached to; for example, α –AA is the one where the amino group is attached to the first carbon atom attaching to the carboxyl group, whereas β –AA is the one where it is attached to the second carbon atom. Among these types, α –AAs are more available and inexpensive because α –AAs have a feature of naturally occurring. There are 20 types of α –AAs (Table 1.1), and some kinds of α –AAs are selected from them in pursuing the thesis research. α –AAs can be classified as neutral, acidic and basic AAs by their side chains or R functional groups as summarized in Table 1.2. It is expected that the acid–base interaction between CO₂ and α –AAs are different depending on the basicity, polarity and steric hindrance of the AA’s side chain [10,15]. In addition to pure α –AAs, amino acid anion-functionalized ionic liquids (AAILs) are synthesized and utilized for the research, as it is anticipated that the amino groups in AAs can become more active for the reaction with CO₂ in the synthetic process of AAILs [16].

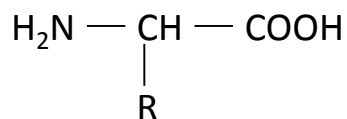


Figure 1.3. General structure of α -AAs (neutral form).

Table 1.1. 20 types of α -AAs, their 3 letter codes and R functional groups.

AA	Code	-R	AA	Code	-R
Glycine	Gly	-H	Aspartic acid	Asp	$-\text{CH}_2\text{COOH}$
Alanine	Ala	$-\text{CH}_3$	Glutamic acid	Glu	$-\text{CH}_2\text{CH}_2\text{COOH}$
Valine	Val	$-\text{CH}(\text{CH}_3)_2$	Asparagine	Asn	$-\text{CH}_2\text{CONH}_2$
Leucine	Leu	$-\text{CH}_2\text{CH}(\text{CH}_3)_2$	Glutamine	Gln	$-\text{CH}_2\text{CH}_2\text{CONH}_2$
Isoleucine	Ile	$-\text{CH}(\text{C}_2\text{H}_5)\text{CH}_3$	Lysine	Lys	$-(\text{CH}_2)_4\text{NH}_2$
Phenylalanine	Phe	$-\text{CH}_2\text{C}_6\text{H}_5$	Arginine	Arg	$-(\text{CH}_2)_3\text{NHC}(\text{NH})\text{NH}_2$
Tyrosine	Tyr	$-\text{CH}_2\text{C}_6\text{H}_4\text{OH}$	Histidine	His	$-\text{C}_4\text{H}_5\text{N}_2$
Tryptophan	Trp	$-\text{C}_9\text{H}_8\text{N}_2$	Proline	Pro	$-\text{C}_3\text{H}_5$
Serine	Ser	$-\text{CH}_2\text{OH}$	Cysteine	Cys	$-\text{CH}_2\text{SH}$
Threonine	Thr	$-\text{CH}(\text{OH})\text{CH}_3$	Methionine	Met	$-\text{CH}_2\text{CH}_2\text{SCH}_3$

Table 1.2. Classification of α -AAs.

Neutral	Non-polar	Glycine, Alanine, Valine, Leucine, Isoleucine, Phenylalanine, Tryptophan, Proline, Methionine
	Polar	Tyrosine, Serine, Threonine, Asparagine, Glutamine, Cysteine
Basic		Lysine, Arginine, Histidine
Acidic		Aspartic acid, Glutamic acid

1.2 Literature review

Although this thesis project is toward fabricating novel amino acid (AA)-based CO₂ adsorbents, there have been much less studies on post-combustion CO₂ capture using AA-based solid sorbents than amine-based solid sorbents so far. AAs have similarities to amines in terms of the molecular structures and the reaction mechanism with CO₂, as both AAs and amines possess amino groups ($-NH_2$) in their structures. Therefore, literature reviews were done for previous studies on CO₂ capture with not only AA-based sorbents, but also amine-based sorbents. Xu et al. are first researchers carrying out a comprehensive investigation on CO₂ adsorption using amine-impregnated solid sorbents [17]; they synthesized polyethyleneimine (PEI)-impregnated mesoporous silica materials for their study. Since then, several researchers have developed different amine-based adsorbents by loading the amines on certain support materials and have investigated the CO₂ adsorption–desorption performances [4,5]. Many of the work have focused on modifying the amine or support to enhance the CO₂ capture performance [5]. Hence, it will be important to find the most active AA-derived material and to synthesize an effective support for the AA-derived material in order to develop promising AA-based solid sorbents with a high CO₂ capture performance. According to Wang et al., the amine-based solid sorbents are classified as

low-temperature CO₂ adsorbents, since the adsorption and desorption temperatures are less than 200 °C [5]. Alkali metal carbonate-based, carbon-based, zeolite-based, MOF-based, silica-based and polymer-based sorbents are categorized as low-temperature CO₂ adsorbents as well; other classifications include intermediate-temperature CO₂ adsorbents (200–400 °C, such as MgO-based sorbents) and high-temperature CO₂ adsorbents (> 400 °C, like CaO-based sorbents). It is considered that the AA-based adsorbents are also low-temperature CO₂ adsorbents due to the similarity of chemical structure to amine-based adsorbents.

Extensive literature search was conducted for studies even on ionic liquids (ILs) and amino acid ionic liquids (AAILs), since many researchers have demonstrated that AAILs are attractive synthetic substances having a high CO₂ sorption–desorption performance for post-combustion CO₂ capture [15,16,18–29]. In fact, AAILs are mainly utilized in my thesis research.

1.2.1 Reaction scheme of AAs with CO₂

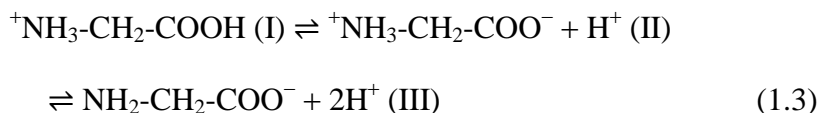
Aqueous alkanolamine solutions are reactive solvents generally used for removal of acid gases such as CO₂ and H₂S from industrial gas streams [11]. The technology of acid gas removal with aqueous alkanolamine solutions is also called amine scrubbing [8]. Monoethanolamine (MEA), diethanolamine (DEA), N-methyldiethanolamine (MDEA) and 2-amino-2-methyl-1-propanol (AMP) are the most commonly used alkanolamines as absorbents in amine scrubbing for post-combustion CO₂ capture [30–32]. Aqueous solutions of amino acid salts (AASs) have also been commercially utilized by BASF for selective removal of CO₂ and H₂S from various gas streams, whose technology is called the Alkazid process [11,33]; BASF employed alanine, dimethyl glycine and diethyl glycine as AAs for the Alkazid process [11]. Besides, in the Giammarco–Vetrocoke process, AAs (especially glycine) have been industrially used as promoters in alkali carbonate solutions for CO₂ removal [34]. Different research groups

have lately suggested AAs including glycine, alanine, proline and taurine as alternatives to amines as well [14].

It is assumed that reaction of AA with CO₂ proceeds through a zwitterion mechanism with two steps in the same manner as amines [12,14]. The first step is that 1 mol of CO₂ reacts with 1 mol of NH₂ species of amino group in AA to form a carbamic acid, R-NHCOOH (Equation 1.1), and the second step is that 1 mol of the generated carbamic acid further reacts with 1 mol of the NH₂ species to form a carbamate anion, R-NHCOO⁻ (Equation 1.2). Thus, in this mechanism, 1 mol of CO₂ reacts with 2 mol of NH₂ species in AA comprehensively.



However, amino groups in pure AAs generally exist as NH₃⁺ rather than NH₂, and chemical forms and distributions of the amino and carboxylic (-COOH) groups change depending on their pH values. For example, in the case of glycine (Gly), which is the simplest type of α-AAs, variations in the chemical forms with the pH range are represented by Equation 1.3, and their distributions calculated with the acid dissociation constants are as shown in Figure 1.3 [14,35]. Guo et al. have clarified that the NH₂ species are much more active for reaction with CO₂ than the NH₃⁺ species [14]. Thus, for AAs to capture CO₂ chemically, NH₃⁺ species in their structures should be deprotonated into the NH₂ species.



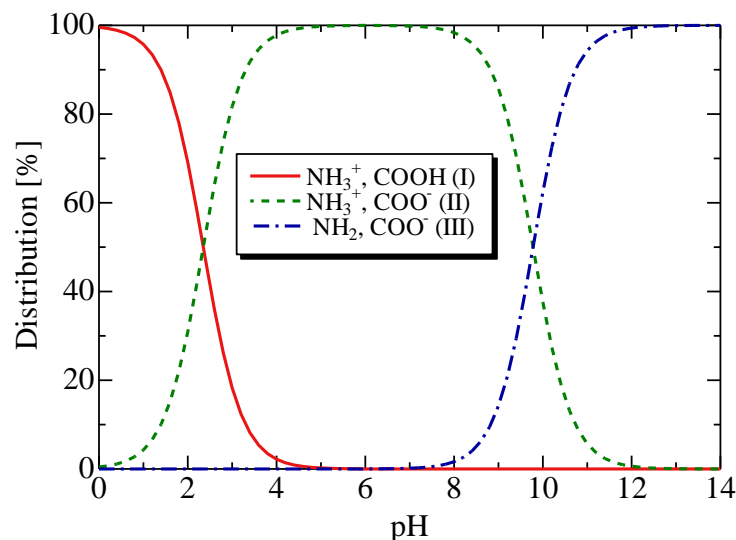


Figure 1.3. Change in chemical forms of amino and carboxylic groups of Gly between the pH ranges of 0–14 at 25 °C [14,35].

1.2.2 Amine-loaded solid sorbents and support materials

The conventional post-combustion CO₂ capture technology by liquid amine absorption and stripping suffers from some intrinsic problems such as equipment corrosion by the amines, solvent losses due to the vaporization and degradation of the amines, and high regeneration energy consumption because of the presence of a huge amount of water in the equipment [5,6]. To avoid those problems, solid sorbents of amines loaded on certain support materials have been extensively investigated in recent years [5]. Several kinds of support materials have been synthesized and applied to develop amine-functionalized solid sorbents for CO₂ adsorption studies, including mesoporous silica, activated carbon, alumina, zeolite and polymer [3,4]. In particular, mesoporous silicas such as MCM-41 [17,36–39], SBA-15[39–46] and KIT-6 [46–48] have been widely studied, since Song's group prepared and investigated PEI-impregnated MCM-41 CO₂ adsorbents for the first time in 2002 [17]. Mesoporous silicas can provide an ordered pore structure with large pore size and pore volume, into which active amine sites can be

uniformly dispersed to enhance the CO₂ sorption-desorption performance [41,44].

The loading methods of amines on supports can be categorized into three classes [49]. Class 1 adsorbents are prepared by loading monomeric or polymeric amines into or onto a support physically, typically by impregnation (Figure 1.4). Song's group first developed this type of adsorbents for their study on CO₂ capture in 2002 [17]. Class 2 adsorbents are based on amines that are covalently grafted to a support like porous silica. This is often achieved by binding amines to oxides with the use of silane chemistry or through preparation of polymeric supports having amine-containing side chains. Class 3 adsorbents are prepared by polymerizing amino-polymers upon porous supports in situ, starting from an amine-containing monomer. This class of sorbents can be regarded as a hybrid of the other two classes [49].

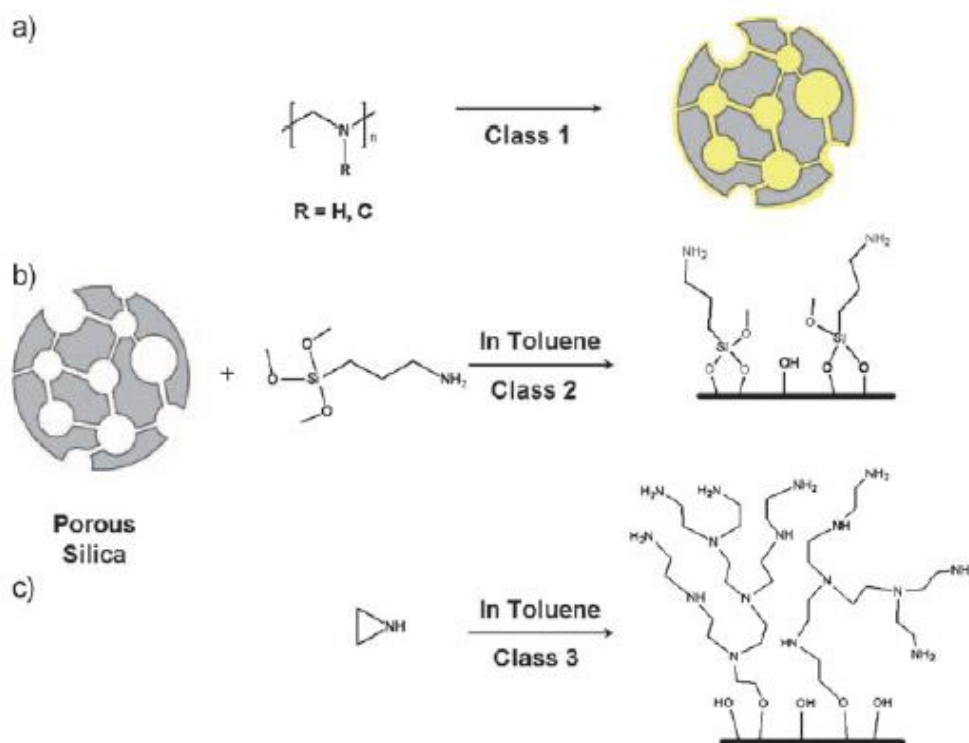


Figure 1.4. Classification of amine-loaded solid sorbents [49].

In general, amine-impregnated sorbents exhibit high CO₂ capture capacities, whereas amine-grafted sorbents display comparatively higher adsorption rates and stabilities during cyclic CO₂ sorption-desorption than amine-impregnated sorbents [3–5]. However, for amine-grafted sorbents, the grafted organic content of amine depends on the surface densities of hydroxyl groups, sometimes causing lower amine loadings as compared with amine-impregnated sorbents. In contrast, for amine-impregnated sorbents, higher loadings may be achieved, but strong diffusion resistances also occur.

It is important to understand what properties of supports predominantly affect the CO₂ capture performances of the supported sorbents. Son et al. have clarified that the pore size of supports significantly influences the CO₂ adsorption capacities of the amine-impregnated mesoporous silica sorbents [47]. They synthesized and used various mesoporous silica supports for their study, namely MCM-41, MCM-48, SBA-15, SBA-16 and KIT-6, and the order of CO₂ adsorption capacities of the supported amine sorbents were KIT-6 > SBA-16 \approx SBA-15 > MCM-48 > MCM-41, which matched that of the average pore diameter. Other research groups have also reported that the pore size and pore volume of mesoporous silicas exerted an impact on the CO₂ capture capacities of the amine-loaded sorbents [39,44]. Pore expansion of supports can lead to better CO₂ capture performances of the supported amines. Sayari's group has developed pore-expanded MCM-41, or PE-MCM-41, and conducted extensive CO₂ capture studies using the amine-loaded PE-MCM-41 sorbents [50–54]. As a result, the PE-MCM-41 gave rise to higher CO₂ adsorption capacities of the supported amines than the conventional MCM-41 and other supports, as the PE-MCM-41 accommodated larger amounts of amines into the pore.

It is assumed that not only the textural properties like pore size, but also the surface chemistry

of supports affect the CO₂ capture performances of the supported amines. Typically, any surfactants are used as templates in synthesizing mesoporous silicas by a sol-gel method, and they are removed from the silica sources to obtain an opened pore structure by extraction and/or calcination (Figure 1.5) [50,55,56]. Yue's group has prepared mesoporous silica supports with the remaining surfactants by not calcination, and they carried out CO₂ capture study using amines immobilized into the supports [38,42]. Their experimental results showed that the remaining surfactants in the supports led to higher CO₂ adsorption capacities of the supported amine sorbents, as the amine bulks dispersed better on the surface of the supports by a surface layer of the surfactants. Heydari-gorji et al. have presented the similar result using amine-loaded PE-MCM-41 with the remaining surfactant [57].

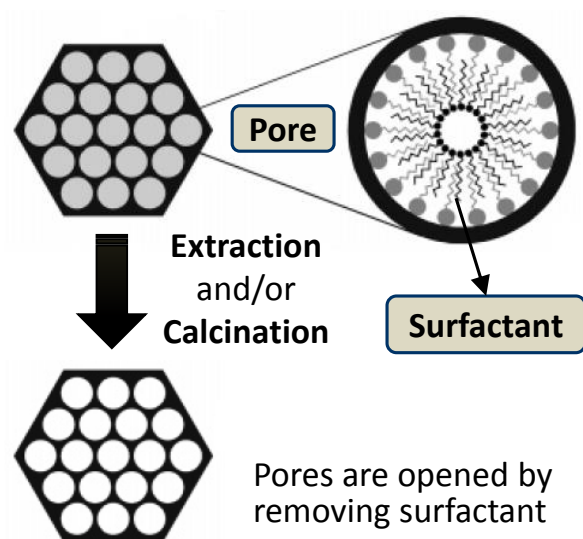
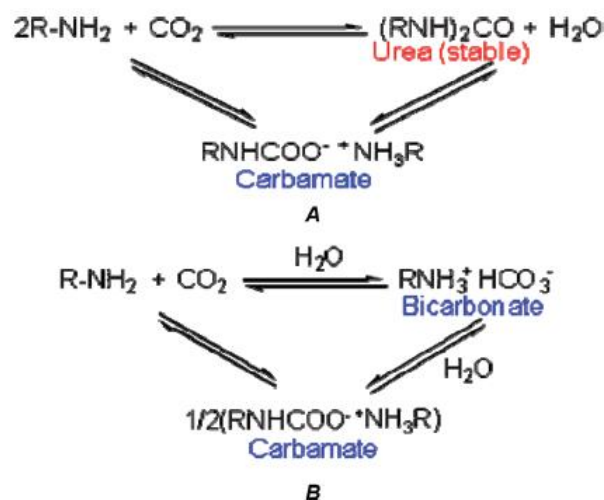
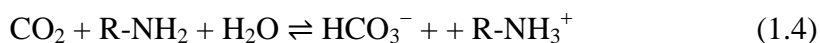


Figure 1.5. Removal of surfactant in synthetic process of mesoporous silicas [50].

1.2.3 Effect of water vapor on CO₂ adsorption–desorption

It is considered important to evaluate the influence of water vapor on CO₂ capture

performances of solid sorbents toward the practical utilization, as real flue gases contain some fraction (nearly 10%) of water vapor. However, CO₂ capture experiments of AA-based solid sorbents have not been carried out in the presence of water vapor so far. For supported amine sorbents, some research groups have reported that water vapor in flow gases exerted a positive effect on the reaction between the amine and CO₂, leading to higher CO₂ uptake [37,40,51–53,58,59]. In the absence of water vapor, 1 mol of CO₂ reacts with 2 mol of NH₂ species in amines via the formation of carbamic acid as an intermediate, as represented by Equations 1.1 and 1.2. On the other hand, in the presence of water vapor, 1 mole of CO₂ can react with 1 mole of the NH₂ species through a different reaction scheme to form a bicarbonate, as expressed by Equation 1.4 [37,53,60–62]. Thus, the amine adsorbs theoretically two times higher amount of CO₂ in the presence of water vapor than the absence of it.

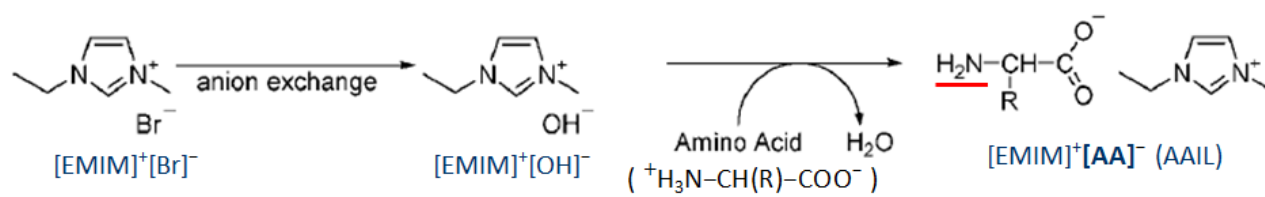


Scheme 1.1. Proposed reaction mechanism of supported amines with CO₂ in (A) the absence and (B) presence of water vapor [53].

Furthermore, Sayari et al. has presented that a cyclic CO₂ adsorption–desorption stability of a supported amine sorbent was retained in a humid gas condition, while it was decreased gradually in a dry gas condition due to formation of urea groups that accumulated on the sorbent, leading to deactivation of the amine (Scheme 1.1) [53].

1.2.4 Amino acid anion-functionalized ionic liquids

Ionic liquids (ILs) are defined as molten salts consisting of only ions that exist in the liquid state at less than 100 °C or room temperature. ILs have very unique characteristics including negligible vapor pressure, high thermal stability, tunable physicochemical properties and non-toxicity [4,5]. ILs have been widely utilized as solvents for catalysis and synthesis. ILs can also be applied to CO₂ capture by either physisorption or chemisorption. For chemisorption, amine-functionalized ILs have recently attracted a great attention as alternatives to the conventional aqueous amines, which are also called task-specific ILs (TSILs) as they are designed by introducing active amino groups to ILs to enhance the CO₂ capture performances [22]. Amino acid anion-functionalized ionic liquids (AAILs) are one type of TSILs that have been applied to CO₂ capture studies. AAILs were developed by Fukumoto et al. in 2005 for the first time; they used 20 α -AAs as anions and 1-ethyl-3-methylimidazolium (EMIM) as a cation to synthesize the AAILs ([EMIM][AAs]) by a neutralization method (Scheme 1.2) [63,64]. Since then, many research groups have vigorously studied CO₂ removal by as-prepared AAILs or AAIL-modified solid sorbents [65]. As seen from Scheme 1.2, NH₃⁺ species (amino groups) in AAs can be deprotonated into active NH₂ species through the preparation process of AAILs, which can enhance the ability of their amino groups for CO₂ capture.



Scheme 1.2. Preparation process of AAILs with [EMIM]⁺ by a neutralization method [64].

Some researchers have investigated the reaction mechanisms of neat AAILs with CO₂, but the reported mechanisms are different depending on the type of cations as well as anions (AAs) in AAILs. For example, Jiang et al. have argued that the reaction of tetraethylammonium amino acid ([N₂₂₂₂][AA]) ILs with CO₂ followed a 2:1 stoichiometry in the same way as that of alkanolamines (Equations 1.1 and 1.2) [27]. Similarly, tetramethylammonium amino acid ([N₁₁₁₁][AA]) and 1-butyl-3-methylimidazolium amino acid ([BMIM][AA]) ILs approached 0.5 mol of CO₂ uptakes per mol of amino group in the AAIL [15,66]. In contrast, Gurkan et al. proposed a 1:1 stoichiometric mechanism for the reaction of trihexyl(tetradecyl)phosphonium amino acid ([P₆₆₆₁₄][AA]) ILs with CO₂, in which only a carbamic acid is produced (Equation 1.1) without formation of carbamate species (Equation 1.2) [21]. Yang et al. have lately clarified that CO₂ absorption of neat phosphonium AAILs actually proceeded through both 2:1 and 1:1 reaction mechanisms, and that the two ratios depended on the type of cations as well as AA anions [24].

One of major disadvantages of AAILs is that they have a high viscosity, resulting in slow CO₂ sorption and desorption rates [16]. An effective way to overcome this drawback and to enhance the CO₂ capture performance is immobilizing AAILs into a porous support with large pore size and pore volume. Some research groups have actually investigated CO₂ adsorption using AAILs

immobilized into support materials in recent years, achieving much more rapid CO₂ sorption than unsupported or as-prepared AAILs [16,19,25,26,29]. It should be highly crucial to investigate the effects of physical and chemical properties of support materials on the CO₂ adsorption of supported AAILs, similarly to that of supported amines. However, no researchers have carried out such investigations with various supports and AAILs.

1.3 Objectives and structure of the thesis

The primary goal of this thesis project is developing novel and efficient AA-based solid sorbents for post-combustion CO₂ capture. Although α -AAs are employed as starting materials for the project, no researchers have examined which pure α -AA has the best reactivity with CO₂. Therefore, the first topic is toward CO₂ capture study of pure solid α -AAs as a screening test to find the most active α -AA. Subsequently, CO₂ capture study of supported α -AAs and AAILs on a certain commercial support is conducted to find a promising AA-derived material that has better reactivity with CO₂. The second topic is evaluating the impact of water vapor on the CO₂ adsorption–desorption of AA-based solid sorbents, as it is important to see how the water vapor contained in actual flue gases affects the CO₂ capture performances of solid sorbents. The third topic is synthesizing various support materials and investigating the effects of their textural properties and surface chemistry on the CO₂ adsorption–desorption of the supported AA-based sorbents to understand what characteristics of supports are crucial to improve the CO₂ capture performances.

Associated with these main topics, the specific objectives of this thesis are arranged as follows:

- 1) Studying the CO₂ capture performances of pure α -AAs as a fundamental screening test to

- find the most active α -AA (Chapter 2);
- 2) Comparing the CO₂ capture performances of supported α -AA and AAIL sorbents on a commercial support with those of pure AAs to find a promising AA-based material that can react better with CO₂ (Chapters 2 and 3);
 - 3) Evaluating the effect of water vapor on the CO₂ adsorption–desorption of the AA-based sorbents (Chapters 3 and 4);
 - 4) Assessing the influence of the AA type in the AA-based sorbents on the CO₂ capture performances (Chapter 4);
 - 5) Conducting the kinetic analysis for the AA-based sorbents (Chapter 4);
 - 6) Investigating the long-term cyclic CO₂ adsorption–desorption stability of the AA-based sorbents (Chapters 2, 3, 5 and 6);
 - 7) Synthesizing several kinds of mesoporous silica supports and investigating the effect of the textural properties on the CO₂ capture of the supported AA-based sorbents (Chapter 5);
 - 8) Comparing the impact of mesoporous silica supports with and without the remaining surfactant on the CO₂ capture of the supported AA-based sorbents (Chapter 6).

This thesis consists of seven chapters, some of which (Chapters 3–6) are organized sequentially in a paper-based format. Chapter 1 has described background, objectives of the thesis project and literature review.

Chapter 2 provides a fundamental study result on CO₂ capture using some kinds of pure α -AAs. Subsequently, pure α -AAs are immobilized into a commercial polymer support by an impregnation method to prepare the supported AA sorbents, and CO₂ adsorption performances of the supported AAs are evaluated and compared with those of pure AAs. The objective of this comparison is to see whether the amino groups in AAs can be activated to enhance the CO₂

capture capacities or not, by immobilizing AAs into a support by impregnation.

From chapter 3, AAILs are mainly used and investigated to develop promising AA-based solid CO₂ adsorbents. Chapter 3 first offers comparative study results of CO₂ capture performances of supported AAIL sorbents with those of supported pure AA sorbents in a dry CO₂ flow condition. Next, the effect of water vapor on CO₂ adsorption–desorption of the supported AAIL and AA sorbents is investigated through the CO₂ capture experiments under a humidified CO₂ flow.

Chapter 4 focuses on the effect of cation as well as anion (AA) of the supported AAIL sorbents on the CO₂ adsorption–desorption in dry or humidified CO₂ flow condition. Two cations, which have substantially different molecular structures and hydrophilicities from each other, are employed to prepare the AAIL and to compare the CO₂ capture performances of the supported AAILs. In addition, six AAs (anions) are used and compared to see how difference in the side chain structure of AAs affect the CO₂ adsorption capacities and rates of the supported AAILs. Kinetic behaviors of these sorbents are also analyzed using a double exponential kinetic model.

From Chapter 5, various mesoporous silica supports are synthesized and used to develop more efficient AAIL-modified solid sorbents for CO₂ capture. The main objective in Chapter 5 is evaluating the impact of textural properties of mesoporous silica supports on CO₂ adsorption of the supported AAIL sorbents. Specifically, the correlation between the CO₂ capture capacities and textural properties (pore size, pore volume and surface area) of the sorbents is analyzed quantitatively. A pore-expanded mesoporous porous silica support is also prepared and applied to aim at further enhancement of the CO₂ adsorption performances.

Chapter 6 presents the effect of remaining surfactant in mesoporous silica supports on CO₂

capture of the supported AAIL sorbents. For this objective, several mesoporous silica supports calcined or not calcined are prepared and compared. The effect of combining remaining surfactant and pore-expansion of a support is also investigated to see how the combined two strategies influence the CO₂ adsorption performances of supported AAIL sorbents.

Chapter 7 finally provides the overall conclusions and some recommendations for future work.

1.4 Outcomes of the thesis

The author has published three peer-reviewed journal papers (Chapters 3, 4 and 5) and submitted the fourth manuscript (Chapter 6) as the first author. A list of these publications is as follows:

Published peer-reviewed journal papers

1. Y. Uehara, D. Karami, N. Mahinpey, Effect of water vapor on CO₂ sorption–desorption behaviors of supported amino acid ionic liquid sorbents on porous microspheres, *Ind. Eng. Chem. Res.* 56 (2017) 14316–14323.
2. Y. Uehara, D. Karami, N. Mahinpey, Roles of cation and anion of amino acid anion-functionalized ionic liquids immobilized into a porous support for CO₂ Capture, *Energy Fuels* 32 (2018) 5345–5354.
3. Y. Uehara, D. Karami, N. Mahinpey, CO₂ adsorption using amino acid ionic liquid-impregnated mesoporous silica sorbents with different textural properties, *Micropor. Mesopor. Mat.* 278 (2019) 378–386.

1. Y. Uehara, D. Karami, N. Mahinpey, Amino acid ionic liquid-modified mesoporous silica sorbents with remaining surfactant for CO₂ capture, submitted to Adsorption in December, 2018.

1.5 References

- [1] Y. Wang, L. Zhao, A. Otto, M. Robinius, D. Stolten, A review of post-combustion CO₂ capture technologies from coal-fired power plants, *Energy Procedia*. 114 (2017) 650–665.
- [2] D. Aaron, C. Tsouris, Separation of CO₂ from flue gas : A review, *Sep Sci Technol* 40 (2011) 321–348.
- [3] A. Sayari, Y. Belmabkhout, R. Serna-guerrero, Flue gas treatment via CO₂ adsorption, *Chem. Eng. J.* 171 (2011) 760–774.
- [4] C.H. Yu, C.H. Huang, C.S. Tan, A review of CO₂ capture by absorption and adsorption, *Aerosol Air Qual. Res.* 12 (2012) 745–769.
- [5] J. Wang, L. Huang, R. Yang, Z. Zhang, J. Wu, Y. Gao, Q. Wang, D.O. Hare, Z. Zhong, Recent advances in solid sorbents for CO₂ capture and new development trends, *Energy Environ. Sci.* 7 (2014) 3478–3518.
- [6] F. Lecomte, P. Broutin, É. Lebas, CO₂ Capture: Technologies to reduce greenhouse gas emissions, Editions Technip, Paris, 2010.
- [7] A. Samanta, A. Zhao, G.K.H. Shimizu, P. Sarkar, R. Gupta, Post-combustion CO₂ capture using solid sorbents: A review, *Ind. Eng. Chem. Res.* 51 (2012) 1438–1463.
- [8] G.T. Rochelle, Amine scrubbing for CO₂ capture, *Science* 325 (2009) 1652–1654.
- [9] M.T. Ho, G.W. Allinson, D.E. Wiley, Reducing the cost of CO₂ capture from flue gases

- using pressure swing adsorption, *Ind. Eng. Chem. Res.* 47 (2008) 4883–4890.
- [10] M.A. Hussain, Y. Soujanya, G.N. Sastry, Evaluating the efficacy of amino acids as CO₂ capturing agents: A first principles investigation, *Environ. Sci. Technol.* 45 (2011) 8582–8588.
- [11] P.S. Kumar, J.A. Hogendoorn, G.F. Versteeg, P.H.M. Feron, Kinetics of the reaction of CO₂ with aqueous potassium salt of taurine and glycine, *AIChE J.* 49 (2003) 203–213.
- [12] M. Kim, H.J. Song, M.G. Lee, H.Y. Jo, J.W. Park, Kinetics and steric hindrance effects of carbon dioxide absorption into aqueous potassium alaninate solutions, *Ind. Eng. Chem. Res.* 51 (2012) 2570–2577.
- [13] H. Knuutila, U.E. Aronu, H.M. Kvamsdal, A. Chikukwa, Post combustion CO₂ capture with an amino acid salt, *Energy Procedia.* 4 (2011) 1550–1557.
- [14] D. Guo, H. Thee, C.Y. Tan, J. Chen, W. Fei, S. Kentish, G.W. Stevens, G. da Silva, Amino acids as carbon capture solvents: Chemical kinetics and mechanism of the glycine + CO₂ reaction, *Energy Fuels* 27 (2013) 3898–3904.
- [15] Y.S. Sistla, A. Khanna, CO₂ Absorption studies in amino acid-anion based ionic liquids, *Chem. Eng. J.* 273 (2015) 268–276.
- [16] X. Wang, N.G. Akhmedov, Y. Duan, D. Luebke, D. Hopkinson, B. Li, Amino acid-functionalized ionic liquid solid sorbents for post-combustion carbon capture, *ACS Appl. Mater. Interfaces.* 5 (2013) 8670–8677.
- [17] X. Xu, C. Song, J.M. Andresen, B.G. Miller, A.W. Scaroni, Novel polyethylenimine-modified mesoporous molecular sieve of MCM-41 type as high-capacity adsorbent for CO₂ capture, *Energy Fuels* 16 (2002) 1463–1469.
- [18] Y. Zhang, S. Zhang, X. Lu, Q. Zhou, W. Fan, Dual aminofunctionalised phosphonium

- ionic liquids for CO₂ capture, *Chem. Eur. J.* 15 (2009) 3003–3011.
- [19] V. Hiremath, A.H. Jadhav, H. Lee, S. Kwon, J. Gil, Highly reversible CO₂ capture using amino acid functionalized ionic liquids immobilized on mesoporous silica, *Chem. Eng. J.* 287 (2016) 602–617.
- [20] F. Chen, K. Huang, Y. Zhou, Z. Tian, X. Zhu, D. Tao, S. Dai, Multi-molar absorption of CO₂ by the activation of carboxylate groups in amino acid ionic liquids, *Angew. Chem.* 128 (2016) 7282–7286.
- [21] B.E. Gurkan, J.C. de la Fuente, E.M. Mindrup, L.E. Ficke, B.F. Goodrich, E.A. Price, W.F. Schneider, J.F. Brennecke, Equimolar CO₂ absorption by anion-functionalized ionic liquids, *J. Am. Chem. Soc.* 132 (2010) 2116–2117.
- [22] E.D. Bates, R.D. Mayton, I. Ntai, J.H. Davis, CO₂ capture by a task-specific ionic liquid, *J. Am. Chem. Soc.* 124 (2002) 926–927.
- [23] B.F. Goodrich, J.C. De La Fuente, B.E. Gurkan, D.J. Zadigian, E.A. Price, Y. Huang, J.F. Brennecke, Experimental measurements of amine-functionalized anion-tethered ionic liquids with carbon dioxide, *Ind. Eng. Chem. Res.* 50 (2011) 111–118.
- [24] Q. Yang, Z. Wang, Z. Bao, Z. Zhang, Y. Yang, Q. Ren, H. Xing, S. Dai, New insights into CO₂ absorption mechanisms with amino-acid ionic liquids, *ChemSusChem* 9 (2016) 806–812.
- [25] J. Ren, L. Wu, B.G. Li, Preparation and CO₂ sorption/desorption of N-(3-aminopropyl)aminoethyl tributylphosphonium amino acid salt ionic liquids supported into porous silica particles, *Ind. Eng. Chem. Res.* 51 (2012) 7901–7909.
- [26] J. Zhang, S. Zhang, K. Dong, Y. Zhang, Y. Shen, X. Lv, Supported absorption of CO₂ by tetrabutylphosphonium amino acid ionic liquids, *Chem. Eur. J.* 12 (2006) 4021–4026.

- [27] Y.Y. Jiang, G.N. Wang, Z. Zhou, Y.T. Wu, J. Geng, Z.B. Zhang, Tetraalkylammonium amino acids as functionalized ionic liquids of low viscosity, *Chem. Commun.* (2008) 505–507.
- [28] S. Saravanamurugan, A.J. Kunov-kruse, R. Fehrmann, A. Riisager, Amine-functionalized amino acid-based ionic liquids as efficient and high-capacity absorbents for CO₂, *ChemSusChem* 7 (2014) 897–902.
- [29] X. Wang, N.G. Akhmedov, Y. Duan, D. Luebke, B. Li, Immobilization of amino acid ionic liquids into nanoporous microspheres as robust sorbents for CO₂ capture, *J. Mater. Chem. A* 1 (2013) 2978–2982.
- [30] H.J. Song, S. Park, H. Kim, A. Gaur, J.W. Park, S.J. Lee, Carbon dioxide absorption characteristics of aqueous amino acid salt solutions, *Int. J. Greenh. Gas Con.* 11 (2012) 64–72.
- [31] A. Aroonwilas, A. Veawab, Integration of CO₂ capture unit using single- and blended-amines into supercritical coal-fired power plants : Implications for emission and energy management, *Int. J. Greenh. Gas Con.* 1 (2007) 143–150.
- [32] M. Ismael, R. Sahnoun, A. Suzuki, M. Koyama, H. Tsuboi, N. Hatakeyama, A. Endou, H. Takaba, M. Kubo, S. Shimizu, C.A. Del, A. Miyamoto, A DFT study on the carbamates formation through the absorption of CO₂ by AMP, *Int. J. Greenh. Gas Con.* 3 (2009) 612–616.
- [33] U.E. Aronu, H.F. Svendsen, K. Anders, Investigation of amine amino acid salts for carbon dioxide absorption, *Int. J. Greenh. Gas Con.* 4 (2010) 771–775.
- [34] A.L. Kohl, R. Nielsen, *Gas purification*, Elsevier, Texas, 1997.
- [35] R.N. Goldberg, N. Kishore, R.M. Lennen, *Thermodynamic quantities for the ionization*

- reactions of buffers, *J. Phys. Chem. Ref. Data.* 31 (2002) 231–370.
- [36] X. Xu, C. Song, J.M. Andr, B.G. Miller, A.W. Scaroni, Preparation and characterization of novel CO₂ “molecular basket” adsorbents based on polymer-modified mesoporous molecular sieve MCM-41, *Micropor. Mesopor. Mat.* 62 (2003) 29–45.
- [37] X. Xu, C. Song, B.G. Miller, A.W. Scaroni, X. Xu, C. Song, B.G. Miller, A.W. Scaroni, Influence of moisture on CO₂ separation from gas mixture by a nanoporous adsorbent based on polyethylenimine-modified molecular sieve MCM-41, *Ind. Eng. Chem. Res.* 44 (2005) 8113–8119.
- [38] M.B. Yue, L.B. Sun, Y. Cao, Y. Wang, Z.J. Wang, J.H. Zhu, Efficient CO₂ capturer derived from as-synthesized MCM-41 modified with amine, *Chem. Eur. J.* 14 (2008) 3442–3451.
- [39] V. Zeleňák, M. Badaničová, D. Halamova, J. Čejka, A. Zukal, N. Murafa, G. Goerigk, Amine-modified ordered mesoporous silica : Effect of pore size on carbon dioxide capture, *Chem. Eng. J.* 144 (2008) 336–342.
- [40] N. Hiyoshi, K. Yogo, T. Yashima, Adsorption of carbon dioxide on amine modified SBA-15 in the presence of water vapor, *Chem. Lett.* 33 (2004) 510–511.
- [41] N. Hiyoshi, K. Yogo, T. Yashima, Adsorption characteristics of carbon dioxide on organically functionalized SBA-15, *Micropor. Mesopor. Mat.* 84 (2005) 357–365.
- [42] M.B. Yue, Y. Chun, Y. Cao, X. Dong, J.H. Zhu, CO₂ capture by as-prepared SBA-15 with an occluded organic template, *Adv. Funct. Mater.* 16 (2006) 1717–1722.
- [43] M.B. Yue, L.B. Sun, Y. Cao, Z.J. Wang, Y. Wang, Q. Yu, J.H. Zhu, Promoting the CO₂ adsorption in the amine-containing SBA-15 by hydroxyl group, *Micropor. Mesopor. Mat.* 114 (2008) 74–81.

- [44] X. Yan, L. Zhang, Y. Zhang, G. Yang, Z. Yan, Amine-modified SBA-15 : Effect of pore structure on the performance for CO₂ capture, *Ind. Eng. Chem. Res.* 50 (2011) 3220–3226.
- [45] M.J. Lashaki, H. Ziaei-azad, A. Sayari, Insights into the hydrothermal stability of triamine-functionalized SBA-15 silica for CO₂ adsorption, *ChemSusChem* 10 (2017) 4037–4045.
- [46] N. Calin, A. Galarneau, T. Cacciaguerra, R. Denoyel, F. Fajula, Epoxy-functionalized large-pore SBA-15 and KIT-6 as affinity chromatography supports, *C. R. Chimie* 13 (2010) 199–206.
- [47] W.J. Son, J.S. Choi, W.S. Ahn, Adsorptive removal of carbon dioxide using polyethyleneimine-loaded mesoporous silica materials, *Micropor. Mesopor. Mat.* 113 (2008) 31–40.
- [48] Y. Liu, J. Shi, J. Chen, Q. Ye, H. Pan, Z. Shao, Y. Shi, Dynamic performance of CO₂ adsorption with tetraethylenepentamine-loaded KIT-6, *Micropor. Mesopor. Mater.* 134 (2010) 16–21.
- [49] W. Li, S. Choi, J.H. Drese, M. Hornbostel, G. Krishnan, P.M. Eisenberger, C.W. Jones, Steam-stripping for regeneration of supported amine-based CO₂ adsorbents, *ChemSusChem* 3 (2010) 899–903.
- [50] R.S. Franchi, P.J.E. Harlick, A. Sayari, Applications of pore-expanded mesoporous silica. 2. Development of a high-capacity, water-tolerant adsorbent for CO₂, *Ind. Eng. Chem. Res.* 44 (2005) 8007–8013.
- [51] P.J.E. Harlick, A. Sayari, Applications of pore-expanded mesoporous silica. 5. Triamine grafted material with exceptional CO₂ dynamic and equilibrium adsorption performance,

- Ind. Eng. Chem. Res. 46 (2007) 446–458.
- [52] R. Serna-Guerrero, E. Da'na, A. Sayari, New insights into the interactions of CO₂ with amine-functionalized silica, Ind. Eng. Chem. Res. 47 (2008) 9406–9412.
- [53] A. Sayari, Y. Belmabkhout, Stabilization of amine-containing CO₂ adsorbents: Dramatic effect of water vapor, J. Am. Chem. Soc. 132 (2010) 6312–6314.
- [54] A. Sayari, Y. Belmabkhout, E. Da'na, CO₂ Deactivation of supported amines: Does the nature of amine matter?, Langmuir 28 (2012) 4241–4247.
- [55] C.T. Kresge, M.E. Leonowicz, W.J. Roth, J.C. Vartuli, J.S. Beck, Ordered mesoporous molecular sieves synthesized by a liquid-crystal template mechanism, Nature 359 (1992) 710–712.
- [56] D. Zhao, J. Feng, Q. Huo, N. Melosh, G.H. Fredrickson, B.F. Chmelka, G.D. Stucky, Triblock copolymer syntheses of mesoporous silica with periodic 50 to 300 angstrom pores, Science 279 (1998) 548–552.
- [57] A. Heydari-gorji, Y. Belmabkhout, A. Sayari, Polyethylenimine-impregnated mesoporous silica: Effect of amine loading and surface alkyl chains on CO₂ adsorption, Langmuir 27 (2011) 12411–12416.
- [58] M.L. Gray, J.S. Hoffman, D.C. Hreha, D.J. Fauth, S.W. Hedges, K.J. Champagne, H.W. Pennline, Parametric study of solid amine sorbents for the capture of carbon dioxide, Energy Fuels. 23 (2009) 4840–4844.
- [59] H.Y. Huang, R.T. Yang, D. Chinn, C.L. Munson, Amine-grafted MCM-48 and silica xerogel as superior sorbents for acidic gas removal from natural gas, Ind. Eng. Chem. Res. 42 (2003) 2427–2433.
- [60] T.L. Donaldson, Y.N. Nguyen, Carbon dioxide reaction kinetics and transport in aqueous

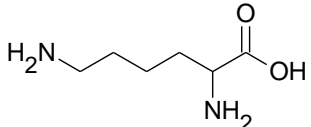
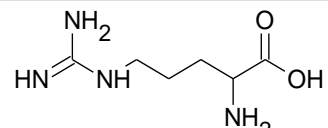
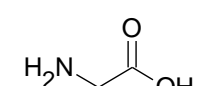
- amine membranes, *Ind. Eng. Chem. Fundam.* 19 (1980) 260–266.
- [61] R.J. Hook, An investigation of some sterically hindered amines as potential carbon dioxide scrubbing compounds, *Ind. Eng. Chem. Res.* 36 (1997) 1779–1790.
- [62] P.D. Vaidya, E.Y. Kenig, CO₂-alkanolamine reaction kinetics: A review of recent studies, *Chem. Eng. Technol.* 30 (2007) 1467–1474.
- [63] K. Fukumoto, M. Yoshizawa, H. Ohno, Room temperature ionic liquids from 20 natural amino acids, *J. Am. Chem. Soc.* 127 (2005) 2398–2399.
- [64] H. Ohno, K. Fukumoto, Amino acid ionic liquids, *Acc. Chem. Res.* 40 (2007) 1122–1129.
- [65] S. Kirchhecker, D. Esposito, Amino acid based ionic liquids: A green and sustainable perspective, *Curr. Opin. Green Sustain. Chem.* 2 (2016) 28–33.
- [66] Z. Feng, F. Cheng-gang, W. You-ting, W. Yuan-tao, Absorption of CO₂ in the aqueous solutions of functionalized ionic liquids and MDEA, *Chem. Eng. J.* 160 (2010) 691–697.

Chapter 2: Fundamental CO₂ capture study using pure solid amino acids and supported amino acids

2.1 Introduction

It is considered important to see how much pure solid amino acids (AAs) can capture CO₂ as a fundamental study, since no researchers have carried out such investigations. In addition, a screening test to find the most active AA for CO₂ removal is required prior to developing a novel promising AA-based solid CO₂ sorbent. Therefore, this chapter first provides a fundamental study result on CO₂ capture using some pure solid α -AAs. Specifically, glycine (Gly), L-lysine (Lys) and L-arginine (Arg) were selected from 20 α -AAs. Lys and Arg have an advantage in that they possess additional amino groups in their side chains (Table 2.1) with stronger basicity than other α -AAs, which might lead to higher CO₂ capture capacities.

Table 2.1. Structures and side chains of Lys, Arg and Gly.

AA type	Structure	Side chain	
Lysine (Lys)		-(CH ₂) ₄ NH ₂	Basic
Arginine (Arg)		-(CH ₂) ₃ NHC(NH)NH ₂	Basic
Glycine (Gly)		-H	Neutral

On the other hand, Gly is the simplest α -AA having only hydrogen in its side chain. Hence, Gly

should be an indicator to examine how differences in the structures and side chain properties of α -AAs influence their CO₂ capture performances.

Next, CO₂ capture performances of supported AAs are evaluated and compared with those of pure AAs in this chapter. The purpose is to see how the CO₂ adsorptivity by amino groups in AAs changes (or enhances) by immobilizing and dispersing the AA bulks into a support. A commercial porous polymer was used as the support.

2.2 Experimental section

2.2.1. Materials

Gly (99%), Lys (98%), Arg ($\geq 98\%$) were purchased from Alfa Aesar Co. (Ward Hill, MA). In the CO₂ capture experiments of pure solid AAs, these AAs were employed as received. Diaion HP-2MG (PMMA microspheres) used as a polymer support was gained from Supelco Co. (Bellefonte, PA), which has the following physical properties: effective particle size, 0.5 mm; pore volume, 1.2 mL/g; specific surface area, 500 m²/g; average pore radius, 17 nm; density, 1.09 g/mL.

2.2.2. Immobilization of AAs into PMMA support

Immobilization of AAs into Diaion HP-2MG (PMMA) support was carried out by an impregnation-vaporization method to prepare the supported AA sorbents [1–4]. PMMA microspheres were dried at 105 °C for 1 h before use, since they include around 60 wt% of moisture. Pure AA was first dissolved in deionized water [5], and the solution was stirred at 200 rpm at room temperature for 30 min. Subsequently, a certain amount of PMMA beads was added to it, and the mixture was further stirred at 100 rpm for 2 h. After evaporation of the solvent and

then drying at 50 °C under vacuum for 24 h, AA-loaded PMMA sorbent was obtained. The supported AA sorbents with various loadings (5, 10, 20 or 30 wt%) were prepared in this way.

2.2.3. CO₂ capture experiment under dry or humidified gas flow

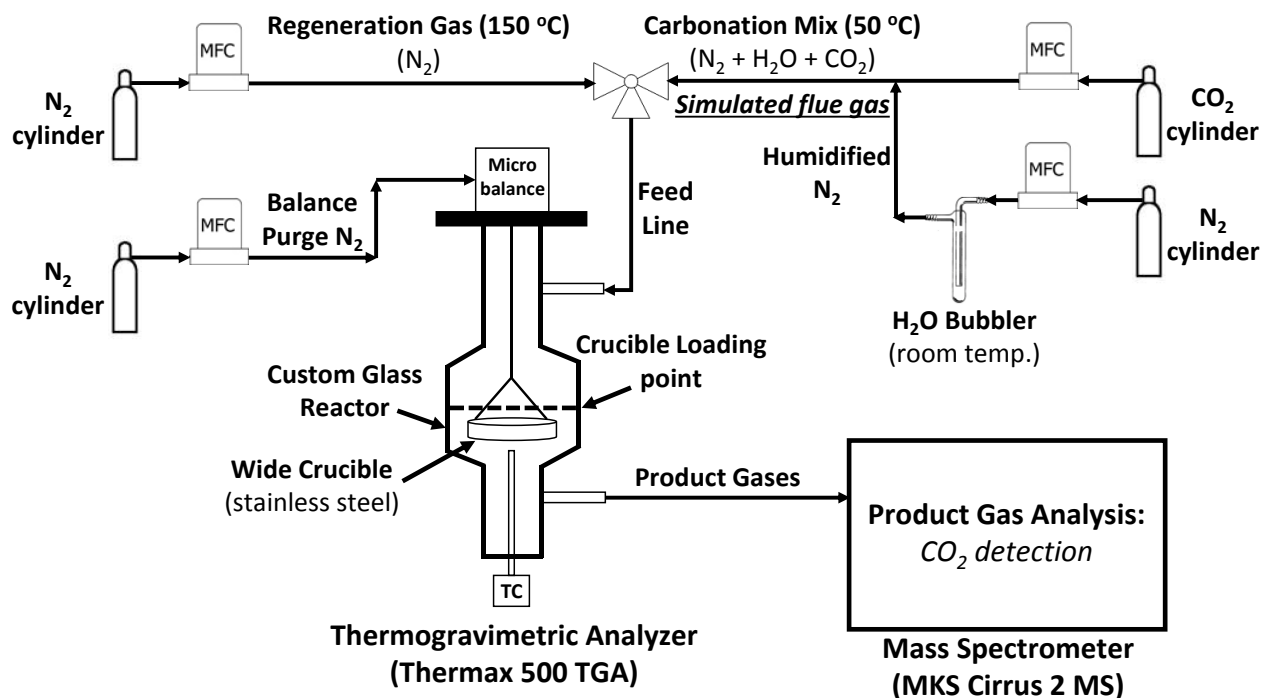


Figure 2.1. The schematic of TGA-MS analysis system [6].

One cyclic or multiple cyclic CO₂ desorption–adsorption experiments of the pure solid AAs and supported AAs were performed under dry or humidified CO₂ gas flow with an analysis system consisting of a coupled thermogravimetric analyzer (TGA) and mass spectrometer (MS) [6]. The TGA-MS analysis system can measure the gas uptakes of not only CO₂ but also H₂O of a sample during the CO₂ adsorption process under the humidified gas inlet. Figure 2.1 presents the schematic of the TGA-MS analysis system. The TGA is a modified Thermax 500 TGA, in

which its furnace and reactor system are replaced by a custom-built glass reactor system with its own independent home-built temperature control system for the required low temperature condition. MS (MKS Cirrus 2) sampling probe is connected to outlet of the glass reactor to measure CO₂ and H₂O concentrations in the outlet gases.

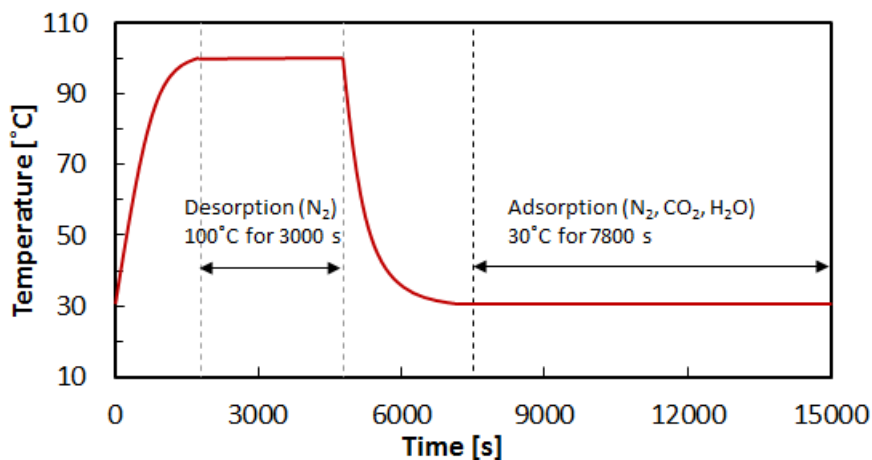


Figure 2.2. CO₂ desorption–adsorption experimental program over one cycle.

Figure 2.2 exhibits the CO₂ desorption–adsorption experimental program over one cycle. In an experiment, nearly 100 mg of a sample was loaded and spread thinly in a wide stainless steel crucible of TGA. The sample was heated to and held at 100 °C for 50 min while supplying only dry N₂ at a flow rate of 152.9 ml/min. After the temperature was decreased to and held at 30 °C taking 75 min, the inlet gas was changed to mixed gases of 2.3 vol% of CO₂ and balance N₂ in dry gas flow condition, or 2.3 vol% of CO₂, 2.1 vol% of H₂O and balance N₂ in humidified gas flow condition at a flow rate of 158.5 ml/min. The mixed gases were fed into TGA for 130 min during the CO₂ adsorption step under either gas inlet condition. The CO₂ and H₂O concentrations in the outlet gases from TGA were recorded every 6 s by the MS sampling probe. A blank run

under the dry or humidified gas flow was also conducted in the same procedure to subtract a buoyancy effect from the TGA weight change data as well as to be used for quantification of CO₂ and H₂O uptakes in humidified gas flow condition. For the experimental results under the humidified gas flow, the CO₂ and H₂O uptakes during the adsorption step were calculated from both MS and TGA data. The detailed quantification procedure is described elsewhere [6].

2.3 Results and discussion

2.3.1 CO₂ adsorption performances of pure solid AAs

Cyclic CO₂ capture experiments of pure solid Gly, Arg and Lys were first conducted under humidified CO₂ gas flow with the TGA-MS system. Figures 2.3, 2.4 and 2.5 present TGA weight changes of pure Gly, Arg and Lys during the 5 cyclic CO₂ desorption–adsorption, respectively.

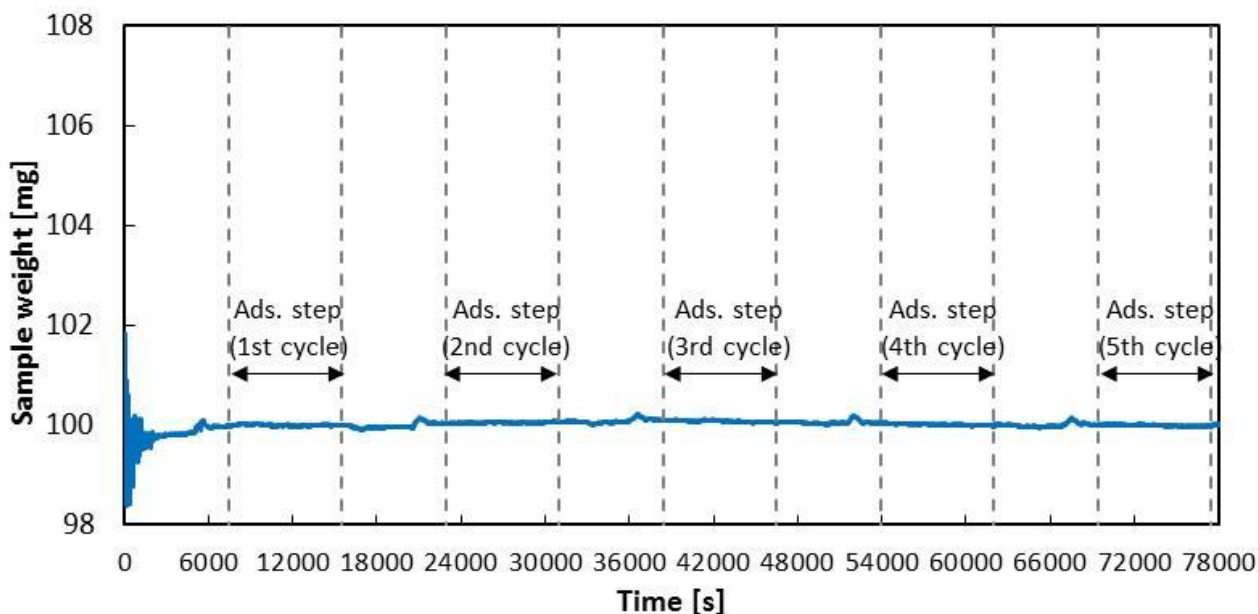


Figure 2.3. TGA weight change of pure Gly in humidified gas flow during 5 cyclic run (adsorption condition of 2.3% CO₂, 2.1% H₂O and balance N₂ flow and 30 °C).

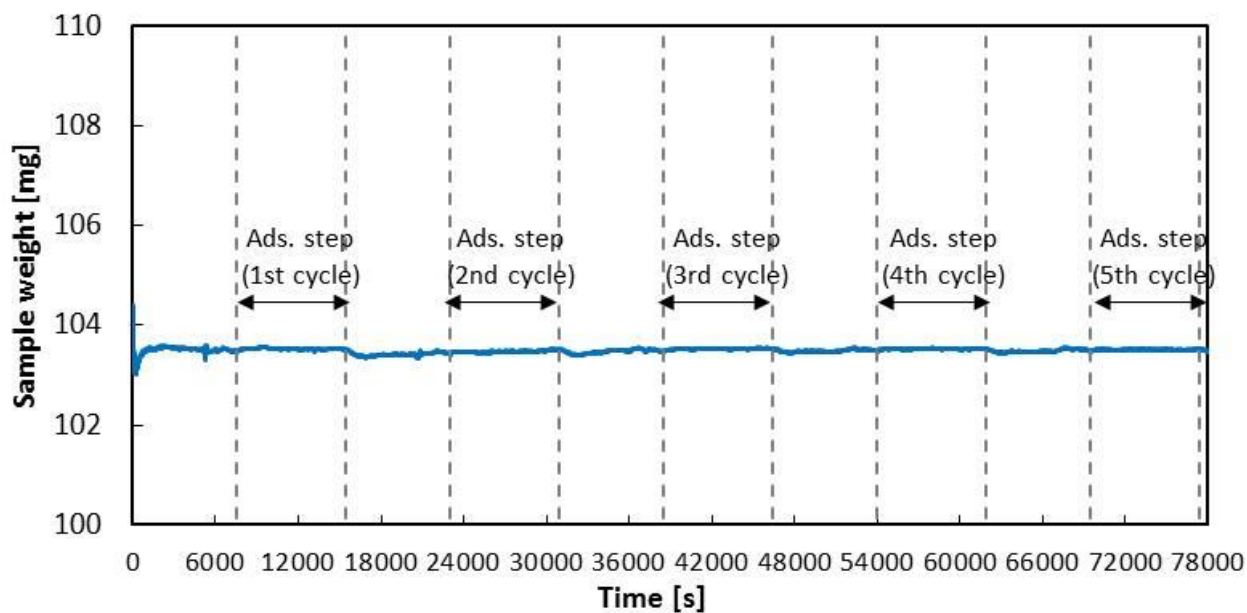


Figure 2.4. TGA weight change of pure Arg in humidified gas flow during 5 cyclic run (adsorption condition of 2.3% CO₂, 2.1% H₂O and balance N₂ flow and 30 °C).

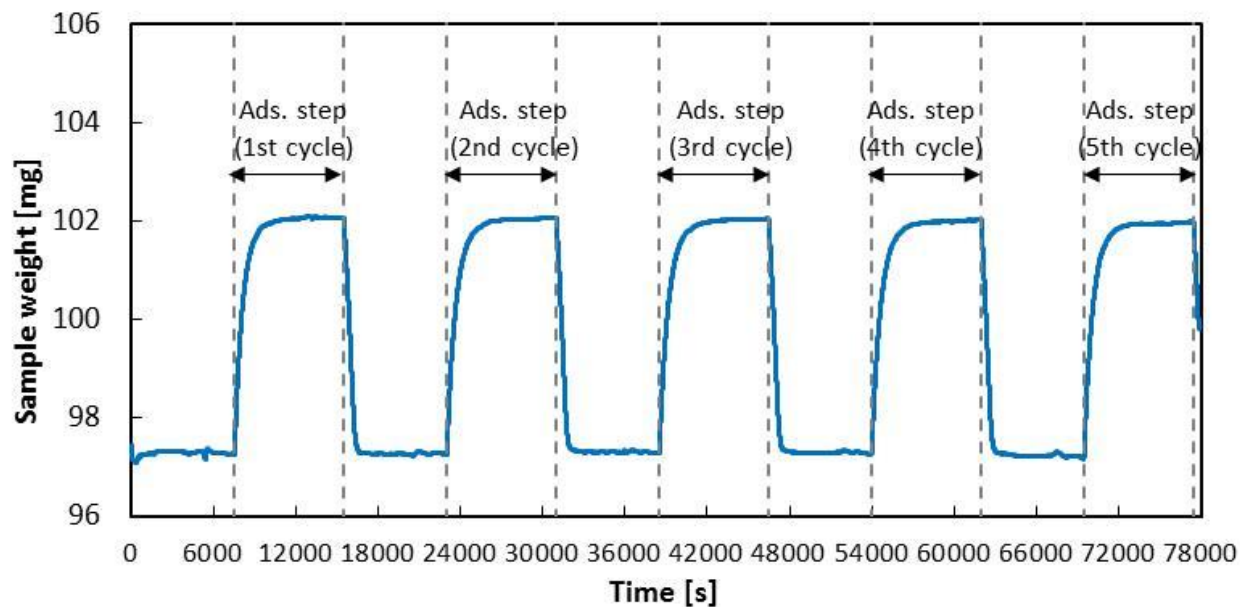


Figure 2.5. TGA weight change of pure Lys in humidified gas flow during 5 cyclic run (adsorption condition of 2.3% CO₂, 2.1% H₂O and balance N₂ flow and 30 °C).

Pure Gly and Arg showed approximately no weight gains in each adsorption step as seen from Figures 2.3 and 2.4, meaning no CO₂ uptakes on these AAs. In contrast, pure Lys exhibited a weight increase during each adsorption step (Figure 2.5). However, this weight increase was due to only H₂O uptake (without CO₂ uptake), which was identified from the quantification result using the MS data as well as TGA weight data. The same experiments for these pure AAs were carried out under dry gas inlet condition as well, but no TGA weight gains were again seen. Thus, pure AAs did not adsorb CO₂ at all under both dry and humidified CO₂ gas inlets. It is considered that no CO₂ uptake on pure AAs would be mainly because pure AAs exist in a zwitterionic state having NH₃⁺ in large particle size, which are inactive for CO₂ capture. Therefore, these AAs were next immobilized into PMMA support by impregnation to change the ionic state of their amino groups as well as to disperse the AA bulks into the support, and the CO₂ capture performances of the supported AAs were evaluated.

2.3.2 CO₂ adsorption performances of supported AA sorbents

Pure Gly, Lys and Arg were loaded on a commercial PMMA, Diaion HP-2MG, with 20 wt% loading by impregnation to prepare the supported AA sorbents. Subsequently, CO₂ adsorption experiments of these sorbents were carried out under dry gas inlet in the same run condition as above. Figure 2.6 presents the dynamic CO₂ adsorption performances at 30 °C under 2.3 % CO₂ and balance N₂ flow. Although the Gly-PMMA sorbent hardly adsorbed CO₂, the Lys- and Arg-PMMA sorbents increased their CO₂ uptakes with time; the CO₂ capture capacities reached almost the equilibrium around 10 min. Furthermore, the supported AA sorbents with different loadings (5, 10 or 30 wt% AA) were also prepared, and the same CO₂ adsorption experiments were conducted.

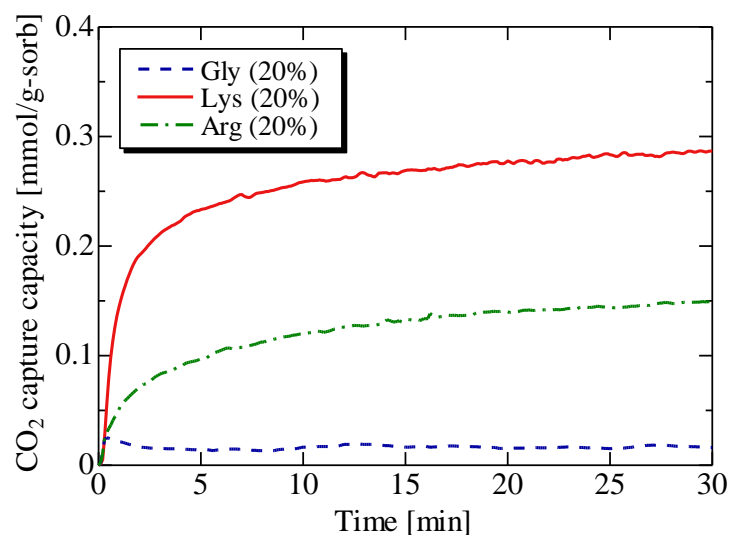


Figure 2.6. Dynamic CO₂ adsorption performances of 20 wt% AA-loaded PMMA sorbents at 30 °C under 2.3 % CO₂ and balance N₂ flow.

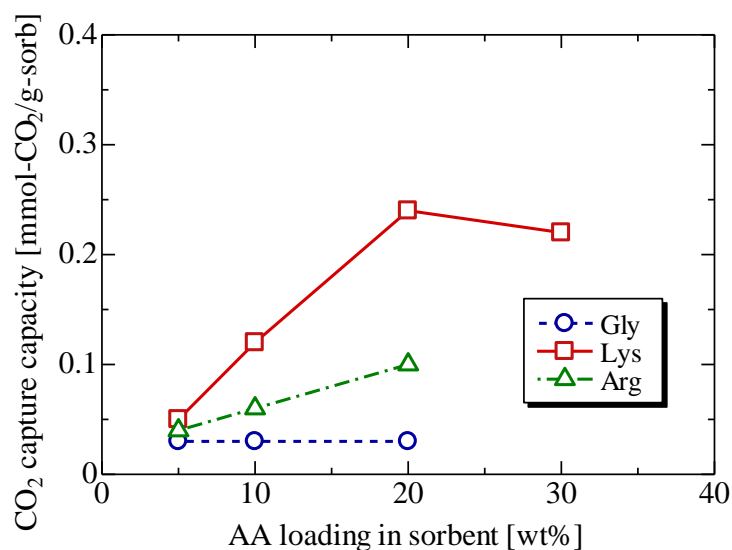


Figure 2.7. Plot of AA loadings vs. CO₂ adsorption capacity of AA-PMMA sorbents with different loadings at 30 °C under 2.3 % CO₂ and balance N₂ flow.

Figure 2.7 depicts the relationship between the AA loading and CO₂ adsorption capacity of the supported AA sorbents. Whereas the Gly-PMMA sorbent exhibit only a few amount of CO₂ uptake at any loadings again, the Gly-PMMA sorbents increased the capacities with higher loadings. Lys and Arg have additional amino groups in their side chains (Table 2.1), leading to stronger basicity than other AAs. The enlargement of capacities of the supported Lys and Arg sorbents with the loading can be because more fractions of their amino groups changed into active NH₂ from NH₃⁺ in the zwitterionic state, when Lys and Arg were impregnated with PMMA with higher loadings. Lys-PMMA sorbent exhibited greater capacity than Arg-PMMA sorbent at any loadings, although Arg has more amino groups than Lys. This implies that the side chain structures of AAs might also influence the reactivity with CO₂, not only the number of their amino groups, as the side chain structures are quite different between Lys and Arg. On the other hand, little CO₂ uptake on the supported Gly sorbent at any loadings suggests that the amino group in Gly remained as inactive NH₃⁺, even when impregnating Gly with PMMA with higher loadings, since Gly has no additional amino groups in its side chain. It was found from these results that activating amino groups in AAs, while dispersing into a porous support, is very important in developing efficient AA-based CO₂ adsorbents.

One of the ways to activate amino groups in AAs is synthesizing amino acid anion-functionalized ionic liquids (AAILs), since the amino groups (NH₃⁺) can be deprotonated into NH₂ in the preparation process of AAILs [4,7]. In the next chapter, CO₂ adsorption of supported AAILs is studied and compared with those of supported AAs.

2.4 Conclusions

CO₂ capture experiments of pure solid AAs were first conducted in dry and humidified CO₂

flow conditions using Gys, Lys and Arg. However, these pure AAs did not exhibit any CO₂ uptakes. Therefore, the AAs were next immobilized into a commercial polymer support, PMMA, by impregnation in order to improve the CO₂ capture performances. The same CO₂ adsorption experiments were then carried out using the supported AA sorbents. As a result, the supported Lys and Arg increased their CO₂ capture capacities with higher loadings, whereas the supported Gly hardly adsorbed CO₂ at any loadings. These results suggested the importance to activate amino groups in AAs from NH₃⁺ in the zwitterionic state into NH₂ for improving the CO₂ capture performances.

2.5 References

- [1] J. Zhang, S. Zhang, K. Dong, Y. Zhang, Y. Shen, X. Lv, Supported absorption of CO₂ by tetrabutylphosphonium amino acid ionic liquids, *Chem. Eur. J.* 12 (2006) 4021–4026.
- [2] J. Ren, L. Wu, B.G. Li, Preparation and CO₂ sorption/desorption of N-(3-aminopropyl)aminoethyl tributylphosphonium amino acid salt ionic liquids supported into porous silica particles, *Ind. Eng. Chem. Res.* 51 (2012) 7901–7909.
- [3] X. Wang, N.G. Akhmedov, Y. Duan, D. Luebke, B. Li, Immobilization of amino acid ionic liquids into nanoporous microspheres as robust sorbents for CO₂ capture, *J. Mater. Chem. A.* 1 (2013) 2978–2982.
- [4] X. Wang, N.G. Akhmedov, Y. Duan, D. Luebke, D. Hopkinson, B. Li, Amino acid-functionalized ionic liquid solid sorbents for post-combustion carbon capture, *ACS Appl. Mater. Interfaces.* 5 (2013) 8670–8677.
- [5] B. Jiang, X. Wang, M.L. Gray, Y. Duan, D. Luebke, B. Li, Development of amino acid and amino acid-complex based solid sorbents for CO₂ capture, *Appl. Energy.* 109 (2013) 112–

118.

- [6] A. Jayakumar, A. Gomez, N. Mahinpey, Post-combustion CO₂ capture using solid K₂CO₃: Discovering the carbonation reaction mechanism, *Appl. Energy*. 179 (2016) 531–543.
- [7] H. Ohno, K. Fukumoto, Amino acid ionic liquids, *Acc. Chem. Res.* 40 (2007) 1122–1129.

CHAPTER 3: Effect of water vapor on CO₂ sorption-desorption behaviors of supported amino acid ionic liquid sorbents on porous microspheres

3.1 Presentation of the article

This paper first presents a comparative investigation on CO₂ capture performances of supported amino acid ionic liquids (AAILs) with those of supported pure amino acids (AAs) under a dry CO₂ inlet condition, using Gly, Lys and Arg. 1-Ethyl-3-methylimidazolium amino acids ([EMIM][AAs]) were synthesized and employed as AAILs, and they were immobilized into a commercial polymer support to prepare the supported AAIL sorbents. The experimental results implied that most fractions of the amino groups in AAs can be deprotonated from NH₃⁺ to active NH₂ in the synthetic process of AAILs, as the supported AAIL sorbents exhibited greater CO₂ adsorption capacities than the corresponding AA sorbents with the same AA contents.

Next, this paper provides different CO₂ capture performances between supported AAIL and AA sorbents in the presence of water vapor, compared with the absence of water vapor. Supported Lys and Arg increased their CO₂ adsorption capacities under a humidified CO₂ flow condition, similarly to supported amine sorbents. On the other hand, the presence of water vapor reduced the capacities of supported [EMIM][Gly] and [EMIM][Lys]. Thus, water vapor exerted a negative impact on CO₂ adsorption of these supported AAIL sorbents, in contrast to that of supported amine sorbents.

Almost all of this work was carried out by Yusuke Uehara. Dr. Davood Karami assisted in setting up an anion-exchange column for the preparation of AAILs and in ordering the chemicals needed for the experiments. Dr. Nader Mahinpey supervised the whole study.

Effect of water vapor on CO₂ sorption-desorption behaviors of supported amino acid ionic liquid sorbents on porous microspheres

This article has been published in Industrial & Engineering Chemistry Research 56 (2017) 14316–14323.

*Yusuke Uehara, Davood Karami, and Nader Mahinpey**

Department of Chemical and Petroleum Engineering, Schulich School of Engineering, University of Calgary, Calgary, AB T2N 1N4, Canada

3.2 Abstract

Immobilizing amino acid ionic liquids (AAILs) into a porous support is a promising way to fabricate robust solid sorbents with high capacities for CO₂ capture. One of important factors to be evaluated toward the practical use is the impact of water vapor in inlet gases on the CO₂ capture performance as real flue gases contain some fraction of water vapor. In this study, CO₂ sorption-desorption experiments of supported 1-ethyl-3-methylimidazolium amino acid ([EMIM][AA]) IL sorbents on porous microspheres were conducted under dry and humidified CO₂ inlet conditions using a TGA-MS analysis system, and their outcomes were compared with those of supported amino acids (AA) sorbents. The presence of water vapor changed the CO₂ sorption behaviors depending on the sorbent types. In humidified CO₂ inlet, the CO₂ capture capacities of supported [EMIM][glycine] and [EMIM][lysine] decreased as the adsorbed water hindered their reaction with CO₂, whereas the CO₂ capture of those with supported lysine and arginine increased, since water content exerted a positive impact on the CO₂ capture behavior.

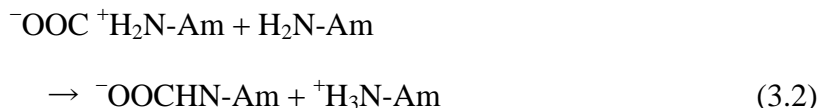
3.3 Introduction

It is widely recognized that carbon dioxide (CO_2) is a major greenhouse gas affecting global climate change. Post-combustion CO_2 capture is one of crucial technologies to reduce CO_2 emitted from industries such as coal- and gas-fired power plants. Aqueous amine scrubbing is a conventional CO_2 capture technology understood well and extensively used with an operating experience of over 80 years [1]. However, it also has some disadvantages such as equipment corrosion, high regeneration energy consumption due to the presence of water and requirement of large absorber [2,3]. Therefore, it is expected to develop novel sorbents to overcome those drawbacks.

Solid sorbents are expected to become alternatives to liquid sorbents like amine solution since solid sorbents can decrease the regeneration energy requirement because of the absence of water [3], leading to reduction in the equipment installation area. Chemical adsorbents will be more suitable as solid sorbents than physical adsorbents because physical adsorbents suffer from low selectivity and sensitivity to moisture that pose considerable complications in capturing only CO_2 from combustion flue gases consisting of several gas components with water vapor [3]. As one kind of chemical adsorbents, amino acids (AAs) are promising choices since AAs have amino ($-\text{NH}_2$) groups in their structures like amines, which can react with CO_2 to adsorb CO_2 chemically [4–6]. Also, AAs show other advantages for CO_2 removal over amines in that they are environmental friendly [7] and have lower vapor pressures than amines [8].

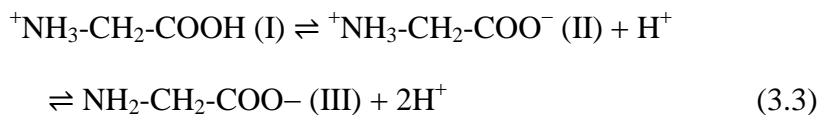
It is assumed that reaction of AA with CO_2 proceed through a zwitterion mechanism with two steps [6,8]. The first step is that 1 mole of CO_2 reacts with 1 mole of NH_2 species of amino group in AA to form a zwitterion (reaction 3.1), and the second step is that 1 mole of the produced

zwitterion further reacts with 1 mole of the NH_2 species in AA to form a carbamate anion (reaction 3.2). Thus, in this mechanism NH_2 species in AA can be the active species to capture CO_2 [5], and 1 mole of CO_2 reacts with 2 moles of the NH_2 species comprehensively.



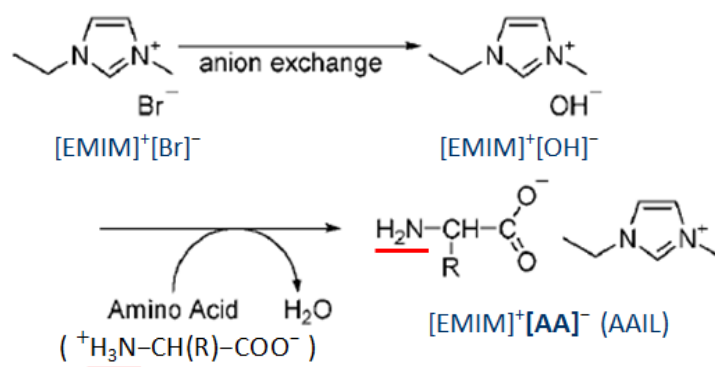
(-Am: $-\text{CH(R)}-\text{COOH}$)

However, the amino groups in AA can also exist as NH_3^+ , not only NH_2 , and both the chemical forms and distribution of amino and carboxylic ($-\text{COOH}$) groups in AAs depend on the pH value. For example, in the case of glycine (Gly), which is the simplest type of α -amino acids (α -AAs), change in the chemical forms with the pH range is represented by reaction 3.3 [8,9]. Thus, for AAs to capture CO_2 chemically, NH_3^+ species in their structures will have to be changed into the NH_2 species.



One of options to change the NH_3^+ into the NH_2 as the active species for CO_2 removal is utilizing amino acid ionic liquids (AAILs). AAILs were developed from 20 types of α -AAs by Fukumoto et al. for the first time [10]. They prepared AAILs with 1-ethyl-3-methylimidazolium cation ($[\text{EMIM}]^+$) by a neutralization method. In this preparation process, NH_3^+ species in AA can be deprotonated into the NH_2 species (Scheme 3.1) [11]. Ionic liquids (ILs) have very unique properties such as negligible vapor pressure, high thermal stability and tunable physicochemical

properties, all of which can also become benefits for uptake of CO₂ [11–14]. In contrast, ILs also have a disadvantage of very high viscosity causing enormous gas diffusion resistance for a gas-liquid reaction. Therefore, it will be a better way to immobilize an AAIL into a porous support with a large surface area and to use it as a solid sorbent for CO₂ capture in order to improve both the mass transfer and dispersion of active sites of the AAIL.



Scheme 3.1. Preparation process of AAILs with [EMIM]⁺ by neutralization method [11].

Recently, some research groups have conducted CO₂ capture experiments of AAILs supported on a porous material [14–17]. According to Wu's and Li's groups, L-lysine (Lys) and Gly based IL supported sorbents showed better CO₂ capture performances than other AA types [14–16]. On the other hand, L-arginine (Arg) and histidine (His) based IL supported sorbents exhibited low CO₂ capture capacities, although they have basic side chains with more amino groups than others. From their results, it is considered that Lys and Gly have a potential to become attractive alternatives to amines as solid sorbents for CO₂ removal. However, the effect of water vapor in inlet gases on the CO₂ capture performance should be evaluated toward the practical utilization since actual flue gases contain some fraction of water vapor [18]. In the case of supported amines,

it has been reported by several groups that water vapor in flow gases exerts a catalytic effect on the reaction between the amine and CO₂ to enhance the amount of CO₂ uptake [18–24]. In contrast, no study have examined CO₂ capture tests of supported AAILs under the presence of water vapor in inlet gases so far, although there is a report that water content contained in supported AAIL sorbents decreased CO₂ sorption capacity [14]. Therefore, the impact of water vapor on CO₂ sorption-desorption behaviors of supported AAILs under a simulated flue gas condition is mainly evaluated in this study. Furthermore, the CO₂ capture performances of supported AAILs are compared with those of supported AAs under both dry and humidified CO₂ flow conditions in terms of AA type and loading in the sorbent.

3.4 Experimental section

3.4.1 Materials

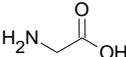
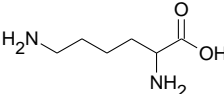
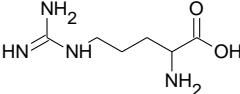
Gly, 99%, Lys, 98%, Arg, ≥98%, 1-ethyl-3-methylimidazolium bromide ([EMIM][Br], ≥98%) and anion exchange resin (Amberlite IRA-402 OH) were purchased from Alfa Aesar Co. (Ward Hill, MA). The molecular structures of the AAs are listed in Table 3.1. Polymethylmethacrylate (PMMA) microspheres (Diaion HP-2MG) were purchased from Supelco Co. (Bellefonte, PA).

3.4.2 Synthesis of [EMIM][AA]

[EMIM][Gly], [EMIM][Lys] and [EMIM][Arg] were prepared by a neutralization method [10,15,16]. In brief, [EMIM][Br] was dissolved in deionized water to prepare the aqueous solution and passed through an anion exchange resin (Amberlite IRA-402 OH) column 5 times to prepare the [EMIM][OH] solution. The [EMIM][OH] solution was then added slowly to a slightly excess equimolar AA aqueous solution. The mixture was stirred at 400 rpm at room

temperature for 24 h. After evaporation of water at around 45 °C and then drying at 50 °C under vacuum for 24 h, a crude product including the desired AAIL and unreacted AA was obtained. Ethanol was added to the crude product, and the mixture was centrifuged at 3800 rpm for 15 min to remove the insoluble AA from it. After drying at 80 °C under vacuum for 24 h, [EMIM][AA] was finally obtained in an overall yield of ~70%.

Table 3.1. Molecular structures of AAs.

AA type		structure
glycine	(Gly)	
L-lysine	(Lys)	
L-arginine	(Arg)	

3.4.3 Preparation of supported [EMIM][AA] or AA on PMMA

Immobilization of [EMIM][AA] into PMMA was carried out by an impregnation-vaporization method [14–17]. PMMA microspheres were dried at 105 °C for 1 h before use as they include around 60 wt% of moisture. Briefly, [EMIM][AA] was dissolved in aqueous ethanol solution at a concentration of 50 mg/mL [15,16], and the mixture was stirred at 200 rpm at room temperature for 30 min. Then, PMMA beads were added to it, and the suspension was further stirred at 100 rpm for 2 h. After evaporation of the solvent and then drying at 50 °C under vacuum for 24 h, supported [EMIM][AA] on PMMA was obtained. Immobilization of AA into PMMA was carried

out by the same impregnation-vaporization way using deionized water as a solvent [25], instead of aqueous ethanol solution. [EMIM][AA]- and AA-PMMA sorbents with various loadings (0, 5, 10, 20, 30, 40, 50 or 70 wt%) were prepared.

3.4.4 Characterization

N₂ adsorption-desorption at −196 °C was conducted for pure PMMA, AA-PMMA and [EMIM][AA] sorbents using a surface area analyzer, Micromeritics ASAP 2020, to measure surface areas and pore volumes of these sorbents by the Brunauer-Emmet-Teller (BET) and Barrett–Joyner–Halenda (BJH) methods. Before the analysis, each sample was degassed at 100 °C for 180 min. Also, thermal stabilities of as-prepared [EMIM][AA] and pure AA as well as the above samples were analyzed under N₂ atmosphere with a heating rate of 10 °C/min using Perkin-Elmer Pyris-STA6000 thermogravimetric analyzer (TGA).

3.4.5 CO₂ capture experiment

CO₂ capture tests of [EMIM][AA]-PMMA and AA-PMMA sorbents were conducted using a TGA-MS analysis system. The equipment configuration is provided in our recent paper [26]. Around 100 mg of sample was loaded in a wide stainless steel crucible of TGA while spreading them thinly to form almost the mono- or bi-layer in the crucible. The sample was heated to and held at 100 °C for 50 min (3000 s) under dry N₂ flow condition for the desorption step. Then, after the temperature was decreased to 30 °C in the dry N₂, the inlet gas was switched to mixed gases of CO₂ with dry or humidified N₂ and fed into TGA for 130 min (7800 s) for the adsorption step. The flow gas components in the adsorption step consisted of CO₂ (2.3%) and balance N₂ for the dry CO₂ condition or CO₂ (2.3%), H₂O (2.1%) and balance N₂ for the humidified CO₂ condition, respectively. 2.3 % of CO₂ was used as enough low CO₂

concentration to avoid additional influence of physisorption on evaluation of the sorbents [21]. Also, the combination of 2.3% of CO₂ and 2.1% of water vapor was adopted for the humidified gas flow condition, considering that actual flue gas contains almost equimolar amounts of CO₂ and H₂O. The MS sampling probe connected to the outlet of the TGA monitored CO₂ concentration in the outlet gases during the adsorption step [26]. Both the data of TGA and MS were recorded every 6 s as a time step (Δt). These desorption-adsorption steps were repeated 5 times when carrying out the cycling tests. Also, blank runs were conducted in the same way for both dry and humidified CO₂ inlet conditions, respectively, to eliminate a buoyancy effect on the data of TGA weight change as well as to be used for quantification of CO₂ and H₂O adsorbed under the humidified CO₂ flow condition as described later.

3.4.6 Quantification of CO₂ and H₂O adsorbed in humidified CO₂ flow condition

The amount of CO₂ and H₂O captured during the adsorption step in the humidified CO₂ inlet condition was calculated using the data of MS as well as TGA since the TGA data contains weight changes due to uptake of H₂O, not only CO₂ [21,26]. The quantification procedure is described elsewhere [26].

3.4.7 Temperature-programmed desorption (TPD)

Temperature-programmed desorption (TPD) tests were also conducted to evaluate and compare desorption behaviors of the sorbents under the dry and humidified CO₂ flow conditions. The experimental condition of TPD is similar with but has some differences from the CO₂ capture tests described above. One of the differences is that duration of the adsorption step was 30 min, not 130 min. In addition, after the adsorption step, the inlet gas was switched to pure N₂ as a purge gas, and the TGA reactor temperature was held at 30 °C for 10 min and then increased

to 170 °C at a rate of 5 °C/ min. The concentration of CO₂ released from the sample in this step was recorded into the MS and evaluated from the MS data as mentioned later.

3.5 Results and discussion

3.5.1 Characterization

In this study, commercial PMMA microspheres, Diaion HP-2MG, were used as a porous support. The BET surface areas and BJH adsorption cumulative pore volumes of PMMA, [EMIM][Lys]-PMMA with 10 wt% and 50 wt% loadings, and Lys-PMMA with 5 wt% and 20 wt% loadings are listed in Table S3.1 of the Supporting Information. It is found that PMMA has a high surface area of 527 m²/g and large pore volume of 1.12 cm³/g, which are beneficial pore properties as a support material. When [EMIM][Lys] IL or Lys was immobilized into PMMA microspheres by an impregnation method, the surface area and pore volume reduced with the loadings, as expected.

Thermal stabilities of PMMA, [EMIM][Lys]-PMMA with different loadings, as-prepared [EMIM][Lys], Lys-PMMA with different loadings and pure Lys were also evaluated through a thermogravimetric analysis under N₂ atmosphere with a heating rate of 10 °C/min. The TGA curves of PMMA, [EMIM][Lys]-PMMA (10 and 50 wt%) and as-prepared [EMIM][Lys] are shown in Figure S3.1, and those of PMMA, Lys-PMMA (5 and 20 wt%) and pure Lys are depicted in Figure S3.2 (Supporting Information). The thermal decompositions of pure PMMA, [EMIM][Lys] and Lys occurred from around 240, 190 and 220 °C, respectively. The start temperature of the thermal decompositions of [EMIM][Lys]-PMMA and Lys-PMMA sorbents were close to that of pure [EMIM][Lys] and Lys. However, the thermal decomposition rates of [EMIM][Lys]-PMMA and Lys-PMMA sorbents were lower than those of pure [EMIM][Lys], Lys

and PMMA. It could be because physical interactions between PMMA and [EMIM][Lys] or Lys immobilized leading to higher thermal stabilities of these sorbents.

3.5.2 Comparison of CO₂ capture performance of [EMIM][AA]- and AA-PMMA under dry CO₂ flow

First, CO₂ adsorption tests of [EMIM][Gly]-, [EMIM][Lys]- and [EMIM][Arg]-PMMA sorbents with the loading of 50 wt% were conducted in the dry CO₂ flow condition (2.3% CO₂ and balance N₂). Similarly, CO₂ adsorption experiments of each AA-PMMA sorbent with the loading of 20 wt% were also carried out. CO₂ adsorption behaviors of those sorbents with time are shown in Figure 3.1.

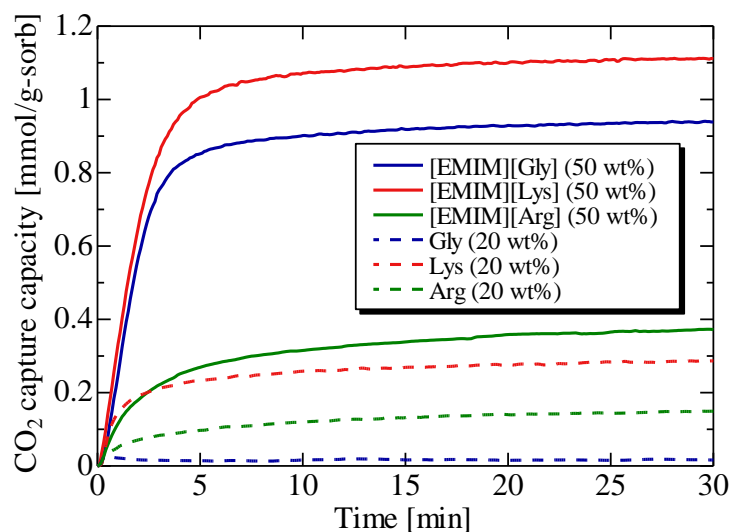


Figure 3.1. CO₂ adsorption behaviors of [EMIM][AA]-PMMA and AA-PMMA sorbents under dry CO₂ flow (2.3% CO₂ and balance N₂) with time.

It is found that CO₂ capture capacities of both the supported [EMIM][AA] and AA sorbents reached almost the equilibrium within 10 min regardless of the AA type. For the Lys-PMMA

sorbent, three repetitions of the experiments were run for the error analysis. Each CO₂ sorption behavior for the three repetitive tests is depicted in Figure S3.3a of the Supporting Information. The three results showed a very similar capture behavior but also had a certain amount of discrepancy with each other due to both systematic and random errors. Fluctuations in concentrations of N₂ and CO₂ in inlet gases, flow gas rates and reactor temperature, vibration of the crucible of TGA and uniformity of the prepared sorbent are considered as factors for the systematic error. The average and standard deviation for CO₂ capture capacity of the Lys-PMMA sorbent were 0.24 and 0.01, respectively, as shown in Table S3.2 of the Supporting Information. Table 3.2 summarizes all the data of CO₂ capture capacity along with literature values conducted with the same loadings but at different temperature and CO₂ inlet concentration. The data of CO₂ uptake of pure PMMA (i.e. 0 wt% loading) is also listed in Table 3.2 with the corresponding literature value, which presents difference in the capacities by the physical adsorption. As seen from Table 3.2, the order of CO₂ capture capacities of [EMIM][AA]-PMMA sorbents was Lys > Gly > Arg, and that of AA-PMMA sorbents was Lys > Arg > Gly, which are the same orders as other groups' results, respectively [15,16]. However, the amounts of CO₂ uptake of these supported sorbents in this work were lower than the literature values. It will be mainly due to a huge difference in CO₂ concentration in the inlet gas [20,21]. Sayari's group has reported that CO₂ adsorption capacities of supported amines increased as CO₂ concentration in the inlet gas increased [20,21]. They considered that CO₂ adsorption of supported amine sorbents under higher CO₂ inlet concentration involve not only chemisorption, but also physisorption, leading to enhancement in the capacity. Thus, physisorption would affect the capacities of these supported AA and AAIL sorbents at higher CO₂ inlet concentration as well as pure PMMA (Table 3.2).

Table 3.2. CO₂ sorption capacities of [EMIM][AA]-PMMA and AA-PMMA sorbents under dry CO₂ inlet condition (2.3% CO₂ and balance N₂) along with corresponding literature values.

type	M.W.	loading	AA content	ads. <i>T</i>	C _{CO₂} in	capacity	ref.
		in sorb.	in sorb.		inlet gases		
	[g/mol]	[wt%]	[mmol/g-sorb]	[°C]	[%]	[mmol/g-sorb]	
[EMIM][Gly]	185.2	50	2.7	30	2.3	0.88	this work
[EMIM][Gly]	185.2	50	2.7	40	100	1.53	15, 16
[EMIM][Lys]	256.4	50	2.0	30	2.3	1.06	this work
[EMIM][Lys]	256.4	50	2.0	40	100	1.67	16
[EMIM][Arg]	284.4	50	1.8	30	2.3	0.28	this work
[EMIM][Arg]	284.4	50	1.8	40	100	1.01	15, 16
Gly	75.1	20	2.7	30	2.3	0.03	this work
Lys	146.2	20	1.4	30	2.3	0.24	this work
Arg	174.2	20	1.1	30	2.3	0.10	this work
Arg	174.2	20	1.1	40	100	0.50	25
PMMA	-	0	0	30	2.3	0.02	this work
PMMA	-	0	0	40	100	0.50	15

CO₂ sorption experiments of these supported sorbents with different loadings (10, 30, 40 and 70 wt% for AAILs, and 5, 10 and 30 wt% for AAs) were carried out, as well. The CO₂ capture capacities of the supported AAILs and AAs with the various loadings are summarized in Tables S3.3 and S3.4 of the Supporting Information, respectively. The relationship between CO₂ capture capacity and AA content in the sorbent is depicted in Figure 3.2.

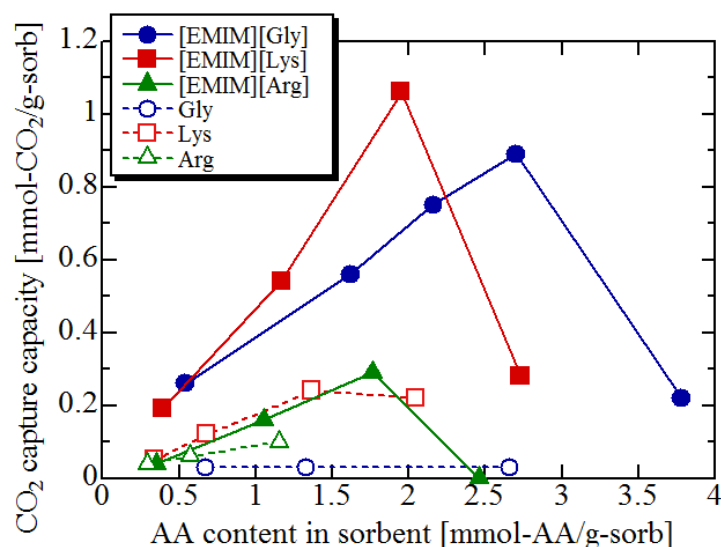


Figure 3.2. Relationship between AA content in the supported sorbent and CO₂ capture capacity obtained under the dry CO₂ flow (2.3% CO₂ and balance N₂).

The capacity of Gly-PMMA sorbent, among all samples, did not increase with increase in the AA content in the sorbent, as indicated in Figure 3.2. This indicates that the amine group in Gly immobilized into PMMA by the impregnation method will exist as NH₃⁺ species rather than NH₂, in which the former one is much less active for reaction with CO₂ [8]. In contrast, the capacities of Lys- and Arg-PMMA sorbents enhanced with the loadings of AA until a certain AA content in the sorbent. This trend can be explained by the fact that Lys and Arg have basic side chains with

more amino groups (Table 3.1), most of which would exist as NH_2 species, not NH_3^+ . The CO_2 uptake of [EMIM][Gly]-PMMA increased with AA content in the sorbent as well as [EMIM][Lys]- and [EMIM][Arg]-PMMA, unlike Gly-PMMA. This implies that most fraction of the amino group in Gly would be deprotonated into NH_2 from NH_3^+ in the preparation process of [EMIM][AA] (Scheme 3.1). However, [EMIM][Arg]-PMMA showed much lower enhancement in the capacity compared with the original AA (i.e. Arg) than [EMIM][Gly]- and [EMIM][Lys]-PMMA, although Arg has the most amount of amino groups among all α -AAs and unsupported (pure) [BMIM][Arg] IL had the highest CO_2 absorption performance in study results by Sistla et al. [27]. In addition, the capacity of Arg was also lower than Lys. On the other hand, Lys displayed the best CO_2 sorption performance in the forms of both the original AA and [EMIM][AA] immobilized into PMMA. The CO_2 uptake of all the sorbents other than Gly-PMMA increased almost linearly with the AA content but decreased from a certain AA content, as found in Figure 3.2. It will suggest that the amounts of NH_2 species in those sorbents enhanced in proportion to the loadings, while too higher loadings caused blockage of the pores of PMMA microspheres, leading to the reduced capacity [15,16,25]. The supported AAIL and AA sorbents exhibited their best CO_2 capture capacities with the loadings of 50 wt% and 20 wt%, respectively (Tables S3.3 and S3.4 in the Supporting Information). The capacity of each sorbent in units of mol/mol-AA are also listed in Tables S3.3 and S3.4. Comparing Table S3.3 with S3.4, it is found that even in units of mol/mol-AA, the capacities of [EMIM][Gly]- and [EMIM][Lys]-PMMA sorbents are much higher than those of the corresponding AA-PMMA sorbents at any AA contents, except for overloadings.

3.5.3 Effect of water vapor in inlet gases on CO₂ sorption of [EMIM][AA]- and AA-PMMA

Next, CO₂ sorption experiments were carried out in the humidified CO₂ flow condition (2.3% CO₂, 2.1% H₂O and balance N₂). [EMIM][AA]-PMMA sorbents with the loadings of 50 wt% and AA-PMMA sorbents with the loadings of 20 wt% were used since they demonstrated the best CO₂ capture performance in dry gas flow condition, respectively. For the Lys-PMMA sorbent, three repetitive runs were conducted for calculating the error analysis, as well. The CO₂ sorption behaviors for the three repetitive runs are shown in Figure S3.3b of the Supporting Information. These behaviors in the humidified CO₂ flow condition displayed more fluctuation noises than the dry CO₂ flow condition (Figure S3.3a), which are due to more error factors. That is, fluctuations in concentration of water vapor in inlet gases and outlet gas concentrations detected by MS are considered as additional factors for the systematic error as well as other factors described above. Nevertheless, the CO₂ capture capacities for these runs converge to approximately the same value. The average and standard deviation of the CO₂ capture capacities for the three runs were 0.36 and 0.01, respectively (Table S3.2 in the Supporting Information). The data of CO₂ sorption capacities for all the sorbents obtained under both the dry and humidified CO₂ inlet conditions are listed in Table 3.3. The influence of water vapor on CO₂ capture capacities of these supported AA and AAIL sorbents was different with the sorbent type, as seen from Table 3.3. In the presence of water vapor, the capacities of both [EMIM][Gly]-PMMA and Gly-PMMA decreased, while those of both [EMIM][Arg]-PMMA and Arg-PMMA increased. On the other hand, water vapor reduced the capacity of [EMIM][Lys]-PMMA but enhanced that of Lys-PMMA. These differences imply that imidazolium cation of the AAILs and side chains of the AAs might affect the CO₂ sorption behavior in the humid CO₂ inlet condition.

Table 3.3. Comparison of CO₂ sorption capacities of [EMIM][AA]-PMMA and AA-PMMA sorbents under dry CO₂ (2.3% CO₂ and balance N₂) and humidified CO₂ (2.3% CO₂, 2.1% H₂O and balance N₂) conditions.

type	loading	capacity	
		[mmol/g-sorb]	
	in sorb. [wt%]	dry	humid
[EMIM][Gly]	50	0.88	0.57
[EMIM][Lys]	50	1.06	0.96
[EMIM][Arg]	50	0.28	0.34
Gly	20	0.03	0.02
Lys	20	0.24	0.36
Arg	20	0.10	0.25
PMMA	0	0.02	0.02

Figures 3.3a and b present the amounts of CO₂ and H₂O uptakes of [EMIM][AA]-PMMA (the loadings of 50 wt%) and AA-PMMA (20 wt%) sorbents during the adsorption step in dry and humidified CO₂ conditions, respectively. Figure 3.2 exhibited that the [EMIM][AA]-PMMA had higher CO₂ sorption capacity than the corresponding AA-PMMA with the same AA contents in the sorbents under the dry CO₂ inlet condition. Comparing Figure 3.3a with 3.3b also displays that the supported [EMIM][AA] sorbents adsorbed much larger amounts of H₂O as well as CO₂ than the supported AA sorbents under the humid CO₂ condition. This is due to higher

hygroscopicities as well as higher loadings of [EMIM][AAs] in the supported AAIL sorbents than AAs in the supported AA sorbents [11].

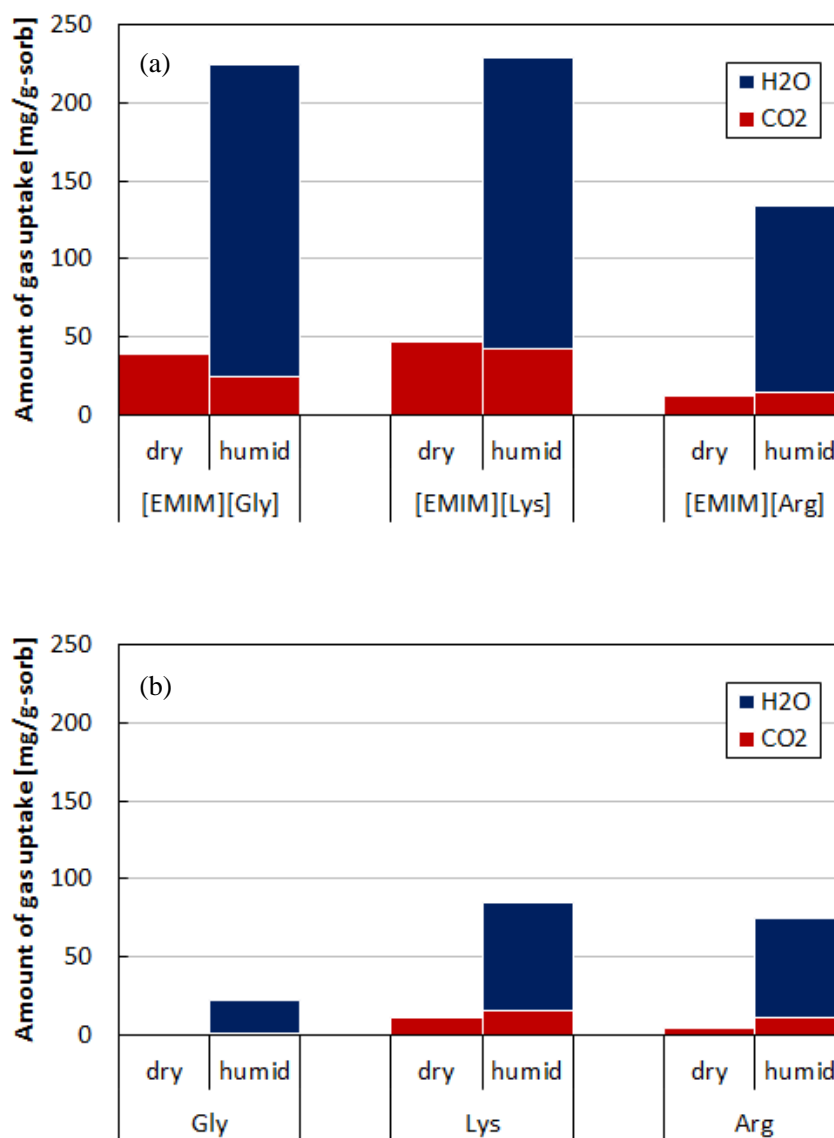


Figure 3.3. Amounts of CO₂ and H₂O uptakes of (a) [EMIM][AA]-PMMA (50 wt%) and (b) AA-PMMA (20 wt%) sorbents during the adsorption step in dry and humidified CO₂ conditions, respectively.

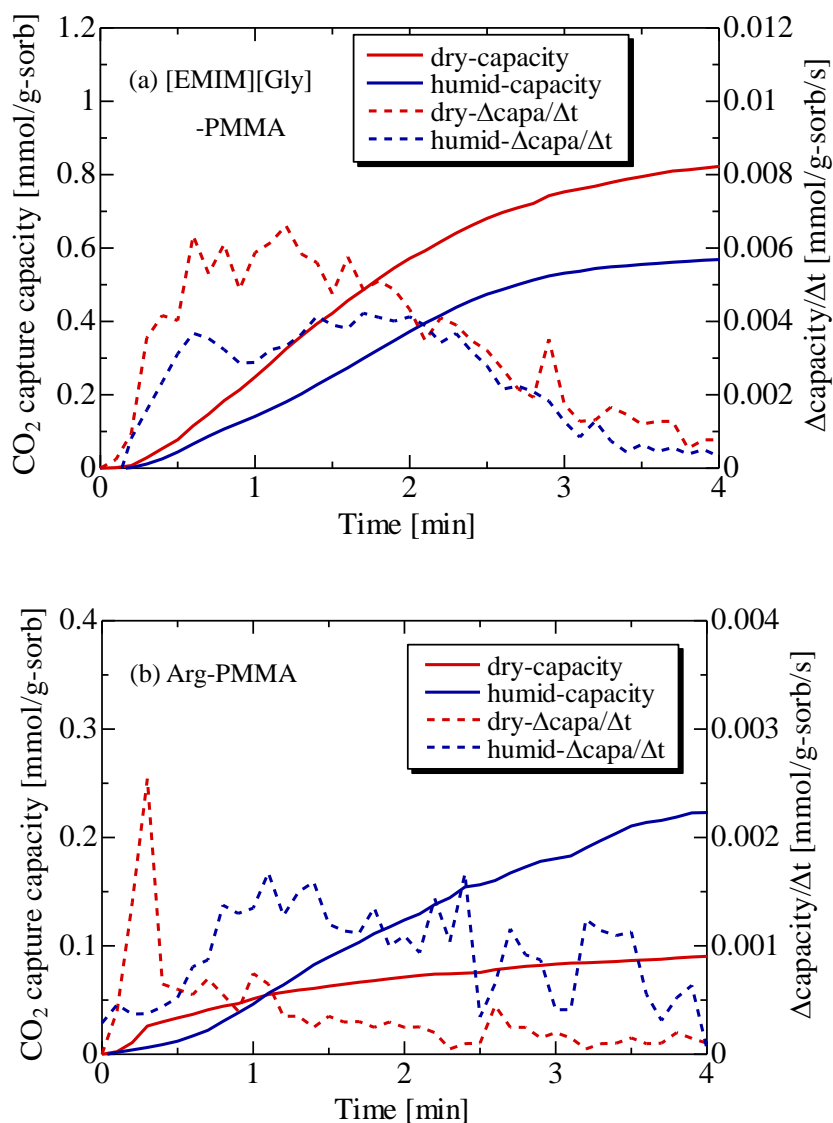


Figure 3.4. Comparison of CO₂ adsorption behaviors of (a) [EMIM][Gly]-PMMA (50 wt%) and (b) Arg-PMMA (20 wt%) with time under dry and humidified CO₂ inlet gas conditions, respectively.

In order to evaluate the influence of water vapor on the CO₂ sorption behaviors in more detail, comparisons of change in CO₂ sorption capacities of [EMIM][Gly]-PMMA (50 wt%) and

Arg-PMMA (20 wt%) with time in dry and humidified CO₂ inlet gas conditions are depicted in Figures 3.4a and b, respectively. These figures also include the behaviors of small change in the capacity per time step, $\Delta\text{capacity}/\Delta t$ ($\Delta t = 6$ s), with time, which represent the CO₂ sorption rate. For [EMIM][Gly]-PMMA, the water vapor decreased the CO₂ sorption rate ($\Delta\text{capacity}/\Delta t$) as well as the capacity, as seen from Figure 3.4a. However, the shapes of curves of $\Delta\text{capacity}/\Delta t$ were similar with a peak at around 1.5 min between dry and humidified CO₂ flow conditions. This fact would mean that water vapor in the inlet gas does not affect the reaction mechanism of [EMIM][Gly] with CO₂. The reason that both the CO₂ sorption capacity and rate reduced under the humid CO₂ flow is that the reaction between the sorbent and CO₂ is hindered by excessive amount of water adsorbed by [EMIM][Gly] [14]. In contrast, the water vapor enhanced both the CO₂ sorption capacity and rate for Arg-PMMA, as found in Figure 3.4b. Furthermore, the shapes of $\Delta\text{capacity}/\Delta t$ curves were also quite different with a peak at different time points between dry and humidified CO₂ inlet conditions. This indicates that the water content had changed the reaction scheme of Arg with CO₂. In most cases of supported amines, CO₂ adsorption capacity in humid CO₂ stream was higher than that in dry CO₂ stream, according to previous research groups [18–24]. These studies suggested that water content had a catalytic effect on the reaction of the amine with CO₂, leading to change in the reaction mechanism to form a bicarbonate, not carbamate [18,22,28–30]. Arg- and Lys-PMMA sorbents might pass through the same reaction scheme with the water content to enhance the capacities. In this reaction scheme, 1 mole of CO₂ will react with 1 mole of NH₂ species in the AA, not 2 moles (reactions 3.1–3.2), as represented by reaction 3.4.



On the other hand, the water vapor did not exert the positive effect on the Gly-PMMA sorbent to increase the capacity. A possible reason for this difference is that most fraction of the amino group in the Gly-PMMA sorbent would exist as NH_3^+ (not NH_2) that is much less active for the reaction. As seen in Table 3.3, the CO_2 sorption capacities of the [EMIM][Lys]-PMMA as well as [EMIM][Gly]-PMMA decreased in the presence of water vapor. This is because an excessive amount of water adsorbed by those sorbents had caused an inhibition of the active sites for the reaction with CO_2 rather than catalytic effect probably due to a hydrogen bond interaction between the AAILs and water [31]. Therefore, the water vapor hindered the reaction to form a carbamate (reactions 3.1–3.2) for those supported AAIL sorbents, without changing the reaction mechanism for formation of bicarbonate (reaction 3.4). In contrast, H_2O uptake of the [EMIM][Arg]-PMMA sorbent was lower than those of the [EMIM][Gly]- and [EMIM][Lys]-PMMA. This fact and positive impact of water vapor on reaction of Arg (or Arg-PMMA sorbent) with CO_2 could be reasons for slightly higher CO_2 capture capacity of the [EMIM][Arg]-PMMA in humidified CO_2 flow.

3.5.4 Effect of water vapor in flow gases on CO_2 desorption behavior

TPD experiments were carried out using [EMIM][Gly]-PMMA (50 wt%) and Arg-PMMA (20 wt%) sorbents under dry and humidified CO_2 inlet gas conditions. The ratio of MS CO_2 signal over MS N_2 signal at a time divided by the initial sample weight loaded in the TGA was evaluated as the CO_2 concentration desorbed from the sample at the time. Figures 3.5a and b show the CO_2 desorption behaviors of [EMIM][Gly]-PMMA and Arg-PMMA with change in TGA reactor temperature from the results of TPD tests, respectively. As found from Figure 3.5a, the amount of CO_2 desorption from [EMIM][Gly]-PMMA sorbent was higher in the dry CO_2 flow than the humid CO_2 flow, which is consistent with the result of CO_2 adsorption described

above (Figure 3.4a).

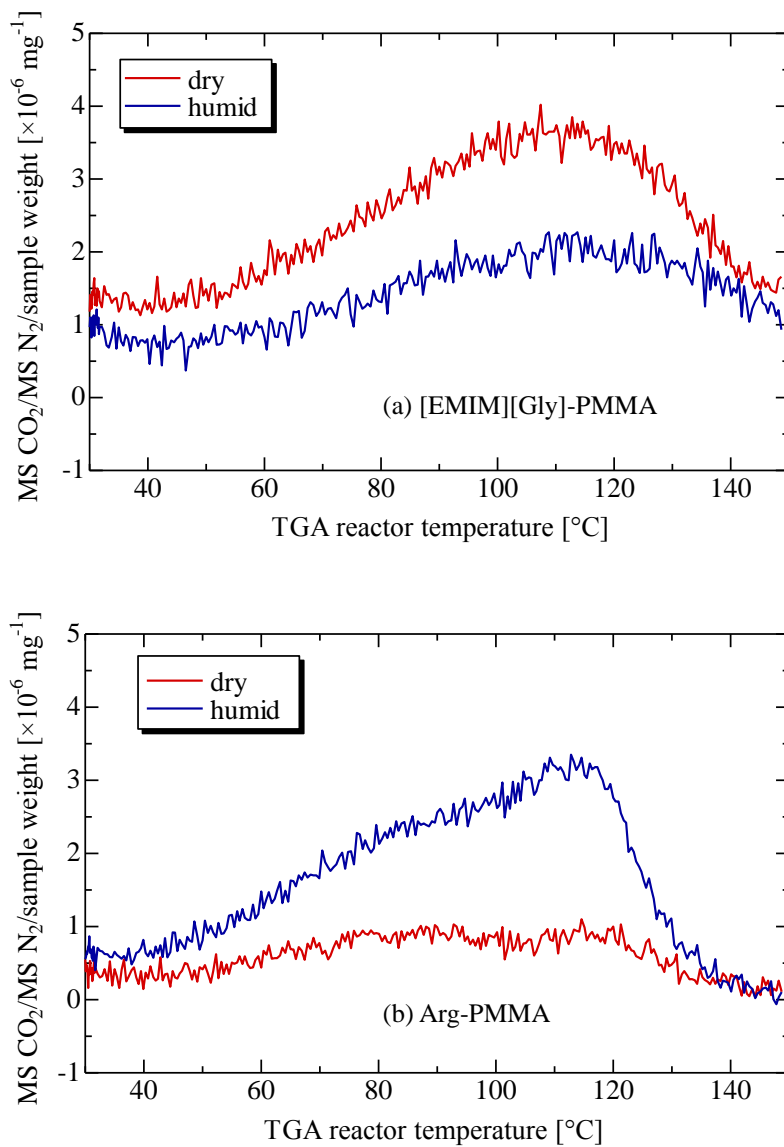


Figure 3.5. CO₂ desorption behaviors of (a) [EMIM][Gly]-PMMA (50 wt%) and (b) Arg-PMMA (20 wt%) with change in TGA reactor temperature under dry and humidified CO₂ inlet gas conditions, respectively.

Also, the shapes of CO₂ desorption profiles with the temperature under the dry and humidified CO₂ conditions were similar, like the CO₂ adsorption behaviors in both the conditions (Figure 3.4a). These results would prove the assumption mentioned previously that water vapor in flow gases does not affect the reaction scheme of [EMIM][Gly] with CO₂. The peaks of CO₂ desorption profiles were at 110 °C in both the dry and humidified CO₂ conditions, which will mean that the peak desorption TGA temperature is 110 °C for this sorbent. On the other hand, Figure 3.5b displays that the amount of CO₂ desorbed from the Arg-PMMA sorbent was higher under the humidified CO₂ condition than the dry CO₂ condition as expected from the CO₂ adsorption test results (Figure 3.4b). Furthermore, the shapes of CO₂ desorption profiles in the dry and humidified CO₂ conditions were quite different: the dry CO₂ condition provided a broad temperature peak from 80 to 120 °C, while the humid CO₂ condition gave a sharp temperature peak at around 120 °C. This will also suggest that in the humid CO₂ flow the reaction mechanism with CO₂ for the Arg-PMMA sorbent was different, and the formation of bicarbonate will be implied (reaction 3.4).

3.5.5 Cyclic CO₂ sorption-desorption in both dry and humidified CO₂ conditions

5 cyclic CO₂ sorption-desorption experiments were conducted using [EMIM][Gly]-, [EMIM][Lys]- and [EMIM][Arg]-PMMA (50 wt%) sorbents under both dry and humidified CO₂ inlet conditions. The adsorption and desorption temperatures were 30 °C and 100 °C, respectively. Changes in the CO₂ sorption capacities of those sorbents with the number of cycles are depicted in Figure 3.6. The CO₂ capture capacity of the [EMIM][Gly]-PMMA sorbent decreased gradually with increasing the number of cycles in both dry and humidified CO₂ flow conditions. One of the reasons of such trend is the incomplete desorption of CO₂ during each regeneration step at 100 °C for 50 min, since the peak desorption temperature is 110 °C in both gas flow

conditions (Figure 3.5a). Another possible reason is that a stable byproduct such as urea had formed and accumulated on the sorbent in the adsorption and/or desorption steps, leading to inhibition of the active site, as Sayari et al. has reported on primary amine-functionalized silica sorbents [22,32]. The similar tendency of decrease in the capacity was found for the [EMIM][Lys]-PMMA sorbent, implying that this sorbent was not also regenerated successfully during each desorption step. The capacities of the supported [EMIM][Gly] and [EMIM][Lys] sorbents under the humid gas inlet were lower than those under the dry gas inlet in any cyclic numbers, since they reduced in the same way in both gas flow conditions with the number of cycles. This fact indicates that the presence of water vapor exerts neither positive nor negative impacts on cyclic stability of the CO₂ capture performance for those sorbents.

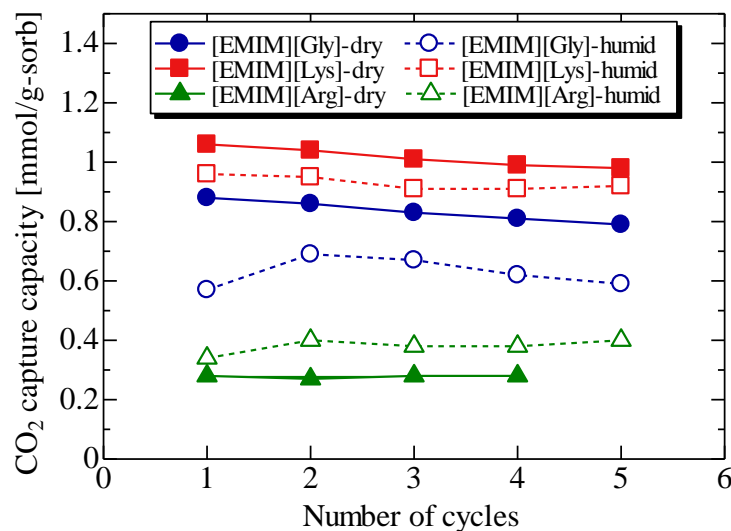


Figure 3.6. Changes in CO₂ capture capacities of [EMIM][AA]-PMMA (50 wt%) run under the dry CO₂ (2.3% CO₂ and balance N₂) and humidified CO₂ (2.3% CO₂, 2.1% H₂O and balance N₂) flow with the number of cycles.

In contrast, the [EMIM][Arg]-PMMA sorbent preserved a stability of the capacity in the multi-cycles, although the capacities of the [EMIM][Gly]- and [EMIM][Lys]-PMMA sorbents are much superior to that of the [EMIM][Arg]-PMMA sorbent up to the fifth cycle. The difference in stability of the capacity might be mainly due to the structures of their amino groups involving formation of byproducts like urea, as Gly and Lys have only primary amino groups, while Arg has secondary amino groups as well as primary ones (Table 3.1). Some researchers have reported that only primary amines exhibited loss of CO₂ uptake during cyclic CO₂ capture tests because of formation of urea linkage in the presence of CO₂ causing the deactivations, whereas secondary and tertiary amines retained a stability of the CO₂ sorption capacity without production of urea groups [32,33]. Thus, cyclic CO₂ capture performance of the supported AAIL sorbents was affected by the type of sorbents as well as the presence of water vapor.

3.6 Conclusions

CO₂ sorption-desorption behaviors of supported [EMIM][AA] sorbents on PMMA were evaluated under dry and humidified CO₂ inlet conditions and also compared with those of supported AA sorbents on PMMA in the same run conditions using Gly, Lys and Arg as AAs. Under the dry CO₂ flow, the supported [EMIM][AA] sorbents exhibited higher CO₂ capture capacities than the corresponding supported AA sorbents with the same AA contents in the sorbents. In the presence of water vapor, CO₂ sorption capacities of the [EMIM][Gly]- and [EMIM][Lys]-PMMA decreased as the adsorbed water inhibited their reaction with CO₂. In contrast, the capacities of Lys-, Arg- and [EMIM][Arg]-PMMA sorbents were higher under the humid CO₂ flow than dry CO₂ flow since the water content exerted a positive effect on these sorbents to enhance the capacities, as considered from the sorption-desorption behaviors. The

cyclic CO₂ sorption-desorption performance of the supported [EMIM][AA] sorbents was also different depending on the structures of the AAs. The CO₂ capture capacities of [EMIM][Gly]- and [EMIM][Lys]-PMMA sorbents decreased gradually with increasing the number of cycles in both the dry and humid CO₂ flow conditions, whereas [EMIM][Arg]-PMMA sorbent kept stable CO₂ capture capacity. In our future studies, different types of IL cations and/or AAs will be examined to fabricate more effective supported AAIL sorbents with higher capacities even in the presence of water vapor.

3.7 Supporting Information

3.7.1 Characterization

Table S3.1. Surface areas and pore volumes of PMMA, [EMIM][Lys]-PMMA with 10 wt% and 50 wt% loadings, and Lys-PMMA with 5 wt% and 20 wt% loadings.

type	BET surface area [m ² /g]	BJH adsorption cumulative pore volume [cm ³ /g]
PMMA	527	1.12
[EMIM][Lys]-PMMA (10%)	327	0.93
[EMIM][Lys]-PMMA (50%)	38	0.35
Lys-PMMA (5%)	298	0.94
Lys-PMMA (20%)	159	0.67

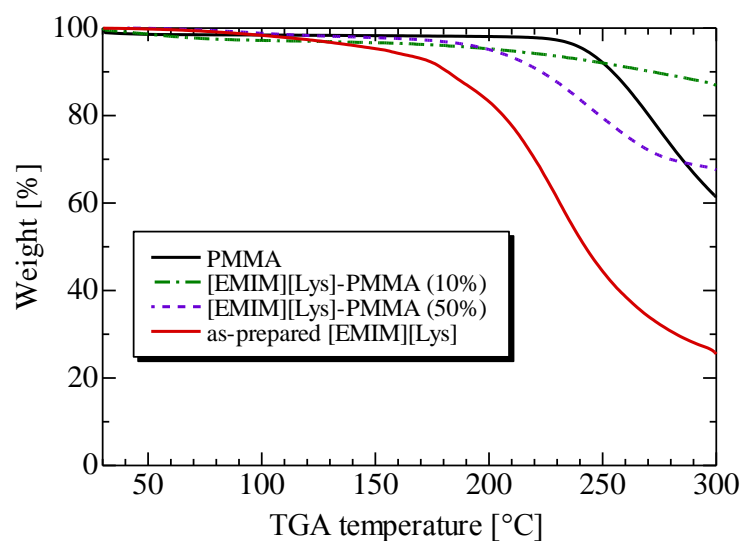


Figure S3.1. TGA curves of PMMA, [EMIM][Lys]-PMMA with 10 wt% and 50 wt% loadings, and as-prepared [EMIM][Lys] (N_2 atmosphere, heating rate of $10\text{ }^{\circ}\text{C}/\text{min}$).

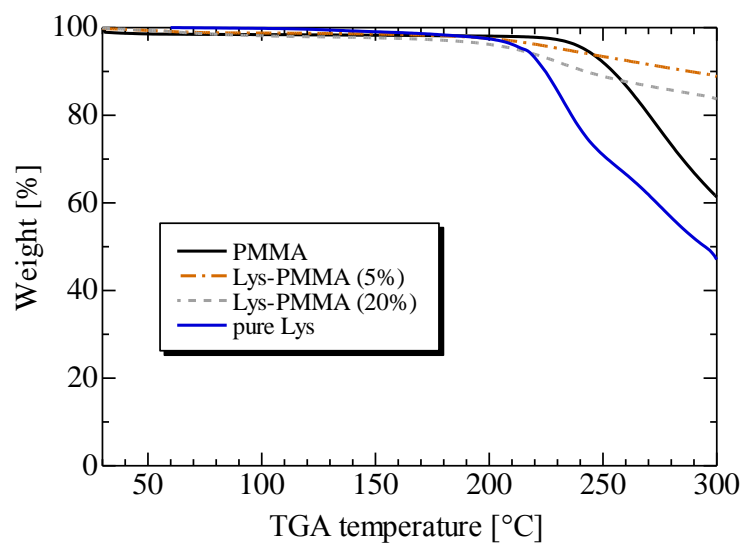


Figure S3.2. TGA curves of PMMA, Lys-PMMA with 5 wt% and 20 wt% loadings, and pure Lys (N_2 atmosphere, heating rate of $10\text{ }^{\circ}\text{C}/\text{min}$).

3.7.2 Error analysis

Three repetitive CO₂ sorption tests were carried out using lysine-polymethylmethacrylate (Lys-PMMA) sorbent with the loading of 20 wt% under both dry and humidified gas inlet conditions to conduct the error analysis. The procedures of sample preparation and CO₂ capture experiment are described in the EXPERIMENTAL SECTION 3.4.3 and 3.4.5, respectively. The three CO₂ sorption run behaviors of the Lys-PMMA sorbent in dry and humidified CO₂ flow conditions are depicted in Figure S3.3a and b, respectively. The experimental values of CO₂ capture capacities for each repetitive run, the averages and standard deviations (S.D.) under dry or humidified gas inlet are summarized in Table S3.2.

Table S3.2. CO₂ capture capacities for three CO₂ sorption runs of Lys-PMMA sorbent with the loading of 20 wt%, the averages and standard deviations (S.D.) in dry and humidified gas inlet conditions, respectively.

gas condition	CO ₂ capture capacity [mmol/g-sorbent]				
	run 1	run 2	run 3	average	S.D.
dry	0.25 (T1)	0.23 (T2)	0.24 (T3)	0.24	0.01
humid	0.36 (T4)	0.38 (T5)	0.35 (T6)	0.36	0.01

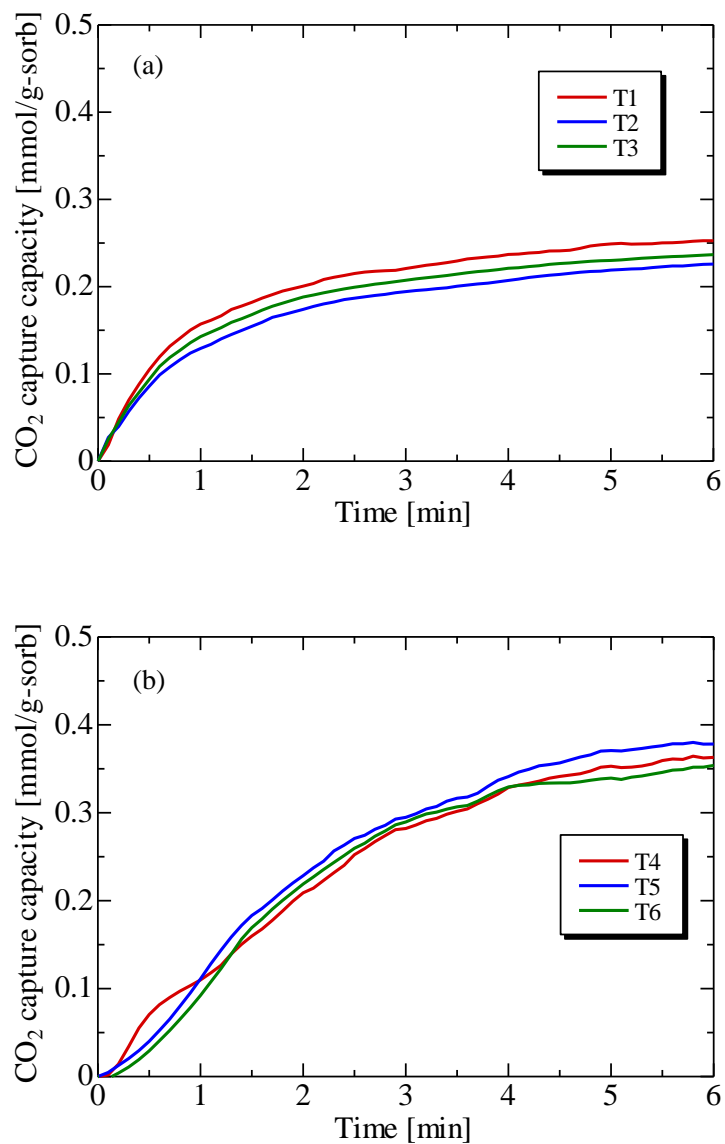


Figure S3.3. Three repetitive CO₂ sorption run behaviors of Lys-PMMA sorbent with the loading of 20 wt% in (a) dry and (b) humidified gas CO₂ conditions, respectively.

3.7.3 Tabular data of CO₂ capture capacities

Table S3.3. CO₂ capture capacities of 1-ethyl-3-methylimidazolium amino acid ([EMIM][AA])-PMMA sorbents with various loadings under dry CO₂ inlet (2.3% CO₂ and balance N₂) and TGA temperature of 30 °C.

type	loading in sorb. [wt%]	AA content in sorb. [mmol/g-sorb]	CO ₂ capture capacity [mmol/g-sorb]	CO ₂ capture capacity [mol/mol-AA]
[EMIM][Gly]	70	3.8	0.22	0.06
	50	2.7	0.88	0.33
	40	2.2	0.75	0.35
	30	1.6	0.56	0.35
	10	0.5	0.25	0.46
[EMIM][Lys]	70	2.7	0.28	0.10
	50	2.0	1.06	0.54
	30	1.2	0.54	0.46
	10	0.4	0.19	0.50
[EMIM][Arg]	70	2.5	0	0
	50	1.8	0.29	0.17
	30	1.1	0.16	0.15
	10	0.4	0.04	0.12

Table S3.4. CO₂ capture capacities of amino acid (AA)-PMMA sorbents with various loadings under dry CO₂ inlet (2.3% CO₂ and balance N₂) and TGA temperature of 30 °C.

type	loading in sorb. [wt%]	AA content in sorb. [mmol/g-sorb]	CO ₂ capture capacity [mmol/g-sorb]	CO ₂ capture capacity [mol/mol-AA]
Gly	20	2.7	0.03	0.01
	10	1.3	0.03	0.02
	5	0.7	0.03	0.04
Lys	30	2.1	0.22	0.11
	20	1.4	0.24	0.18
	10	0.7	0.12	0.18
	5	0.3	0.05	0.16
Arg	20	2.5	0.10	0.09
	10	1.8	0.06	0.11
	5	0.4	0.04	0.14

3.8 References

- [1] G.T. Rochelle, Amine scrubbing for CO₂ capture, Science 325 (2009) 1652–1654.
- [2] C.H. Yu, C.H. Huang, C.S. Tan, A review of CO₂ capture by absorption and adsorption,

Aerosol Air Qual. Res. 12 (2012) 745–769.

- [3] A. Samanta, A. Zhao, G.K.H. Shimizu, P. Sarkar, R. Gupta, Post-combustion CO₂ capture using solid sorbents: A review, *Ind. Eng. Chem. Res.* 51 (2012) 1438–1463.
- [4] M.A. Hussain, Y. Soujanya, G.N. Sastry, Evaluating the efficacy of amino acids as CO₂ capturing agents: A first principles investigation, *Environ. Sci. Technol.* 45 (2011) 8582–8588.
- [5] P.S. Kumar, J.A. Hogendoorn, G.F. Versteeg, P.H.M. Feron, Kinetics of the reaction of CO₂ with aqueous potassium salt of taurine and glycine, *AIChE J.* 49 (2003) 203–213.
- [6] M. Kim, H.J. Song, M.G. Lee, H.Y. Jo, J.W. Park, Kinetics and steric hindrance effects of carbon dioxide absorption into aqueous potassium alaninate solutions, *Ind. Eng. Chem. Res.* 51 (2012) 2570–2577.
- [7] H. Knuutila, U.E. Aronu, H.M. Kvamsdal, A. Chikukwa, Post combustion CO₂ capture with an amino acid salt, *Energy Procedia.* 4 (2011) 1550–1557.
- [8] D. Guo, H. Thee, C.Y. Tan, J. Chen, W. Fei, S. Kentish, G.W. Stevens, G. da Silva, Amino acids as carbon capture solvents: Chemical kinetics and mechanism of the glycine + CO₂ reaction, *Energy Fuels* 27 (2013) 3898–3904.
- [9] R.N. Goldberg, N. Kishore, R.M. Lennen, Thermodynamic quantities for the ionization reactions of buffers, *J. Phys. Chem. Ref. Data.* 31 (2002) 231–370.
- [10] K. Fukumoto, M. Yoshizawa, H. Ohno, Room temperature ionic liquids from 20 natural amino acids, *J. Am. Chem. Soc.* 127 (2005) 2398–2399.
- [11] H. Ohno, K. Fukumoto, Amino acid ionic liquids, *Acc. Chem. Res.* 40 (2007) 1122–1129.
- [12] B.E. Gurkan, J.C. de la Fuente, E.M. Mindrup, L.E. Ficke, B.F. Goodrich, E.A. Price, W.F. Schneider, J.F. Brennecke, Equimolar CO₂ absorption by anion-functionalized ionic

- liquids, *J. Am. Chem. Soc.* 132 (2010) 2116–2117.
- [13] B.F. Goodrich, J.C. De La Fuente, B.E. Gurkan, D.J. Zadigian, E.A. Price, Y. Huang, J.F. Brennecke, Experimental measurements of amine-functionalized anion-tethered ionic liquids with carbon dioxide, *Ind. Eng. Chem. Res.* 50 (2011) 111–118.
- [14] J. Ren, L. Wu, B.G. Li, Preparation and CO₂ sorption/desorption of N-(3-aminopropyl)aminoethyl tributylphosphonium amino acid salt ionic liquids supported into porous silica particles, *Ind. Eng. Chem. Res.* 51 (2012) 7901–7909.
- [15] X. Wang, N.G. Akhmedov, Y. Duan, D. Luebke, B. Li, Immobilization of amino acid ionic liquids into nanoporous microspheres as robust sorbents for CO₂ capture, *J. Mater. Chem. A*. 1 (2013) 2978–2982.
- [16] X. Wang, N.G. Akhmedov, Y. Duan, D. Luebke, D. Hopkinson, B. Li, Amino acid-functionalized ionic liquid solid sorbents for post-combustion carbon capture, *ACS Appl. Mater. Interfaces*. 5 (2013) 8670–8677.
- [17] J. Zhang, S. Zhang, K. Dong, Y. Zhang, Y. Shen, X. Lv, Supported absorption of CO₂ by tetrabutylphosphonium amino acid ionic liquids, *Chem. Eur. J.* 12 (2006) 4021–4026.
- [18] X. Xu, C. Song, B.G. Miller, A.W. Scaroni, X. Xu, C. Song, B.G. Miller, A.W. Scaroni, Influence of moisture on CO₂ separation from gas mixture by a nanoporous adsorbent based on polyethylenimine-modified molecular sieve MCM-41, *Ind. Eng. Chem. Res.* 44 (2005) 8113–8119.
- [19] N. Hiyoshi, K. Yogo, T. Yashima, Adsorption of carbon dioxide on amine modified SBA-15 in the presence of water vapor, *Chem. Lett.* 33 (2004) 510–511.
- [20] P.J.E. Harlick, A. Sayari, Applications of pore-expanded mesoporous silica. 5. Triamine grafted material with exceptional CO₂ dynamic and equilibrium adsorption performance,

- Ind. Eng. Chem. Res. 46 (2007) 446–458.
- [21] R. Serna-Guerrero, E. Da'na, A. Sayari, New insights into the interactions of CO₂ with amine-functionalized silica, Ind. Eng. Chem. Res. 47 (2008) 9406–9412.
- [22] A. Sayari, Y. Belmabkhout, Stabilization of amine-containing CO₂ adsorbents: Dramatic effect of water vapor, J. Am. Chem. Soc. 132 (2010) 6312–6314.
- [23] M.L. Gray, J.S. Hoffman, D.C. Hreha, D.J. Fauth, S.W. Hedges, K.J. Champagne, H.W. Pennline, Parametric study of solid amine sorbents for the capture of carbon dioxide, Energy Fuels. 23 (2009) 4840–4844.
- [24] H.Y. Huang, R.T. Yang, D. Chinn, C.L. Munson, Amine-grafted MCM-48 and silica xerogel as superior sorbents for acidic gas removal from natural gas, Ind. Eng. Chem. Res. 42 (2003) 2427–2433.
- [25] B. Jiang, X. Wang, M.L. Gray, Y. Duan, D. Luebke, B. Li, Development of amino acid and amino acid-complex based solid sorbents for CO₂ capture, Appl. Energy. 109 (2013) 112–118.
- [26] A. Jayakumar, A. Gomez, N. Mahinpey, Post-combustion CO₂ capture using solid K₂CO₃: Discovering the carbonation reaction mechanism, Appl. Energy. 179 (2016) 531–543.
- [27] Y.S. Sistla, A. Khanna, CO₂ Absorption studies in amino acid-anion based ionic liquids, Chem. Eng. J. 273 (2015) 268–276.
- [28] T.L. Donaldson, Y.N. Nguyen, Carbon dioxide reaction kinetics and transport in aqueous amine membranes, Ind. Eng. Chem. Fundam. 19 (1980) 260–266.
- [29] R.J. Hook, An investigation of some sterically hindered amines as potential carbon dioxide scrubbing compounds, Ind. Eng. Chem. Res. 36 (1997) 1779–1790.
- [30] P.D. Vaidya, E.Y. Kenig, CO₂–alkanolamine reaction kinetics: A review of recent studies,

- Chem. Eng. Technol. 30 (2007) 1467–1474.
- [31] W. Zhao, G. He, L. Zhang, J. Ju, H. Dou, F. Nie, C. Li, H. Liu, Effect of water in ionic liquid on the separation performance of supported ionic liquid membrane for CO₂/N₂, J. Memb. Sci. 350 (2010) 279–285.
- [32] A. Sayari, Y. Belmabkhout, E. Da'na, CO₂ Deactivation of supported amines: Does the nature of amine matter?, Langmuir 28 (2012) 4241–4247.
- [33] D.H. Jo, H. Jung, D.K. Shin, C.H. Lee, S.H. Kim, Effect of amine structure on CO₂ adsorption over tetraethylenepentamine impregnated poly methyl methacrylate supports, Sep. Purif. Technol. 125 (2014) 187–193.

CHAPTER 4: Roles of cation and anion of amino acid anion-functionalized ionic liquids immobilized into a porous support for CO₂ capture

4.1 Presentation of the article

This paper first presents the effect of cation of amino acid anion-functionalized ionic liquids (AAILs) immobilized into a commercial polymer support on the CO₂ adsorption. The cations selected to synthesize the supported AAILs and to compare the CO₂ capture performances were 1-ethyl-3-methylimidazolium (EMIM) cation and tetrabutylphosphonium (P₄₄₄₄) cation, because they possess substantially different molecular structures and hydrophilicities from each other. As a result, the supported [P₄₄₄₄][AA] sorbents exhibited greater CO₂ adsorption capacities than the corresponding supported [EMIM][AA] sorbents with the same AA loading in units of mol/mol-AAIL under a dry CO₂ gas inlet condition. It was especially noteworthy that the supported [P₄₄₄₄][Gly] sorbent slightly surpassed 0.5 mol/mol-AAIL, in contrast to the supported [EMIM][Gly] sorbent, suggesting that the reaction stoichiometry of the supported [P₄₄₄₄][Gly] with CO₂ was closer to 1:1 than 2:1 ratio, as Gly has only one amino group in the molecule.

The effect of not only cation, but also AA anion in the supported AAIL sorbents on the CO₂ adsorption is evaluated in this paper. The experimental results showed that Gly and Lys anions having linear side chains with only primary amino groups led to greater CO₂ adsorption capacities than His and Arg anions having complicated side chains with secondary and tertiary amino groups, although His and Arg have more amino groups. In other words, the side chain structures of AAs, in addition to the number of amino groups, influenced the CO₂ capture performances.

The kinetic analysis study of the supported [EMIM][AA] and [P₄₄₄₄][AA] sorbents on the CO₂

adsorption is also performed and compared in this paper. From the analysis, it was found that a double exponential kinetic model fitted the dynamic CO₂ adsorption behaviors of all the AAIL-loaded solid sorbents very well.

This paper finally offers the impact of water vapor on CO₂ adsorption of the supported AAIL sorbents with a different cation. The supported [P₄₄₄₄][AA] sorbents adsorbed much less amount of water vapor than the corresponding supported [EMIM][AA] sorbents under a humidified CO₂ inlet condition. Nevertheless, both the supported [EMIM][AA] and [P₄₄₄₄][AA] sorbents decreased their CO₂ capture capacities in a similar manner in the presence of water vapor. It was found from the kinetic behaviors that much more rapid initial adsorption rate of H₂O than CO₂ on these sorbents, not the total H₂O uptakes, caused inhibition of the AAIL active sites for the surface reaction with CO₂.

Nearly all of this study was conducted by Yusuke Uehara. Dr. Davood Karami assisted in ordering the chemicals needed for the synthesis of AAILs and gave advice on the kinetic study. Dr. Nader Mahinpey supervised the whole research.

Roles of cation and anion of amino acid anion-functionalized ionic liquids immobilized into a porous support for CO₂ capture

This article has been published in *Energy & Fuels* 32 (2018) 5345–5354.

*Yusuke Uehara, Davood Karami, and Nader Mahinpey**

Department of Chemical and Petroleum Engineering, Schulich School of Engineering,
University of Calgary, Calgary, AB T2N 1N4, Canada

4.2 Abstract

The impact of cation and anion of amino acid (AA) anion-functionalized ionic liquids (ILs) immobilized into a porous support on the CO₂ capture performance was investigated in dry or humidified gas flow condition. 1-ethyl-3-methylimidazolium ([EMIM]) cation and tetrabutylphosphonium ([P₄₄₄₄]) cation were used as a cation for synthesizing AAILs and compared, since they have different molecular structures and hydrophilicities with each other affecting gas sorption behaviors. The experimental results showed that supported [P₄₄₄₄][AAs] had higher CO₂ capture capacities than the corresponding supported [EMIM][AAs] in units of mol/mol-AAIL under dry gas inlet, exhibiting the effect of cation on the CO₂ adsorption performance. Under humidified gas flow, supported [P₄₄₄₄][AAs] adsorbed much less amounts of water vapor than supported [EMIM][AAs]. On the other hand, CO₂ capture capacities of both supported [EMIM][AAs] and [P₄₄₄₄][AAs] slightly reduced in the presence of water vapor, due to much more rapid sorption of H₂O than CO₂.

4.3 Introduction

Mitigating CO₂ emission from combustion of fossil fuels has been a considerable concern since we have recognized that CO₂ can contribute to global warming as a greenhouse gas. Amine-functionalized ionic liquids (ILs) have lately received a great attention as alternatives to aqueous amines used for the conventional CO₂ capture technology because of their unique features like negligible vapor pressure, high thermal stability and tunability of physicochemical properties. Among them, amino acid ionic liquids (AAILs) have been energetically studied as sorbents for CO₂ removal in recent years [1–7]. Amino acids (AAs) themselves are attractive materials since they are inexpensive and also have little impact on environment, high biodegradability and low volatility [8–10].

One disadvantage of AAILs is their high viscosity leading to slow CO₂ sorption and desorption rates. Therefore, immobilizing AAILs into a porous support with a large specific surface area and pore volume is a better way to enhance their CO₂ capture performance as solid sorbents. Some research groups have investigated CO₂ adsorption of AAILs immobilized into support materials using several kinds of AAs as anions, achieving much more rapid CO₂ sorption than unsupported or pure AAILs [1,4–6,11]. Supported AAIL sorbents can also have a good stability of cyclic CO₂ capture, although the durability can depend on the type of AAILs [4–6,12]. However, no study has used two or more types of cations in studying CO₂ capture of supported AA anion-functionalized ILs. It is considered important to evaluate the impact of cations as well as AA anions of supported AAILs on the CO₂ adsorption behaviors to design further promising AAIL- functionalized solid sorbents because of a couple of reasons. First, cations of AAILs can also affect the CO₂ sorption mechanism, not only AA anions. Reaction stoichiometries of AAILs with CO₂ have been reported by some researchers based on their experimental studies using pure

AILs with one or two kinds of cations, but they are different depending on the type of cations. For example, Jiang et al. argued that the reaction of pure tetraethylammonium amino acid ([N₂₂₂₂][AA]) ILs with CO₂ followed a 2:1 stoichiometry [2]. This mechanism is similar with that on alkanolamines used for aqueous amine scrubbing [13], which is expressed by Equations 1 and 2. In these consecutive reactions, 1 mole of amine group reacts with 1 mole of CO₂ to form a carbamic acid (Equation 4.1), and then the generated carbamic acid further reacts with 1 mol of another amine group to form a carbamate anion (Equation 4.2). Similarly, tetramethylammonium amino acid ([N₁₁₁₁][AA]) and 1-butyl-3-methylimidazolium amino acid ([BMIM][AA]) ILs approached 0.5 mol of CO₂ absorption per mol of amino group in the AAIL [10,14]. On the other hand, Gurkan et al. proposed a 1:1 stoichiometric mechanism for reaction of trihexyl(tetradecyl) phosphonium amino acid ([P₆₆₆₁₄][AA]) ILs with CO₂, in which only a carbamic acid is produced (equation 4.1) without the formation of carbamate species (Equation 4.2) [3]. Yang et al. have recently demonstrated that CO₂ absorption of pure phosphonium AAILs actually proceeded through both 2:1 and 1:1 reaction mechanisms, and that the two ratios depended on the type of cations as well as AA anions [7].



Second, AAILs generally have a high hydrophilicity, which depends on the type of cations. For instance, tetrabutylphosphonium amino acid ([P₄₄₄₄][AAs]) ILs exhibit a larger hydrophobicity than [BMIM][AAs] due to hydrophobic alkyl chains of P₄₄₄₄ cation [15]. Hydrophobicity of AAILs might be a crucial factor for CO₂ removal because actual flue gases contain some percentage of water vapor. In other words, high hydrophilic AAILs could capture

huge amounts of water as well as CO₂ in flue gases, leading to inhibition of active sites in the AAILs for CO₂ uptake.

In this work, impacts of both cation and anion of AAILs immobilized into a porous support on their CO₂ adsorption performance under dry CO₂ inlet condition are evaluated through experimental study using a TGA-MS analysis system. Furthermore, the same experiments are carried out under humidified CO₂ flow condition to compare adsorption behaviors of H₂O as well as CO₂ for those supported AAILs. 1-ethyl-3-methylimidazolium cation ([EMIM]⁺) and tetrabutylphosphonium cation ([P₄₄₄₄]⁺) are used as a cation for synthesizing AAILs since they have different chemical structures and hydrophilicities. Polymethylmethacrylate (PMMA) microspheres are selected as a support, since PMMA supports have shown good performances for CO₂ capture [5,6,16–18]. The advantages of PMMA microspheres are that they are inexpensive and have large surface area, pore volume and pore size [16].

4.4 Experimental section

1-ethyl-3-methylimidazolium bromide ([EMIM][Br]), ≥98%, glycine (Gly), 99%, L-lysine (Lys), 98%, L-histidine (His), ≥98%, L-alanine (Ala), 99%, β-alanine (BALA), 98%, L-arginine (Arg), ≥98%, and anion exchange resin (Amberlite IRA-402 OH) were obtained from Alfa Aesar Co. (Ward Hill, MA). Tetrabutylphosphonium bromide ([P₄₄₄₄][Br]), 98%, were purchased from Sigma Aldrich Co. (St. Louis, MO). Diaion HP-2MG that is polymethylmethacrylate (PMMA) microspheres as a support material were bought from Supelco Co. (Bellefonte, PA), which have the following physical properties: effective particle size, 0.5 mm; pore volume, 1.2 mL/g; specific surface area, 500 m²/g; average pore radius, 17 nm; density, 1.09 g/mL. Molecular structures of AAs (anions), EMIM and P₄₄₄₄ cations are listed in Tables 4.1 and 4.2, respectively.

Table 4.1. Molecular structures of AA anions.

AA		structure of AA anion
glycine	[Gly]	
L-lysine	[Lys]	
L-histidine	[His]	
L-alanine	[Ala]	
β-alanine	[BALA]	
L-arginine	[Arg]	

Table 4.2. Molecular structures of EMIM and P₄₄₄₄ cations.

cation	structure
[EMIM] ⁺	
[P ₄₄₄₄] ⁺	

4.4.1 Synthesis of [EMIM][AA] and [P₄₄₄₄][AA]

AILs of [EMIM][AAs] and [P₄₄₄₄][AAs] were synthesized by a neutralization method [1,5,6,19]. [EMIM][Br] or [P₄₄₄₄][Br] was first dissolved in deionized water to prepare each aqueous solution, and the solution was passed through an anion exchange resin (Amberlite IRA-402 OH) column to prepare [EMIM][OH] or [P₄₄₄₄][OH] aqueous solution. Next, a slight excess of equimolar AA aqueous solution was added to the [EMIM][OH] or [P₄₄₄₄][OH] aqueous solution. Then, the mixture was gently stirred at room temperature for 24 h. After evaporating water from the mixture at around 45 °C and then drying it at 50 °C under vacuum for 24 h, a crude product including both the desired AAIL and unreacted AA was gained. Ethanol was added to the crude product, and the suspension was centrifuged at 3800 rpm for 15 min to separate the insoluble AA from it. After drying the ethanol solution at 80 °C under vacuum for 24 h, AAIL of [EMIM][AA] or [P₄₄₄₄][AA] was finally prepared.

4.4.2 Immobilization of AAIL into PMMA microspheres

The prepared [EMIM][AA] or [P₄₄₄₄][AA] was immobilized into PMMA microspheres by an impregnation method.[1,4–6] PMMA microspheres were dried at 105 °C for 1 h before usage since they contain approximately 60 wt% of water content. The [EMIM][AA] or [P₄₄₄₄][AA] was first dissolved in aqueous ethanol solution at a concentration of 50 mg/mL, and the solution was stirred at 200 rpm at room temperature for 30 min. Next, the dried PMMA microspheres were added to it, and the suspension was stirred further at 100 rpm for 2 h. By evaporating the solvent, followed by drying the residue at 50 °C under vacuum for 24 h, [EMIM][AA]- or [P₄₄₄₄][AA]-PMMA solid sorbent was obtained.

4.4.3 Characterization

BET surface area and BJH pore volume analyses were carried out for pure PMMA, [EMIM][AA]-PMMA and [P₄₄₄₄][AA]-PMMA sorbents through N₂ adsorption-desorption isotherm at -196 °C using a surface area analyzer, Micromeritics ASAP 2020. The samples were degassed at 100 °C for 180 min before the analysis. In addition, thermogravimetric analyses of pure PMMA, the as-prepared AAILs and the AAIL-PMMA sorbents were conducted under N₂ atmosphere with a heating rate of 10 °C/min using Perkin-Elmer Pyris-STA 6000 thermogravimetric analyzer (TGA). Around 10 mg of a sample was used for each thermogravimetric analysis.

4.4.4 CO₂ sorption test under dry or humidified gas flow

CO₂ adsorption experiments of [EMIM][AA]- or [P₄₄₄₄][AA]-PMMA sorbent in dry or humid gas flow condition were carried out mainly using a TGA-MS analysis system. The schematic and equipment configuration of the TGA-MS system are described elsewhere [20]. The TGA used is a modified Thermax 500 TGA, in which the furnace and reactor system were replaced by a custom-built glass reactor system with an independent home-built temperature control system for the required low temperature conditions. Nearly 100 mg of a prepared sorbent sample was loaded and spread thinly in a wide stainless steel crucible of TGA. The sample was heated to and held at 100 °C for 50 min while flowing only dry N₂ at a flow rate of 152.9 ml/min. After the temperature was decreased to and held at 30 °C in the dry N₂ taking 75 min, the inlet gas was changed to mixed gases of 2.3 vol% of CO₂ and balance N₂ in dry gas flow condition, or 2.3 vol% of CO₂, 2.1 vol% of H₂O and balance N₂ in humidified gas flow condition at a flow rate of 158.5 ml/min. The mixed gases were fed into TGA for 130 min to conduct CO₂ sorption experiment in either gas inlet condition. CO₂ and H₂O concentrations in the outlet gases from

TGA was recorded every 6 s by MS sampling probe connected to the outlet of TGA, whose data were used for quantification of the CO₂ and H₂O uptakes by the sample in humidified gas flow condition [12,20]. A blank run under the dry or humidified gas flow was also conducted in the same procedure to subtract a buoyancy effect from TGA weight change data as well as to be used for quantification of CO₂ and H₂O uptakes in humidified gas flow condition. The procedure for quantification of CO₂ and H₂O uptakes is described elsewhere [12,20]. The experimental errors of CO₂ capture capacities in both dry and humidified CO₂ flow conditions are estimated at $\pm 5\%$ [12].

The CO₂ adsorption experiments were performed even at different temperatures (50, 70 and 90 °C) and CO₂ inlet concentrations (15, 50 and 80 vol%) in dry gas flow condition using Perkin-Elmer Pyris-STA 6000 TGA instead of the above TGA-MS system. The activation energy of CO₂ adsorption was calculated from the kinetic data under the different adsorption temperatures by the Arrhenius equation.

4.4.5 Temperature programmed desorption (TPD)

Temperature programmed desorption (TPD) experiment was carried out to evaluate a desorption behavior of CO₂ adsorbed in dry or humidified gas flow. This experiment was started from CO₂ adsorption step, followed by TPD step. The CO₂ adsorption step was conducted under dry or humidified gas flow in the same procedure as the CO₂ sorption test described above. For the next TPD step, flow gas was switched to dry pure N₂ again while holding the TGA temperature at 30 °C for 60 min. Then, the temperature was risen to 150 °C at a rate of 5 °C/min in the dry N₂ flow. The CO₂ concentration released from the sample was recorded with the MS.

4.5 Results and discussion

In this study, EMIM cation and P₄₄₄₄ cation were selected to investigate the impact of cations on CO₂ adsorption behaviors of supported AA anion-functionalized ILs, since imidazolium-based and phosphonium-based cations have different hydrophilicities as well as molecular structures (Table 4.2) [15]. Also, several kinds of AAs were used as the anions to find promising AA types for CO₂ capture of AAIL- functionalized solid sorbents.

The synthesized [EMIM][AA] or [P₄₄₄₄][AA] IL was immobilized into commercial PMMA microspheres, Diaion HP-2MG, with various loadings by an impregnation method. The PMMA microspheres have large surface area and pore volume (527 m²/g and 1.12 cm³/g), as shown in Table S4.1 of the Supporting Information. As the AAIL was supported on the PMMA microspheres, both the surface area and pore volume of PMMA reduced with higher AAIL loadings (Table S4.1). TGA curves of PMMA, [EMIM][Lys]-PMMA and [P₄₄₄₄][Lys]-PMMA with 10 and 50 wt% loadings, and as-prepared [EMIM][Lys] and [P₄₄₄₄][Lys] under N₂ atmosphere are depicted in Figure S4.1 of the Supporting Information. The thermal decomposition of PMMA occurred from around 240 °C, whereas that of as-prepared [EMIM][Lys] and [P₄₄₄₄][Lys] started from lower temperature of around 190 °C. The starting temperature of thermal decomposition of [EMIM][Lys]-PMMA and [P₄₄₄₄][Lys]-PMMA sorbents were close to that of as-prepared [EMIM][Lys] and [P₄₄₄₄][Lys], respectively. In contrast, the decomposition rates of the supported AAIL sorbents were lower than pure PMMA and as-prepared AAILs, which is likely due to enhanced thermal stabilities of the supported sorbents by physical interaction between the AAILs and PMMA.

4.5.1 Effect of cation of AAIL on CO₂ adsorption performance under dry CO₂ inlet

CO₂ sorption experiments of [EMIM][AA]-PMMA and [P₄₄₄₄][AA]-PMMA sorbents (50 wt% loadings) under dry CO₂ inlet condition were first conducted using Gly, Lys and His as AA anions at 30 °C. A low CO₂ concentration of 2.3% in the feed gases was adopted in order to avoid additional influence of physisorption on CO₂ capture of the sorbents [21]. Figure 4.1 shows change in CO₂ uptakes of the [EMIM][AA]- and [P₄₄₄₄][AA]-PMMA sorbents with time.

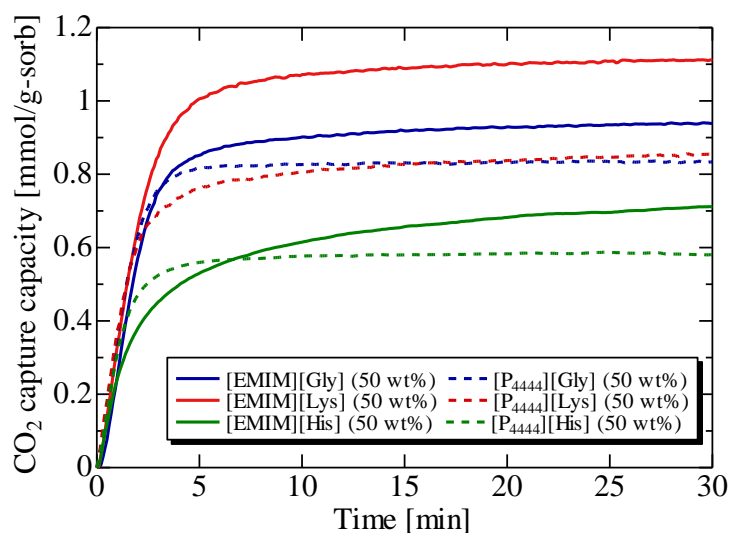


Figure 4.1. Change in CO₂ uptake of [EMIM][AA]-PMMA and [P₄₄₄₄][AA]-PMMA sorbents with the loadings of 50 wt% under dry CO₂ inlet condition (2.3% CO₂ and balance N₂) with time at 30 °C (AA: Gly, Lys or His).

The CO₂ uptakes of almost all the sorbents reached approximately their equilibrium within 15 min regardless of the type of sorbents. In addition, it is found that the CO₂ adsorption processes have two steps: the first step is a fast process with exponential weight increase, and the second step is a much slower process in which the weight change levels off [22]. The same experiment

using pure PMMA was conducted as well, but it did not virtually adsorb CO₂ (only 0.03 mmol/g-PMMA). It means that CO₂ is not captured physically on PMMA under the low CO₂ concentration gas flow. Therefore, CO₂ uptakes of the AAIL-PMMA sorbents in this gas flow condition are just due to chemisorption by active species of the AAILs immobilized into the PMMA support.

The CO₂ sorption experiments of these sorbents with various AAIL loadings (10, 30, 40 or 70 wt%) were also carried out. Figure 4.2 presents relationship between AAIL loadings and CO₂ capture capacities of the supported sorbents.

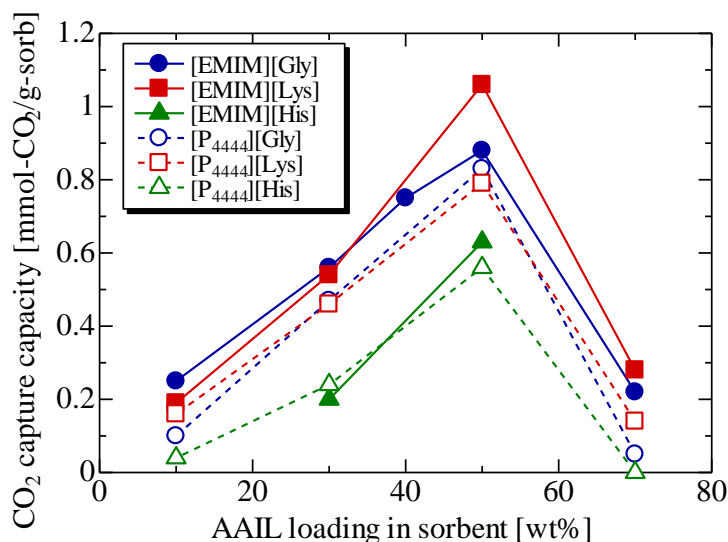


Figure 4.2. Relationship between AAIL loadings and CO₂ capture capacities of [EMIM][AA]- or [P₄₄₄₄][AA]-PMMA sorbent under dry CO₂ flow condition (2.3% CO₂ and balance N₂) at 30 °C (AA: Gly, Lys or His).

The capacities of both [EMIM][AA]- and [P₄₄₄₄][AA]-PMMA sorbents increases almost linearly with the IL loadings and reached their maximum values at 50 wt%. On the other hand, the

capacities dramatically decreases to 70 wt%, indicating that higher loading of AAIL blocks pores of the PMMA support, leading to reduction in accessible surface areas for dispersion of active species of the IL [5].

Table 4.3. CO₂ capture capacities of [EMIM][AA]-PMMA (50 wt%) and [P₄₄₄₄][AA]-PMMA (50 wt%) in dry CO₂ flow condition (2.3% CO₂ and balance N₂) at 30 °C.

AAIL	M.W. [g/mol]	capacity [mmol/g-sorb]	capacity [mol/mol-AAIL]
[EMIM][Gly]	185.2	0.88	0.33
[EMIM][Lys]	256.4	1.06	0.54
[EMIM][His]	265.3	0.63	0.36
[EMIM][Ala]	199.3	0.80	0.30
[EMIM][BALA]	199.3	0.80	0.30
[EMIM][Arg]	284.4	0.28	0.17
[P ₄₄₄₄][Gly]	333.5	0.83	0.55
[P ₄₄₄₄][Lys]	404.6	0.79	0.64
[P ₄₄₄₄][His]	413.6	0.56	0.46

The CO₂ uptakes of [EMIM][Gly]- and [EMIM][Lys]-PMMA were slightly greater than [P₄₄₄₄][Gly]- and [P₄₄₄₄][Lys]-PMMA in any AAIL loadings, respectively, as seen from Figure 4.2. The unit of the capacity should be changed from mmol/g-sorbent to mol/mol-AAIL in order to discuss about reaction stoichiometry of the supported AAILs with CO₂. Hence, the CO₂

capture capacities of each sorbent with the loading of 50 wt% in terms of mol/mol-AAIL as well as mmol/g-sorbent are tabulated in Table 4.3. In units of mol/mol-AAIL, the capacities of [P₄₄₄₄][Gly]- and [P₄₄₄₄][Lys]-PMMA (50 wt%) are higher than those of [EMIM][Gly]- and [EMIM][Lys]-PMMA (50 wt%), respectively, unlike the orders in terms of mmol/g-sorbent. In addition, it is noteworthy that the capacity of [P₄₄₄₄][Gly]-PMMA (50 wt%) surpasses 0.5 mol/mol-AAIL under the low CO₂ concentration gas flow in which the influence of physisorption is negligible, although high AAIL loading can lead to low CO₂/AAIL ratio for supported sorbents prepared by impregnation methods [23]. It is improbable for CO₂ uptake of Gly anion-functionalized solid sorbent with high loading to exceed 0.5 mol/mol-AAIL, if the reaction proceeds in a 2:1 stoichiometry (Equations 4.1 and 4.2) without physical adsorption, since Gly has only one primary amino group in its structure (Table 4.1) that can react with CO₂. Yang et al. have demonstrated that CO₂ absorption on pure phosphonium AAILs, [P₄₄₄₄][AAs] and [P₆₆₆₁₄][AAs], occurred in both 1:1 and 2:1 stoichiometries (AAIL:CO₂), while their CO₂ capture capacities approached 1.0 mol/mol-AAIL rather than 0.5 mol/mol-AAIL [7]. Thus, our experimental results imply that even CO₂ adsorption on phosphonium AAIL-functionalized solid sorbents can take place via 1:1 as well as 2:1 stoichiometries. In contrast, the capacity of [EMIM][Gly]-PMMA (50 wt%) was only 0.33 mol/mol-AAIL (Table 4.3), emphasizing the effect of cation on reaction stoichiometry of AAIL-functionalized solid sorbents with CO₂. This difference can be attributed to the ion size of EMIM cation smaller than P₄₄₄₄ cation (Table 4.2) as larger cations can reduce cation-anion interactions in AAILs, leading to increase in basicity of the AA anions that can facilitate the CO₂ sorption [7]. The similar experimental result is seen in a published paper by Khanna's group, in which CO₂ absorption capacity of another imidazolium AAIL, [BMIM][Gly], did not also achieve 0.5 mol/mol-AAIL [10]. [EMIM][Lys]- and

[P₄₄₄₄][Lys]-PMMA (50 wt%) showed higher CO₂/AAIL ratios than [EMIM][Gly]- and [P₄₄₄₄][Gly]-PMMA (50 wt%) as found in Table 4.3. This is because Lys has another amino group in its side chain, and it could react with CO₂ to some degree.

4.5.2 Effect of anion of AAIL on CO₂ adsorption performance under dry CO₂ inlet

CO₂ sorption experiments of [EMIM][AA]-PMMA with various loadings using other AAs (Ala, BALA and Arg) as anions were also carried out in dry CO₂ flow condition. The relationship between AAIL loadings and CO₂ capture capacities of all the [EMIM][AA]-PMMA sorbents is depicted in Figure 4.3.

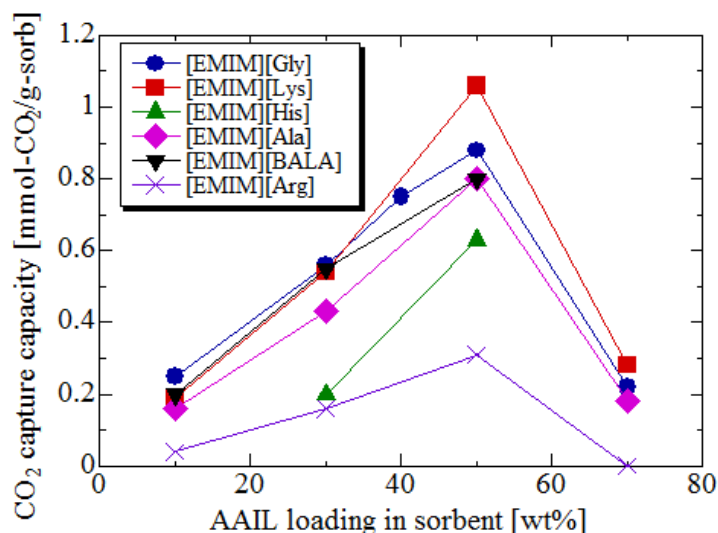


Figure 4.3. Relationship between AAIL loadings and CO₂ capture capacities of [EMIM][AA]-PMMA sorbents under dry CO₂ flow condition (2.3% CO₂ and balance N₂) at 30 °C (AA: Gly, Lys, His, Ala, BALA or Arg).

All the [EMIM][AA]-PMMA sorbents reached their maximum CO₂ capture capacities at 50 wt% loading. The capacities of these other [EMIM][AA]-PMMA sorbents with 50 wt% loadings in

both units of mmol/g-sorbent and mol/mol-AAIL are also listed in Table 4.3. [EMIM][Ala]- and [EMIM][BALA]-PMMA (50 wt%) showed comparable capacities with [EMIM][Gly]-PMMA (50 wt%) especially in units of mol/mol-AAIL, despite small differences in the molecular structures among the three AAs (Table 4.1). On the other hand, [EMIM][His]- and [EMIM][Arg]-PMMA (50 wt%) exhibited lower capacities than these sorbents, although His and Arg have more amine groups in their side chains (Table 4.1). Also, the capacity of [P₄₄₄₄][His]-PMMA (50 wt%) were lower than that of [P₄₄₄₄][Gly]-PMMA (50 wt%). The similar tendencies are found in previous reports on CO₂ adsorption studies using supported AAIL solid sorbents [4,6], while pure His and Arg anion-functionalized ILs have displayed good CO₂ absorption capacities owing to their more amine groups [10,24]. However, [EMIM][Lys]- and [P₄₄₄₄][Lys]-PMMA showed a better CO₂ capture performance due to another amino group in Lys side chain. This discrepancy might be attributed to differences in steric complexity of the side chain and the forms of amino groups in AA that can affect the interaction with CO₂, since Lys has a linear side chain with primary amino groups, whereas His and Arg have complicated side chains with secondary (and tertiary) amino groups as well as primary ones. Thus, it is indicated that AAs having simpler structures with only primary amino groups, like Gly and Lys, can become more promising platforms for AAIL-functionalized solid sorbents with better CO₂ capture performance.

4.5.3 Kinetic analysis of CO₂ adsorption in dry CO₂ flow

In order to analyze the CO₂ adsorption kinetics of [EMIM][AA]- and [P₄₄₄₄][AA]-PMMA sorbents, the following double exponential model was adopted [25]:

$$M_t/M_e = A_S(1 - \exp(-k_S t)) + A_D(1 - \exp(-k_D t)) \quad (4.3)$$

where M_t and M_e are experimental mass gains of the sorbent due to CO₂ adsorption at time t and after reaching the equilibrium, A_S and A_D are the relative contributions of surface and diffusion barriers controlling the overall adsorption process, with $A_S + A_D = 1$, and k_S and k_D are the corresponding surface and diffusion rate constants, respectively [22]. This model has adjusted to CO₂ adsorption study data using other solid sorbents successfully [6,22,26]. Equation 4.3 can be further rewritten to obtain an equation representing molar CO₂ uptake per unit weight of sorbent, C_t , at time t as follows:

$$C_t = C_e - A_1 \exp(-k_S t) - A_2 \exp(-k_D t) \quad (4.4)$$

where $C_t = M_t / (44 W_{\text{sorbent}})$, $C_e = M_e / (44 W_{\text{sorbent}})$, $A_1 = M_e A_S / (44 W_{\text{sorbent}})$, $A_2 = M_e A_D / (44 W_{\text{sorbent}})$, respectively. 44 is molecular weight of CO₂, and W_{sorbent} is sample weight of the sorbent. The experimental data of CO₂ uptake with time for all the [EMIM][AA]- and [P₄₄₄₄][AA]-PMMA sorbents with several loadings were fitted with Equation 4.4. The fitted curves are shown in Figures S4.2 to S4.10 of the Supporting Information along with the experimental data. In addition, the obtained parameters in equation 4.4 (A_1 , A_2 , k_S and k_D) and the coefficient of determination, R^2 , are listed in each figure. It is found that the CO₂ adsorption processes for all the sorbents also have two steps as described above, regardless of the type and loading of AAILs: fast exponential weight gain, followed by much slow weight change. Furthermore, the double exponential model (Equation 4.4) fits the experimental CO₂ adsorption data of nearly all the sorbents very well with R^2 of over 0.99. k_S values are larger than k_D values by approximately one order of magnitude for each sorbent. These facts indicate that the two steps in CO₂ adsorption for all the sorbents could be interpreted as follows [6]: CO₂ adsorption occurs first on the surface of sorbent (k_S), where CO₂ reacts with active species on the surface rapidly; then, once the surface

active species bonds with CO_2 , CO_2 diffuses into the sorbent to further reacts with the inner active species (k_D), which is a much slow process. Subsequently, k_S and k_D values were plotted with respect to AAIL loadings in the sorbents in Figure 4.4a and b, respectively.

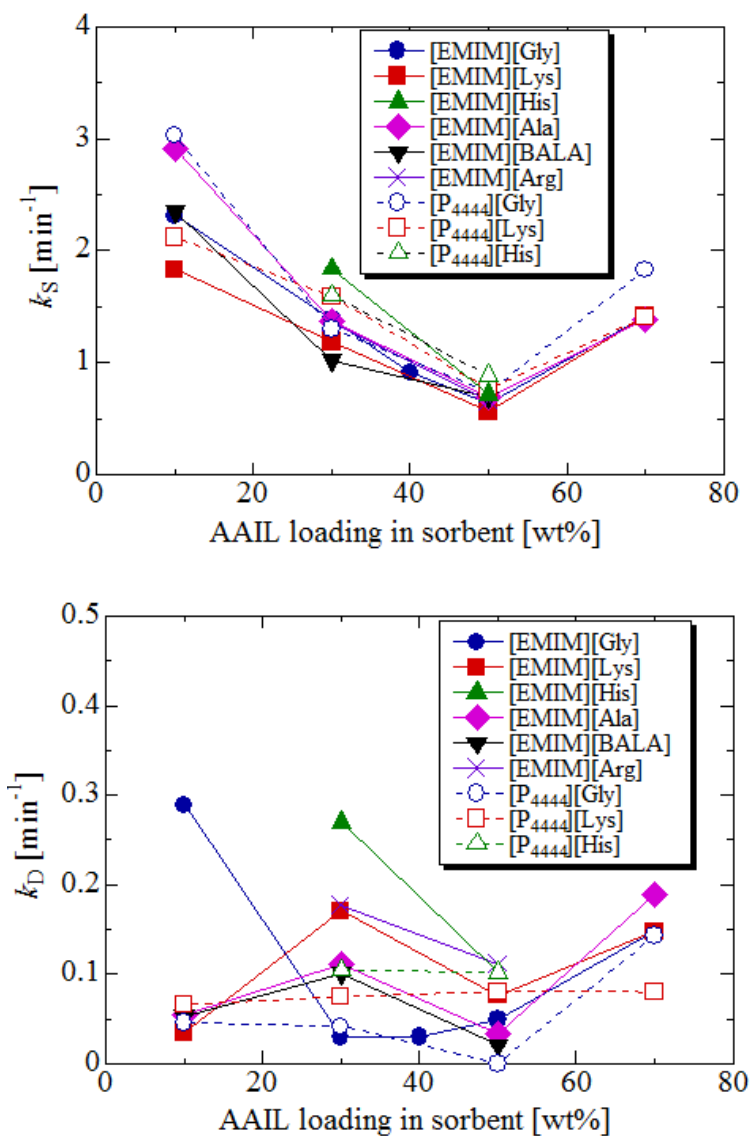


Figure 4.4. Plot of (a) k_S and (b) k_D of AAIL-PMMA sorbent under dry CO_2 flow condition (2.3% CO_2 and balance N_2) at 30 °C vs AAIL loading in the sorbent, respectively.

Interestingly, k_s values decreases with higher AAIL loadings, reaches the minimum values at 50 wt% but increases at 70 wt% for all the sorbents. This trend is opposite to that of CO₂ capture capacities as seen from Figures 4.2 and 4.3. The decreases in k_s until 50 wt% mean that the surface reaction resistances on the AAIL active sites increase with higher loadings. This can be partly attributed to an impregnation method used for synthesizing the sorbents, since it has been reported that supported amine sorbents prepared by impregnation methods caused reduction in the CO₂ adsorption rates with higher loadings while enhancing the capacities [23]. However, k_s values at 70 wt% gets greater than 50 wt%, although the CO₂ capture capacities at 70 wt% are much lower than other loadings (Figures 4.2 and 4.3). This might be because at 70 wt% most of the active species in AAILs would deposit on the surface without finely dispersing into the pores of PMMA, causing less surface reaction resistances but also much lower capacities. On the other hand, k_D values do not show an identical trend in relationships with AAIL loadings for all the sorbents. Thus, a strong correlation is seen just between AAIL loadings and k_s values. At 50 wt% all the sorbents exhibited their largest capacities but lowest surface reaction rates (k_s). Obviously, both higher CO₂ adsorption capacity and rate are desirable in developing promising sorbents. Therefore, novel support materials and supporting procedures should be examined in our future work.

Also, CO₂ sorption experiments of [EMIM][Lys]-PMMA, [P₄₄₄₄][Lys]-PMMA (50 wt%) and pure PMMA were performed at different adsorption temperatures (30, 50, 70 and 90 °C) and CO₂ inlet concentrations (2.3, 15, 50 and 80%) in dry gas flow condition using Perkin-Elmer Pyris-STA 6000 TGA instead of the TGA-MS system (Thermax 500 TGA). The kinetic data for those experimental results were analyzed with the double exponential model, as well. The CO₂ capture capacities and k_s values for [EMIM][Lys]-PMMA (50 wt%) and pure PMMA obtained

under the different CO₂ concentrations and 30 °C of the adsorption temperature are tabulated in Table 4.4.

Table 4.4. CO₂ capture capacities and k_s values of [EMIM][Lys]-PMMA (50 wt%) and pure PMMA obtained at different CO₂ inlet concentrations and 30 °C using Thermax 500 or Perkin-Elmer STA 6000 TGA.

sample	TGA	C _{CO2} [vol%]	capacity [mmol/g-sorb]	k_s [min ⁻¹]
[EMIM][Lys] -PMMA (50 wt%)	Thermax 500	2.3	1.06	0.56
		2.3	1.09	0.96
	Perkin-Elmer	15	1.25	2.26
	STA 6000	50	1.38	5.99
		80	1.37	13.4
PMMA	Thermax 500	2.3	0.03	1.68
		2.3	0.10	2.31
	Perkin-Elmer	15	0.20	3.95
	STA 6000	50	0.38	5.90
		80	0.53	13.4

The capacities and k_s increased with higher CO₂ concentration for both the [EMIM][Lys]-PMMA and pure PMMA. The similar tendency of enhancement in CO₂ capture capacity with

higher CO₂ concentration has been reported by Wu's group using other types of supported AAILs [4]: the capacities of supported N-(3-Aminopropyl) aminoethyl tributylphosphonium or [apaeP₄₄₄][Lys] and [apaeP₄₄₄][Gly] (50 wt% loadings) were 1.87 and 1.65 mmol/g-sorbent at 100% of CO₂ concentration, but they decreased to 1.54 and 1.37 mmol/g-sorbent at 14% of CO₂ concentration, respectively (higher capacities for these sorbents than our results can be because these sorbents have more amino groups in not only the anions but also the cations).

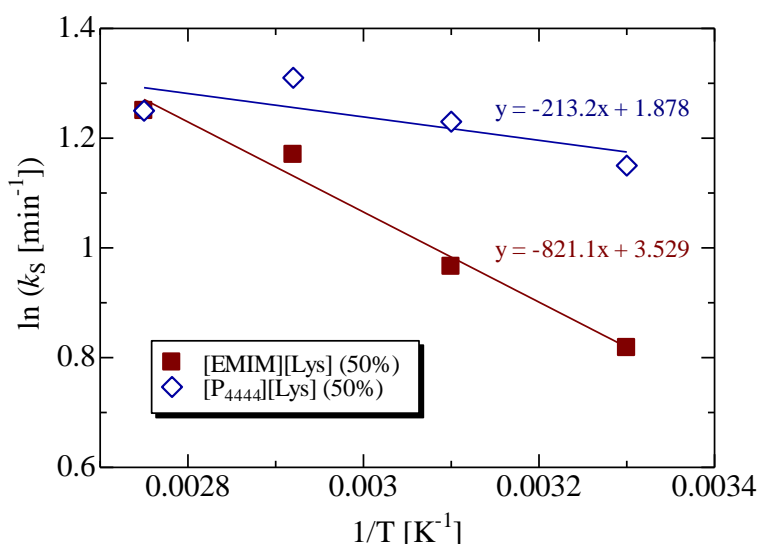


Figure 4.5. Arrhenius plots of k_s for [EMIM][Lys]-PMMA and [P₄₄₄][Lys]-PMMA (50 wt%) adsorption data obtained at different adsorption temperatures and 15% of CO₂ concentration.

In contrast, these values at 2.3% of CO₂ concentration with Perkin-Elmer STA 6000 were close to those in the same run condition with Thermax 500 TGA. CO₂ adsorption on pure PMMA occurs by only physisorption. Therefore, it is considered that enhancements in the CO₂ sorption capacity and rate for the [EMIM][Lys]-PMMA sorbent with higher CO₂ concentration are attributed to not only chemisorption but also physisorption. Figure 4.5 shows Arrhenius plots of

k_s for the [EMIM][Lys]-PMMA and [P₄₄₄₄][Lys]-PMMA (50 wt%) adsorption data obtained under the different adsorption temperatures and 15% of CO₂ concentration. For both sorbents, k_s values increased with higher adsorption temperature, and almost linear relationships were gained between $\ln k_s$ and $1/T$. The activation energies for the [EMIM][Lys]-PMMA and [P₄₄₄₄][Lys]-PMMA (50 wt%) sorbents calculated by the Arrhenius equation were 6.8 and 1.8 kJ/mol, respectively. Thus, the activation barrier of the [P₄₄₄₄][Lys]-PMMA (50 wt%) is less than that of the [EMIM][Lys]-PMMA (50 wt%). Larger ion size of [P₄₄₄₄] cation than [EMIM] cation might contribute to lower activation barrier as well as higher CO₂/AAIL molar ratio (Table 4.3) of the [P₄₄₄₄][Lys]-PMMA than those of the [EMIM][Lys]-PMMA.

4.5.4 Comparison of CO₂ and H₂O adsorption behaviors under humidified CO₂ inlet

Next, CO₂ capture experiments in humidified CO₂ inlet condition were conducted to evaluate the effect of water vapor on the CO₂ adsorption behaviors. [EMIM][AA]-PMMA and [P₄₄₄₄][AA]-PMMA sorbents with 50 wt% loadings (AA: Gly, Lys and His) were used since all the sorbents exhibited their best CO₂ capture capacities at 50 wt% in dry gas flow. 2.3% of CO₂ and 2.1% of water vapor were selected for the humidified gas condition, assuming that actual flue gas contains almost equimolar amounts of CO₂ and water vapor. The amounts of CO₂ and H₂O uptakes for the [EMIM][AA]- and [P₄₄₄₄][AA]-PMMA sorbents are shown in Figure 4.6a and b, respectively. Comparing Figure 4.6b with 4.6a, it is seen that the [P₄₄₄₄][AA]-PMMA sorbents adsorbed only approximately half amounts of H₂O of the corresponding [EMIM][AA]-PMMA sorbents under the humidified gas flow, regardless of the type of AA anion. The less H₂O uptakes of [P₄₄₄₄][AA]-PMMA sorbents can be attributed to hydrophobic alkyl chains of P₄₄₄₄ cation. It is expected that a significant difference in H₂O uptakes due to the cation types could affect the CO₂ adsorption capacities. However, the amounts of CO₂ uptakes of both

[EMIM][AA]- and [P₄₄₄₄][AA]-PMMA sorbents slightly reduced in a similar way in the presence of water vapor.

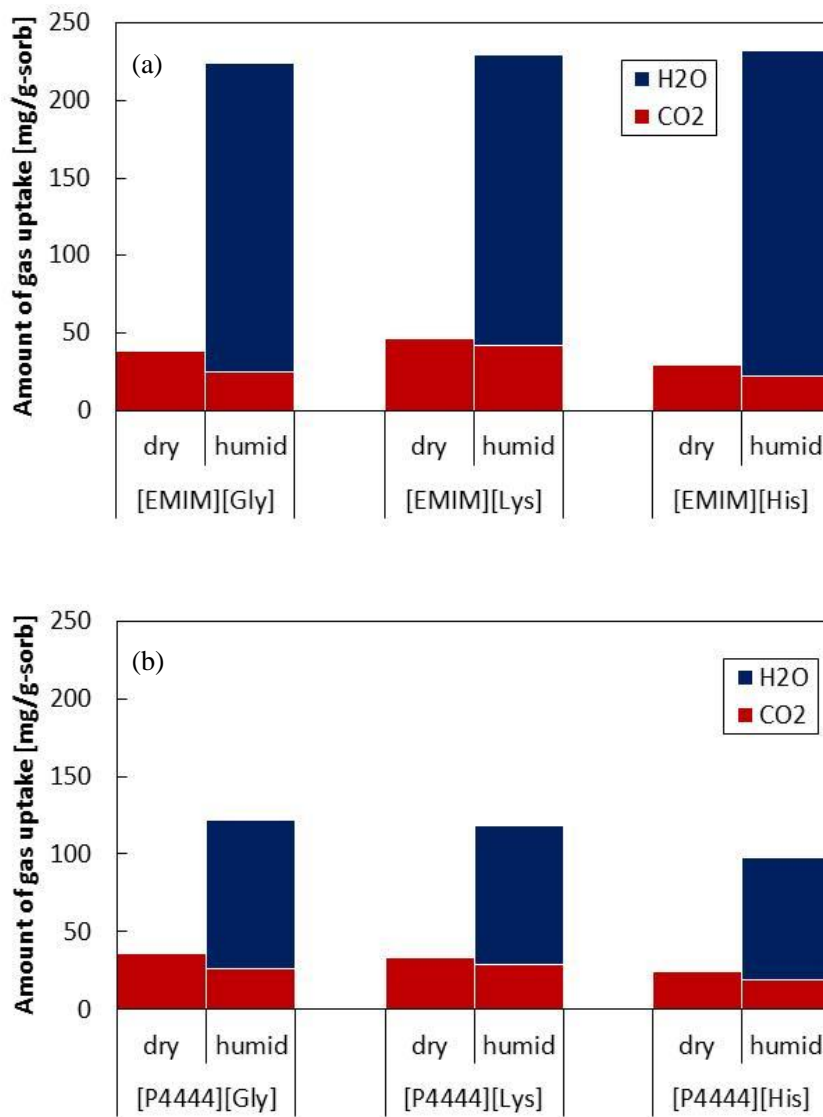


Figure 4.6. Amounts of CO₂ and H₂O uptakes of (a) [EMIM][AA]-PMMA (50 wt%), and (b) [P₄₄₄₄][AA]-PMMA (50 wt%) sorbents in dry (2.3% CO₂ and balance N₂) and humidified gas (2.3% CO₂, 2.1% H₂O and balance N₂) inlets at 30 °C, respectively (AA: Gly, Lys or His).

The same experiments were also conducted using pure Lys immobilized into PMMA (20 wt% loading) prepared in the same manner as AAIL-PMMA sorbents, designated as Lys-PMMA. As a result, the Lys-PMMA sorbent slightly increased the amount of CO₂ uptake in the presence of water vapor while adsorbing much larger amount of water vapor than CO₂ as well, as shown in Figure 4.7. Thus, water vapor exerted a negative impact on CO₂ capture performance of AAIL-PMMA sorbents but a positive impact on that of Lys-PMMA sorbent, despite difference in the total amounts of H₂O uptakes.

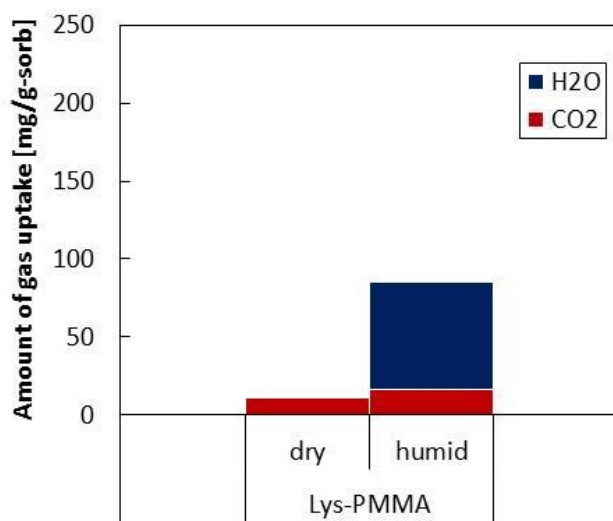


Figure 4.7. Amounts of CO₂ and H₂O uptakes of Lys-PMMA (20 wt%) sorbent in the dry and humidified gas inlets at 30 °C.

In order to compare the CO₂ adsorption behaviors of AAIL-PMMA sorbents with that of Lys-PMMA in the presence of water vapor more deeply, changes in CO₂ uptakes of [EMIM][Lys]-PMMA (50 wt%), [P₄₄₄₄][Lys]-PMMA (50 wt%) and Lys-PMMA (20 wt%) sorbents with time under dry and humidified gas inlets are depicted in Figure 4.8a, b and c, respectively.

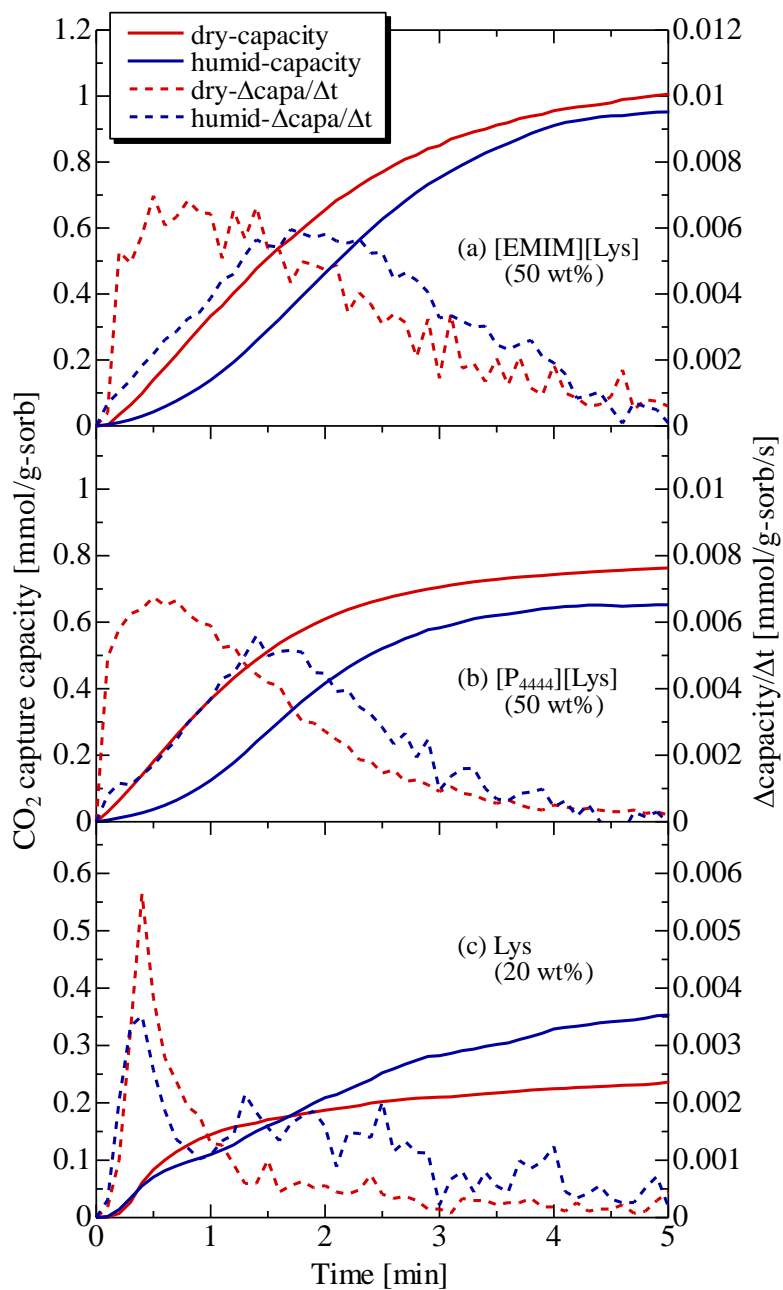
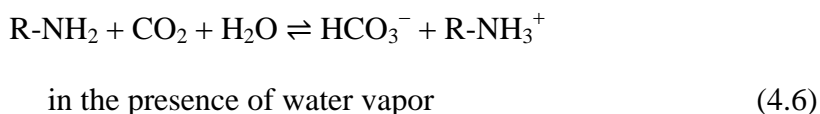
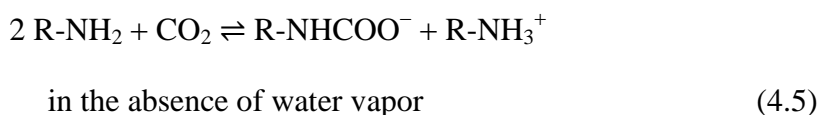


Figure 4.8. CO₂ sorption behaviors of (a) [EMIM][Lys]-PMMA (50 wt%), (b) [P₄₄₄₄][Lys]-PMMA (50 wt%) and (c) Lys-PMMA (20 wt%) sorbents with time under dry (2.3% CO₂ and balance N₂) and humidified gas (2.3% CO₂, 2.1% H₂O and balance N₂) inlets at 30 °C, respectively.

Small changes in CO₂ uptakes per time step of the TGA-MS analysis, $\Delta\text{capacity}/\Delta t$ ($\Delta t = 6$ s), with time are also depicted in this figure, representing the apparent CO₂ sorption rates. From Figure 4.8, considerable differences are seen in the CO₂ sorption rates as well as capacities. For the [EMIM][Lys]- and [P₄₄₄₄][Lys]-PMMA sorbents, not only the capacities, but also the sorption rates ($\Delta\text{capacity}/\Delta t$) greatly decreased in the presence of water vapor until 1.5 min from beginning of the CO₂ adsorption, although the rates overtook those in the dry gas flow after 1.5 min. The reductions in CO₂ sorption rates as well as capacities at the beginning stages indicate that water vapor inhibited the surface reactions of active species in the AAILs with CO₂. In contrast, for the Lys-PMMA sorbent, although the CO₂ sorption rate reduced before 1.5 min in the presence of water vapor, the rate increased after 1.5 min, leading to higher capacity. It has been reported that supported amine sorbents enhanced their CO₂ capture capacities in the presence of water vapor by increasing the CO₂/amine stoichiometric ratios through a different reaction scheme with CO₂ from that in the absence of water vapor, as seen from Equations 4.5 and 4.6 [17,21,27–31].



It is possible that the Lys-PMMA sorbent passed the similar reaction mechanism with CO₂ as supported amines under the humidified gas flow (Equation 4.6) to increase the sorption rate and uptake. These differences in the CO₂ sorption rates and capacities between Lys

anion-functionalized IL and pure Lys supported sorbents imply that cations of AAILs hinder reaction of the active species with CO₂ in the presence of water vapor maybe due to a hydrogen bond interaction between the cations and water vapor.

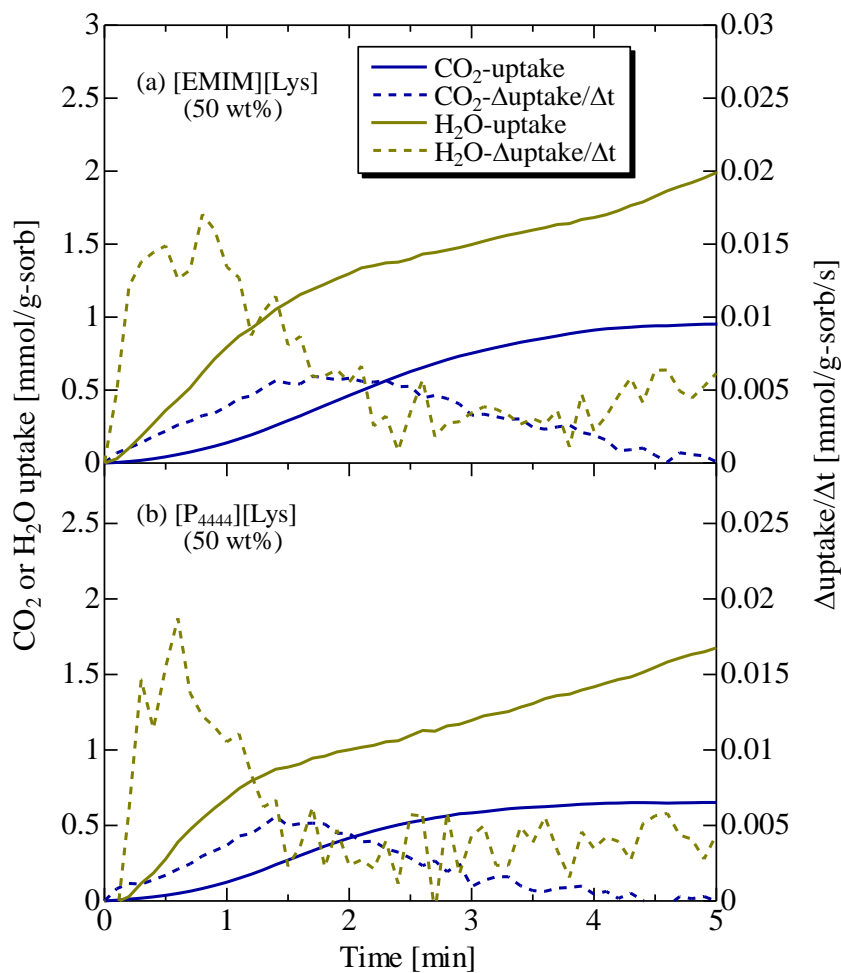


Figure 4.9. CO₂ and H₂O sorption behaviors of (a) [EMIM][Lys]-PMMA (50 wt%) and (b) [P₄₄₄₄][Lys]-PMMA (50 wt%) sorbents with time under humidified gas flow (2.3% CO₂, 2.1% H₂O and balance N₂) at 30 °C, respectively.

Comparisons of gas uptake behaviors of H₂O and CO₂ for [EMIM][Lys]- and [P₄₄₄₄][Lys]-PMMA sorbents (50 wt%) at beginning stages of the adsorption in the humidified gas flow are depicted in Figure 4.9a and b, respectively. $\Delta \text{uptake} / \Delta t$ in this figure represents the apparent sorption rates of each gas. It is seen that not only the uptakes, but also the sorption rates of H₂O are much higher than those of CO₂ until 1.5 min from the beginning for both sorbents to nearly same degrees, despite difference in the total amounts of H₂O uptakes between these sorbents (Figure 4.6); the H₂O uptake of the [EMIM][Lys]-PMMA sorbent continued increasing much longer time and much larger than that of the [P₄₄₄₄][Lys]-PMMA sorbent. This fact indicates that much faster initial H₂O uptake inhibits surface reaction of the AAIL active sites with CO₂ to decrease the CO₂ sorption rates and capacities in the presence of water vapor for [EMIM][AA]- and [P₄₄₄₄][AA]-PMMA sorbents.

4.5.5 TPD behaviors of CO₂ adsorbed in dry and humidified gas flow

TPD experiments of [EMIM][Lys]-PMMA (50 wt%), [P₄₄₄₄][Lys]-PMMA (50 wt%) and Lys-PMMA (20 wt%) sorbents were carried out to compare the desorption behaviors of CO₂ adsorbed in dry and humidified gas flow conditions. The TPD behaviors of these sorbents are shown in Figure 4.10a, b and c. The ratio of MS signals of CO₂ over N₂ at a time divided by the initial sample weight loaded in the TGA, $\text{MS CO}_2 / \text{MS N}_2 / \text{sample weight}$, in this figure represents CO₂ concentration released from the sample at the time. The amounts of CO₂ desorbed from the [EMIM][Lys]- and [P₄₄₄₄][Lys]-PMMA sorbents are higher under the dry gas inlet than humidified gas inlet, whereas that from the Lys-PMMA sorbent is higher under the humidified gas inlet than dry gas inlet. These different trends agree with the CO₂ sorption test results for each sorbent in the two gas flow conditions (Figure 4.7).

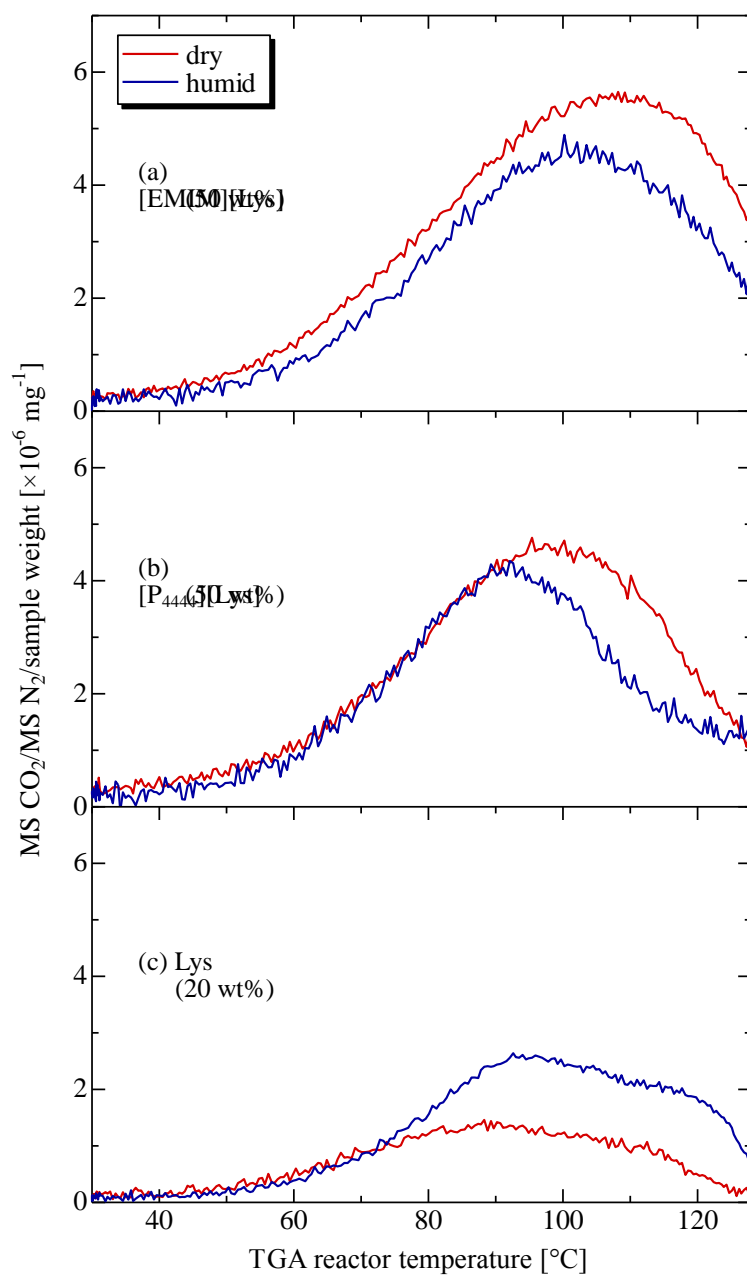


Figure 4.10. TPD behaviors of CO₂ adsorbed in dry and humidified gas flow conditions for (a) [EMIM][Lys]-PMMA (50 wt%), (b) [P₄₄₄₄][Lys]-PMMA (50 wt%) and (c) Lys-PMMA (20 wt%) sorbents with TGA temperature, respectively.

In addition, the CO₂ desorption peak temperature of the [EMIM][Lys]- and [P₄₄₄₄][Lys]-PMMA sorbents is slightly higher in the dry gas flow than humidified gas flow, while that of the Lys-PMMA sorbent is slightly higher in the humidified gas flow than dry gas flow. These facts indicate that, for the AAIL-PMMA sorbents, not only the amounts of CO₂ adsorbed, but also the stabilities of CO₂ bonded chemically with the AAILs reduce in the presence of water vapor. In contrast, for the Lys-PMMA sorbent, it is possible that in the presence of water vapor more stable bicarbonate than carbamate is produced (Equation 4.6), leading to the higher CO₂ desorption peak temperature as well as amount desorbed.

4.6 Conclusions

CO₂ capture performance of [EMIM][AA]-PMMA and [P₄₄₄₄][AA]-PMMA sorbents were compared using a TGA-MS analysis system under dry or humidified gas flow conditions. [P₄₄₄₄][AA]-PMMA sorbents showed higher CO₂ capture capacities than the corresponding [EMIM][AA]-PMMA sorbents in units of mol/mol-AAIL under dry gas inlet, exhibiting the effect of AAIL cation on the CO₂ adsorption. Especially, [P₄₄₄₄][Gly]-PMMA slightly exceeded 0.5 mol/mol-AAIL in the low CO₂ concentration flow condition, implying that the reaction stoichiometry of AAIL with CO₂ gets closer to 1:1 from 2:1 ratio, unlike [EMIM][Gly]-PMMA. Gly and Lys anions having linear side chains with only primary amino groups contributed to better CO₂ sorption performance than His and Arg anions having more complicated side chains with secondary and tertiary amino groups, although His and Arg have more amino groups. The CO₂ sorption behaviors of all the sorbents fitted in a double exponential model very well. At 50 wt% loading, the CO₂ capture capacities for all the sorbents reached their maximum values, whereas the surface reaction rates (k_s) reached their minimum values, regardless of AAIL cation

and anion types.

Under humidified gas flow, [P₄₄₄₄][AA]-PMMA sorbents adsorbed much less amounts of water vapor than [EMIM][AA]-PMMA sorbents. Nevertheless, CO₂ capture capacities of both types of sorbents slightly reduced in a similar way in the presence of water vapor. This can be attributed to much more rapid initial sorption rate of H₂O than CO₂ on the AAIL-PMMA sorbents, not total amounts of H₂O uptakes, leading to inhibition of the AAIL active sites for the surface reaction with CO₂.

4.7 Supporting Information

Table S4.1. Surface areas and pore volumes of PMMA, [EMIM][Lys]-PMMA, [P₄₄₄₄][Lys]-PMMA and [P₄₄₄₄][Gly]-PMMA with various loadings.

type	BET surface area [m ² /g]	BJH adsorption cumulative pore volume [cm ³ /g]
PMMA	527	1.12
[EMIM][Lys]-PMMA (10%)	327	0.93
[EMIM][Lys]-PMMA (50%)	38	0.35
[P ₄₄₄₄][Lys]-PMMA (10%)	256	0.99
[P ₄₄₄₄][Lys]-PMMA (50%)	37	0.32
[P ₄₄₄₄][Gly]-PMMA (10%)	378	1.04
[P ₄₄₄₄][Gly]-PMMA (30%)	118	0.69
[P ₄₄₄₄][Gly]-PMMA (50%)	26	0.25
[P ₄₄₄₄][Gly]-PMMA (70%)	9.0	0.02

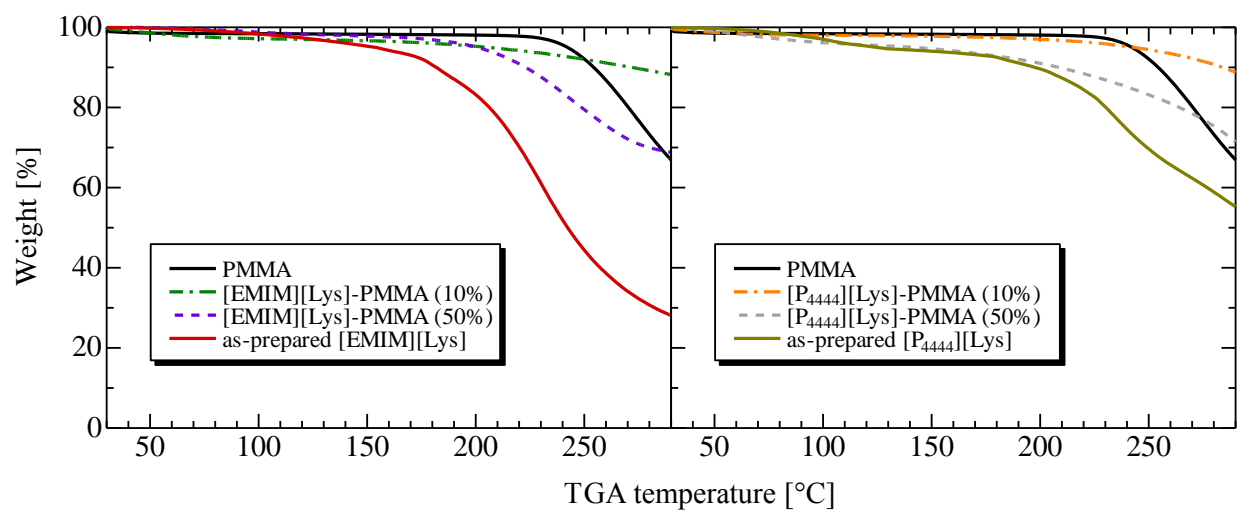


Figure S4.1. TGA curves of PMMA, [EMIM][Lys]-PMMA and [P₄₄₄₄][Lys]-PMMA with 10 and 50 wt% loadings, and as-prepared [EMIM][Lys] and [P₄₄₄₄][Lys] under N₂ atmosphere at a heating rate of 10 °C /min.

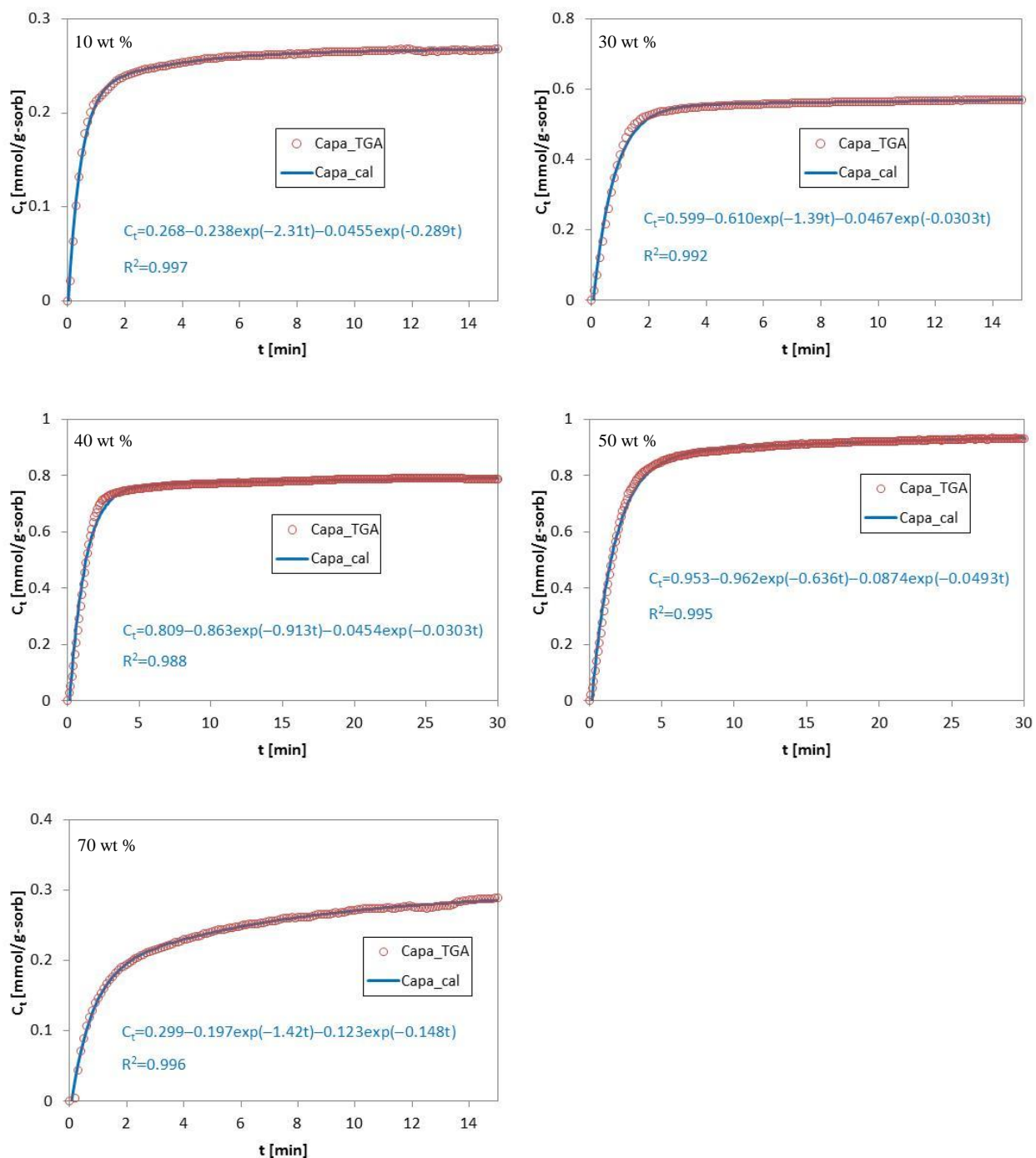


Figure S4.2. Fitted curves for CO₂ sorption experimental data of [EMIM][Gly]-PMMA sorbents with different loadings (Capa_TGA and Capa_cal represent the experimental and calculated data, respectively).

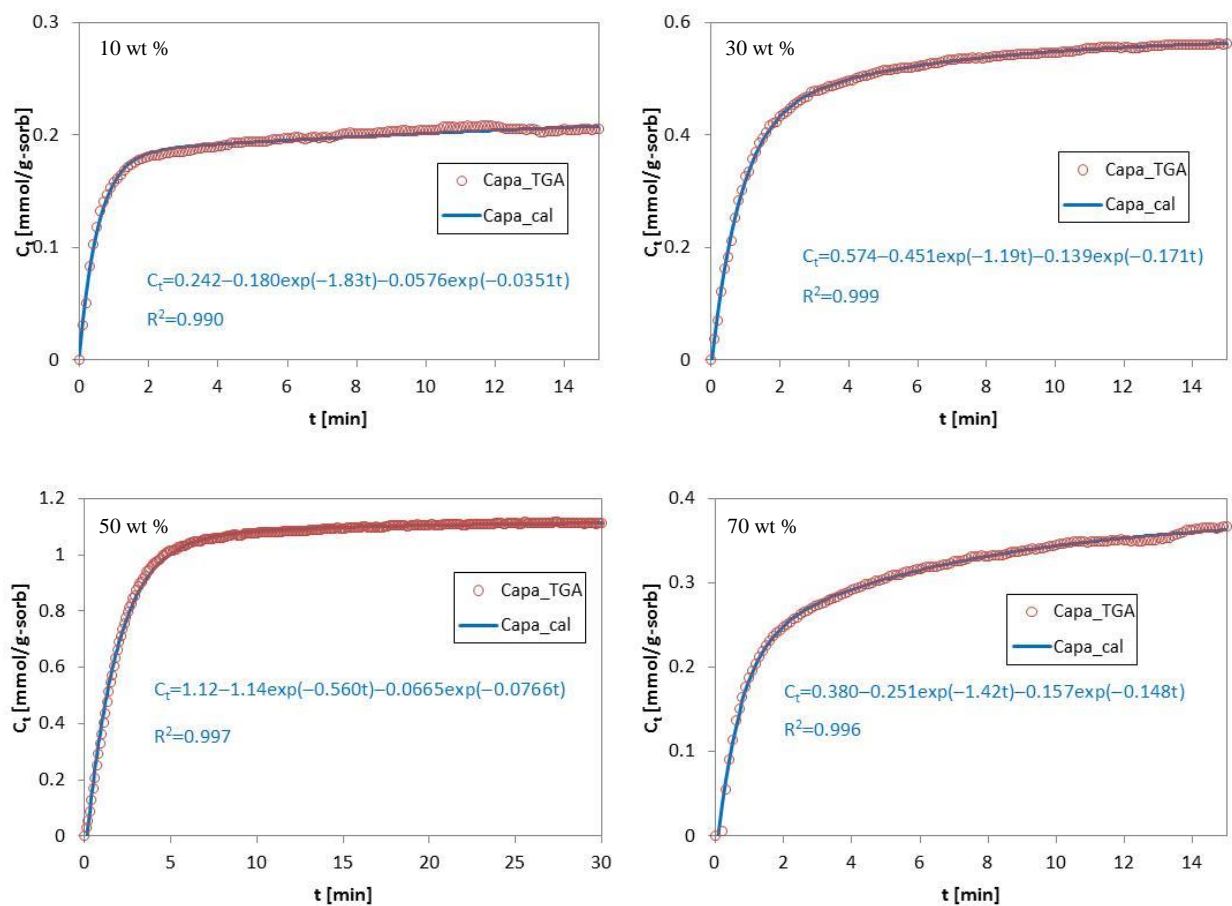


Figure S4.3. Fitted curves for CO₂ sorption experimental data of [EMIM][Lys]-PMMA sorbents with different loadings (Capa_TGA and Capa_cal represent the experimental and calculated data, respectively).

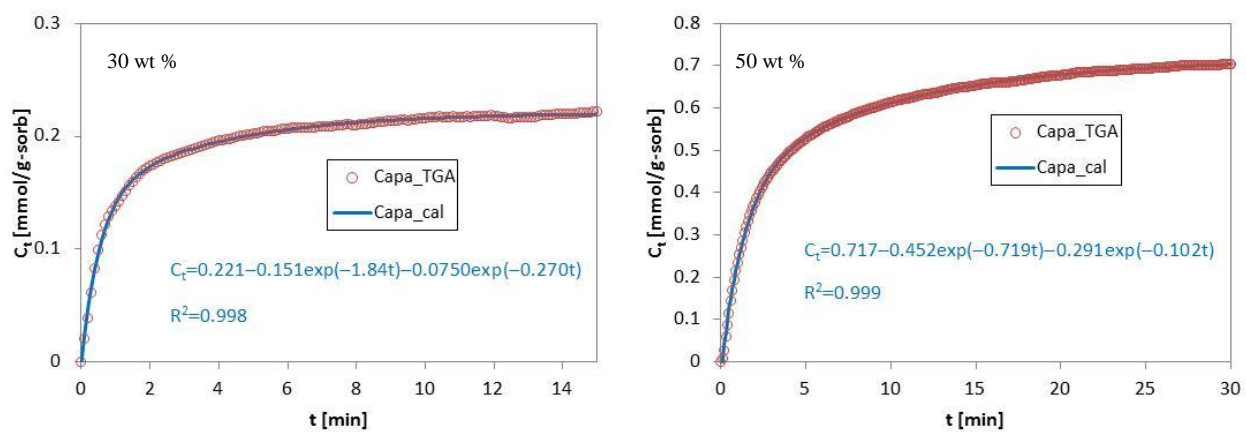


Figure S4.4. Fitted curves for CO₂ sorption experimental data of [EMIM][His]-PMMA sorbents with different loadings (Capa_TGA and Capa_cal represent the experimental and calculated data, respectively).

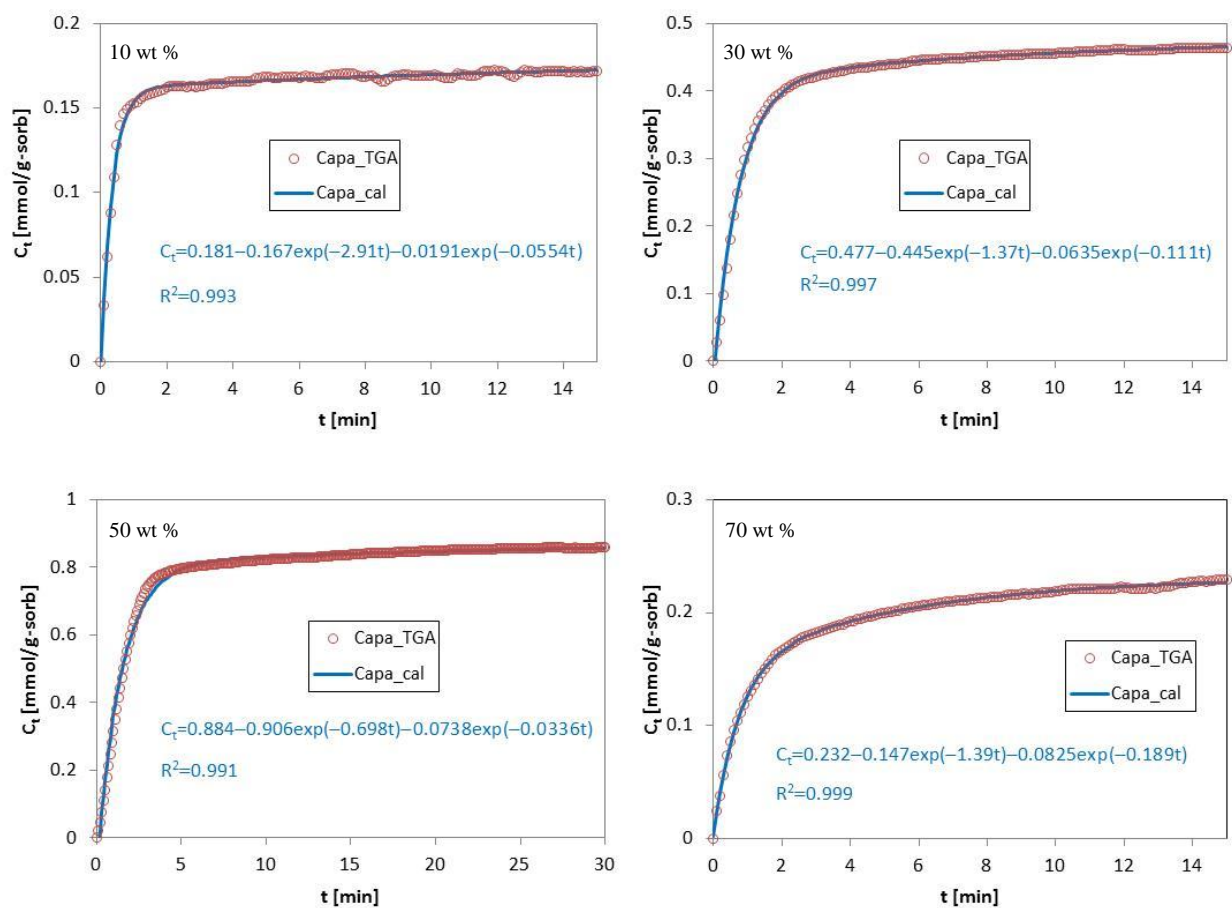


Figure S4.5. Fitted curves for CO₂ sorption experimental data of [EMIM][Ala]-PMMA sorbents with different loadings (Capa_TGA and Capa_cal represent the experimental and calculated data, respectively).

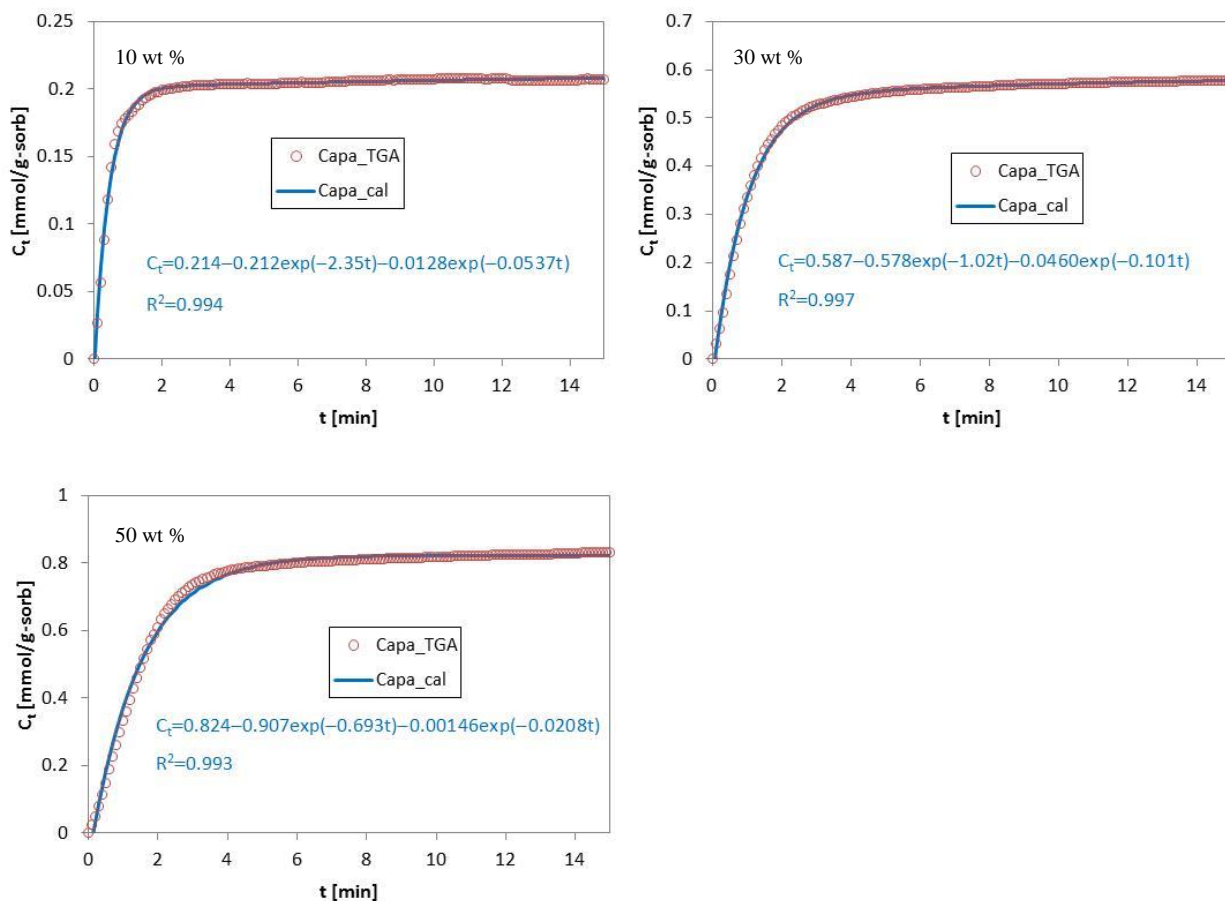


Figure S4.6. Fitted curves for CO₂ sorption experimental data of [EMIM][BALA]-PMMA sorbents with different loadings (Capa_TGA and Capa_cal represent the experimental and calculated data, respectively).

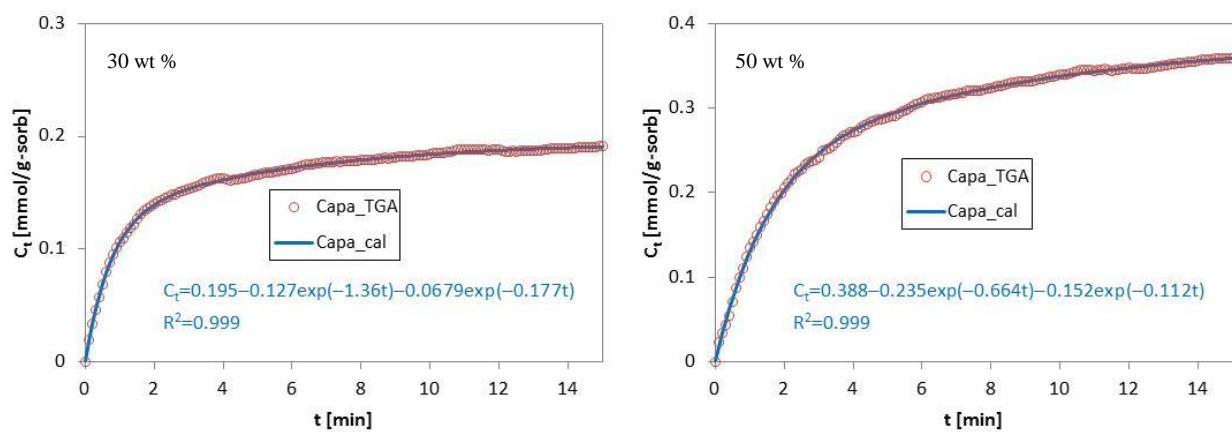


Figure S4.7. Fitted curves for CO₂ sorption experimental data of [EMIM][Arg]-PMMA sorbents with different loadings (Capa_TGA and Capa_cal represent the experimental and calculated data, respectively).

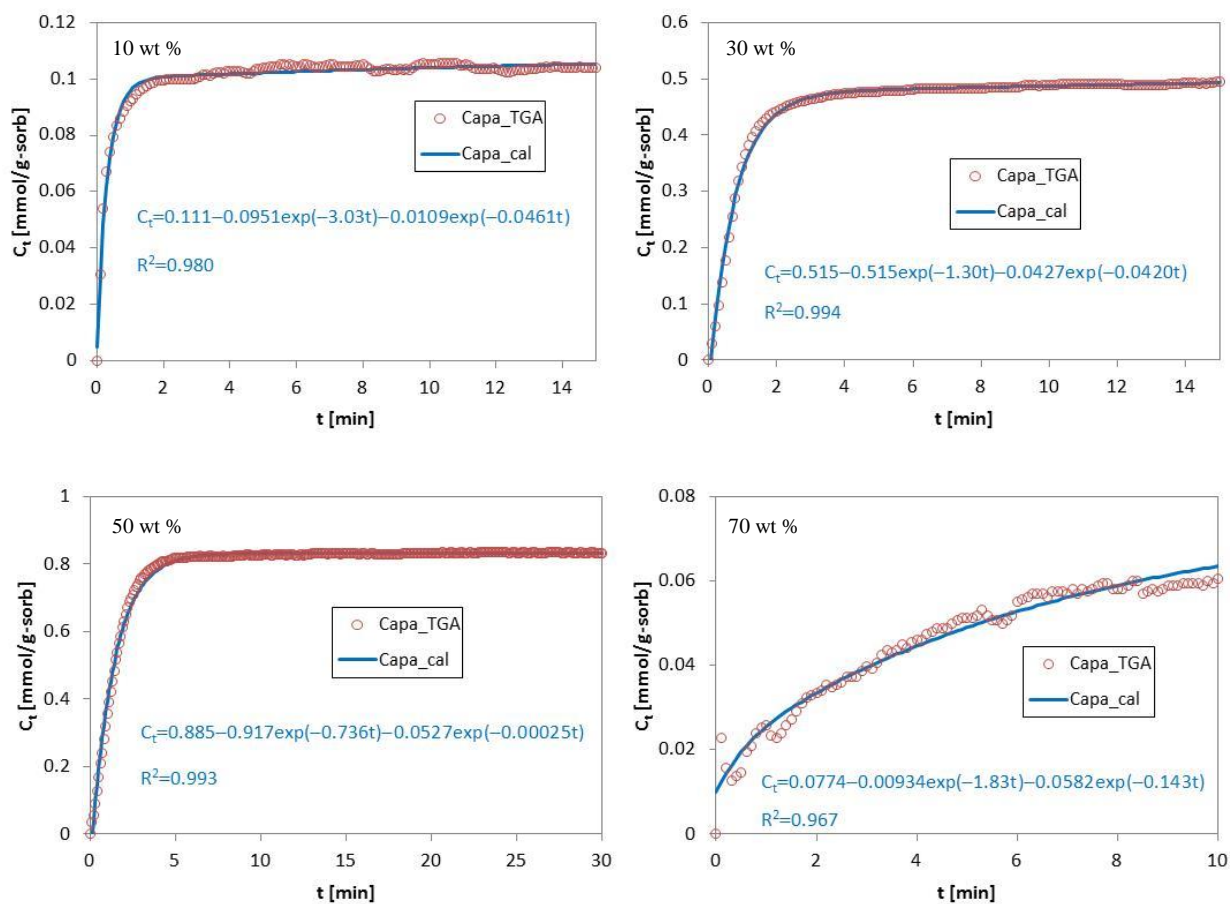


Figure S4.8. Fitted curves for CO₂ sorption experimental data of [P₄₄₄₄][Gly]-PMMA sorbents with different loadings (Capa_TGA and Capa_cal represent the experimental and calculated data, respectively).

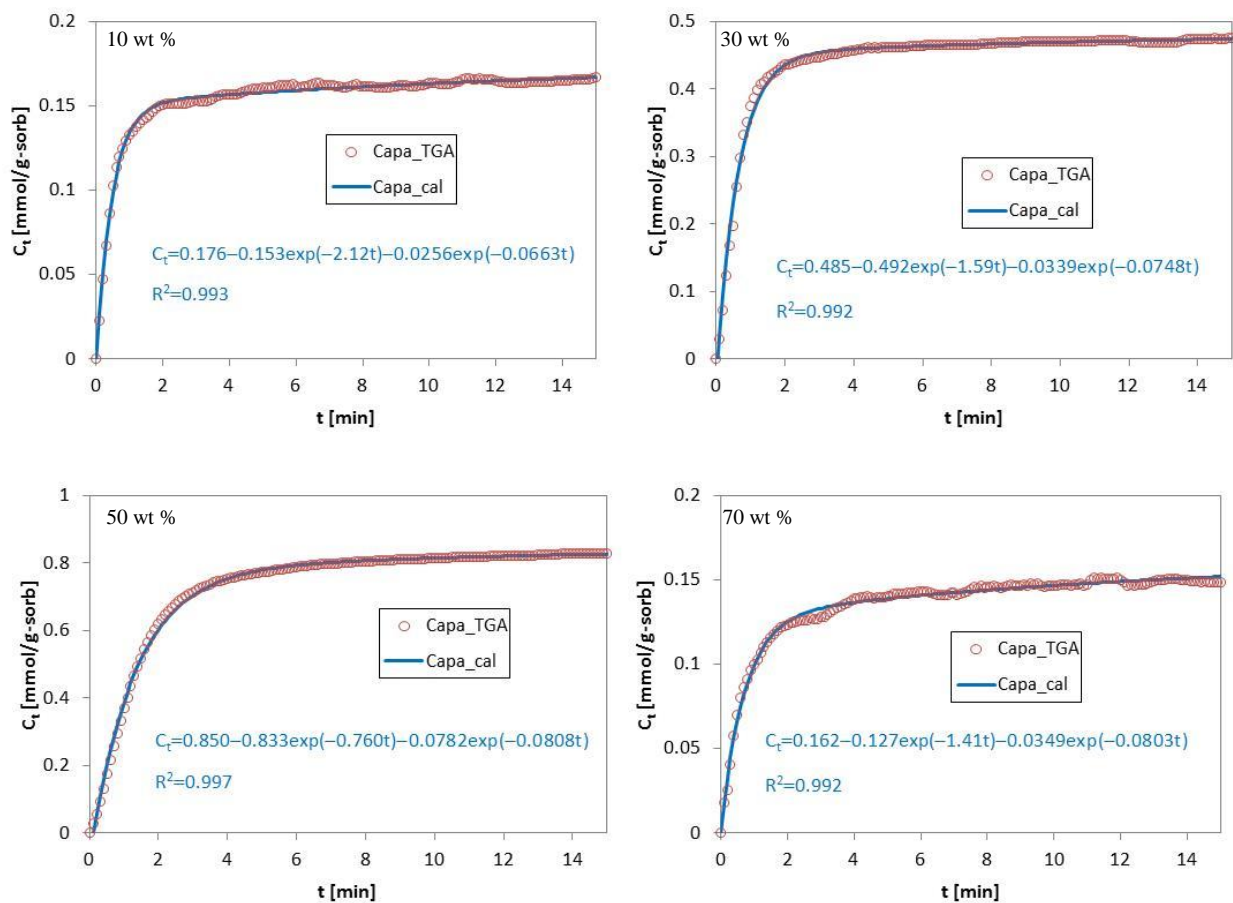


Figure S4.9. Fitted curves for CO₂ sorption experimental data of [P₄₄₄₄][Lys]-PMMA sorbents with different loadings (Capa_TGA and Capa_cal represent the experimental and calculated data, respectively).

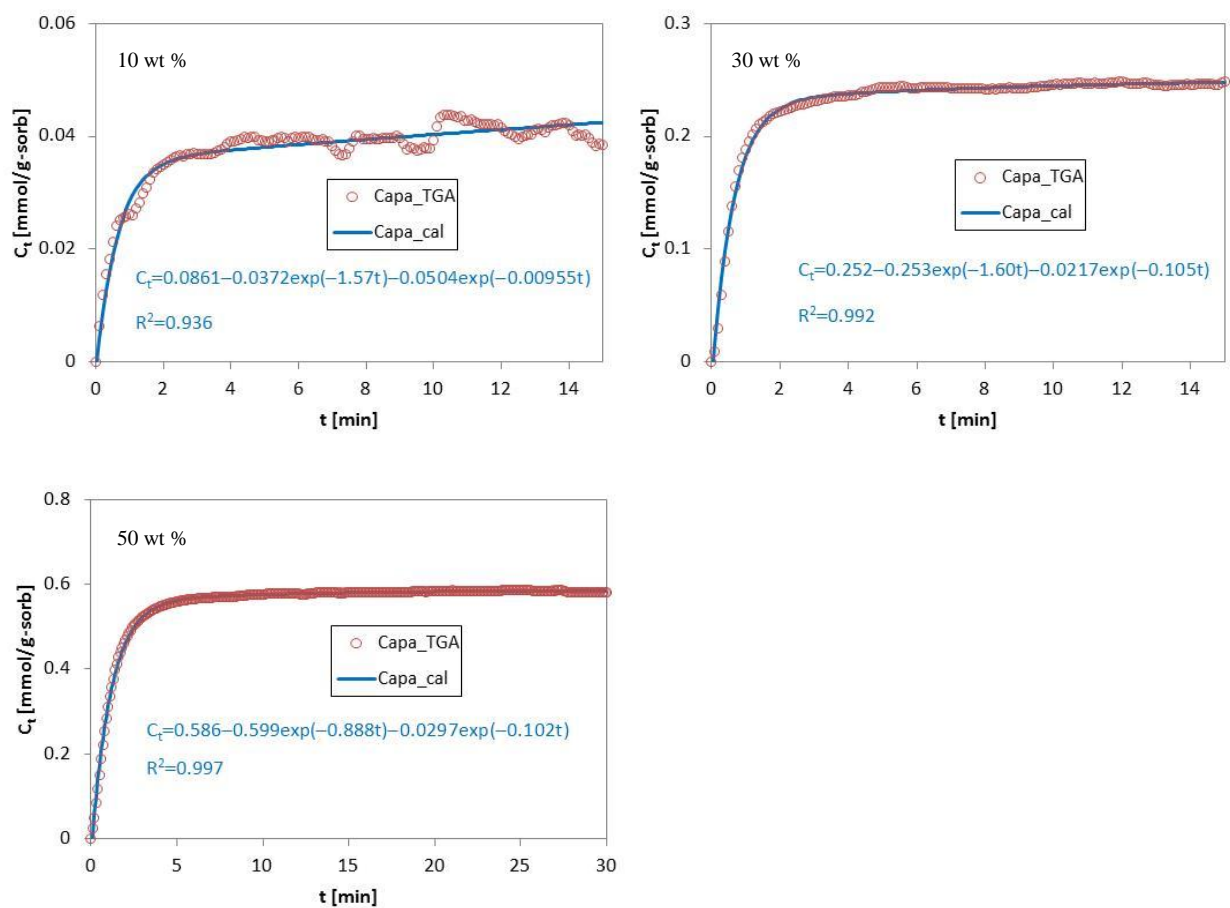


Figure S4.10. Fitted curves for CO₂ sorption experimental data of [P₄₄₄₄][His]-PMMA sorbents with different loadings (Capa_TGA and Capa_cal represent the experimental and calculated data, respectively).

4.8 References

- [1] J. Zhang, S. Zhang, K. Dong, Y. Zhang, Y. Shen, X. Lv, Supported absorption of CO₂ by tetrabutylphosphonium amino acid ionic liquids, *Chem. Eur. J.* 12 (2006) 4021–4026.
- [2] Y.Y. Jiang, G.N. Wang, Z. Zhou, Y.T. Wu, J. Geng, Z.B. Zhang, Tetraalkylammonium amino acids as functionalized ionic liquids of low viscosity, *Chem. Commun.* (2008) 505–507.
- [3] B.E. Gurkan, J.C. de la Fuente, E.M. Mindrup, L.E. Ficke, B.F. Goodrich, E.A. Price, W.F. Schneider, J.F. Brennecke, Equimolar CO₂ absorption by anion-functionalized ionic liquids, *J. Am. Chem. Soc.* 132 (2010) 2116–2117.
- [4] J. Ren, L. Wu, B.G. Li, Preparation and CO₂ sorption/desorption of N-(3-aminopropyl)aminoethyl tributylphosphonium amino acid salt ionic liquids supported into porous silica particles, *Ind. Eng. Chem. Res.* 51 (2012) 7901–7909.
- [5] X. Wang, N.G. Akhmedov, Y. Duan, D. Luebke, B. Li, Immobilization of amino acid ionic liquids into nanoporous microspheres as robust sorbents for CO₂ capture, *J. Mater. Chem. A.* 1 (2013) 2978–2982.
- [6] X. Wang, N.G. Akhmedov, Y. Duan, D. Luebke, D. Hopkinson, B. Li, Amino acid-functionalized ionic liquid solid sorbents for post-combustion carbon capture, *ACS Appl. Mater. Interfaces.* 5 (2013) 8670–8677.
- [7] Q. Yang, Z. Wang, Z. Bao, Z. Zhang, Y. Yang, Q. Ren, H. Xing, S. Dai, New insights into CO₂ absorption mechanisms with amino-acid ionic liquids, *ChemSusChem* 9 (2016) 806–812.
- [8] H. Knuutila, U.E. Aronu, H.M. Kvamsdal, A. Chikukwa, Post combustion CO₂ capture with an amino acid salt, *Energy Procedia.* 4 (2011) 1550–1557.

- [9] D. Guo, H. Thee, C.Y. Tan, J. Chen, W. Fei, S. Kentish, G.W. Stevens, G. da Silva, Amino acids as carbon capture solvents: Chemical kinetics and mechanism of the glycine + CO₂ reaction, *Energy Fuels* 27 (2013) 3898–3904.
- [10] Y.S. Sistla, A. Khanna, CO₂ Absorption studies in amino acid-anion based ionic liquids, *Chem. Eng. J.* 273 (2015) 268–276.
- [11] V. Hiremath, A.H. Jadhav, H. Lee, S. Kwon, J. Gil, Highly reversible CO₂ capture using amino acid functionalized ionic liquids immobilized on mesoporous silica, *Chem. Eng. J.* 287 (2016) 602–617.
- [12] Y. Uehara, D. Karami, N. Mahinpey, Effect of water vapor on CO₂ sorption–desorption behaviors of supported amino acid ionic liquid sorbents on porous microspheres, *Ind. Eng. Chem. Res.* 56 (2017) 14316–14323.
- [13] P.D. Vaidya, E.Y. Kenig, CO₂–alkanolamine reaction kinetics: A review of recent studies, *Chem. Eng. Technol.* 30 (2007) 1467–1474.
- [14] Z. Feng, F. Cheng-gang, W. You-ting, W. Yuan-tao, Absorption of CO₂ in the aqueous solutions of functionalized ionic liquids and MDEA, *Chem. Eng. J.* 160 (2010) 691–697.
- [15] K. Fukumoto, H. Ohno, Design and synthesis of hydrophobic and chiral anions from amino acids as precursor for functional ionic liquids, *Chem. Commun.* (2006) 3081–3083.
- [16] D.H. Jo, H. Jung, D.K. Shin, C.H. Lee, S.H. Kim, Effect of amine structure on CO₂ adsorption over tetraethylenepentamine impregnated poly methyl methacrylate supports, *Sep. Purif. Technol.* 125 (2014) 187–193.
- [17] M.L. Gray, J.S. Hoffman, D.C. Hreha, D.J. Fauth, S.W. Hedges, K.J. Champagne, H.W. Pennline, Parametric study of solid amine sorbents for the capture of carbon dioxide, *Energy Fuels*. 23 (2009) 4840–4844.

- [18] M.L. Gray, K.J. Champagne, D. Fauth, J.P. Baltrus, H. Pennline, Performance of immobilized tertiary amine solid sorbents for the capture of carbon dioxide, *Int. J. Greenh. Gas Con.* 2 (2012) 3–8.
- [19] K. Fukumoto, M. Yoshizawa, H. Ohno, Room temperature ionic liquids from 20 natural amino acids, *J. Am. Chem. Soc.* 127 (2005) 2398–2399.
- [20] A. Jayakumar, A. Gomez, N. Mahinpey, Post-combustion CO₂ capture using solid K₂CO₃: Discovering the carbonation reaction mechanism, *Appl. Energy.* 179 (2016) 531–543.
- [21] R. Serna-Guerrero, E. Da'na, A. Sayari, New insights into the interactions of CO₂ with amine-functionalized silica, *Ind. Eng. Chem. Res.* 47 (2008) 9406–9412.
- [22] M.J. Al-Marri, M.M. Khader, M. Taw, G. Qi, E.P. Giannelis, CO₂ Sorption kinetics of scaled-up polyethylenimine-functionalized mesoporous silica sorbent, *Langmuir* 31 (2015) 3569–3576.
- [23] A. Sayari, Y. Belmabkhout, R. Serna-guerrero, Flue gas treatment via CO₂ adsorption, *Chem. Eng. J.* 171 (2011) 760–774.
- [24] S. Saravanamurugan, A.J. Kunov-kruse, R. Fehrmann, A. Riisager, Amine-functionalized amino acid-based ionic liquids as efficient and high-capacity absorbents for CO₂, *ChemSusChem* 7 (2014) 897–902.
- [25] A.J. Fletcher, E.J. Cussen, D. Bradshaw, M.J. Rosseinsky, K.M. Thomas, Adsorption of gases and vapors on nanoporous templated with methanol and ethanol : structural effects in adsorption kinetics, *J. Am. Chrm. Soc.* 126 (2004) 9750–9759.
- [26] A. Kondo, N. Kojima, H. Kajiro, H. Noguchi, Y. Hattori, F. Okino, K. Maeda, T. Ohba, K. Kaneko, H. Kanoh, Gas adsorption mechanism and kinetics of an elastic layer-structured metal–organic framework, *J. Phys. Chem. C* 116 (2012) 4157–4162.

- [27] X. Xu, C. Song, B.G. Miller, A.W. Scaroni, X. Xu, C. Song, B.G. Miller, A.W. Scaroni, Influence of moisture on CO₂ separation from gas mixture by a nanoporous adsorbent based on polyethylenimine-modified molecular sieve MCM-41, *Ind. Eng. Chem. Res.* 44 (2005) 8113–8119.
- [28] N. Hiyoshi, K. Yogo, T. Yashima, Adsorption of carbon dioxide on amine modified SBA-15 in the presence of water vapor, *Chem. Lett.* 33 (2004) 510–511.
- [29] P.J.E. Harlick, A. Sayari, Applications of pore-expanded mesoporous silica. 5. Triamine grafted material with exceptional CO₂ dynamic and equilibrium adsorption performance, *Ind. Eng. Chem. Res.* 46 (2007) 446–458.
- [30] A. Sayari, Y. Belmabkhout, Stabilization of amine-containing CO₂ adsorbents: Dramatic effect of water vapor, *J. Am. Chem. Soc.* 132 (2010) 6312–6314.
- [31] H.Y. Huang, R.T. Yang, D. Chinn, C.L. Munson, Amine-grafted MCM-48 and silica xerogel as superior sorbents for acidic gas removal from natural gas, *Ind. Eng. Chem. Res.* 42 (2003) 2427–2433.

CHAPTER 5: CO₂ adsorption using amino acid ionic liquid-impregnated mesoporous silica sorbents with different textural properties

5.1 Presentation of the article

This paper mainly presents the effect of textural properties of mesoporous silica supports on CO₂ adsorption of the supported amino acid ionic liquid (AAIL) sorbents. In this study, an AAIL of 1-ethyl-3-methylimidazolium lysine ([EMIM][Lys]) was impregnated with mesoporous silica supports having different textural properties to prepare the AAIL-loaded mesoporous silica sorbents. A commercial polymer support, PMMA, was also employed for the comparison. The textural properties of the as-prepared supports and supported AAIL sorbents, including the pore size distribution, were characterized using a BET analyzer. Subsequently, CO₂ adsorption experiments of the supported AAIL sorbents were conducted with a TGA under a dry CO₂ gas flow condition. It was found that average pore size (D_P) of the as-prepared mesoporous silica supports exerted a dominant impact on the CO₂ capture capacities of the supported AAIL sorbents compared with the pore volume (V_P) and surface area (S_{BET}), as a result of the quantitative evaluation.

This paper next offers the effect of pore-expansion of a support on CO₂ adsorption of the supported AAIL sorbents, based on the above relationship. Pore-expanded SBA-15 (PE-SBA-15) was synthesized and compared with SBA-15 for the purpose. The comparative experimental results exhibited that pore expansion of a support led to greater capacity of the supported AAIL sorbent, although the capacity did not approach the theoretical maximum value only by the pore expansion.

This work was almost completely performed by Yusuke Uehara under the supervision of Dr.

Nader Mahinpey. Dr. Davood Karami assisted in ordering some chemicals needed for the synthesis of mesoporous silicas, instructed how to use TGA before starting the CO₂ adsorption experiments and gave some advices when revising the manuscript of the paper.

CO₂ adsorption using amino acid ionic liquid-impregnated mesoporous silica sorbents with different textural properties

This article has been published in *Microporous and Mesoporous Materials* 278 (2019) 378–386.

*Yusuke Uehara, Davood Karami, and Nader Mahinpey**

Department of Chemical and Petroleum Engineering, Schulich School of Engineering,
University of Calgary, Calgary, AB T2N 1N4, Canada

5.2 Abstract

An amino acid ionic liquid (AAIL) was impregnated with several kinds of mesoporous silica supports having various textural properties to prepare solid sorbents of the AAIL immobilized into the mesoporous silicas. The main objective of this work is evaluating the impact of textural properties of the supports on CO₂ adsorption of the supported AAIL sorbents, which has not been investigated by any researchers previously. A commercial polymer support was also utilized for comparison as it has quite different shape and pore size distribution from the mesoporous silicas. 1-Ethyl-3-methylimidazolium lysine ([EMIM][Lys]) was synthesized and used as the AAIL. Each [EMIM][Lys]-loaded sorbent exhibited a different CO₂ adsorption performance depending on the type of the support. Quantitative evaluation with the textural properties clarified that there is an extremely strong correlation between the average pore size of the pure supports and the CO₂ capture capacities of the [EMIM][Lys]-impregnated sorbents. Based on the trend, pore expanded mesoporous silica was prepared and evaluated accordingly. It was found that the pore expansion of a support can improve the CO₂ adsorption performances of the AAIL-loaded

sorbents, although pore expansion may not be the only factor causing the CO₂ capture capacity of the sorbent to approach the theoretical maximum capacity.

5.3 Introduction

Carbon dioxide (CO₂) is generally considered as one of major greenhouse gases causing climate changes. Huge quantities of CO₂ are emitted from fired power plants using combustion of coals, oils or natural gases. A technology for directly capturing CO₂ in flue gases from these plants and other industries is called post-combustion CO₂ capture. Aqueous amine scrubbing is a widely used and matured technology with long operating experience for post-combustion CO₂ capture [1]. However, this technology suffers from some drawbacks such as equipment corrosion and high regeneration energy requirement due to the presence of large amounts of water [2,3].

Amine-functionalized ionic liquids (ILs) have recently drawn our interest as substitute materials to aqueous amines because ILs hold attractive characteristics including negligible volatility, high thermal stability and physicochemical tunability [4]. They are also called task-specific ionic liquids (TSILs) as they are designed by introducing active amino groups to ILs to improve their CO₂ capture performances [5]. Amino acid ionic liquids (AAILs) are one type of TSILs that have been extensively studied for CO₂ capture in recent years [6–20], since they were developed by Fukumoto et al. for the first time with 20 kinds of natural amino acids (AAs) [21]. AAs themselves have advantages to be CO₂ sorbents in that they are inexpensive, biodegradable and environmental friendly [12,22,23]. Many research groups have focused on investigations of the capacities and reaction mechanisms for CO₂ absorption by as-prepared or pure AAILs [8–13]. One of drawbacks of AAILs is their high viscosities causing strong gas diffusion resistances, which in turn leads to slow CO₂ sorption rates. Therefore, for practical

application, it will be highly desirable to dispersedly immobilize the bulk of AAIL into a porous support in order to overcome the gas diffusion limitation. Some workers have reported that the CO₂ sorption rates of AAILs were in fact significantly enhanced when they were immobilized into a support material [6,14–16]. However, there have been still limited investigations on CO₂ capture using supported AAILs, and no researches have examined what properties of supports affect their CO₂ sorption performances.

To date, several kinds of support materials have been utilized to develop amine-modified solid sorbents for CO₂ capture studies, including mesoporous silica, silica gel, activated carbon, alumina, zeolite and polymer [2,24]. Among them, mesoporous silicas, such as MCM-41 [25–29], SBA-15 [29–36] and KIT-6 [36–38], have been widely investigated in particular. Mesoporous silicas can offer an ordered pore structure with large pore size and surface area into which the active sites of amines can be dispersed uniformly, leading to improvement of the CO₂ adsorption performance [33,35]. Some research groups have reported that the pore size and pore volume of mesoporous silica supports exert an impact on the CO₂ capture capacities of the amine-loaded sorbents [29,33,37]. Pore expansions of mesoporous silicas have also been examined to accommodate higher loadings of amines into the pores for further enhancement of the CO₂ uptakes [39–41]. Amine-functionalized solid sorbents have been classified into two types according to intensity of the interaction between the amine groups and support: 1) amine-impregnated sorbents with weak interactions, and 2) amine-grafted sorbents with strong covalent bonding [2]. Amine-impregnated sorbents generally display higher CO₂ capture capacities than amine-grafted sorbents, as higher amine loadings can be accomplished by impregnation methods. On the other hand, amine-impregnated sorbents suffer from strong diffusion resistances, leading to lower adsorption rates than amine-grafted sorbents.

In this work, various kinds of mesoporous silica materials with different textural properties are first impregnated with an AAIL to prepare AAIL-functionalized mesoporous silica sorbents. Subsequently, CO₂ adsorption experiments are carried out using those sorbents to investigate the effect of textural properties of supports on the CO₂ capture performances, which is the main objective of this study. L-lysine (Lys) is selected as an AA anion to synthesize an AAIL because Lys has shown better CO₂ sorption capacity than other AA types in previous experimental studies using supported AAIL sorbents due to its more amino groups and higher basicity [14,16,19,20].

5.4 Experimental

5.4.1 Synthesis of AAIL

1-Ethyl-3-methylimidazolium ([EMIM]) and Lys were chosen as a cation and anion, respectively, to prepare an AAIL of [EMIM][Lys]. The [EMIM][Lys] was synthesized by a neutralization method with [EMIM][Br] ($\geq 98\%$, Alfa Aesar). The detail on the preparation of [EMIM][Lys] is described elsewhere [19,20].

5.4.2 Synthesis of mesoporous silica supports

Various mesoporous silica supports, SBA-15, MCM-41 and KIT-6 were prepared according to the procedures reported by Son et al. [37]. The synthesis of SBA-15 involved the use of triblock copolymer EO20-PO70-EO20 (Pluronic P123, Aldrich) as a structure-directing agent and tetraethyl orthosilicate (TEOS, 98%, Aldrich) as a silica source. Typically, 1 g of P123 was first added to 38 mL of 1.6 M HCl (37%, VWR). After stirring it for 1 h, 2.13 g of TEOS was added to the solution with stirring. The mixture was aged for 24 h at 35 °C, followed by statically heating for 24 h at 100 °C. The resultant solid product was recovered by filtration, washed with

ethanol, and then dried overnight at 100 °C. SBA-15 was finally obtained by calcining the dried product for 4 h at 550 °C.

The synthesis of MCM-41 was performed using cetyltrimethylammonium bromide (CTAB, Sigma) as a templating agent and colloidal silica HS-40 (40 wt%, Aldrich) [37]. In a typical process, 0.4 g of NaOH was dissolved in 10 g of deionized water. Subsequently, 2.8 g of HS-40 was added to the NaOH solution with stirring at 50 °C to prepare a silicate solution. 1.84 g of CTAB was dissolved in 10 g of deionized water to prepare a CTAB solution, which was then added to the silicate solution with stirring at room temperature. 1 M acetic acid ($\geq 99.7\%$, Sigma-Aldrich) was used in adjusting pH of the solution to 11. The solution was further stirred for 6 h at room temperature, followed by aging for 24 h at 100 °C. The solid product obtained was collected by filtration and washed with deionized water. MCM-41 was finally gained after drying for 24 h at 50 °C and then calcination of the product for 5 h at 550 °C.

KIT-6 was prepared using P123 and n-butanol (99.8%, Sigma-Aldrich) as a structure-directing mixture [37]. In a typical synthesis, 0.8 g of P123 was dissolved in a mixture of 28.8 g of deionized water and 1.58 g of 35 wt% HCl under vigorous stirring at 35 °C. Then, 0.8 g of n-butanol was added to the mixture. After stirring it for 1 h, 1.72 g of TEOS was next added to the clear solution. The mixture was left under stirring for 24 h at 35 °C, followed by statically aging for 24 h at 100 °C. The resultant precipitate was hot-filtered and subsequently dried overnight at 100 °C. The dried product was extracted with a mixture of ethanol-HCl (1:1 ratio, 10 mL) using a centrifuge (Centrifuge 5702, eppendorf) at 300 rpm for 1 min or at 3000 rpm for 5 min to remove the templating agents. After calcination for 5 h at 550 °C, two types of KIT-6 were finally obtained by the different extraction conditions; the former and latter were named KIT-6S and KIT-6L, respectively.

Pore-expanded SBA-15 or PE-SBA-15 was also synthesized by just modifying the preparation method of SBA-15 described above using 1,3,5-trimethylbenzene (TMB, $\geq 98\%$, Alfa Aesar) as a swelling agent [36,42,43]. The changes on the process of SBA-15 to obtain PE-SBA-15 are as follows: 1) 1.0 g of TMB were added with TEOS to the P123 solution dissolved in 1.6 M HCl before the aging at 35 °C, and 2) the heating after the aging at 35 °C was conducted at 130 °C for 24 h, instead of 100 °C.

5.4.3 Immobilization of AAIL into supports

Immobilization of the [EMIM][Lys] into the prepared mesoporous silica was conducted mainly by an impregnation method [19,20]. Commercial poly(methyl methacrylate) or PMMA microspheres (Diaion HP-2MG, Supelco) were also used as a support for comparison since they have displayed good performance on CO₂ sorption using supported amine or AAIL sorbents [15,16,44–46]. Briefly, the [EMIM][Lys] was dissolved in aqueous ethanol solution at a concentration of 50 mg/mL, which was stirred at 200 rpm for 30 min at room temperature. After adding a support (the prepared mesoporous silica or PMMA) to solution with different ratios (20, 30, 50, 60 or 70 wt% [EMIM][Lys] loadings), the suspension was further stirred at 100 rpm for 2 h. Evaporating the solvent and then drying the residue at 50 °C under vacuum for 24 h gave the solid sorbent of [EMIM][Lys] impregnated with the support. Each sorbent prepared was designated by combining the name of support with the loading of [EMIM][Lys]. For example, a solid sorbent of 20 wt% [EMIM][Lys] impregnated with SBA-15 was named “SBA-15-20”.

Physical mixing was also employed to evaluate the effect of immobilization method on the textural properties and CO₂ capture behaviors of the supported AAIL. In brief, the [EMIM][Lys] was mechanically mixed with a support using a motor. Then, the mixture was dried at 50 °C under vacuum for 24 h. The obtained sorbent was designated by adding “PM” to the behind of

the name of support and [EMIM][Lys] loading.

5.4.4 Characterization

N₂ adsorption–desorption isotherms of the as-prepared support materials and supported [EMIM][Lys] sorbents were determined at –196 °C using a surface area analyzer (ASAP 2020, Micromeritics). Before the measurement, degas was conducted for 120 min at 180 °C for the as-prepared supports or at 100 °C for the supported [EMIM][Lys] sorbents. From the obtained data, the surface areas were calculated by the Brunauer-Emmet-Teller (BET) method, and the pore volumes and pore sizes were computed by the Barrett–Joyner–Halenda (BJH) method. In the BJH analysis, a cylindrical pore model was assumed. The experimental errors of those textural properties were estimated within ±5% from three repetitive measurements with the as-prepared MCM-41 support.

Thermal stabilities of the as-prepared supports, as-prepared [EMIM][Lys] and supported [EMIM][Lys] were examined using a thermogravimetric analyzer (TGA STA 6000, PerkinElmer). For the analysis, the TGA temperature was raised under N₂ atmosphere at a heating rate of 10 °C/min.

5.4.5 CO₂ adsorption experiments

CO₂ adsorption experiments of the supported [EMIM][Lys] sorbents and as-prepared support materials were carried out using the TGA. Around 10 mg of a sample was loaded in a crucible of the TGA and heated to 100 °C in a pure N₂ gas at a flow rate of 100 mL/min. After holding the sample for 50 min under the N₂ gas flow, the temperature was lowered to 30 °C, and then the feed gas was switched to mixed gases of CO₂ and N₂. The mixed gases consisted of 15% CO₂ and balance N₂, which were fed at a flow rate of 130 mL/min. The CO₂ adsorption process was

performed for 30 min in the dry gas flow condition. The experimental error in the CO₂ capture capacity of a sample was estimated within $\pm 5\%$ from three repetitive adsorption tests using the [EMIM][Lys]-impregnated PMMA sorbent (50 wt% loading). Cyclic CO₂ adsorption–desorption experiments were also conducted to evaluate the long-term stability of the CO₂ capture performance. In the cyclic experiments, after one adsorption process, the sample was again heated to and kept at 100 °C for 50 min under the pure N₂ gas flow for a desorption process, followed by lowering the temperature to 30 °C for the next adsorption process.

5.5 Results and discussion

5.5.1 Characterization of pure and [EMIM][Lys]-impregnated mesoporous silicas

Table 5.1 lists BET surface area (S_{BET}), BJH adsorption cumulative pore volume (V_{P}) and average pore diameter (D_{P}) of the as-prepared mesoporous silicas (SBA-15, MCM-41 and KIT-6) and commercial PMMA (Diaion HP-2MG). The shapes of all the mesoporous silicas were powdery, while that of PMMA was spherical (beadlike). The textural properties of S_{BET} , V_{P} and D_{P} were different by the type of the supports; MCM-41 had much larger surface area but smaller pore size than others, whereas PMMA possessed the smallest surface area but the biggest pore size among these supports. Two kinds of KIT-6 (KIT-6S and KIT-6L) were synthesized in this study by changing the ethanol-HCl extraction condition with a centrifuge. KIT-6L exhibited larger S_{BET} and V_{P} than KIT-6S possibly due to more sufficient extraction of the templating agents from the pores for KIT-6L. On the other hand, D_{P} of the KIT-6S and KIT-6L did not become significantly different from each other.

Table 5.1. Textural properties of as-prepared mesoporous silica and PMMA supports.

Support	$S_{\text{BET}}^{\text{a}}$ [m ² /g]	V_{P}^{b} [cm ³ /g]	D_{P}^{c} [nm]
SBA-15	725	0.94	5.2
MCM-41	1735	1.12	2.6
KIT-6S ^d	842	1.13	5.3
KIT-6L ^e	970	1.31	5.4
PMMA	527	1.12	8.4
PE-SBA-15	503	2.30	19.1

^a BET surface area.

^b BJH adsorption cumulative pore volume.

^c BJH adsorption average pore diameter.

^d Ethanol-HCl extraction was carried out with centrifuge at 300 rpm for 1 min.

^e Ethanol-HCl extraction was carried out with centrifuge at 3000 rpm for 5 min.

Table 5.2 summarizes S_{BET} and V_{P} of [EMIM][Lys]-impregnated mesoporous silica and PMMA sorbents with various loadings. Figures 5.1 and 5.2 depict N₂ adsorption–desorption isotherms of the [EMIM][Lys]-loaded mesoporous silica and PMMA sorbents, as well as the corresponding as-prepared supports, respectively. Both S_{BET} and V_{P} of all the supports decreased when the [EMIM][Lys] was immobilized into them with higher loadings, as found by comparing Tables 5.1 and 5.2.

Table 5.2. Textural properties of [EMIM][Lys]-loaded mesoporous silica and PMMA sorbents with different loadings.

Sorbent	S_{BET} [m ² /g]	V_{P} [cm ³ /g]
SBA-15-20	265	0.58
SBA-15-30	223	0.48
SBA-15-50	75	0.15
SBA-15-60	33	0.05
MCM-41-50	36	0.11
KIT-6S-50	87	0.17
KIT-6S-50-PM ^a	83	0.15
PMMA-50 [19]	38	0.35
PE-SBA-15-50	191	1.07

^a [EMIM][Lys] was immobilized into KIT-6S by physical mixing with 50 wt% loading.

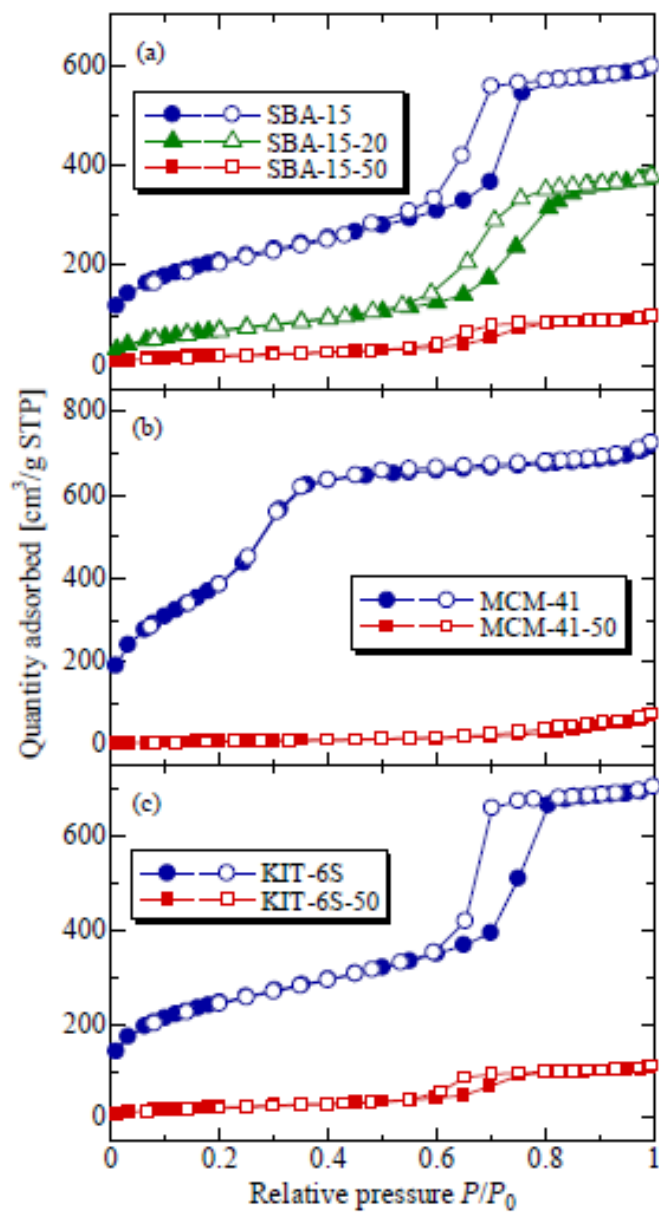


Figure 5.1. N₂ adsorption–desorption isotherms of as-prepared and [EMIM][Lys]-impregnated (a) SBA-15, (b) MCM-41 and (c) KIT-6S; filled and opened marks represent the adsorption and desorption branches, respectively..

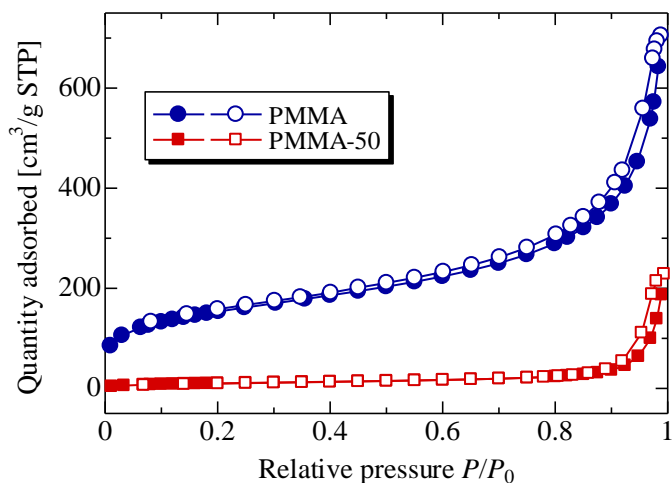


Figure 5.2. N₂ adsorption–desorption isotherms of as-prepared and [EMIM][Lys]-impregnated PMMA; filled and opened marks represent the adsorption and desorption branches, respectively.

Figure 5.3a, b and c present BJH pore size distributions of the as-prepared and [EMIM][Lys]-impregnated SBA-15, MCM-41 and KIT-6S, respectively. Without [EMIM][Lys] loadings, all the mesoporous silicas exhibited sharp pore size distributions between 2 and 12 nm of pore diameter. However, at 50 wt% [EMIM][Lys] loading, these mesoporous silicas lost most parts of their meso-pore spaces in each narrow range.

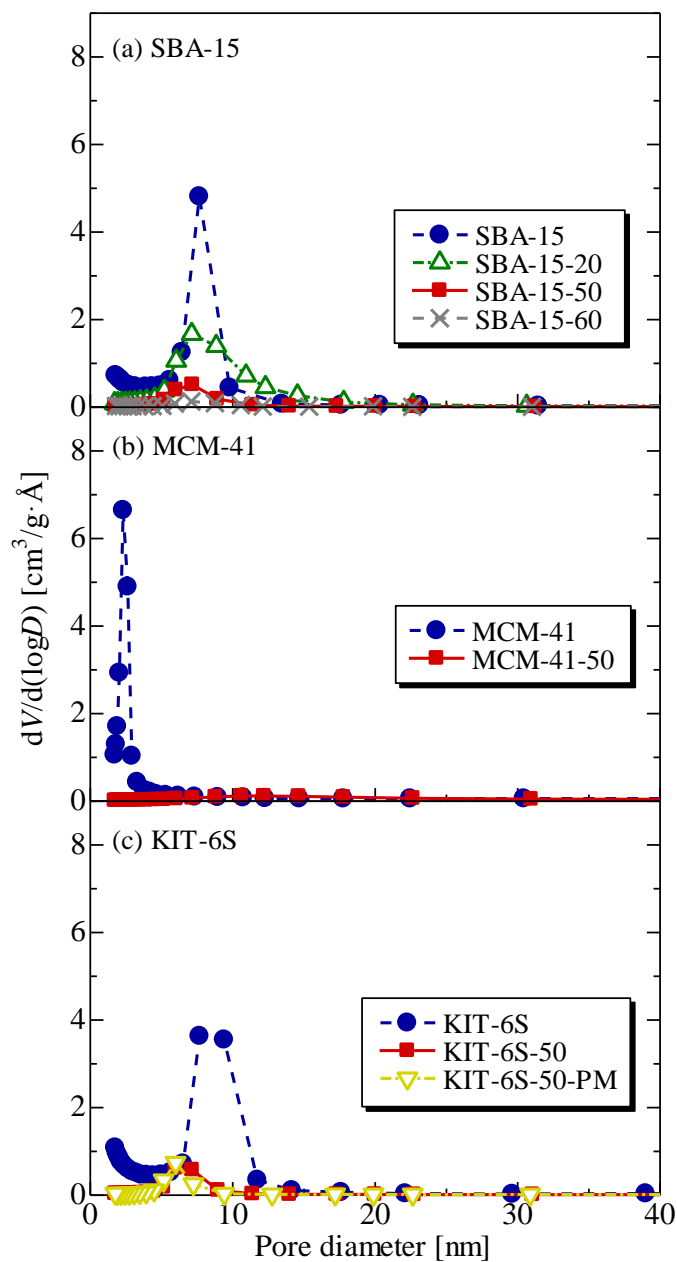


Figure 5.3. BJH pore size distributions of as-prepared and [EMIM][Lys]-impregnated (a) SBA-15, (b) MCM-41 and (c) KIT-6S.

[EMIM][Lys] was also immobilized into KIT-6S by a physical mixing method with 50 wt% loading, which is designated as “KIT-6S-50-PM”. Interestingly, KIT-6S-50-PM showed similar pore size distribution as well as S_{BET} and V_{P} (Table 5.2) to KIT-6S-50 on which the [EMIM][Lys] was supported by an impregnation method with the same loading, regardless of the different immobilization methods. Figure 5.4 presents BJH pore size distributions of pure and [EMIM][Lys]-impregnated PMMA on a semi-logarithmic graph. In contrast to the mesoporous silicas, the pure PMMA displayed extremely broad pore size distribution. At 50 wt% [EMIM][Lys] loading, the pore space of PMMA greatly decreased as well; especially, the PMMA lost almost all of the pore space in the smaller pore diameter than 10 nm.

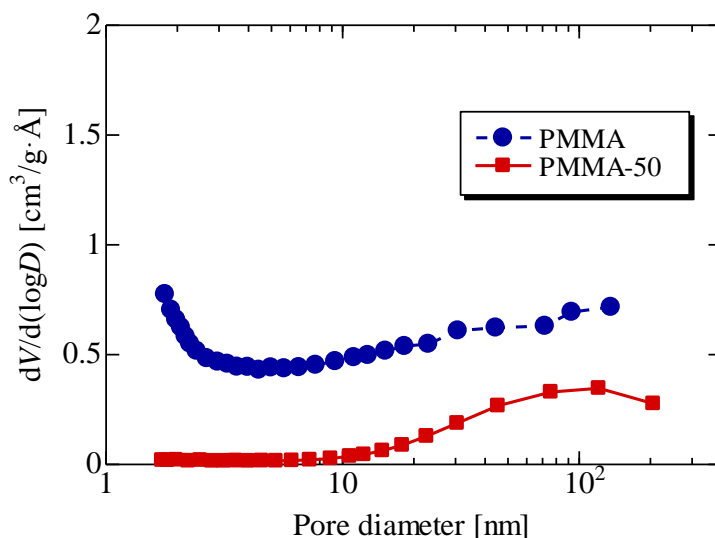


Figure 5.4. BJH pore size distributions of as-prepared and [EMIM][Lys]-impregnated (50 wt%) PMMA.

Figure 5.5a depicts TGA curves of the pure [EMIM][Lys], pure supports (SBA-15, KIT-6S and PMMA) and [EMIM][Lys]-impregnated SBA-15 sorbents with various loadings under N_2

atmosphere at a heating rate of 10 °C/min. The corresponding differential thermogravimetric analysis (DTGA) results are also described in Figure 5.5b.

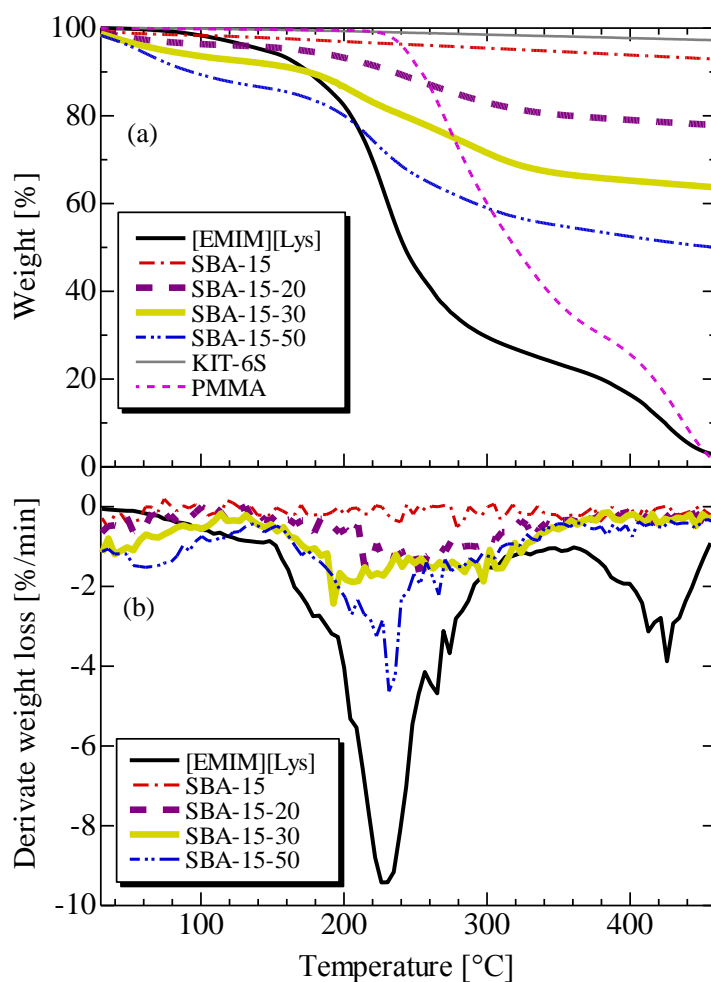


Figure 5.5. (a) TGA curves and (b) DTGA curves of pure [EMIM][Lys], pure supports (SBA-15, KIT-6S and PMMA) and [EMIM][Lys]-impregnated SBA-15 sorbents with various loadings under N₂ atmosphere at a heating rate of 10 °C/min.

The as-prepared mesoporous silica supports exhibited good thermal stabilities, while the pure PMMA support underwent thermal decomposition from 240 °C, continuing to 460 °C. Thermal

decomposition of the as-prepared [EMIM][Lys] started occurring slowly from 160 °C and then progressed more rapidly from 200 to 280 °C. On the other hand, the [EMIM][Lys]-impregnated SBA-15 sorbents showed larger weight losses below 100 °C with higher loadings. The reason can be mainly due to desorption of moisture remaining in the pores of the sorbents prepared by the impregnation method, based on quantification results with a mass spectrometer. The rate of the weight loss reduced between 100 and 160 °C, meaning that the moisture desorption almost completed before 100 °C. At higher temperature than 160 °C, the [EMIM][Lys]-impregnated SBA-15 sorbents displayed the similar thermal decomposition behaviors to the pure [EMIM][Lys], and the thermal decomposition rates and weight losses increased with higher loadings. According to previous literature, when amines were loaded into mesoporous silicas by an impregnation method, thermal decompositions of the amines happened at lower and narrower temperature range than the pure amines [26,37]. Xu et al. attributed those variations to the uniform dispersion of the amine into the mesoporous silica because the melting or thermal decomposition temperature can decrease as the particle size of a material reduces [26,47]. On the other hand, the [EMIM][Lys]-impregnated SBA-15 did not exhibit such phenomena, demonstrating a high thermal stability of the AAIL in that its uniform dispersion into the support did not change the thermal decomposition temperature range. This is also due to an extremely high thermal stability of the mesoporous silica compared with PMMA.

5.5.2 CO₂ adsorption performances of the [EMIM][Lys]-impregnated sorbents with 50 wt% loading

The [EMIM][Lys]-impregnated mesoporous silica (SBA-15, MCM-41, KIT-6S and KIT-6L) and PMMA sorbents with 50 wt% loading were first used for comparative CO₂ capture experiments with a TGA. Figure 5.6a and b present the CO₂ adsorption performances of the

[EMIM][Lys]-loaded sorbents and the as-prepared SBA-15 and KIT-6S supports at 30 °C in the units of mmol per gram of sorbent or support, respectively. All the [EMIM][Lys]-impregnated mesoporous silica sorbents showed CO₂ uptake behaviors with time, whereas the pure SBA-15 and KIT-6S supports hardly adsorbed CO₂. This difference indicates that the active sites of [EMIM][Lys] immobilized into the individual mesoporous silica supports have a substantial potential for CO₂ capture in this adsorption experimental condition.

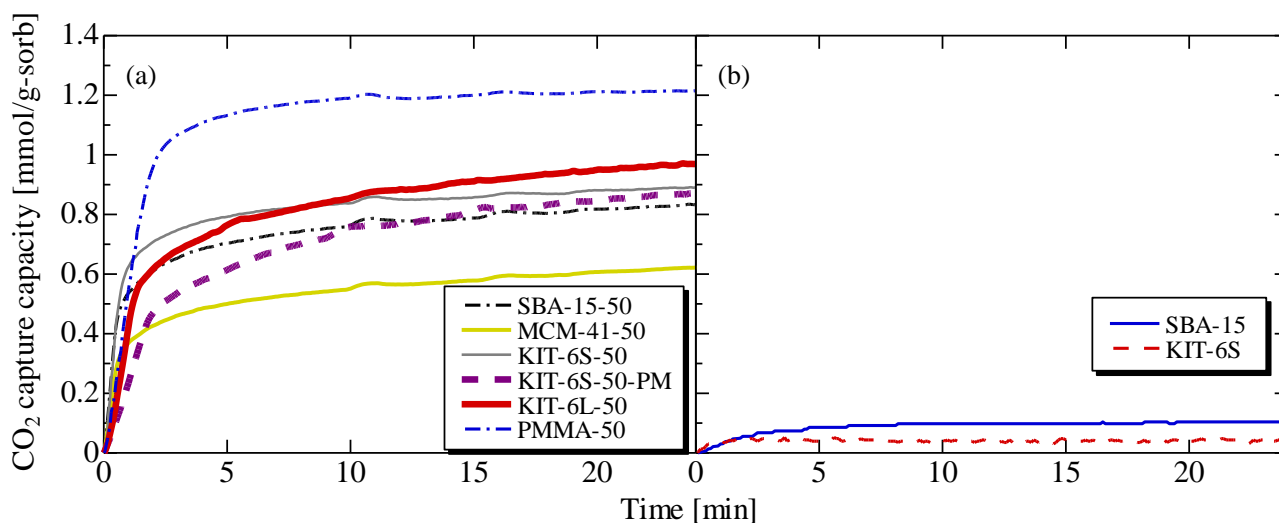


Figure 5.6. CO₂ adsorption performances of (a) [EMIM][Lys]-loaded sorbents with 50 wt% loading and (b) as-prepared SBA-15 and KIT-6S supports with time at 30 °C.

The CO₂ adsorption process can be categorized into two steps with time, namely fast adsorption step with exponential weight increment and subsequent much slow adsorption step, which have been seen for other AAIL-modified or amine-modified solid sorbents [20,48]. The CO₂ capture performances of the [EMIM][Lys]-impregnated sorbents varied by the type of supports. In other words, the individual supports exerted a different impact on the CO₂ capture capacities. PMMA

gave rise to much higher capacity than the mesoporous silicas, while MCM-41 resulted in the lowest capacity; the order of supports on the capacities was PMMA > KIT-6L > KIT-6S > SBA-15 > MCM-41. It is assumed that the CO₂ capture capacities of [EMIM][Lys]-impregnated sorbents are influenced by the different textural properties of the as-prepared supports described in the previous section. The same CO₂ adsorption experiment was also carried out using KIT-6S-50-PM prepared by physical mixing. Obviously, KIT-6S-50-PM displayed slower CO₂ adsorption rate than KIT-6S-50 and other sorbents prepared by impregnation. This result suggests that impregnation methods can offer more uniform and finer dispersion of AAILs into supports than physical mixing methods, leading to lower gas diffusion resistance that can improve the adsorption rate. However, the CO₂ capture capacity of KIT-6S-50-PM finally converged to the nearly same value as that of KIT-6S-50, regardless of the difference in the adsorption rates. The textural properties of as-prepared supports and sorbents again appear to cause the comparable capacity of KIT-6S-50-PM with KIT-6S-50, as these sorbents exhibited the approximately same pore size distributions (Figure 5.3c) as well as S_{BET} and V_{P} (Table 5.2).

In order to evaluate the influence of the textural properties of as-prepared supports on the CO₂ capture capacities of [EMIM][Lys]-impregnated sorbents quantitatively, D_{P} , S_{BET} and V_{P} of the as-prepared supports were plotted with the capacities of the supported sorbents at 30 °C in Figures 5.7, 5.8 and 5.9, respectively. D_{P} of the as-prepared supports evidently showed a much better linear relationship with the capacities of sorbents than S_{BET} and V_{P} . It is remarkable that the average pore size (D_{P}) of the pure supports exactly exerted a dominant impact on the capacities of the supported sorbents in this way, since the mesoporous silica and PMMA supports had quite different shapes and pore size distributions (Figures 5.3 and 5.4) from each other; in addition, KIT-6 possesses more complex geometry than MCM-41 and SBA-15 [37].

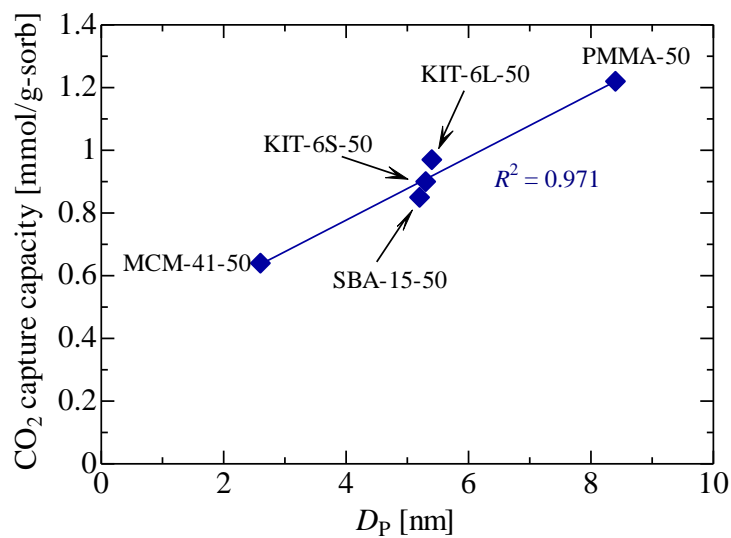


Figure 5.7. Plot of D_p of as-prepared supports with CO_2 capture capacities of [EMIM][Lys]-impregnated (50 wt%) sorbents at 30 °C.

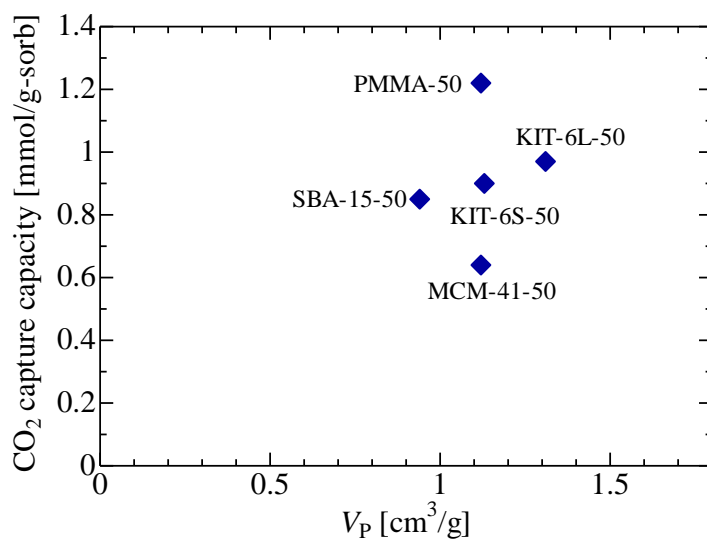


Figure 5.8. Plot of V_p of as-prepared supports with CO_2 capture capacities of [EMIM][Lys]-impregnated (50 wt%) sorbents at 30 °C.

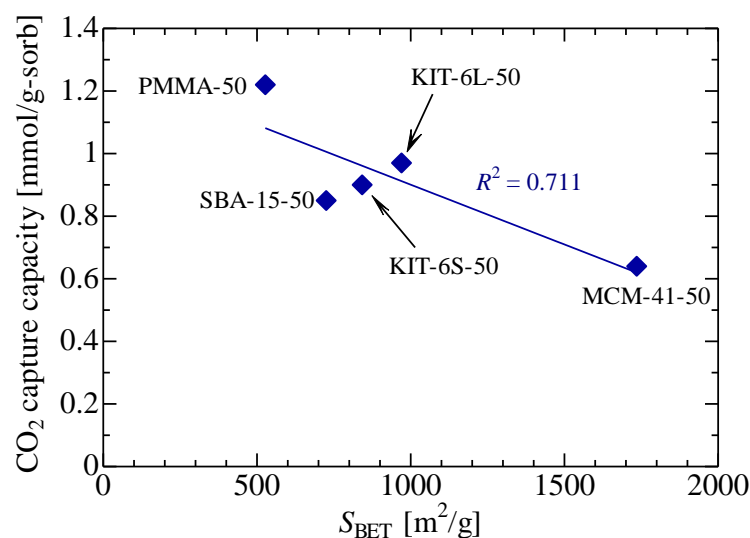


Figure 5.9. Plot of S_{BET} of as-prepared supports with CO_2 capture capacities of [EMIM][Lys]-impregnated (50 wt%) sorbents at 30 °C.

Although S_{BET} exhibited a moderate correlation with the capacities, it is not reasonable that the capacities of the supported sorbents decrease with increasing in the surface area of the pure supports. Son et al. have reported that the pore size of mesoporous silica supports predominantly affect the CO_2 adsorption performances of amine-impregnated mesoporous silica sorbents [37]. Thus, our study clarified that the pore size of supports is very important factor influencing CO_2 capture performances of the AAIL- loaded sorbents similar to amine-loaded sorbents. Not only the average pore size, but also the maximum pore size in BJH pore size distributions of the as-prepared supports varied in the order of PMMA > KIT-6 > SBA-15 > MCM-41 (Figures 5.3 and 5.4). It is assumed that AAIL bulks can be penetrated more effectively into supports with large pore under the impregnation process than those with small pore, because AAILs have high

viscosities. This difference can, in turn, affect the CO₂ adsorption of the AAIL-loaded sorbents. Therefore, supports with larger average (or maximum) pore size will result in higher capacities of the AAIL-loaded sorbents. Although pore geometry may be another crucial factor influencing penetration of AAIL bulks, pore size will exert more dominant impact on the penetration than pore geometry, since KIT-6 with more intricate pore geometry also exhibited the good linear correlation between D_P and the capacity as well as other supports (Figure 5.7).

5.5.3 Effect of pore expansion of support on the CO₂ adsorption performance

The relationships derived from the experimental data in previous sections indicate that mesoporous silica supports with larger pore size can result in increasing the CO₂ capture capacities of AAIL-impregnated mesoporous silica sorbents. Based on this expectation, pore-expanded SBA-15 (PE-SBA-15) was next synthesized and used as the support to evaluate the effect of pore expansion of a support on the CO₂ capture performance of the [EMIM][Lys]-loaded sorbent. The pore expansion of SBA-15 was carried out by modifying the synthesis method of SBA-15, namely addition of TMB and statically heating at a higher temperature of 130 °C in brief [36,42,43]. S_{BET} , V_P and D_P of the as-prepared PE-SBA-15 are listed in Table 5.1. Compared with SBA-15, V_P and D_P of PE-SBA-15 were highly enlarged. PE-SBA-15 possessed much larger D_P than any other supports as well. Figure 5.10 depicts pore size distributions of the pure PE-SBA-15 and [EMIM][Lys]-impregnated PE-SBA-15 sorbent with 50 wt% loading (PE-SBA-15-50). The peak of pore size distribution of PE-SBA-15 was shifted to larger pore size range and became broader than that of SBA-15 (Fig. 5.3a). At 50 wt% [EMIM][Lys] loading, the pore space of PE-SBA-15 also greatly reduced as well as the S_{BET} and V_P (Table 5.2).

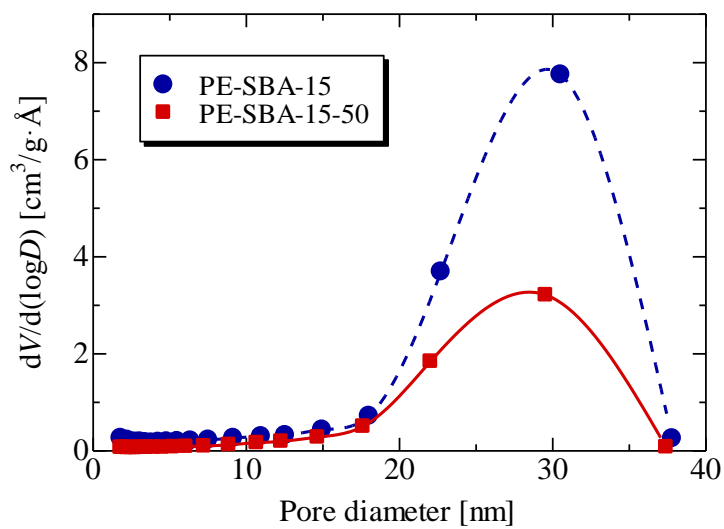


Figure 5.10. BJH pore size distributions of as-prepared and [EMIM][Lys]-impregnated (50 wt%) PE-SBA-15.

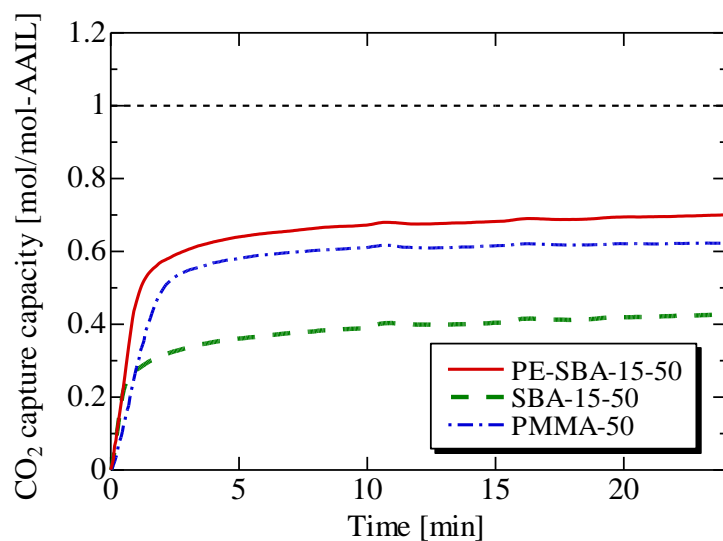


Figure 5.11. CO₂ adsorption performances of [EMIM][Lys]-impregnated (50 wt%) PE-SBA-15, SBA-15 and PMMA sorbents with time at 30 °C in the units of mol/mol-AAIL.

Figure 5.11 presents the CO₂ adsorption behaviors of the [EMIM][Lys]-impregnated PE-SBA-15, SBA-15 and PMMA sorbents with 50 wt% loading (named PE-SBA-15-50, SBA-15-50 and PMMA-50, respectively) at 30 °C. The CO₂ capture capacities are represented in the units of mole per mole of AAIL. The capacity of PE-SBA-15-50 surpassed that of PMMA-50 as well as SBA-15-50, demonstrating that the pore expansion of supports can enhance the CO₂ capture performances of supported AAILs; PE-SBA-15-50 exhibited approximately 1.5 times higher capacity than SBA-15-50. Nevertheless, the improvement in the capacity by the pore expansion seems low, from the viewpoint of much larger average pore size of PE-SBA-15 than PMMA (Table 5.1). Figure 5.12 describes the relationship between D_P of the pure supports and the CO₂ capture capacities of [EMIM][Lys]-impregnated sorbents in the units of mol/mol-AAIL, including the data of PE-SBA-15-50.

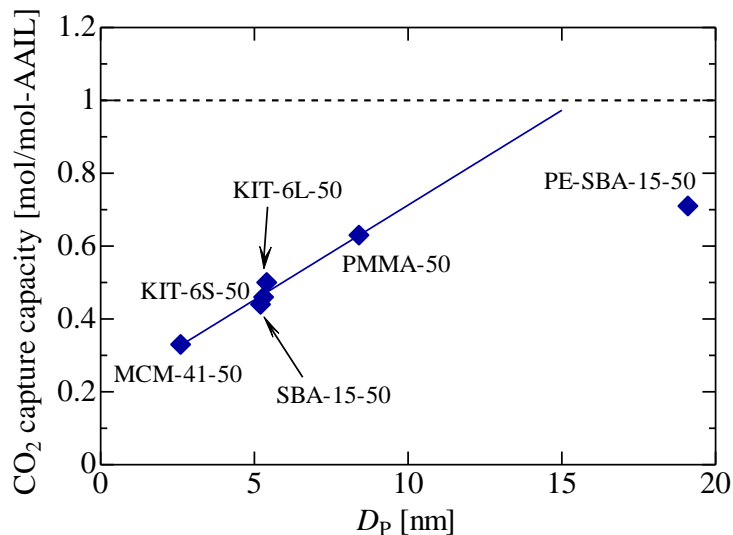
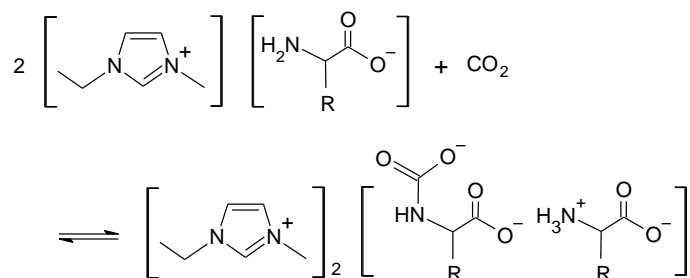


Figure 5.12. Relationship between D_P of pure supports and CO₂ capture capacities of [EMIM][Lys]-impregnated (50 wt%) sorbents in the units of mol/mol-AAIL.

The point of PE-SBA-15-50 is much lower than the linear regression line obtained from other data. It is expected that the reaction of amino groups in supported imidazolium AAIL, such as [EMIM][AA], with CO₂ proceeds in a 2:1 stoichiometry [12,15,20]; the assumed reaction scheme of [EMIM][AAs] with CO₂ is described in Scheme 5.1.



Scheme 5.1. Assumed reaction scheme of [EMIM][AAs] with CO₂.

Based on the stoichiometry, the theoretical maximum CO₂ capture capacity of [EMIM][Lys]-loaded sorbent should be 1.0 mol/mol-AAIL, as Lys has two amino groups in its molecule. However, the experimental capacity of PE-SBA-15-50 did not highly approach to the theoretical maximum value either. This inadequate enhancement of the capacity indicates that dispersion of the AAIL bulk into the support is not greatly improved only by the pore expansion. For supported amine sorbents, the amine efficiency, or CO₂/N ratio, is also a crucial factor, in addition to the capacity. It has been reported that the CO₂/N ratios of 50 wt% polyethylenimine (PEI)-impregnated MCM-41, SBA-15 and KIT-6 sorbents were 0.18, 0.27 and 0.17 in a dry gas flow condition at a low CO₂ concentration (5 to 15%), respectively [24]. From our results, the CO₂/N ratios of 50 wt% [EMIM][Lys]-impregnated MCM-41, SBA-15 and KIT-6 sorbents were 0.17, 0.22 and 0.23, respectively, which were comparable to those of the above PEI-impregnated

mesoporous silica sorbents. It is important to enhance not only the capacity, but also the CO_2/N ratio to the maximum value of 0.5 under a dry CO_2 gas inlet for supported amine and AAIL sorbents, by promoting dispersion of the active phases into the supports. The CO_2/N ratio of the [EMIM][Lys]-loaded sorbent was increased to 0.36 when using PE-SBA-15 support. There is still room to improve the CO_2/N ratio to the maximum value. It is considered that surface modification of the support can also be involved in the enhancement of AAIL dispersion. For example, Yue et al. have reported that SBA-15 and MCM-41 supports prepared without calcination enabled finer dispersion of amines into the pores owing to the remaining surfactants in the supports, compared with the surfactant-free counterparts, leading to higher CO_2 capture capacities of the amine-loaded sorbents [28,31]. Similarly, Sayari's group has reported that a surface layer of long alkyl chains of the surfactant left in a mesoporous silica support enhanced dispersion of the loaded amine, resulting in improvement of the CO_2 adsorption performance [49].

The CO_2 adsorption experiments were also conducted using the [EMIM][Lys]-impregnated PE-SBA-15, SBA-15 and PMMA sorbents with various loadings (20, 30, 50, 60 and 70 wt%). Figure 5.13a and b depict the relationships of the loadings with the CO_2 capture capacities in the different units of mmol/g-sorb and mol/mol-AAIL for these sorbents, respectively. PE-SBA-15 caused higher CO_2 capture capacities of the supported sorbent than SBA-15 at any [EMIM][Lys] loading. The mesoporous silica and PMMA supports exerted a different impact on the capacities with the change in the loadings. For the PMMA support, until 50 wt% loading the capacity of the supported sorbent increased linearly (Figure 5.13a), and the reaction stoichiometric ratio of CO_2/AAIL was approximately constant (Figure 5.13b).

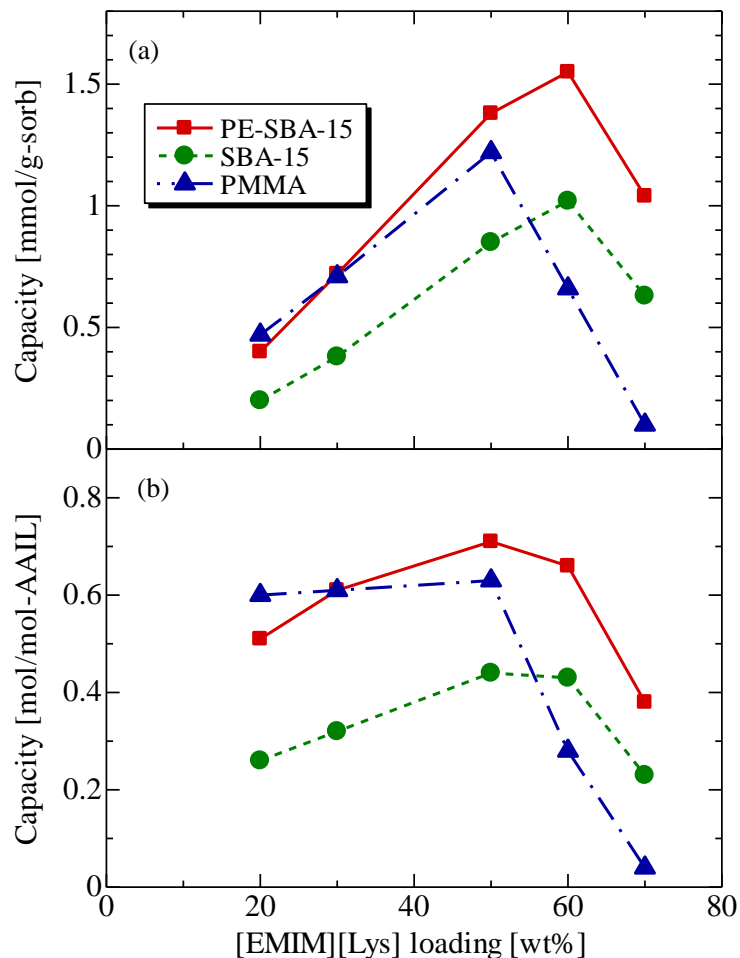


Figure 5.13. Plot of [EMIM][Lys] loadings with CO₂ capture capacities of [EMIM][Lys]-impregnated PE-SBA-15, SBA-15 and PMMA sorbents in the units of (a) mmol/g-sorb and (b) mol/mol-AAIL.

However, both the capacity and CO₂/AAIL ratio remarkably reduced from 60 wt% loading. On the other hand, for the PE-SBA-15 and SBA-15 supports, the CO₂/AAIL ratio gradually increased to 50 wt% loading and did not significantly decrease at 60 wt% loading. Xu et al. has reported a similar trend of gradual increase in the chemical adsorptivity of CO₂ by an

amine-impregnated MCM-41 sorbent with higher loadings [26]. It is possible that the difference in the pore size distributions of the supports affects the relationship between the loadings and CO₂ capture performances. Since the PMMA support has a broad and shallow pore space (Figure 5.4), AAILs can be loaded on the front part of the pore wall, resulting in less diffusion resistance that can improve their reactivity with CO₂ even at lower loadings; however, at excessively higher loadings (i.e. over 60 wt%), AAILs can cover the surface instead of being dispersedly supported into the pore, leading to reduction in the CO₂ adsorption performance.

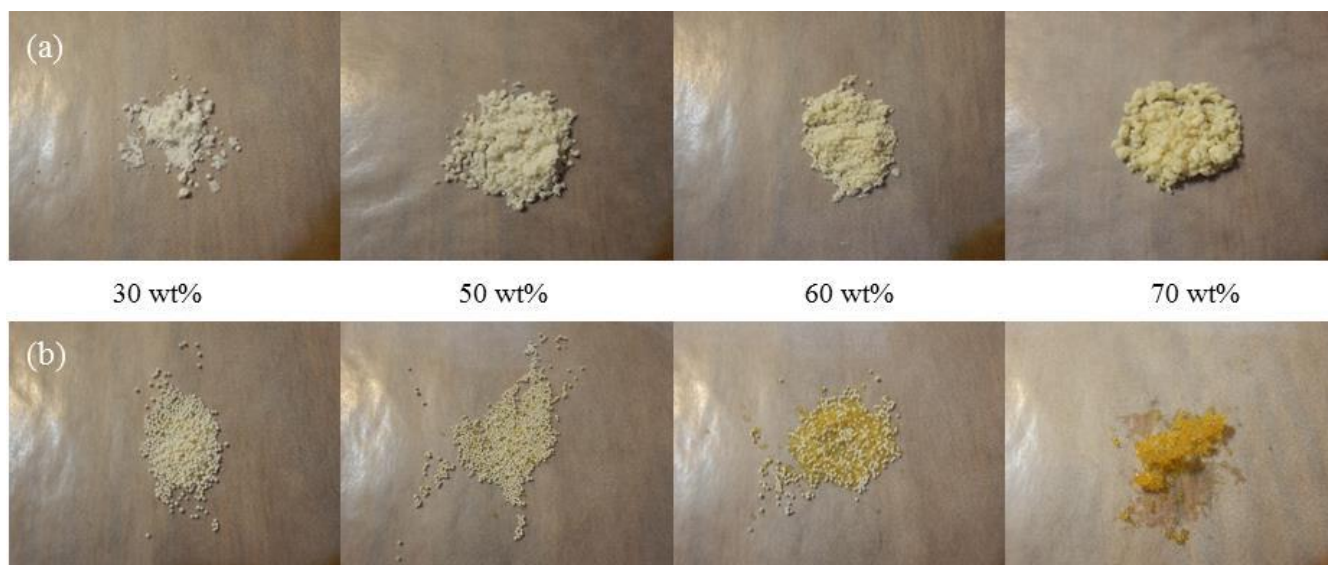


Figure 5.14. Appearances of [EMIM][Lys]-impregnated (a) SBA-15 and (b) PMMA sorbents with various loadings.

In contrast, as the PE-SBA-15 and SBA-15 supports hold narrow and deep pore spaces (Figures 5.3 and 5.10), AAILs can be immobilized into the inner part of the pore channels at low loading, causing little contact with CO₂ [26]; the contact and reactivity with CO₂ can improve with higher loadings as AAILs can be supported into the front part as well as inner part of the pore walls.

These mesoporous silicas could load higher amounts of AAILs into the pores without covering of the surfaces than the PMMA due to the difference in the pore structures, which is a possible reason that the capacities of the [EMIM][Lys]-impregnated mesoporous silicas did not decrease at 60 wt% loading. The difference in the dispersivity of AAIL into the pores of supports can also be speculated from the appearances of the sorbents. Figure 5.14 a and b show the appearances of [EMIM][Lys]-impregnated SBA-15 and PMMA sorbents with various loadings, respectively. The [EMIM][Lys] is a yellow IL having a high viscosity. When the [EMIM][Lys] was loaded into the PMMA at 60 wt% loading, the surface of PMMA particles were largely dyed yellow while becoming stickier, meaning that most of the external surface of PMMA particles were covered with the [EMIM][Lys]. In contrast, such changes were not clearly seen for the [EMIM][Lys]-loaded SBA-15 with 60 wt% loading.

Cyclic CO₂ adsorption–desorption experiments were finally carried out using PE-SBA-15-50, SBA-15-50 and PMMA-50 sorbents. The adsorption and desorption conditions were at 30 °C for 30 min and at 100 °C for 50 min, respectively. Figure 5.15 presents changes in the CO₂ adsorption capacities of the sorbents with the number of cycles. The capacities of these sorbents gradually decreased with the cycle number. The reduction in the capacity with higher cycle number can occur due to the incomplete CO₂ desorption as well as the weight loss of AAIL during desorption processes [14,15]. The capacities of PE-SBA-15-50, SBA-15-50 and PMMA-50 decreased by 14, 19 and 7% after five cycles, respectively, and thus PE-SBA-15-50 and SBA-15-50 showed higher capacity losses than PMMA-50. It is considered that difference in the pore size distributions of supports can influence even the desorption performances of the supported sorbents, as CO₂ could be desorbed more easily and adequately from the sorbent, if CO₂ is adsorbed mainly on the front wall of the pore having broader and shallower space, such as

PMMA. We will further examine the effect of pore structure of supports as well as CO₂ adsorption and desorption run conditions on the cyclic CO₂ capture performances of AAIL-loaded sorbents to improve the long-term stability in our future study.

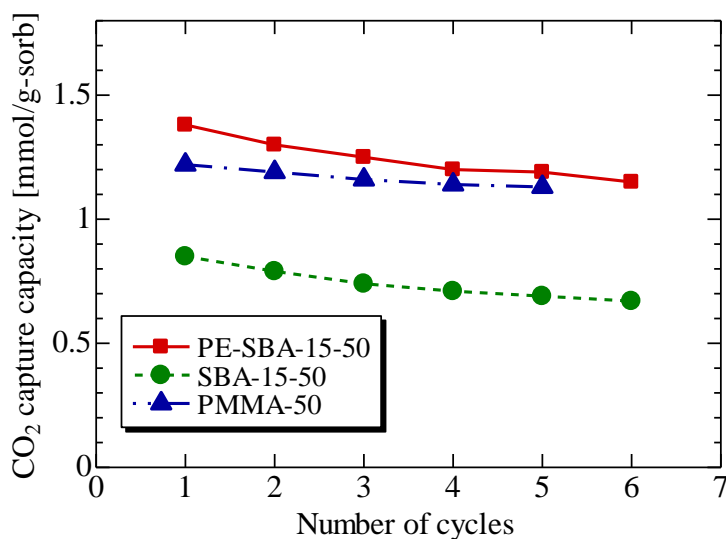


Figure 5.15. Changes in CO₂ adsorption capacities of [EMIM][Lys]-impregnated (50 wt%) PE-SBA-15, SBA-15 and PMMA sorbents with the number of CO₂ adsorption–desorption cycles.

5.6 Conclusions

An AAIL of [EMIM][Lys] was impregnated with various mesoporous silica supports having different textural properties to prepare the [EMIM][Lys]-loaded sorbents. The textural properties and thermal stabilities of the mesoporous silica supports before and after loading of the [EMIM][Lys] were analyzed and also compared with those of a commercial PMMA support. The pore volume (V_P) and surface area (S_{BET}) of the supports reduced with higher loadings. It was also found that the [EMIM][Lys]-impregnated mesoporous silica sorbents retained a high

thermal stability regardless of the loadings, because the thermal decomposition temperature range of the [EMIM][Lys] did not decrease even when it was loaded on the mesoporous silica with higher loadings.

CO₂ adsorption experiments of the [EMIM][Lys]-impregnated sorbents were carried out in a dry CO₂ flow condition at 30 °C with a TGA. Then, the main objective of this study, the effect of textural properties of the pure supports on the CO₂ adsorption performances of the supported AAIL sorbents was evaluated. The average pore size (D_p) of the pure supports exhibited much better linear relationship with the CO₂ capture capacities of the sorbents than V_p and S_{BET} , despite of difference in the shapes and pore size distributions of the supports. Based on this relationship, pore expanded SBA-15 (PE-SBA-15) was next prepared and used as the support. The additional experimental results showed that pore expansion of a support led to higher CO₂ capture capacity of the supported AAIL sorbent, although the capacity did not approach the theoretical maximum value only by the pore expansion. In cyclic CO₂ adsorption–desorption experiments, the mesoporous silica supports (even PE-SBA-15) caused greater losses in the CO₂ capture capacities with the number of cycle than PMMA support. Further investigations to enhance the long-term stabilities of supported AAIL sorbents will be made in our future work.

5.7 References

- [1] G.T. Rochelle, Amine scrubbing for CO₂ capture, *Science* 325 (2009) 1652–1654.
- [2] C.H. Yu, C.H. Huang, C.S. Tan, A review of CO₂ capture by absorption and adsorption, *Aerosol Air Qual. Res.* 12 (2012) 745–769.
- [3] A. Samanta, A. Zhao, G.K.H. Shimizu, P. Sarkar, R. Gupta, Post-combustion CO₂ capture using solid sorbents: A review, *Ind. Eng. Chem. Res.* 51 (2012) 1438–1463.

- [4] J. Wang, L. Huang, R. Yang, Z. Zhang, J. Wu, Y. Gao, Q. Wang, D.O. Hare, Z. Zhong, Recent advances in solid sorbents for CO₂ capture and new development trends, *Energy Environ. Sci.* 7 (2014) 3478–3518.
- [5] E.D. Bates, R.D. Mayton, I. Ntai, J.H. Davis, CO₂ capture by a task-specific ionic liquid, *J. Am. Chem. Soc.* 124 (2002) 926–927.
- [6] J. Zhang, S. Zhang, K. Dong, Y. Zhang, Y. Shen, X. Lv, Supported absorption of CO₂ by tetrabutylphosphonium amino acid ionic liquids, *Chem. Eur. J.* 12 (2006) 4021–4026.
- [7] Y.Y. Jiang, G.N. Wang, Z. Zhou, Y.T. Wu, J. Geng, Z.B. Zhang, Tetraalkylammonium amino acids as functionalized ionic liquids of low viscosity, *Chem. Commun.* (2008) 505–507.
- [8] B.E. Gurkan, J.C. de la Fuente, E.M. Mindrup, L.E. Ficke, B.F. Goodrich, E.A. Price, W.F. Schneider, J.F. Brennecke, Equimolar CO₂ absorption by anion-functionalized ionic liquids, *J. Am. Chem. Soc.* 132 (2010) 2116–2117.
- [9] B.F. Goodrich, J.C. De La Fuente, B.E. Gurkan, D.J. Zadigian, E.A. Price, Y. Huang, J.F. Brennecke, Experimental measurements of amine-functionalized anion-tethered ionic liquids with carbon dioxide, *Ind. Eng. Chem. Res.* 50 (2011) 111–118.
- [10] B.F. Goodrich, J.C. De Fuente, B.E. Gurkan, Z.K. Lopez, E.A. Price, Y. Huang, J.F. Brennecke, Effect of water and temperature on absorption of CO₂ by amine-functionalized anion-tethered ionic liquids, *J. Phys. Chem. B* 115 (2011) 9140–9150.
- [11] S. Saravanamurugan, A.J. Kunov-kruse, R. Fehrmann, A. Riisager, Amine-functionalized amino acid-based ionic liquids as efficient and high-capacity absorbents for CO₂, *ChemSusChem* 7 (2014) 897–902.
- [12] Y.S. Sistla, A. Khanna, CO₂ absorption studies in amino acid-anion based ionic liquids,

- Chem. Eng. J. 273 (2015) 268–276.
- [13] Q. Yang, Z. Wang, Z. Bao, Z. Zhang, Y. Yang, Q. Ren, H. Xing, S. Dai, New insights into CO₂ absorption mechanisms with amino-acid ionic liquids, *ChemSusChem* 9 (2016) 806–812.
- [14] J. Ren, L. Wu, B.G. Li, Preparation and CO₂ sorption/desorption of N-(3-aminopropyl)aminoethyl tributylphosphonium amino acid salt ionic liquids supported into porous silica particles, *Ind. Eng. Chem. Res.* 51 (2012) 7901–7909.
- [15] X. Wang, N.G. Akhmedov, Y. Duan, D. Luebke, B. Li, Immobilization of amino acid ionic liquids into nanoporous microspheres as robust sorbents for CO₂ capture, *J. Mater. Chem. A*. 1 (2013) 2978–2982.
- [16] X. Wang, N.G. Akhmedov, Y. Duan, D. Luebke, D. Hopkinson, B. Li, Amino acid-functionalized ionic liquid solid sorbents for post-combustion carbon capture, *ACS Appl. Mater. Interfaces*. 5 (2013) 8670–8677.
- [17] Y. Zhang, S. Zhang, X. Lu, Q. Zhou, W. Fan, X.P. Zhang, Dual amino-functionalised phosphonium ionic liquids for CO₂ capture, *Chem. Eur. J.* 15 (2009) 3003–3011.
- [18] V. Hiremath, A.H. Jadhav, H. Lee, S. Kwon, J.G. Seo, Highly reversible CO₂ capture using amino acid functionalized ionic liquids immobilized on mesoporous silica, *Chem. Eng. J.* 287 (2016) 602–617.
- [19] Y. Uehara, D. Karami, N. Mahinpey, Effect of water vapor on CO₂ sorption–desorption behaviors of supported amino acid ionic liquid sorbents on porous microspheres, *Ind. Eng. Chem. Res.* 56 (2017) 14316–14323.
- [20] Y. Uehara, D. Karami, N. Mahinpey, Roles of cation and anion of amino acid anion-functionalized ionic liquids immobilized into a porous support for CO₂ Capture,

- Energy Fuels 32 (2018) 5345–5354.
- [21] K. Fukumoto, M. Yoshizawa, H. Ohno, Room temperature ionic liquids from 20 natural amino acids, *J. Am. Chem. Soc.* 127 (2005) 2398–2399.
 - [22] H. Knuutila, U.E. Aronu, H.M. Kvamsdal, A. Chikukwa, Post combustion CO₂ capture with an amino acid salt, *Energy Procedia* 4 (2011) 1550–1557.
 - [23] D. Guo, H. Thee, C.Y. Tan, J. Chen, W. Fei, S. Kentish, G.W. Stevens, G. da Silva, Amino acids as carbon capture solvents: Chemical kinetics and mechanism of the glycine + CO₂ reaction, *Energy Fuels* 27 (2013) 3898–3904.
 - [24] A. Sayari, Y. Belmabkhout, R. Serna-guerrero, Flue gas treatment via CO₂ adsorption, *Chem. Eng. J.* 171 (2011) 760–774.
 - [25] X. Xu, C. Song, J.M. Andresen, B.G. Miller, A.W. Scaroni, Novel polyethylenimine-modified mesoporous molecular sieve of MCM-41 type as high-capacity adsorbent for CO₂ capture, *Energy Fuels* 16 (2002) 1463–1469.
 - [26] X. Xu, C. Song, J.M. Andr, B.G. Miller, A.W. Scaroni, Preparation and characterization of novel CO₂ “molecular basket” adsorbents based on polymer-modified mesoporous molecular sieve MCM-41, *Micropor. Mesopor. Mat.* 62 (2003) 29–45.
 - [27] X. Xu, C. Song, B.G. Miller, A.W. Scaroni, X. Xu, C. Song, B.G. Miller, A.W. Scaroni, Influence of moisture on CO₂ separation from gas mixture by a nanoporous adsorbent based on polyethylenimine-modified molecular sieve MCM-41, *Ind. Eng. Chem. Res.* 44 (2005) 8113–8119.
 - [28] M.B. Yue, L.B. Sun, Y. Cao, Y. Wang, Z.J. Wang, J.H. Zhu, Efficient CO₂ capturer derived from as-synthesized MCM-41 modified with amine, *Chem. Eur. J.* 14 (2008) 3442–3451.
 - [29] V. Zelenák, M. Badaničová, D. Halamova, J. Čejka, A. Zukal, N. Murafa, G. Goerigk,

- Amine-modified ordered mesoporous silica : Effect of pore size on carbon dioxide capture, *Chem. Eng. J.* 144 (2008) 336–342.
- [30] N. Hiyoshi, K. Yogo, T. Yashima, Adsorption of carbon dioxide on amine modified SBA-15 in the presence of water vapor, *Chem. Lett.* 33 (2004) 510–511.
- [31] M.B. Yue, Y. Chun, Y. Cao, X. Dong, J.H. Zhu, CO₂ capture by as-prepared SBA-15 with an occluded organic template, *Adv. Funct. Mater.* 16 (2006) 1717–1722.
- [32] M.B. Yue, L.B. Sun, Y. Cao, Z.J. Wang, Y. Wang, Q. Yu, J.H. Zhu, Promoting the CO₂ adsorption in the amine-containing SBA-15 by hydroxyl group, *Micropor. Mesopor. Mat.* 114 (2008) 74–81.
- [33] X. Yan, L. Zhang, Y. Zhang, G. Yang, Z. Yan, Amine-modified SBA-15 : Effect of pore structure on the performance for CO₂ capture, *Ind. Eng. Chem. Res.* 50 (2011) 3220–3226.
- [34] M.J. Lashaki, H. Ziaei-azad, A. Sayari, Insights into the hydrothermal stability of triamine-functionalized SBA-15 silica for CO₂ adsorption, *ChemSusChem* 10 (2017) 4037–4045.
- [35] N. Hiyoshi, K. Yogo, T. Yashima, Adsorption characteristics of carbon dioxide on organically functionalized SBA-15, *Micropor. Mesopor. Mat.* 84 (2005) 357–365.
- [36] N. Calin, A. Galarneau, T. Cacciaguerra, R. Denoyel, F. Fajula, Epoxy-functionalized large-pore SBA-15 and KIT-6 as affinity chromatography supports, *C. R. Chimie* 13 (2010) 199–206.
- [37] W.J. Son, J.S. Choi, W.S. Ahn, Adsorptive removal of carbon dioxide using polyethyleneimine-loaded mesoporous silica materials, *Micropor. Mesopor. Mat.* 113 (2008) 31–40.
- [38] Y. Liu, J. Shi, J. Chen, Q. Ye, H. Pan, Z. Shao, Y. Shi, Dynamic performance of CO₂

- adsorption with tetraethylenepentamine-loaded KIT-6, *Micropor. Mesopor. Mater.* 134 (2010) 16–21.
- [39] R.S. Franchi, P.J.E. Harlick, A. Sayari, Applications of pore-expanded mesoporous silica. 2. Development of a high-capacity, water-tolerant adsorbent for CO₂, *Ind. Eng. Chem. Res.* 44 (2005) 8007–8013.
- [40] P.J.E. Harlick, A. Sayari, Applications of pore-expanded mesoporous silica. 5. Triamine grafted material with exceptional CO₂ dynamic and equilibrium adsorption performance, *Ind. Eng. Chem. Res.* 46 (2007) 446–458.
- [41] A. Olea, E.S. Sanz-Pérez, A. Arencibia, R. Sanz, G. Calleja, Amino-functionalized pore-expanded SBA-15 for CO₂ adsorption, *Adsorption* 19 (2013) 589–600.
- [42] T.P.B. Nguyen, J.W. Lee, W.G. Shim, H. Moon, Synthesis of functionalized SBA-15 with ordered large pore size and its adsorption properties of BSA, *Micropor. Mesopor. Mater.* 110 (2008) 560–569.
- [43] Y. Wang, M. Noguchi, Y. Takahashi, Y. Ohtsuka, Synthesis of SBA-15 with different pore sizes and the utilization as supports of high loading of cobalt catalysts, *Catal. Today* 68 (2001) 3–9.
- [44] D.H. Jo, H. Jung, D.K. Shin, C.H. Lee, S.H. Kim, Effect of amine structure on CO₂ adsorption over tetraethylenepentamine impregnated poly methyl methacrylate supports, *Sep. Purif. Technol.* 125 (2014) 187–193.
- [45] M.L. Gray, J.S. Hoffman, D.C. Hreha, D.J. Fauth, S.W. Hedges, K.J. Champagne, H.W. Pennline, Parametric study of solid amine sorbents for the capture of carbon dioxide, *Energy Fuels* 23 (2009) 4840–4844.
- [46] M.L. Gray, K.J. Champagne, D. Fauth, J.P. Baltrus, H. Pennline, Performance of

- immobilized tertiary amine solid sorbents for the capture of carbon dioxide, *Int. J. Greenh. Gas Con.* 2 (2012) 3–8.
- [47] P. Zeng, S. Zajac, P.C. Clapp, J.A. Rifkin, Nanoparticle sintering simulations 1, *Mat. Sci. Eng. A-Struct.* 252 (1998) 301–306.
- [48] M.J. Al-Marri, M.M. Khader, M. Tawfik, G. Qi, E.P. Giannelis, CO₂ Sorption kinetics of scaled-up polyethylenimine-functionalized mesoporous silica sorbent, *Langmuir* 31 (2015) 3569–3576.
- [49] A. Heydari-gorji, Y. Belmabkhout, A. Sayari, Polyethylenimine-impregnated mesoporous silica: Effect of amine loading and surface alkyl chains on CO₂ adsorption, *Langmuir* 27 (2011) 12411–12416.

CHAPTER 6: Amino acid ionic liquid-modified mesoporous silica sorbents with remaining surfactant for CO₂ capture

6.1 Presentation of the article

This paper mainly presents the effect of remaining surfactants in mesoporous silica supports on CO₂ capture of the supported amino acid ionic liquid (AAIL) sorbents. MCM-41 and SBA-15 calcined and not calcined were first synthesized and used as mesoporous silica supports. 1-Ethyl-3-methylimidazolium lysine ([EMIM][Lys]) was again employed as an AAIL and loaded on these supports to prepare the supported AAIL sorbents. Then, CO₂ adsorption experiments of the [EMIM][Lys]-loaded mesoporous silica sorbents were carried out using a TGA in a dry CO₂ gas flow condition. Very interestingly, the supports not calcined, named MCM-41-SA and SBA-15-SA, gave rise to greater CO₂ adsorption capacities of the supported AAIL sorbents than the counterparts calcined, although the as-prepared MCM-41-SA and SBA-15-SA themselves hardly adsorbed CO₂ in the same run condition. It was found that the surfactants remaining in the supports not calcined can enhance the CO₂ adsorption performances of the supported AAIL sorbents.

This paper also provides the effect of combining remaining surfactant and pore-expansion of a mesoporous silica support on CO₂ adsorption of the supported AAIL sorbent. This was explored, since it has been found that pore-expansion of supports can also led to higher capacities of the sorbents. Pore-expanded SBA-15 (PE-SBA-15) calcined and not calcined were synthesized and used for the examination. Although a synergetic effect between the remaining surfactant and pore-expansion was expected, PE-SBA-15 not calcined, or PE-SBA-15-SA, caused lower capacity of the supported [EMIM][Lys] sorbent at any loadings. In other words, the effects of

both the remaining surfactant and remaining surfactant were not obtained at the same time on CO₂ capture of supported AAIL sorbents.

This study was carried out almost entirely by Yusuke Uehara under the supervision of Dr. Nader Mahinpey. Dr. Davood Karami assisted in conducting BET analyses in other group's lab and provided some advices in writing the paper.

Amino acid ionic liquid-modified mesoporous silica sorbents with remaining surfactant for CO₂ capture

This article has been published to Adsorption in December, 2018.

*Yusuke Uehara, Davood Karami, and Nader Mahinpey**

Department of Chemical and Petroleum Engineering, Schulich School of Engineering,
University of Calgary, Calgary, AB T2N 1N4, Canada

6.2 Abstract

An amino acid ionic liquid (AAIL) was immobilized into a few kinds of mesoporous silica supports, namely MCM-41 and SBA-15, calcined or not calcined by an impregnation method. 1-Ethyl-3-methylimidazolium lysine ([EMIM][Lys]) was synthesized and employed as an AAIL. CO₂ adsorption experiments were then carried out using the [EMIM][Lys]-loaded mesoporous silica sorbents. Although the as-prepared supports not calcined, denoted as MCM-41-SA and SBA-15-SA, themselves did not adsorb CO₂ almost at all, these supports led to higher CO₂ adsorption capacities of the supported [EMIM][Lys] sorbents than the counterparts calcined, because of the remaining surfactant in the supports. Despite the improved adsorption performances for supported AAIL sorbents, the remaining surfactants did not enhance the regeneration performances in cyclic CO₂ adsorption-desorption. Pore-expanded SBA-15 (PE-SBA-15) was also synthesized and used as a support to see the effect of pore-expansion of support on CO₂ adsorption by the AAIL-loaded sorbents, not only the remaining surfactant. The calcined PE-SBA-15 caused greater capacities than the calcined SBA-15 at any [EMIM][Lys]

loadings, displaying that pore-expansion can also improve the CO₂ adsorption performances. On the other hand, PE-SBA-15 not calcined (PE-SBA-15-SA) did not result in higher capacities of the sorbents than the counterpart calcined, in contrast to SBA-15-SA and MCM-41-SA. Thus, a synergetic effect by combination of the remaining surfactant and pore-expansion of support was not seen on the CO₂ adsorption of supported AAIL sorbents.

6.3 Introduction

Moderating anthropogenic CO₂ emission from coal- and natural gas-fired power plants has been a matter of concern as a serious environmental issue, since it is widely accepted that CO₂ is one of major greenhouse gases causing climate change. Although aqueous amine scrubbing has been applied to post-combustion CO₂ capture as a matured technology with long years' operating experience [1], this technology has some disadvantages including corrosion of the equipment, thermal and oxidative degradation of the solvents, solvent losses and high regeneration energy requirement [2]. To overcome those drawbacks of liquid amine absorption, many efforts have been directed to developing promising alternative materials and technologies so far [3,4].

Amine-functionalized ionic liquids (ILs), or so-called task-specific ionic liquids (TSILs) for the selective removal of CO₂, are attractive materials as alternatives to liquid amines because of their unique characteristics such as negligible vapor pressure, excellent thermal stability and tunable physicochemical properties [5,6]. Amino acid anion-functionalized ionic liquids (AAILs), which were developed by Ohno's group for the first time in 2005 with 20 α -amino acids (AAs) [7], are one of TSILs energetically studied for CO₂ capture in particular [8–12]. Although AAILs have active amino groups ($-NH_2$) in their anions for the reaction with CO₂ like amines, it is extremely desirable to immobilize the AAIL bulks into a porous support dispersedly to enhance

the CO₂ sorption–desorption rates, because ILs possess a high viscosity causing firm gas diffusion resistance [13–15]. It is considered greatly important to investigate the impact of physical and chemical properties of support materials on the CO₂ capture performances of supported AAILs. However, no researchers have conducted such studies using various supports and AAILs.

Many efforts have been devoted to developing effective amine-modified solid sorbents for removal of CO₂ by immobilizing amines into a certain support, such as mesoporous silica, activated carbon, zeolite and polymer [6,16]. For mesoporous silica supports, various materials, including MCM-41 [17–21], SBA-15 [22–26] and KIT-6 [27–29], have been synthesized and employed to study the influence of textural properties and surface chemistry of the amine-loaded solid sorbents on the CO₂ adsorption–desorption. Ahn’s group has clarified that the pore size of supports exerted a dominant impact on the CO₂ adsorption capacities of the amine-impregnated sorbents using several kinds of mesoporous silica supports [27]. Other researchers have also presented that the pore size and pore volume of mesoporous silicas were important factors affecting the CO₂ adsorption capacities of amine-loaded sorbents [21,30]. Sayari’s group has developed pore-expanded MCM-41 (PE-MCM-41) supports and carried out CO₂ capture studies using the amine-functionalized PE-MCM-41 sorbents [31–33]. The PE-MCM-41 led to higher CO₂ capture capacities of the amine-modified solid sorbents than the conventional MCM-41 and other supports, due to larger amounts of amines loaded into the pore channels of PE-MCM-41.

Apart from the textural properties such as pore size, it is assumed that the surface chemistry of supports is another crucial factor to improve the CO₂ capture performance of the supported chemisorbents. Some researchers have examined the effect of leaving the surfactants in the as-prepared mesoporous silica supports on the CO₂ adsorption–desorption of the amine-modified

solid sorbents [20,24,34]. As a result, the remaining surfactants in the supports gave rise to higher CO₂ adsorption capacities of the supported amine sorbents, since they allowed the amine bulks to disperse better on the surface of the supports to enhance the interaction between the amines and CO₂. This strategy can also contribute to saving of energy and time, as the surfactants do not need to be removed in the preparation process of the supports. In this study, the effect of remaining surfactants in mesoporous silica supports (MCM-41, SBA-15 and pore-expanded SBA-15) on the CO₂ capture of AAIL-modified solid sorbents is investigated using 1-ethyl-3-methylimidazolium lysine ([EMIM][Lys]) as an AAIL.

6.4 Experimental section

6.4.1 Synthesis of materials

6.4.4.1 [EMIM][Lys]

1-Ethyl-3-methylimidazolium bromide ([EMIM][Br], ≥98%) and L-lysine (Lys, 98%) were used as materials to synthesize an AAIL of [EMIM][Lys] by a neutralization method, both of which were purchased from Alfa Aesar Co. (Ward Hill, MA). The detailed preparation procedure of [EMIM][Lys] is described elsewhere [35,36].

6.4.4.2 Mesoporous silica supports

MCM-41 and SBA-15 supports were synthesized based on the procedures reported by Ahn's group [27]. The preparation of MCM-41 required the use of colloidal silica HS-40 (40 wt%, Aldrich) as a silica source and cetyltrimethylammonium bromide (CTAB, Sigma) as a templating agent. Typically, 0.4 g of NaOH was dissolved in 10 g of deionized water. 2.8 g of HS-40 was then added to the NaOH solution while stirring at 50 °C to prepare a silicate solution. 1.84 g of

CTAB was dissolved in 10 g of deionized water to prepare a CTAB solution, followed by adding it to the silicate solution with stirring at room temperature. To adjust pH of the solution to 11, a proper quantity of 1 N acetic acid ($\geq 99.7\%$, Sigma-Aldrich) was added. After stirring the solution for further 6 h at room temperature, it was aged for 72 h at 100 °C to get a crude solid product. The solid product was filtered, washed with deionized water, and then dried for 24 h at 100 °C. Around half of the dried product was calcined for 5 h at 550 °C to obtain a final product of the surfactant-free “MCM-41”. The other half was not calcined to leave the surfactant (CTAB) in the support, which was denoted as “MCM-41-SA”.

The synthesis of SBA-15 was carried out using tetraethyl orthosilicate (TEOS, 98%, Aldrich) as a silica source and triblock copolymer EO20-PO70-EO20 (Pluronic® P123, Aldrich) as a templating agent [27]. The first step was adding 1 g of P123 to 38 mL of 1.6 M HCl (prepared with 37% HCl, VWR), which was then stirred for 1 h. Subsequently, 2.13 g of TEOS was added to the solution while continuously stirring. After the mixture was aged for 24 h at 35 °C, it was heated statically for 24 h at 100 °C to gain a crude solid product. The crude product was collected by filtration. Then, washing the solid product with deionized water, followed by drying overnight at 100 °C provided the SBA-15 with the remaining surfactant (P123), which was named “SBA-15-SA”. Almost half of the SBA-15-SA was calcined for 4 h at 550 °C to obtain the surfactant-free “SBA-15”.

Also, pore-expanded SBA-15, or PE-SBA-15, was synthesized by modifying the preparation process of SBA-15, which involved the use of 1,3,5-trimethylbenzene (TMB, $\geq 98\%$, Alfa Aesar) as a swelling agent [28,37,38]. The specific modifications are as follows: 1) 1.0 g of TMB were added to the solution of P123 dissolved in 1.6 M HCl along with TEOS before the aging at 35 °C, and 2) after the aging at 35 °C, the mixture was heated for 24 h at 130 °C, instead of 100 °C.

PE-SBA-15 and PE-SBA-15-SA were finally obtained with and without the calcination, respectively, through the same process as the above supports.

6.4.4.3 [EMIM][Lys]-loaded mesoporous silica sorbents

The [EMIM][Lys] was immobilized into the mesoporous silica supports by an impregnation method to gain the supported AAIL sorbents. The first step was dissolving the [EMIM][Lys] in an aqueous ethanol solution at a concentration of 50 mg/mL, followed by stirring at 200 rpm for 30 min at room temperature. Subsequently, the mesoporous silica was added to the solution in different weight ratios so that the [EMIM][Lys] loading meets 10, 20, 30, 50, 60 or 70 wt%, which was stirred further at 100 rpm for 2 h. Evaporation of the solvent, followed by drying the residue at 50 °C in vacuo for 24 h provided the [EMIM][Lys]-loaded mesoporous silica sorbent. [EMIM][Lys]-loaded mesoporous silica sorbents with an added surfactant were also prepared, in order to see the effect of adding a surfactant to the surfactant-free sorbents on the CO₂ adsorption of supported AAIL sorbents. Specifically, certain amounts of calcined MCM-41 and CTAB were added to the [EMIM][Lys] dissolved in an aqueous ethanol solution (50 mg/mL) so that the weight ratio meets “50% [EMIM][Lys] + 25% MCM-41 + 25% CTAB” or “50% [EMIM][Lys] + 37.5% MCM-41 + 12.5% CTAB”. Then, 50 wt% [EMIM][Lys]-loaded MCM-41 sorbents with the added CTAB (50 wt% or 25 wt% CTAB in the support) were obtained through the same steps as described above.

6.4.4.4 Characterization

Thermogravimetric analyses (TGAs) of the as-prepared [EMIM][Lys] and mesoporous silica supports were performed using a thermogravimetric analyzer (TGA 8000, PerkinElmer). The analyses were conducted under N₂ atmosphere while raising the TGA temperature at a heating

rate of 10 °C/min.

N₂ adsorption–desorption isotherms of the as-prepared mesoporous silicas and [EMIM][Lys]-loaded mesoporous silica sorbents were measured at –196 °C with a surface area analyzer (ASAP 2020, Micromeritics). Prior to the measurement, the samples were degassed for 120 min at 100 °C. The calculation of surface areas by the Brunauer-Emmet-Teller (BET) method and of pore volumes and pore sizes by the Barrett–Joynes–Halenda (BJH) method were carried out from the data obtained. The experimental errors were estimated within ±5% based on three repetitive analysis data with the pure MCM-41.

6.4.4.5 CO₂ adsorption test

CO₂ capture tests were performed for the as-prepared supports and [EMIM][Lys]-loaded sorbents using a TGA (TG 209 F1 Libra, NETZSCH). One experiment consisted of desorption step and then adsorption step. Specifically, nearly 10 mg of a sample was loaded in the TGA crucible and heated to 100 °C in 100% N₂ gas at a flow rate of 33 mL/min. After holding the sample for 50 min under this condition to desorb any gases from the sample, the temperature was lowered to 30 °C. Subsequently, the feed gas was changed to mixed gases of CO₂ and N₂ at CO₂ concentration of 15%, which were supplied at a flow rate of 39 mL/min. The CO₂ adsorption process was conducted for 30 min under this condition. The experimental errors of the CO₂ adsorption capacities obtained were estimated within ±5% from three repetitive run data using 50 wt% [EMIM][Lys]-loaded MCM-41-SA sorbent.

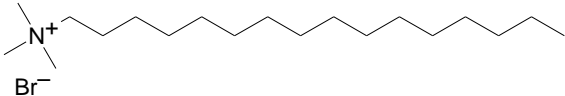
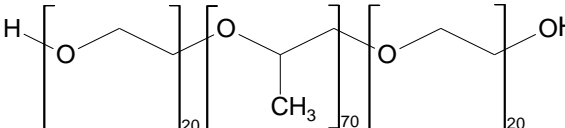
Cyclic CO₂ desorption–adsorption tests were also carried out to see the long-term CO₂ capture stability. The same desorption and adsorption steps as above were repeated 10 times for a cyclic experiment; the desorption was conducted for 50 min under 100 °C and 100% N₂ flow, followed by the adsorption for 30 min under 30 °C and 15% CO₂ (balance N₂) flow. In addition,

the cyclic experiments were also performed under different desorption temperature of 80 or 120 °C, instead of 100 °C, to see the effect of desorption temperature on the cyclic stability.

6.5 Results and discussion

In this work, six mesoporous silica supports (MCM-41, SBA-15 and PE-SBA-15), which were either calcined or not calcined, were prepared and used to develop supported AAIL sorbents for CO₂ capture study. Table 6.1 summarizes the description of these mesoporous silicas.

Table 6.1. Description of the mesoporous silica supports used in this work.

Support	Calcination	Additive	Surfactant
MCM-41	Calcined (550 °C)		CTAB
MCM-41-SA	Not calcined	—	
SBA-15	Calcined (550 °C)		P123
SBA-15-SA	Not calcined	—	
PE-SBA-15	Calcined (550 °C)	TMB	
PE-SBA-15-SA	Not calcined		

The surfactants used to synthesize the supports were CTAB for MCM-41 and P123 for SBA-15 and PE-SBA-15, respectively. [EMIM][Lys] (AAIL) was synthesized by a neutralization method, which was then immobilized into each support with different loadings by an impregnation

method to prepare the [EMIM][Lys]-loaded mesoporous silica sorbents. Lys was chosen as an AA (anion) to synthesize the AAIL, since Lys has exhibited greater CO₂ sorption performance than other AAs in previous studies using supported AAIL sorbents, because of an additional amino group in its side chain and the higher basicity [13,15,35,36].

6.5.1 Characterization

6.5.5.1 TGA behavior

Figure 6.1 depicts TGA profiles of the as-prepared [EMIM][Lys] and mesoporous silica supports under N₂ atmosphere at a heating rate of 10 °C/min. MCM-41, SBA-15 and PE-SBA-15 exhibited a similar behavior of very slight weight reduction with temperature, and those weight losses to 700 °C were only 3.9, 3.1 and 1.1%, respectively. The negligible weight losses for these supports imply that almost all of each surfactant was removed from the individual supports in their preparation processes. On the other hand, MCM-41-SA, SBA-15-SA and PE-SBA-15-SA, which were the supports not calcined, showed large weight decreases, meaning that each surfactant used for the synthesis remained in these supports. The weight losses of MCM-41-SA, SBA-15-SA and PE-SBA-15-SA to 700 °C were 51, 32 and 18%, respectively. Higher weight loss of MCM-41-SA than the others suggests that larger amount of the surfactant remained in this support. PE-SBA-15-SA exhibited smaller and slower weight decrease than SBA-15-SA after 350 °C, although the same mass ratio of silica (TEOS) to surfactant (P123) was employed to synthesize these supports. In the preparation of PE-SBA-15-SA, it was washed with ethanol, not pure water, to remove TMB used as a pore-expander. If TMB exists in a support, any significant weight reduction would occur before 350 °C, or near the boiling point of TMB (165 °C). However, PE-SBA-15-SA did not show such a phenomenon, indicating that TMB was

completely removed from the support by the ethanol extraction. It is rather assumed that not only TMB but also a part of P123 were removed by the ethanol extraction, which is a possible reason for lower weight loss of PE-SBA-15-SA than SBA-15-SA.

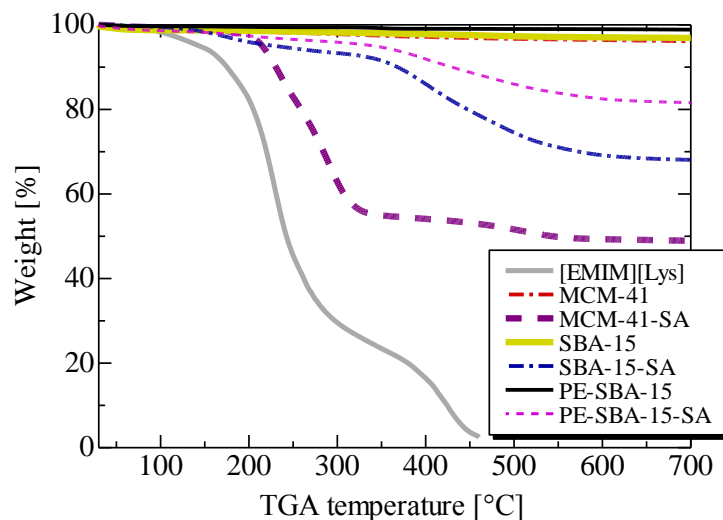


Figure 6.1. TGA profiles of as-prepared [EMIM][Lys] and mesoporous silica supports under N₂ atmosphere at a heating rate of 10 °C/min.

6.5.5.2 Pore property

Table 6.2 lists BET surface area (S_{BET}) and BJH adsorption cumulative pore volume (V_{p}) of the as-prepared mesoporous silica supports. MCM-41-SA, SBA-15-SA and PE-SBA-15-SA showed lower S_{BET} and V_{p} than the corresponding counterparts calcined, indicating that each surfactant used for the synthesis not only remained in the supports, but also blocked their pores. The decreases in S_{BET} and V_{p} of MCM-41 by the remaining surfactant were much larger than those of SBA-15 and PE-SBA-15. This difference agrees with greater weight loss of MCM-41-SA in the thermogravimetry (Figure 6.1) that indicates more amount of surfactant left

in the support than the other supports.

Table 6.2. Textural properties of as-prepared mesoporous silica supports.

Support	$S_{\text{BET}}^{\text{a}}$ [m^2/g]	V_{p}^{b} [cm^3/g]
MCM-41	1213	0.83
MCM-41-SA	20	0.06
SBA-15	725	0.94
SBA-15-SA	377	0.67
PE-SBA-15	503	2.30
PE-SBA-15-SA	304	1.50

^a BET surface area.

^b BJH adsorption cumulative pore volume.

Zhu's group has presented the same discrepancy between MCM-41 and SBA-15 not calcined [20]. According to their interpretation, for MCM-41, a stronger electrostatic force between the silica wall and surfactant (CTAB) existing in the silica makes the removal of the surfactant by just water washing more difficult than SBA-15. Figure 6.2 describes the BJH pore size distributions of the as-prepared supports. PE-SBA-15 exhibited the peak of pore size distribution in larger pore size range than MCM-41 and SBA-15, owing to the pore expansion by addition of TMB and aging at higher temperature (130 °C). When each surfactant remained in these supports

without calcination, their peaks of pore size distribution did not shift, whereas their pore spaces reduced.

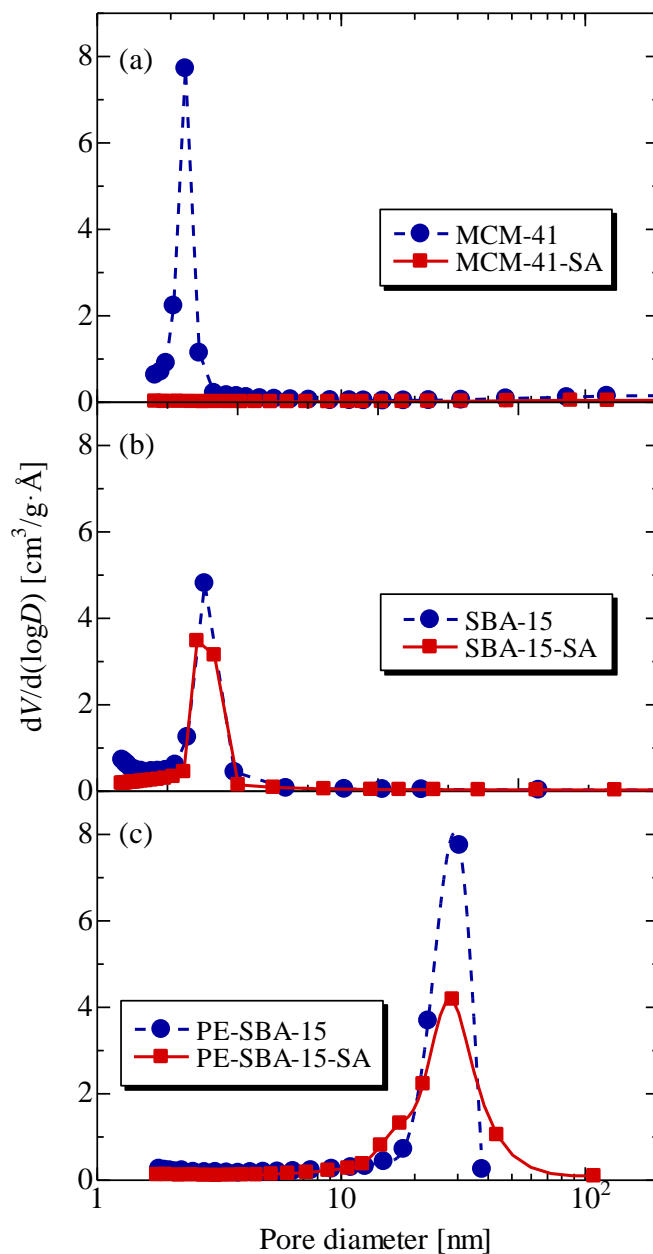


Figure 6.2. BJH pore size distributions of as-prepared (a) MCM-41, (b) SBA-15 and (c) PE-SBA-15.

Table 6.3. Textural properties of [EMIM][Lys]-loaded mesoporous silica sorbents with different [EMIM][Lys] loadings.

Support	$S_{\text{BET}}^{\text{a}}$ [m^2/g]	V_{P}^{b} [cm^3/g]
MCM-41 (50%)	36	0.11
SBA-15 (20%)	265	0.58
SBA-15 (30%)	223	0.48
SBA-15 (50%)	75	0.15
SBA-15 (60%)	33	0.05
SBA-15-SA (30%)	110	0.30
SBA-15-SA (50%)	3.4	0.01
PE-SBA-15 (50%)	191	1.07
PE-SBA-15-SA (50%)	24	0.15

Table 6.3 summarizes S_{BET} and V_{P} of the [EMIM][Lys]-loaded mesoporous silica sorbents with different [EMIM][Lys] loadings. It is found by comparing data in Tables 6.2 and 6.3 that all the mesoporous silica supports reduced both their S_{BET} and V_{P} when the [EMIM][Lys] was loaded on them with higher loadings. This gives a strong evidence that the [EMIM][Lys] was successfully located within the channels of these supports, regardless of the presence or absence

of the remaining surfactant in the support [34].

6.5.2 CO₂ capture performance

6.5.2.1 As-prepared mesoporous silicas

It is important to evaluate the CO₂ adsorption performances of as-prepared mesoporous silica supports separately from those of AAIL-loaded mesoporous silica sorbents, in order to understand how the supports act on the CO₂ adsorption of AAIL when the AAIL is loaded on them. Therefore, CO₂ adsorption experiments of the as-prepared mesoporous silicas were first conducted under TGA experimental condition of 15% CO₂ (balance N₂) flow and 30 °C. Figure 6.3a and b present the dynamic CO₂ adsorption performances of pure MCM-41 and SBA-15 supports with and without the remaining surfactant, respectively.

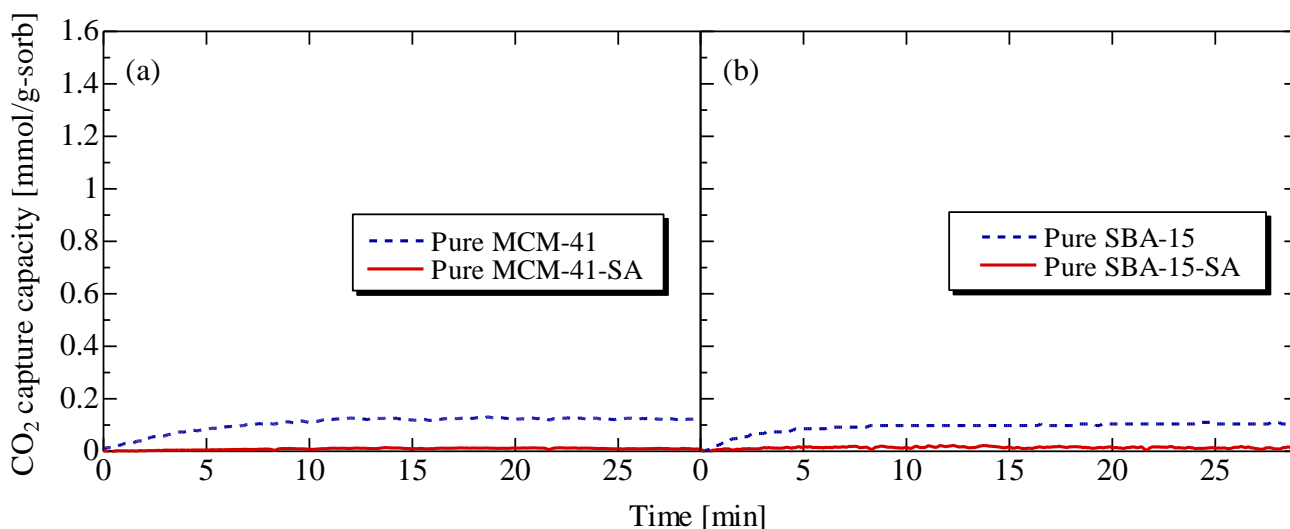


Figure 6.3. Dynamic CO₂ adsorption performances of as-prepared (a) MCM-41 and (b) SBA-15 with and without the remaining surfactant under 15% CO₂ (balance N₂) flow and 30 °C.

The CO₂ capture capacities of MCM-41 and SBA-15 were only around 0.1 mmol/g. Moreover, MCM-41-SA and SBA-15-SA adsorbed further less amounts of CO₂, whose capacities were almost zero. When the same CO₂ capture experiment was carried out using pure CTAB powder, it also did not exhibit any CO₂ uptake, as reported by Zhu's group previously [20]. Mesoporous silicas can physically adsorb CO₂ into the pores [3]. It is considered that reduction in the surface area and pore volume of MCM-41-SA and SBA-15-SA by the remaining surfactant (Table 6.2) caused their lower physical adsorption capacities than the corresponding counterparts calcined.

6.5.2.2 *[EMIM][Lys]-loaded mesoporous silica sorbents with remaining surfactant*

Next, CO₂ adsorption experiments of the [EMIM][Lys]-loaded mesoporous silica sorbents (50 wt% loading) were carried out under the same run condition as the as-prepared supports. Figure 6.4a and b show the dynamic CO₂ capture performances of 50 wt% [EMIM][Lys]-loaded MCM-41 and SBA-15 sorbents with and without the remaining surfactant, respectively. The supported [EMIM][Lys] sorbents exhibited much greater CO₂ adsorption capacities than the pure supports (Figure 6.3), suggesting that the [EMIM][Lys] loaded on the support possesses a substantial potential to capture CO₂. It is very noteworthy that MCM-41-SA and SBA-15-SA caused higher capacities of the supported AAIL sorbents, although these pure supports themselves adsorbed less amounts of CO₂ than the corresponding counterparts calcined (Figure 6.3). It is also interesting that both CTAB and P123 remaining in each support contributed to increase in the capacities of the corresponding AAIL-loaded sorbents, regardless of their different chemical structures (Table 6.1) and properties. For supported amine sorbents, Wang et al. have demonstrated using various surfactants with different ionicities, including CTAB and P123, that a surfactant existing in a porous silica support enhanced the CO₂ adsorption capacity and kinetics, despite the type of surfactants [39]. They explained that the surfactants on the

surface of support acted as a promoter of CO₂ diffusion into the amine films, leading to better CO₂ capture performance. Hence, our experimental results illustrated that surfactants remaining in mesoporous silica supports can improve the CO₂ capture capacities even for supported AAILs by promoting the contact between the AAILs and CO₂. This strategy can also result in saving energy and time due to no necessity to remove surfactants from the supports [24].

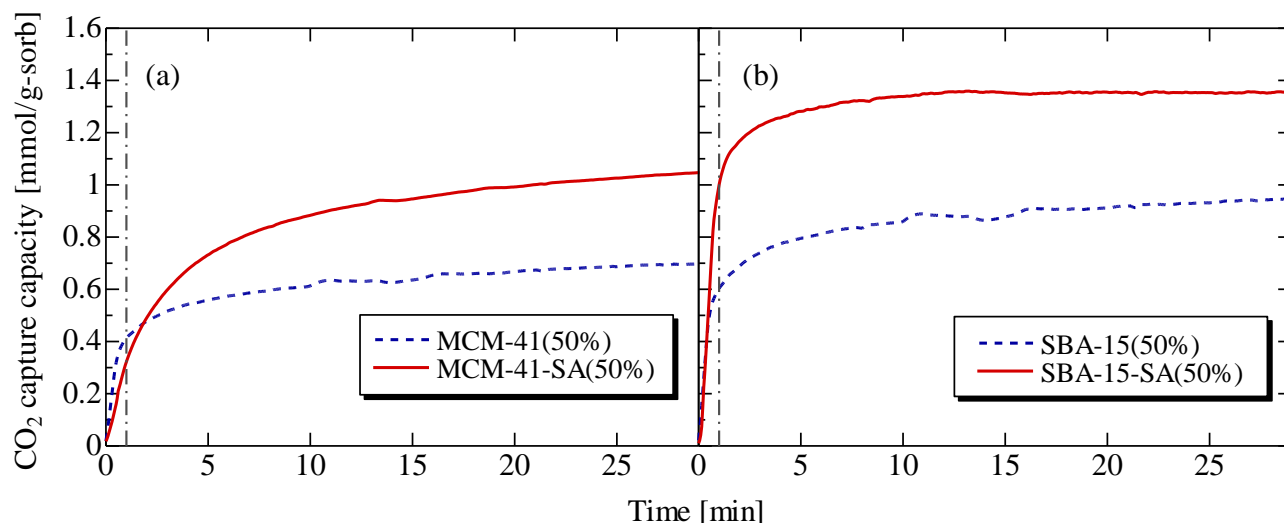


Figure 6.4. Dynamic CO₂ adsorption performances of 50 wt% [EMIM][Lys]-loaded (a) MCM-41 and (b) SBA-15 sorbents with and without the remaining surfactant under 15% CO₂ (balance N₂) flow and 30 °C.

As seen from Figure 6.4, the CO₂ adsorption by supported AAIL sorbents occurred in two stage process, similarly to supported amine sorbents [40]. The first stage is a fast reaction with CO₂ accompanying a sharp weight gain, which takes place on the surface of sorbent (surface reaction). The second stage proceeds much more slowly, in which the weight change gradually ceases. For MCM-41, although the remaining surfactant enhanced the CO₂ adsorption capacity

of the 50 wt% AAIL-loaded sorbent, it lowered the surface reaction rate. For example, at the adsorption time of 1 min, the capacity of 50 wt% [EMIM][Lys]-loaded MCM-41-SA was 31% of the total capacity, whereas that of 50 wt% [EMIM][Lys]-loaded MCM-41 was 59% (Figure 6.4a). On the other hand, the surfactant remaining in SBA-15 did not decrease the surface reaction rate; the capacities of the [EMIM][Lys]-loaded SBA-15-SA and SBA-15 (50 wt%) at 1 min were 73% and 64% of the total capacities, respectively (Figure 6.4b). Lower initial adsorption rate of the AAIL-loaded MCM-41-SA than MCM-41 can be because too huge amount of the surfactant existing on the support's surface delayed the occurrence of the surface reaction, as expected from the characterization of MCM-41-SA described above.

The same experiments were conducted using the supported AAIL sorbents with different [EMIM][Lys] loadings as well. Figure 6.5a and b plot the relationship between the [EMIM][Lys] loading and CO₂ adsorption capacity in different units of mmol/g-sorbent and mol/mol-AAIL, respectively. SBA-15-SA led to higher capacities of the sorbents than SBA-15 at the [EMIM][Lys] loadings of 50, 60 and 70 wt%, implying that the remaining surfactant in the support can offer better CO₂ diffusion into the AAIL active sites with higher AAIL loading. From 60 to 70 wt% loadings, both the capacities of the [EMIM][Lys]-loaded SBA-15 and SBA-15-SA sorbents reduced. This means that too higher AAIL loadings inhibit the CO₂ diffusion regardless of the presence of remaining surfactant as a diffusion promoter, resulting in lower CO₂ adsorption performance. As well as SBA-15, MCM-41 with the remaining surfactant caused higher capacity than the surfactant-free MCM-41 at enough high [EMIM][Lys] loadings of 30 and 50 wt%. However, MCM-41-SA decreased the capacity at 60 wt% loading, unlike MCM-41. Also, MCM-41-SA caused slower surface reaction rate than the calcined MCM-41 at this loading, in the same manner as 50 wt% loading (Fig. 4a). The reasons can be again due to too large

amount of the surfactant existing on the support, in addition to the AAIL. In other words, surfactants would hinder CO₂ diffusion into AAIL's active sites in the sorbent rather than promoting it, when both the AAIL and surfactant exist on the support in too higher ratios.

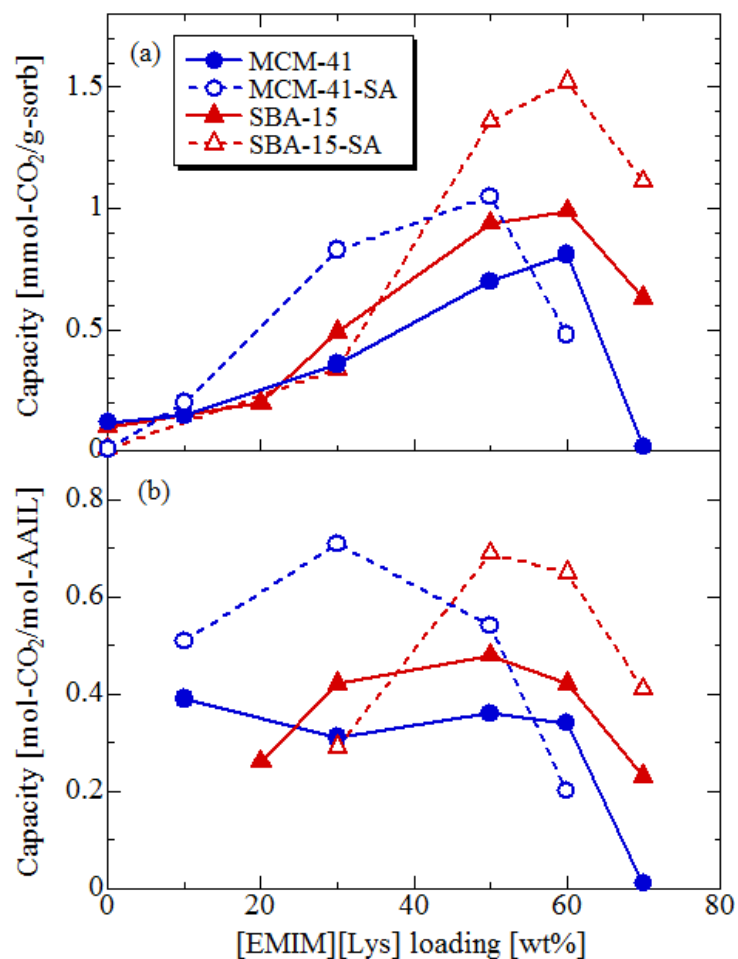


Figure 6.5. Plot of [EMIM][Lys] loading vs. CO₂ adsorption capacity of [EMIM][Lys]-loaded MCM-41 and SBA-15 sorbents with and without the remaining surfactant under 15% CO₂ (balance N₂) flow and 30 °C in units of (a) mmol/g-sorbent and (b) mol/mol-AAIL.

According to previous reports, an amino group in imidazolium AAILs, including

[EMIM][AA], can react with CO₂ in 2:1 stoichiometry, similarly to amines with CO₂ [12,14]. As Lys has an additional amino group in its side chain, 1 mol of [EMIM][Lys] should theoretically capture 1 mol of CO₂ at most, based on this stoichiometry. The experimental reaction stoichiometric ratios of all the supported [EMIM][Lys] sorbents prepared in this study did not reach the theoretical maximum value of 1.0 mol/mol-AAIL (Fig. 5b). However, MCM-41-SA and SBA-15-SA led to a high value of approximately 0.7 mol/mol-AAIL at 30 and 50 wt% [EMIM][Lys] loadings, which were over 1.5 times greater than the corresponding surfactant-free counterparts, respectively.

6.5.2.3 Cyclic CO₂ capture performances of [EMIM][Lys]-loaded mesoporous silica sorbents

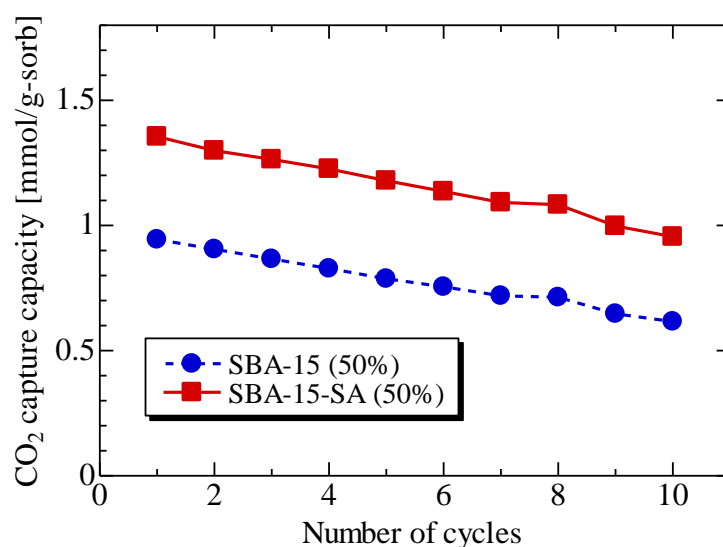


Figure 6.6. Cyclic CO₂ capture performances of 50wt% [EMIM][Lys]-loaded SBA-15 and SBA-15-SA sorbents under the adsorption condition of 15% CO₂ (balance N₂) flow and 30 °C, and desorption condition of 100% N₂ flow and 100 °C.

Cyclic CO₂ capture performance tests were conducted using 50 wt% [EMIM][Lys]-loaded

SBA-15 and SBA-15-SA sorbents, in order to see the long-term stabilities. Figure 6.6 presents changes in the CO₂ capture capacities of these sorbents during 10 cyclic CO₂ adsorption–desorption carried out under the adsorption condition of 15% CO₂ flow and 30 °C, and the desorption condition of 100% N₂ flow and 100 °C. SBA-15-SA resulted in higher capacity of the sorbent at any cycles than SBA-15. However, both these sorbents gradually decreased their capacities with the number of cycle in a similar way, regardless of the presence or absence of the remaining surfactant in the support; the reduction rates in the capacities of the [EMIM][Lys]-loaded SBA-15 and SBA-15-SA sorbents after 10 cycles were 35% and 30%, respectively. In other words, the surfactant in SBA-15-SA did not change (or improve) the cyclic CO₂ capture stability of the supported AAIL sorbents.

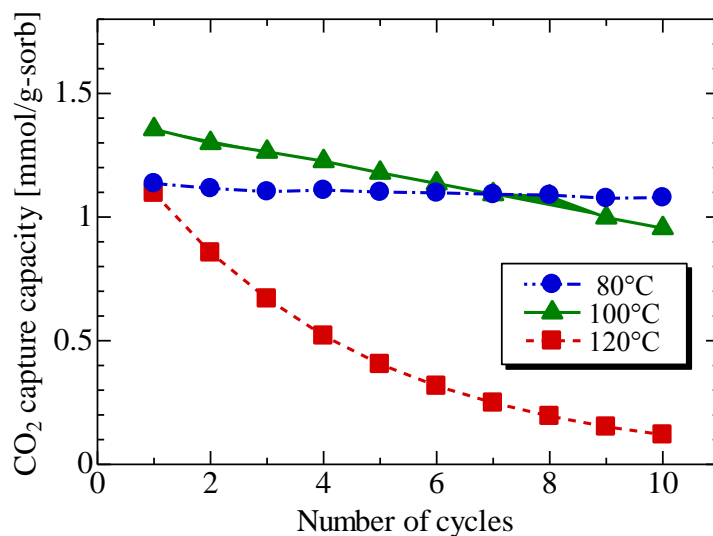


Figure 6.7. Cyclic CO₂ capture performance of 50wt% [EMIM][Lys]-loaded SBA-15-SA sorbent under different desorption temperature of 80, 100 or 120 °C in 100% N₂ flow; the adsorption condition is 15% CO₂ (balance N₂) flow and 30 °C.

Reductions in the capacities of AAIL-loaded mesoporous silica sorbents with higher cycle can occur due to incomplete desorption of CO₂ and weight losses of the AAIL bulks by their volatilization from the sorbents during the regeneration steps [14,15]. It is assumed that regeneration temperature is an important factor for these phenomena, which can in turn highly influence the cyclic CO₂ capture stabilities. Therefore, the cyclic CO₂ adsorption–desorption experiments were also carried out while changing the regeneration temperature to 80 or 120 °C (instead of 100 °C) in each desorption step to see the effect of regeneration temperature on the cyclic CO₂ capture performance of supported AAIL sorbent. Figure 6.7 depicts change in the capacity of 50 wt% [EMIM][Lys]-loaded SBA-15-SA sorbent during 10 cyclic CO₂ capture test conducted under the desorption temperature of 80, 100 or 120 °C; the other experimental condition was same as above. The cyclic stability of the supported AAIL sorbent was quite different by the regeneration temperature. After 10 cycles, the reduction rate of the capacity was 89% under the desorption temperature of 120 °C, whereas it was only 5% under that of 80 °C. In addition to the capacity, the weight of sorbent (sample) also greatly reduced during each desorption step at 120 °C; on the other hand, it hardly decreased at 80 °C. It has been found from our previous studies that the peak temperature of CO₂ desorption from supported [EMIM][AA] sorbents was around 110 °C [35,36]. Nevertheless, a huge reduction in the cyclic stability of supported [EMIM][Lys] sorbent occurred predominantly due to enormous weight loss of the loaded AAIL by its volatilization at the regeneration temperature of 120 °C, rather than incomplete CO₂ desorption. On the other hand, the cyclic performance considerably stabilized at the regeneration temperature of 80 °C due to the highly moderated weight loss. However, the capacity in the first cycle was lower than at that of 100 °C. This might be because water content left in the sorbent was not completely desorbed at 80 °C, which decreased the CO₂ adsorption

performance, since it has been known that water content exerts a negative impact on the CO₂ capture of supported AAIL sorbents, according to our previous studies [35,36]. Thus, these experimental results indicate that optimizing regeneration temperature is very crucial to enhance both the capacities and long-term stabilities of supported AAIL sorbents during cyclic CO₂ capture, which will be further investigated in our future work.

6.5.2.4 *Effect of addition of surfactant*

It is interesting to examine whether a surfactant added to mesoporous silica supports can also improve the CO₂ capture performances of supported AAILs, in a similar manner to the remaining surfactants, or not. For supported amine sorbents, Wang et al. have reported that an addition of only 5% surfactant enhanced the CO₂ adsorption capacities of 65% PEI-loaded sorbents on a surfactant-free porous silica by 6.8 to 17.4%; the effect was different by the type of surfactants [39]. It is assumed from Fig. 1 that the as-prepared MCM-41-SA contains around 50 wt% surfactant (CTAB) in it. Therefore, 50 wt% [EMIM][Lys]-loaded MCM-41-SA sorbent should include 50% [EMIM][Lys], 25% silica (MCM-41) and 25% remaining CTAB approximately in the weight ratio. In order to compare the effect of an added surfactant on the CO₂ adsorption with that of the remaining surfactant, [EMIM][Lys]-loaded MCM-41 sorbents with an added CTAB were prepared so that the weight ratio satisfies “50% [EMIM][Lys] + 25% MCM-41 + 25% CTAB” or “50% [EMIM][Lys] + 37.5% MCM-41 + 12.5% CTAB”, which are denoted as “MCM-41-CTAB50% (50%)” and “MCM-41-CTAB25% (50%)”, respectively. Figure 6.8 compares the CO₂ adsorption capacities of the two sorbents with those of the 50 wt% [EMIM][Lys]-loaded MCM-41 and MCM-41-SA sorbents (without the addition of CTAB). It is considered that MCM-41-CTAB50% (50%) has an equivalent composition, or CTAB, to MCM-41-SA (50%). However, MCM-41-CTAB50% (50%) exhibited much lower capacity than

MCM-41 (50%), instead of surpassing it. Even MCM-41-CTAB25% (50%), which contains half amount of CTAB of MCM-41-CTAB50% (50%), showed the same tendency.

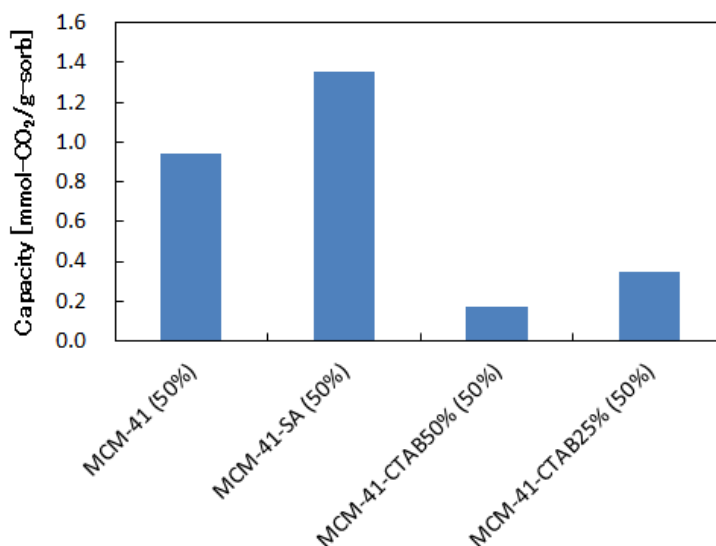


Figure 6.8. CO₂ adsorption capacities of 50 wt% [EMIM][Lys]-loaded MCM-41 (or MCM-41-SA) sorbents with and without an added CTAB under 15% CO₂ (balance N₂) flow and 30 °C.

Zhu's group has gained similar CO₂ adsorption performance results using supported amine sorbents on SBA-15 with and without an added surfactant (P123); calcined SBA-15 with the added P123 caused lower capacities of the sorbents than the surfactant-free counterpart at high amine loadings (over 40 wt%), whereas SBA-15 with the remaining P123 led to higher capacities than these supports [24]. They explained that the diminished performance by SBA-15 with the added P123 was because at high amine loadings, the amine just coated the external surface of the support without being dispersed into it, since the added P123 reduced the pore space of the support more than the remaining P123, although the amount of P123 contained was

equal (40 wt% in the support). Thus, it was found from our results that an addition of surfactant into a support can deteriorate the CO₂ adsorption performances even for supported AAIL sorbents by hindering the AAIL dispersion, rather than promoting it, when both the loaded amounts of surfactant and AAIL are large, in contrast to the remaining surfactant.

6.5.2.5 *Effect of pore-expansion*

For supported amine sorbents, some researchers have demonstrated that pore-expanded mesoporous silica supports gave rise to higher CO₂ capture capacities, as they accommodated more amounts of the amines dispersedly into their larger pores [31,32,41]. There has also been a report that pore size of mesoporous silica supports exerted a predominant impact on the CO₂ adsorption of supported amine sorbents [27]. It is expected from these facts that CO₂ adsorption performances of supported AAILs could be further enhanced by loading AAILs into a pore-expanded mesoporous silica support with the remaining surfactant. Sayari's group has actually presented that a pore-expanded MCM-41 (PE-MCM-41) with the remaining surfactant led to greater CO₂ capture capacities of the amine-loaded sorbents than the surfactant-free PE-MCM-41 as well as other supports [34]. Therefore, the same experiments were conducted using [EMIM][Lys]-loaded PE-SBA-15 and PE-SBA-15-SA sorbents with different [EMIM][Lys] loadings, and those results were compared to see both the effects of pore-expansion and remaining surfactant on the CO₂ adsorption. Figure 6.9 depicts the relationship between the [EMIM][Lys] loading and capacity of the [EMIM][Lys]-loaded SBA-15 and PE-SBA-15 sorbents with and without the remaining surfactant. Regarding the supports calcined, PE-SBA-15 resulted in higher CO₂ capture capacities of the sorbents than SBA-15 at any [EMIM][Lys] loadings. This result indicates that pore-expansion can contribute to better dispersion of even AAILs into the support, leading to greater CO₂ adsorption capacities by the

supported AAILs.

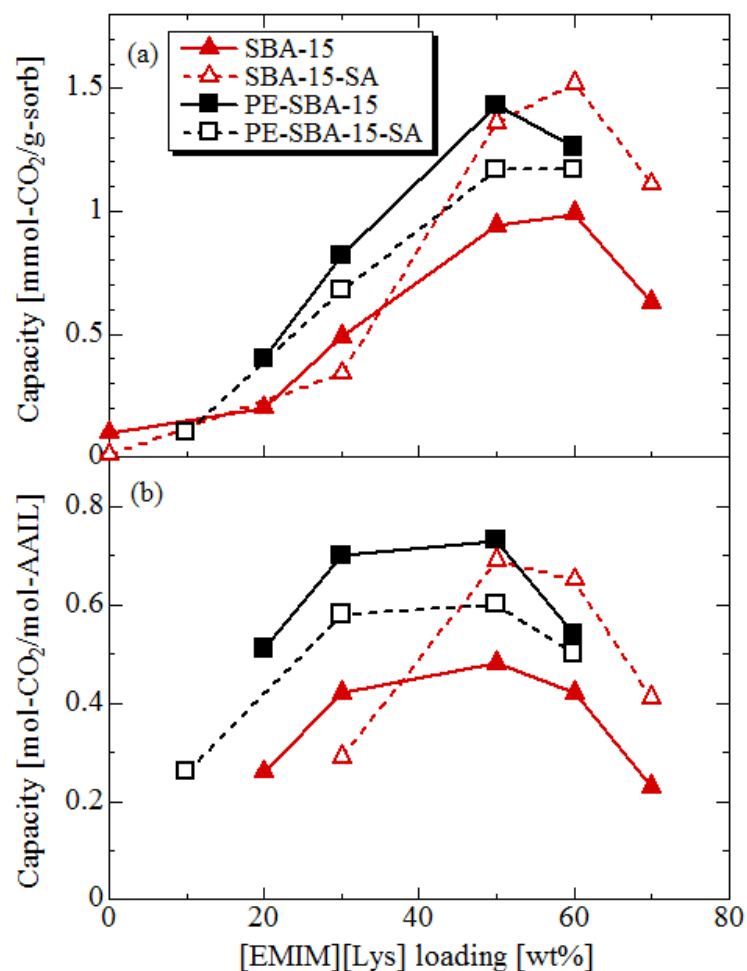


Figure 6.9. Plot of [EMIM][Lys] loading vs. CO₂ adsorption capacity of [EMIM][Lys]-loaded SBA-15 and PE-SBA-15 sorbents with and without the remaining surfactant under 15% CO₂ (balance N₂) flow and 30 °C in units of (a) mmol/g-sorbent and (b) mol/mol-AAIL.

However, PE-SBA-15-SA caused lower capacities than the counterpart calcined (PE-SBA-15), unlike SBA-15-SA and MCM-41-SA: the surface reaction rate also decreased by the remaining surfactant for PE-SBA-15-SA. Furthermore, increase in the capacities by PE-SBA-15-SA was

lower than that by SBA-15-SA especially at high [EMIM][Lys] loadings. Thus, combination of the remaining surfactant and pore-expansion of a support did not exhibit a synergetic effect on CO₂ adsorption of the supported AAILs. When a support having large and deep pore space, like PE-SBA (Fig. 6.2c), contains a surfactant within the channels, more amount of the loaded AAIL might be just confined within inner part of the pore by the surfactant, instead of being dispersed better on the surface, than the surfactant-free support. It is a possible reason for the reduced performance by PE-SBA-15-SA compared with PE-SBA-15.

6.6 Conclusions

CO₂ adsorption study was first conducted using solid sorbents of [EMIM][Lys] loaded on mesoporous silica supports (MCM-41 and SBA-15) calcined or not calcined. Very interestingly, the supports not calcined (MCM-41-SA and SBA-15-SA) caused higher CO₂ capture capacities of the supported AAIL sorbents than the counterparts calcined owing to the remaining surfactant in the supports, although the as-prepared MCM-41-SA and SBA-15-SA themselves hardly adsorbed CO₂ under the same run condition. In contrast to the adsorption performances, the remaining surfactants did not improve the regeneration performances during cyclic CO₂ adsorption–desorption. It was also found that regeneration temperature had a huge impact on the cyclic CO₂ capture stabilities of supported AAIL sorbents, since the capacity greatly decreased with the number of cycle at the desorption temperature of 120 °C due to enormous weight loss of the loaded AAIL by its volatilization, whereas it highly stabilized at 80 °C.

Pore-expanded SBA-15 (PE-SBA-15) was also employed as a support to evaluate the effect of pore-expansion as well as the remaining surfactant of support on CO₂ adsorption of the supported AAILs. It was found that pore-expansion can improve the CO₂ adsorption

performances, as the calcined PE-SBA-15 led to higher capacities of the sorbents than the calcined SBA-15 at any AAIL loadings. However, contrary to expectation, PE-SBA-15 with the remaining surfactant (PE-SBA-15-SA) did not give rise to greater capacities than the surfactant-free counterpart, unlike SBA-15-SA and MCM-41-SA. Thus, combining the remaining surfactant and pore-expansion of support did not provide a synergetic effect on the CO₂ adsorption of supported AAIL sorbents.

6.7 References

- [1] G.T. Rochelle, Amine scrubbing for CO₂ capture, *Science* 325 (2009) 1652–1654.
- [2] F. Lecomte, P. Broutin, É. Lebas, CO₂ Capture: Technologies to reduce greenhouse gas emissions, Editions Technip, Paris, 2010.
- [3] C.H. Yu, C.H. Huang, C.S. Tan, A review of CO₂ capture by absorption and adsorption, *Aerosol Air Qual. Res.* 12 (2012) 745–769.
- [4] A. Samanta, A. Zhao, G.K.H. Shimizu, P. Sarkar, R. Gupta, Post-combustion CO₂ capture using solid sorbents: A review, *Ind. Eng. Chem. Res.* 51 (2012) 1438–1463.
- [5] E.D. Bates, R.D. Mayton, I. Ntai, J.H. Davis, CO₂ capture by a task-specific ionic liquid, *J. Am. Chem. Soc.* 124 (2002) 926–927.
- [6] J. Wang, L. Huang, R. Yang, Z. Zhang, J. Wu, Y. Gao, Q. Wang, D.O. Hare, Z. Zhong, Recent advances in solid sorbents for CO₂ capture and new development trends, *Energy Environ. Sci.* 7 (2014) 3478–3518.
- [7] K. Fukumoto, M. Yoshizawa, H. Ohno, Room temperature ionic liquids from 20 natural amino acids, *J. Am. Chem. Soc.* 127 (2005) 2398–2399.
- [8] B.E. Gurkan, J.C. de la Fuente, E.M. Mindrup, L.E. Ficke, B.F. Goodrich, E.A. Price, W.F.

- Schneider, J.F. Brennecke, Equimolar CO₂ absorption by anion-functionalized ionic liquids, *J. Am. Chem. Soc.* 132 (2010) 2116–2117.
- [9] B.F. Goodrich, J.C. De Fuente, B.E. Gurkan, Z.K. Lopez, E.A. Price, Y. Huang, J.F. Brennecke, Effect of water and temperature on absorption of CO₂ by amine-functionalized anion-tethered ionic liquids, *J. Phys. Chem. B* 115 (2011) 9140–9150.
- [10] B.F. Goodrich, J.C. De La Fuente, B.E. Gurkan, D.J. Zadigian, E.A. Price, Y. Huang, J.F. Brennecke, Experimental measurements of amine-functionalized anion-tethered ionic liquids with carbon dioxide, *Ind. Eng. Chem. Res.* 50 (2011) 111–118.
- [11] S. Saravanamurugan, A.J. Kunov-kruse, R. Fehrmann, A. Riisager, Amine-functionalized amino acid-based ionic liquids as efficient and high-capacity absorbents for CO₂, *ChemSusChem* 7 (2014) 897–902.
- [12] Y.S. Sistla, A. Khanna, CO₂ absorption studies in amino acid-anion based ionic liquids, *Chem. Eng. J.* 273 (2015) 268–276.
- [13] J. Ren, L. Wu, B.G. Li, Preparation and CO₂ sorption/desorption of N-(3-aminopropyl)aminoethyl tributylphosphonium amino acid salt ionic liquids supported into porous silica particles, *Ind. Eng. Chem. Res.* 51 (2012) 7901–7909.
- [14] X. Wang, N.G. Akhmedov, Y. Duan, D. Luebke, B. Li, Immobilization of amino acid ionic liquids into nanoporous microspheres as robust sorbents for CO₂ capture, *J. Mater. Chem. A* 1 (2013) 2978–2982.
- [15] X. Wang, N.G. Akhmedov, Y. Duan, D. Luebke, D. Hopkinson, B. Li, Amino acid-functionalized ionic liquid solid sorbents for post-combustion carbon capture, *ACS Appl. Mater. Interfaces* 5 (2013) 8670–8677.
- [16] A. Sayari, Y. Belmabkhout, R. Serna-guerrero, Flue gas treatment via CO₂ adsorption,

- Chem. Eng. J. 171 (2011) 760–774.
- [17] X. Xu, C. Song, J.M. Andresen, B.G. Miller, A.W. Scaroni, Novel polyethylenimine-modified mesoporous molecular sieve of MCM-41 type as high-capacity adsorbent for CO₂ capture, *Energy Fuels* 16 (2002) 1463–1469.
- [18] X. Xu, C. Song, J.M. Andr, B.G. Miller, A.W. Scaroni, Preparation and characterization of novel CO₂ “molecular basket” adsorbents based on polymer-modified mesoporous molecular sieve MCM-41, *Micropor. Mesopor. Mat.* 62 (2003) 29–45.
- [19] X. Xu, C. Song, B.G. Miller, A.W. Scaroni, X. Xu, C. Song, B.G. Miller, A.W. Scaroni, Influence of moisture on CO₂ separation from gas mixture by a nanoporous adsorbent based on polyethylenimine-modified molecular sieve MCM-41, *Ind. Eng. Chem. Res.* 44 (2005) 8113–8119.
- [20] M.B. Yue, L.B. Sun, Y. Cao, Y. Wang, Z.J. Wang, J.H. Zhu, Efficient CO₂ capturer derived from as-synthesized MCM-41 modified with amine, *Chem. Eur. J.* 14 (2008) 3442–3451.
- [21] V. Zelenák, M. Badaničová, D. Halamova, J. Čejka, A. Zukal, N. Murafa, G. Goerigk, Amine-modified ordered mesoporous silica : Effect of pore size on carbon dioxide capture, *Chem. Eng. J.* 144 (2008) 336–342.
- [22] N. Hiyoshi, K. Yogo, T. Yashima, Adsorption of carbon dioxide on amine modified SBA-15 in the presence of water vapor, *Chem. Lett.* 33 (2004) 510–511.
- [23] N. Hiyoshi, K. Yogo, T. Yashima, Adsorption characteristics of carbon dioxide on organically functionalized SBA-15, *Micropor. Mesopor. Mat.* 84 (2005) 357–365.
- [24] M.B. Yue, Y. Chun, Y. Cao, X. Dong, J.H. Zhu, CO₂ capture by as-prepared SBA-15 with an occluded organic template, *Adv. Funct. Mater.* 16 (2006) 1717–1722.
- [25] M.B. Yue, L.B. Sun, Y. Cao, Z.J. Wang, Y. Wang, Q. Yu, J.H. Zhu, Promoting the CO₂

- adsorption in the amine-containing SBA-15 by hydroxyl group, *Micropor. Mesopor. Mat.* 114 (2008) 74–81.
- [26] M.J. Lashaki, H. Ziaei-azad, A. Sayari, Insights into the hydrothermal stability of triamine-functionalized SBA-15 silica for CO₂ adsorption, *ChemSusChem* 10 (2017) 4037–4045.
- [27] W.J. Son, J.S. Choi, W.S. Ahn, Adsorptive removal of carbon dioxide using polyethyleneimine-loaded mesoporous silica materials, *Micropor. Mesopor. Mat.* 113 (2008) 31–40.
- [28] N. Calin, A. Galarneau, T. Cacciaguerra, R. Denoyel, F. Fajula, Epoxy-functionalized large-pore SBA-15 and KIT-6 as affinity chromatography supports, *C. R. Chimie* 13 (2010) 199–206.
- [29] Y. Liu, J. Shi, J. Chen, Q. Ye, H. Pan, Z. Shao, Y. Shi, Dynamic performance of CO₂ adsorption with tetraethylenepentamine-loaded KIT-6, *Micropor. Mesopor. Mater.* 134 (2010) 16–21.
- [30] X. Yan, L. Zhang, Y. Zhang, G. Yang, Z. Yan, Amine-modified SBA-15 : Effect of pore structure on the performance for CO₂ capture, *Ind. Eng. Chem. Res.* 50 (2011) 3220–3226.
- [31] R.S. Franchi, P.J.E. Harlick, A. Sayari, Applications of pore-expanded mesoporous silica. 2. Development of a high-capacity, water-tolerant adsorbent for CO₂, *Ind. Eng. Chem. Res.* 44 (2005) 8007–8013.
- [32] P.J.E. Harlick, A. Sayari, Applications of pore-expanded mesoporous silica. 5. Triamine grafted material with exceptional CO₂ dynamic and equilibrium adsorption performance, *Ind. Eng. Chem. Res.* 46 (2007) 446–458.
- [33] R. Serna-Guerrero, E. Da'na, A. Sayari, New insights into the interactions of CO₂ with

- amine-functionalized silica, *Ind. Eng. Chem. Res.* 47 (2008) 9406–9412.
- [34] A. Heydari-gorji, Y. Belmabkhout, A. Sayari, Polyethylenimine-impregnated mesoporous silica: Effect of amine loading and surface alkyl chains on CO₂ adsorption, *Langmuir* 27 (2011) 12411–12416.
- [35] Y. Uehara, D. Karami, N. Mahinpey, Effect of water vapor on CO₂ sorption–desorption behaviors of supported amino acid ionic liquid sorbents on porous microspheres, *Ind. Eng. Chem. Res.* 56 (2017) 14316–14323.
- [36] Y. Uehara, D. Karami, N. Mahinpey, Roles of cation and anion of amino acid anion-functionalized ionic liquids immobilized into a porous support for CO₂ Capture, *Energy Fuels* 32 (2018) 5345–5354.
- [37] T.P.B. Nguyen, J.W. Lee, W.G. Shim, H. Moon, Synthesis of functionalized SBA-15 with ordered large pore size and its adsorption properties of BSA, *Micropor. Mesopor. Mater.* 110 (2008) 560–569.
- [38] Y. Wang, M. Noguchi, Y. Takahashi, Y. Ohtsuka, Synthesis of SBA-15 with different pore sizes and the utilization as supports of high loading of cobalt catalysts, *Catal. Today* 68 (2001) 3–9.
- [39] J. Wang, D. Long, H. Zhou, Q. Chen, X. Liu, L. Ling, Surfactant promoted solid amine sorbents for CO₂ capture, *Energy Environ. Sci.* 5 (2012) 5742–5749.
- [40] M.J. Al-Marri, M.M. Khader, M. Tawfik, G. Qi, E.P. Giannelis, CO₂ Sorption kinetics of scaled-up polyethylenimine-functionalized mesoporous silica sorbent, *Langmuir* 31 (2015) 3569–3576.
- [41] S. Loganathan, M. Tikmani, A.K. Ghoshal, Novel pore-expanded MCM-41 for CO₂ capture: Synthesis and characterization, *Langmuir* 29 (2013) 3491–3499.

Chapter 7: Conclusions and recommendations for future study

7.1 Relation between chapters

The principal goal of this thesis project was developing novel and efficient AA-based adsorbents for post-combustion CO₂ capture. Associated with the main goal, several research topics have been arranged, which have been investigated in Chapters 2–6. Figure 7.1 presents the relation between each Chapter.

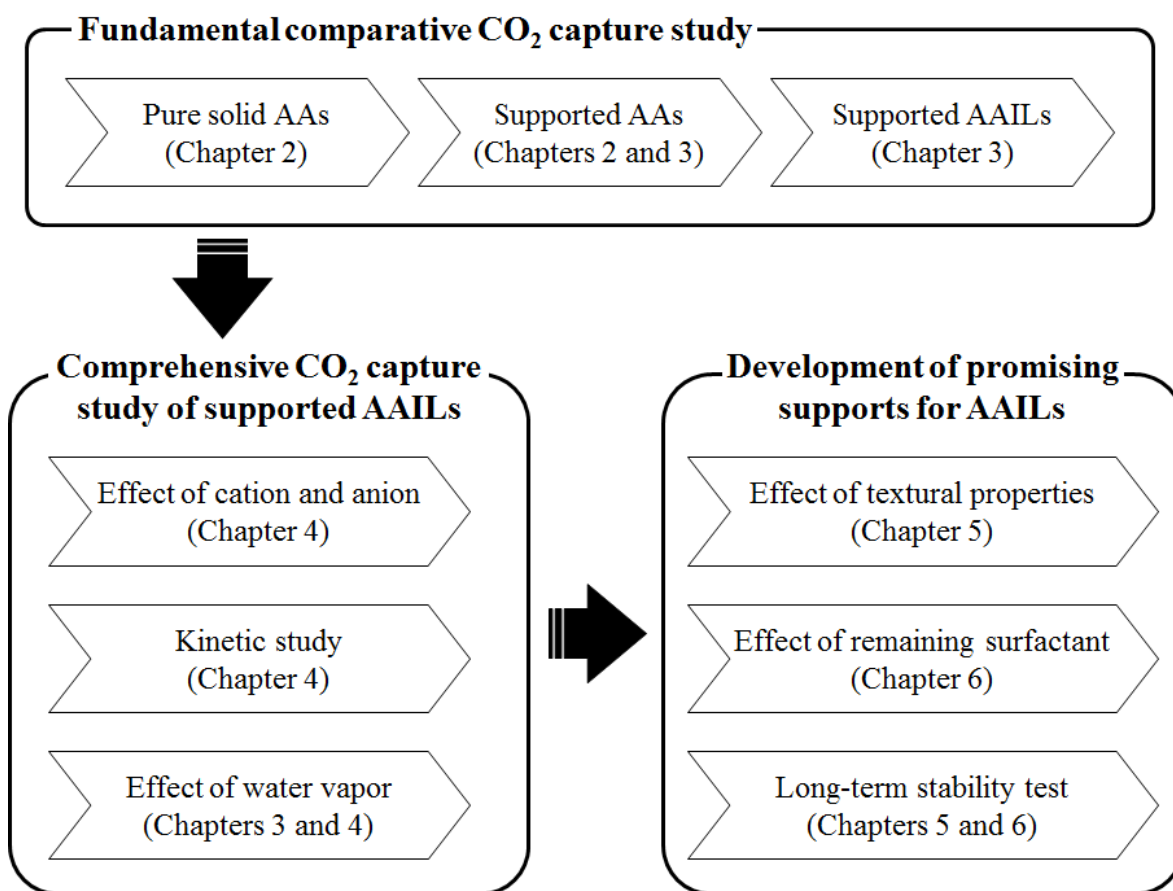


Figure 7.1. Relation between Chapters.

The research topics can be categorized into three themes. The first topic is a fundamental comparative CO₂ capture study in Chapters 2–3. Chapter 2 first focused on CO₂ capture performances of pure solid amino acids (AAs). Subsequently, CO₂ capture study of supported AAs on a commercial support was conducted and compared to see whether amino groups in AAs can be activated by immobilizing and dispersing AA bulks into the support. From Chapter 3, amino acid anion-functionalized ionic liquids (AAILs) have been mainly employed as AA-based materials, since amino groups in AAs can be deprotonated from NH₃⁺ (zwitterionic state) into active NH₂ through the preparation process of AAILs. Chapter 3 compared CO₂ adsorption performances of supported AAIL sorbents with those of supported AA sorbents. The effect of water vapor on CO₂ adsorption–desorption of the supported AA and AAIL sorbents was also investigated.

The second topic is a comprehensive CO₂ capture study of supported AAIL sorbents through Chapters 3–4. Chapter 4 mainly provided the effect of cation and anion of supported AAILs on the CO₂ adsorption. In addition to six AAs (anions), two cations were used for the comparative study. Kinetic analyses were also carried out using a double exponential kinetic model. The effect of water vapor on the CO₂ adsorption–desorption was again studied for these supported AAILs with different cations or anions.

The third topic is development of promising supports for AAILs to improve the CO₂ capture performances. In Chapters 5–6, various mesoporous silica supports were synthesized and employed, and the influence of physical properties or surface chemistry of the supports on CO₂ capture of the supported AAIL sorbents were investigated. Chapter 5 mainly focused on the effect of textural properties of the mesoporous silica supports. Specifically, the correlation of CO₂ adsorption capacities of the sorbents with pore size, pore volume and surface area of the

as-prepared supports was quantitatively assessed. Chapter 5 also presented that pore-expansion of mesoporous silica supports can lead to enhancement of the capacities of the supported AAIL sorbents. Chapter 6 offered the impact of remaining surfactants in the supports on the CO₂ adsorption–desorption. For the exploration, mesoporous silica supports calcined and not calcined were prepared and compared. In Chapter 6, the effect of combining remaining surfactant and pore-expansion of a support was also explored to see whether a synergetic effect on CO₂ adsorption of the supported AAIL sorbents can be obtained or not by the combination.

7.2 Summaries

The summaries for the three major topics described above (Figure 7.1) are first outlined individually. Then, the overall conclusions of the thesis project are summarized at the end.

7.2.1 Fundamental comparative CO₂ capture study

In Chapter 2, fundamental CO₂ adsorption experiments of pure solid AAs were first conducted at 30 °C under a dry or humidified CO₂ gas flow, using Gly, Lys and Arg. Lys and Arg were selected, since they possess additional amino groups in their side chains with higher basicity, which might be beneficial for better reactivity with CO₂. Gly was also chosen for comparison, as Gly is the simplest α -AA, having only hydrogen in its side chain. The same experiments were subsequently carried out using the supported AAs on a commercial PMMA support, in order to see how the adsorption performances change by immobilizing and dispersing the AA bulks into the support. In Chapter 3, AAIL-loaded PMMA sorbents were employed for CO₂ adsorption study, and the results were compared with those of AA-loaded PMMA sorbents. 1-Ethyl-3-methylimidazolium amino acids ([EMIM][AAs]) were synthesized and used as AAILs. The effect of water vapor on CO₂ adsorption–desorption of the supported AA and AAIL sorbents

were evaluated and compared as well. Through these experimental studies, the following conclusions have been obtained:

- Pure AAs (Gly, Lys and Arg) did not adsorb CO₂ almost at all, regardless of the presence or absence of water vapor;
- It was considered that no CO₂ uptake on pure AAs would be mainly because pure AAs exist in a zwitterionic state with inactive NH₃⁺ in large particle size;
- Lys- and Arg-loaded PMMA sorbents adsorbed CO₂ and increased the CO₂ uptakes with higher AA loadings under a dry CO₂ flow condition, whereas Gly-loaded PMMA sorbents hardly adsorbed CO₂ at any loadings;
- This difference indicated that more fractions of the amino groups in Lys and Arg changed into active NH₂ from NH₃⁺ (in zwitterionic state), when Lys and Arg were impregnated with PMMA with higher loadings, in contrast to Gly having no additional amino groups in its side chain;
- [EMIM][AA]-loaded PMMA sorbents exhibited higher CO₂ capture capacities than the corresponding AA-loaded PMMA sorbents with the same AA contents;
- The improved capacities by supported AAIL sorbents can be because most fractions of the amino groups in AAs are deprotonated from NH₃⁺ to active NH₂ in the synthetic process of AAILs;
- Water vapor negatively influenced CO₂ adsorption of the supported [EMIM][Gly] and [EMIM][Lys] sorbents, in contrast to supported amine and AA sorbents, as the water vapor hindered the reaction of the AAILs with CO₂ because of a hydrogen bond interaction formed between the AAILs and H₂O.

7.2.2 Comprehensive CO₂ capture study of supported AAILs

From Chapter 3, AAILs loaded on a certain support have been mainly employed for CO₂ capture study, since the supported AAIL sorbents exhibited good CO₂ adsorption performances. In Chapter 4, the effect of cations as well as anions (AAs) in supported AAILs on the CO₂ adsorption–desorption was first investigated under a dry CO₂ flow condition. Two cations, namely EMIM and tetrabutylphosphonium (P₄₄₄₄) cations, were chosen, as they possess significantly different molecular structures and hydrophilicities from each other. In addition, six AAs (Gly, Lys, His, Ala, BALA and Arg) were selected as AA anions. A commercial PMMA support was again employed to prepare the supported AAIL ([EMIM][AA] and [P₄₄₄₄][AA]) sorbents. Kinetic study on the CO₂ adsorption was then performed using a double exponential model. The effect of water vapor on CO₂ adsorption–desorption of the [EMIM][AA]- and [P₄₄₄₄][AA]-loaded PMMA sorbents was again evaluated and compared in Chapter 4. From these investigations, the following conclusions have been gained:

- [P₄₄₄₄][AA]-loaded PMMA sorbents exhibited higher CO₂ adsorption capacities than the corresponding [EMIM][AA]-loaded PMMA sorbents with the same AA loading in units of mol/mol-AAIL under a dry gas flow condition;
- Especially interesting result was that 50 wt% [P₄₄₄₄][Gly]-loaded sorbent slightly exceeded 0.5 mol/mol-AAIL under a low CO₂ (2.3%) gas flow condition, indicating that the reaction stoichiometry of the supported [P₄₄₄₄][Gly] with CO₂ was closer to 1:1 than 2:1 ratio, since Gly holds only one amino group in its molecule;
- These results suggested that molecular size of the cation in AAIL-modified solid sorbents can affect the reactivity with CO₂;
- Regarding the effect of AA anions, Gly and Lys anions having linear side chains with only

primary amino groups resulted in higher CO₂ adsorption capacities of the supported AAIL sorbents than His and Arg anions having complex side chains with secondary and tertiary amino groups, although His and Arg possess more amino groups in their side chains;

- It was thus found that the side chain structures of AA anions can influence the CO₂ capture performances of the supported AAIL sorbents, in addition to the number of the amino groups;
- In units of mmol/g-sorbent, 50 wt% [EMIM][Lys]-loaded PMMA sorbent exhibited the highest capacity of 1.06 mmol/g-sorbent at 30 °C in the dry gas inlet (2.3% CO₂ concentration) among the AAIL-PMMA sorbents examined;
- The kinetic analyses revealed that a double exponential model very accurately fitted the dynamic CO₂ adsorption behaviors of all the supported AAIL sorbents at any loadings;
- In a humidified CO₂ flow condition, the supported [P₄₄₄₄][AA] sorbents adsorbed much less amount of water vapor than the corresponding supported [EMIM][AA] sorbents, due to less hydrophilicity of P₄₄₄₄ cation than EMIM cation;
- Despite less H₂O uptakes, the supported [P₄₄₄₄][AA] sorbents decreased the CO₂ capture capacities in a similar manner to the supported [EMIM][AA] sorbents in the presence of water vapor;
- From the kinetic behaviors, it was found that much more rapid initial adsorption rate of H₂O than CO₂ on these sorbents, not the total H₂O uptakes, caused inhibition of the surface reaction of AAILs with CO₂, resulting in lower CO₂ capture capacities in the presence of water vapor.

7.2.3 Development of promising supports for AAILs

Through Chapters 5-6, several mesoporous silica supports (MCM-41, SBA-15 and KIT-6)

have been synthesized. Subsequently, an AAIL of [EMIM][Lys] was loaded on the individual mesoporous silica support by impregnation to prepare the supported AAIL sorbent. Chapter 5 mainly focused on the influence of textural properties, namely pore size, pore volume and surface area, of the mesoporous silica supports on CO₂ capture of the supported [EMIM][Lys] sorbent. The impact of pore-expansion of a support was also explored using pore-expanded SBA-15 (PE-SBA-15). In Chapter 6, the main objective was investigation on the effect of remaining surfactant in mesoporous silica supports on the CO₂ capture. The effect of combining remaining surfactant and pore-expansion of a support was also examined. In addition, cyclic CO₂ adsorption–desorption stability of the AAIL-loaded mesoporous silica sorbent was evaluated under different regeneration temperatures. These experiments and analyses have provided the following conclusions:

- All of the AAIL-loaded calcined mesoporous silica sorbents adsorbed CO₂, but the capacities were different by the type of the supports;
- It was found from quantitative analyses that average pore size (D_P) of the as-prepared mesoporous silica supports exerted a dominant impact on the CO₂ capture capacities of the supported AAIL sorbents, compared with the pore volume (V_P) and surface area (S_{BET});
- Pore expansion of a support (PE-SBA-15 calcined) contributed to improvement in the capacity of supported AAIL sorbent, although the capacity did not approach the theoretical maximum value only by the pore expansion;
- Mesoporous silica supports not calcined, named MCM-41-SA and SBA-15-SA, led to greater CO₂ adsorption capacities of the supported AAIL sorbents than the counterparts calcined, due to the remaining surfactant in the supports;
- In contrast to the improved adsorption capacities, the remaining surfactants did not

enhance the regeneration performances in cyclic CO₂ adsorption–desorption;

- The cyclic CO₂ capture stability greatly reduced at the desorption temperature of 120 °C due to enormous weight loss of the loaded AAIL by its volatilization, whereas it highly enhanced at 80 °C because of the moderated weight loss;
- Thus, it was found that regeneration temperature exerted a significant impact on the cyclic stabilities of supported AAIL sorbents;
- PE-SBA-15 not calcined (PE-SBA-15-SA) caused lower capacity of the supported AAIL sorbent than PE-SBA-15 calcined at high AAIL loadings, although a synergetic effect between remaining surfactant and pore-expansion was expected on the CO₂ adsorption.

7.2.4 Overall conclusions

The overall conclusions of the thesis project are finally summarized here. In order to aim at the primary goal of developing novel and efficient AA-based solid sorbents for post-combustion CO₂ capture, various AAILs and mesoporous silica supports have been synthesized and evaluated mainly through CO₂ adsorption–desorption experiments in the absence or presence of water vapor. Regarding the type of AAs, it has been uncovered that Lys and Gly having linear side chains with only primary amino groups are more promising than other AAs, since Lys- and Gly-based AAIL adsorbents exhibited higher capacities per gram of the sorbent.

Some strategies to improve the performances of mesoporous silica supports have been investigated as well. As a result, it has been found that pore-expansion of or leaving the surfactant in a support are effective ways to enhance the capacities of supported AAIL sorbents; however, combining the two strategies does not provide a synergetic effect for supported AAIL sorbents, as described so far. Leaving the surfactant appears to be more efficient than pore-expansion in terms of saving the cost, time and energy [7].

In the presence of water vapor, most supported AAIL sorbents slightly decreased their CO₂ adsorption capacities, in contrast to supported amine and AA sorbents, as the water content inhibited the reaction of the AAILs with CO₂ by rapidly forming a hydrogen bond interaction between the AAIL cations and H₂O. Therefore, it is said that water vapor is an unfavorable impurity in flue gases for CO₂ capture by supported AAIL sorbents.

Despite many advances in development of novel and efficient AA-based CO₂ adsorbents, some problems and subjects have still remained unsettled, which are listed in the next section.

7.3 Recommendations for future study

The following are the subjects that should be addressed in future work, which correspond to the criteria described in Chapter 1 (1.1) that promising CO₂ adsorbents should satisfy:

- CO₂ adsorption capacity: the CO₂ capture capacities of AA-based (supported AAIL) adsorbents need to be further increased, as optimum capacities of CO₂ adsorbents are in a range of 2–4 mmol/g-sorbent [1];
- CO₂/N ratio: it is crucial to improve not only the capacity, but also the CO₂/N ratio (or amine efficiency);
- Long-term stability in cyclic CO₂ adsorption–desorption: finding an optimum regeneration condition (temperature) will be predominantly important to enhance the cyclic CO₂ adsorption–desorption stabilities of supported AAIL sorbents;
- Tolerance to impurities: tolerance to impurities contained in actual flue gases, such as SO₂, should be explored.

The details on these subjects and recommendations are described below.

7.3.1 CO₂ adsorption capacity

In this thesis project, various supported AAIL sorbents have been synthesized and employed for CO₂ capture study. Also, some attempts to increase the CO₂ adsorption capacities of the AAIL-loaded solid sorbents have been carried out by the selection of more active AAs (anions) and modification of support materials (pore-expansion of and/or leaving the surfactant in a support). Among the sorbents investigated so far, 60 wt% [EMIM][Lys]-impregnated PE-SBA-15 and SBA-15-SA sorbents exhibited the highest capacities of 1.5 mmol/g-sorbent at 30 °C in a dry gas inlet condition at 15% CO₂ concentration (refer to Figures 5.11 and 6.5). However, the capacities need to be further elevated to a range of 2–4 mmol/g-sorbent that is an optimum capacity for promising CO₂ adsorbents reported by Ho et al. [1].

It is expected that the CO₂ adsorption capacities of supported AAIL sorbents can increase by introducing more amino groups or nitrogen content into anions and/or cations of the AAILs. For example, Ren et al. have synthesized AAILs with multiple amino groups in both the cations and anions using several AAs as anions, and then conducted CO₂ capture experiments of the AAIL-loaded silica sorbents [2]. As a result, the Lys-based AAIL adsorbent with 4 amino groups showed a high capacity of 1.87 mmol/g-sorbent at 25 °C in 100% CO₂ flow condition. Zhang et al. have also prepared dual amino-functionalized AAILs for CO₂ study to increase the molar CO₂ capacities; the supported dual amino-functionalized AAIL sorbents exhibited twice higher molar capacities than single amino-functionalized AAIL adsorbents [3]. In the case of supported amine sorbents, amines with high nitrogen content, such as polyethyleneimine (PEI) and tetraethylenepentamine (TEPA) (Figure 7.2), have been often utilized to improve the CO₂ adsorption capacities as well [4,5]. For instance, 50 wt% TEPA-loaded MCM-41 sorbent with the remaining surfactant (CTAB) exhibited the capacity as high as 4.5 mmol/g-sorbent at 75 °C in a

dry gas flow (5% CO₂ concentration) [6]. It is interesting to attempt mixing AAILs and amines to increase the nitrogen content in the sorbent.

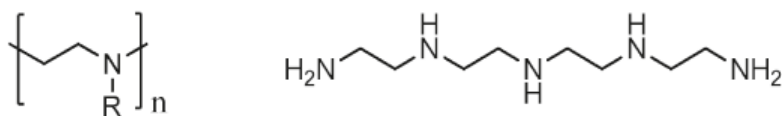


Figure 7.2. Molecular structures of PEI (left) and TEPA (right) [5].

Developing more efficient support materials will be also crucial. In this thesis project, the effects of textural properties and remaining surfactants (surface chemistry) of mesoporous silica supports on CO₂ capture of the supported AAIL sorbents have been investigated through Chapters 5–6. Understanding the influence of other characteristics of supports, such as geometry and interaction between the supports and AAILs, might be further required for the purpose. It will be also important to try other loading methods, like grafting.

7.3.2 CO₂/N ratio

In addition to CO₂ adsorption capacity, CO₂/N ratio (or amine efficiency) is a crucial factor for chemical adsorbents with amino groups. Regarding supported amine sorbents, the maximum CO₂/N ratio should be 0.5 under a dry CO₂ inlet condition, as the reaction of an amino group in amines with CO₂ occurs in a 2:1 stoichiometry in the absence of water content, as expressed by Equations 1.1–1.2 [8]. It has been reported that the CO₂/N ratios of 50 wt% PEI-loaded MCM-41, SBA-15 and KIT-6 sorbents were 0.18, 0.27 and 0.17 under a dry gas inlet at a low CO₂ concentration (5 to 15%), respectively [9].

Chapter 4 has revealed that cations with larger molecular size can lead to greater reaction

stoichiometry of the supported AAIL sorbents with CO₂. For instance, 50 wt% [P₄₄₄₄][Gly]-loaded PMMA sorbent exceeded the CO₂/N ratio of 0.5 in a dry CO₂ flow condition, which is higher than the maximum value of supported amine sorbents. On the other hand, the CO₂/N ratios of 50 wt% [EMIM][Gly]- and [EMIM][Lys]-loaded PMMA sorbents were less than 0.35. Thus, selection of cations as well as anions (AAs) can affect the CO₂/N ratio of the supported AAIL sorbents. It is recommended to explore further enhancement of both the CO₂/N ratio and capacity using other cations with larger molecular size, such as trihexyl(tetradecyl)ammonium ([N₆₆₆₁₄]⁺) and trihexyl(tetradecyl)phosphonium ([P₆₆₆₁₄]⁺) cations [10,11].

7.3.3 Stability in cyclic CO₂ adsorption–desorption

Chapter 6 has disclosed that regeneration temperature significantly affected the cyclic CO₂ capture stabilities of supported AAIL sorbents, since larger weight loss of the AAIL occurred at higher regeneration temperature by its volatilization, causing lower cyclic stability. Among 3 conditions of the regeneration temperatures examined, 80 °C was much better than the other temperatures (100 and 120 °C) to enhance the cyclic stability. However, further exploration on the regeneration condition will be required to improve the cyclic CO₂ capture performances.

7.3.4 Tolerance to impurities

Combustion flue gases from coal– and oil–fired power plants generally contain some impurities, including SO_x, NO_x and water vapor [5]. This thesis project has investigated only the effect of water vapor on CO₂ capture performances of AA-based solid sorbents (in Chapters 3-4); water vapor exerted a negative impact on CO₂ adsorption–desorption of most supported AAIL sorbents, in contrast to supported amine and AA sorbents. The effect of other impurities, such as SO₂, should be evaluated in future study to see whether they negatively influence the CO₂ capture

performances as well as water vapor, or not.

7.4 References

- [1] M.T. Ho, G.W. Allinson, D.E. Wiley, Reducing the cost of CO₂ capture from flue gases using pressure swing adsorption, *Ind. Eng. Chem. Res.* 47 (2008) 4883–4890.
- [2] J. Ren, L. Wu, B.G. Li, Preparation and CO₂ sorption/desorption of N-(3-aminopropyl)aminoethyl tributylphosphonium amino acid salt ionic liquids supported into porous silica particles, *Ind. Eng. Chem. Res.* 51 (2012) 7901–7909.
- [3] Y. Zhang, S. Zhang, X. Lu, Q. Zhou, W. Fan, Dual aminofunctionalised phosphonium ionic liquids for CO₂ capture, *Chem. Eur. J.* 15 (2009) 3003–3011.
- [4] C.H. Yu, C.H. Huang, C.S. Tan, A review of CO₂ capture by absorption and adsorption, *Aerosol Air Qual. Res.* 12 (2012) 745–769.
- [5] A. Samanta, A. Zhao, G.K.H. Shimizu, P. Sarkar, R. Gupta, Post-combustion CO₂ capture using solid sorbents: A review, *Ind. Eng. Chem. Res.* 51 (2012) 1438–1463.
- [6] M.B. Yue, L.B. Sun, Y. Cao, Y. Wang, Z.J. Wang, J.H. Zhu, Efficient CO₂ capturer derived from as-synthesized MCM-41 modified with amine, *Chem. Eur. J.* 14 (2008) 3442–3451.
- [7] M.B. Yue, Y. Chun, Y. Cao, X. Dong, J.H. Zhu, CO₂ capture by as-prepared SBA-15 with an occluded organic template, *Adv. Funct. Mater.* 16 (2006) 1717–1722.
- [8] P.D. Vaidya, E.Y. Kenig, CO₂-alkanolamine reaction kinetics: A review of recent studies, *Chem. Eng. Technol.* 30 (2007) 1467–1474.
- [9] A. Sayari, Y. Belmabkhout, R. Serna-guerrero, Flue gas treatment via CO₂ adsorption, *Chem. Eng. J.* 171 (2011) 760–774.
- [10] S. Saravanamurugan, A.J. Kunov-kruse, R. Fehrmann, A. Riisager, Amine-functionalized

- amino acid-based ionic liquids as efficient and high-capacity absorbents for CO₂, ChemSusChem 7 (2014) 897–902.
- [11] Q. Yang, Z. Wang, Z. Bao, Z. Zhang, Y. Yang, Q. Ren, H. Xing, S. Dai, New insights into CO₂ absorption mechanisms with amino-acid ionic liquids, ChemSusChem 9 (2016) 806–812.

Appendix: Copyright permissions



[Home](#) [Account Info](#) [Help](#)

 **ACS Publications**
Most Trusted. Most Cited. Most Read.

Title: Effect of Water Vapor on CO₂ Sorption-Desorption Behaviors of Supported Amino Acid Ionic Liquid Sorbents on Porous Microspheres

Author: Yusuke Uehara, Davood Karami, Nader Mahinpey

Publication: Industrial & Engineering Chemistry Research

Publisher: American Chemical Society

Date: Dec 1, 2017

Copyright © 2017, American Chemical Society

Logged in as:
Yusuke Uehara
Account #: 3001336154
[LOGOUT](#)

PERMISSION/LICENSE IS GRANTED FOR YOUR ORDER AT NO CHARGE

This type of permission/license, instead of the standard Terms & Conditions, is sent to you because no fee is being charged for your order. Please note the following:

- Permission is granted for your request in both print and electronic formats, and translations.
- If figures and/or tables were requested, they may be adapted or used in part.
- Please print this page for your records and send a copy of it to your publisher/graduate school.
- Appropriate credit for the requested material should be given as follows: "Reprinted (adapted) with permission from (COMPLETE REFERENCE CITATION). Copyright (YEAR) American Chemical Society." Insert appropriate information in place of the capitalized words.
- One-time permission is granted only for the use specified in your request. No additional uses are granted (such as derivative works or other editions). For any other uses, please submit a new request.

[BACK](#)[CLOSE WINDOW](#)

Copyright © 2018 [Copyright Clearance Center, Inc.](#) All Rights Reserved. [Privacy statement](#). [Terms and Conditions](#).
Comments? We would like to hear from you. E-mail us at customercare@copyright.com



RightsLink®

Home

Account
Info

Help



ACS Publications
Most Trusted. Most Cited. Most Read.

Title: Roles of Cation and Anion of Amino Acid Anion-Functionalized Ionic Liquids Immobilized into a Porous Support for CO₂ Capture
Author: Yusuke Uehara, Davood Karami, Nader Mahinpey
Publication: Energy & Fuels
Publisher: American Chemical Society
Date: Apr 1, 2018
Copyright © 2018, American Chemical Society

Logged in as:
Yusuke Uehara
Account #:
3001336154

LOGOUT

PERMISSION/LICENSE IS GRANTED FOR YOUR ORDER AT NO CHARGE

This type of permission/license, instead of the standard Terms & Conditions, is sent to you because no fee is being charged for your order. Please note the following:

- Permission is granted for your request in both print and electronic formats, and translations.
- If figures and/or tables were requested, they may be adapted or used in part.
- Please print this page for your records and send a copy of it to your publisher/graduate school.
- Appropriate credit for the requested material should be given as follows: "Reprinted (adapted) with permission from (COMPLETE REFERENCE CITATION). Copyright (YEAR) American Chemical Society." Insert appropriate information in place of the capitalized words.
- One-time permission is granted only for the use specified in your request. No additional uses are granted (such as derivative works or other editions). For any other uses, please submit a new request.

BACK

CLOSE WINDOW

Copyright © 2018 [Copyright Clearance Center, Inc.](#) All Rights Reserved. [Privacy statement](#). [Terms and Conditions](#).

Comments? We would like to hear from you. E-mail us at customercare@copyright.com



RightsLink®

[Home](#)[Account Info](#)[Help](#)

Title: CO₂ adsorption using amino acid ionic liquid-impregnated mesoporous silica sorbents with different textural properties

Author: Yusuke Uehara, Davood Karami, Nader Mahinpey

Publication: Microporous and Mesoporous Materials

Publisher: Elsevier

Date: April 2019

© 2019 Elsevier Inc. All rights reserved.

Logged in as:
Yusuke Uehara

Account #:
3001336154

[LOGOUT](#)

Please note that, as the author of this Elsevier article, you retain the right to include it in a thesis or dissertation, provided it is not published commercially. Permission is not required, but please ensure that you reference the journal as the original source. For more information on this and on your other retained rights, please visit: <https://www.elsevier.com/about/our-business/policies/copyright#Author-rights>

[BACK](#)[CLOSE WINDOW](#)

Copyright © 2019 [Copyright Clearance Center, Inc.](#) All Rights Reserved. [Privacy statement](#). [Terms and Conditions](#). Comments? We would like to hear from you. E-mail us at customer@copyright.com